

# Radiochemical synthesis of $^{18}\text{F}$ -radiolabelled ProTides for Positron Emission Tomography

A thesis submitted in accordance with the conditions  
governing candidates for the degree of  
Philosophiae Doctor in Cardiff University

by

Alessandra Cavaliere

January 2018

Cardiff School of Pharmacy and Pharmaceutical Science

Cardiff University



# Acknowledgments

I want to take the opportunity to express my gratitude to all my supervisors for their great support provided during these years.

In particular, I would like to thank Prof. Andrew Westwell for the amazing positive attitude, patient guidance, encouragement and advice he has provided throughout my time as his student. I have been extremely lucky to have a supervisor who cared so much about my work and me and who responded always promptly to my queries.

I thank Dr. Katrin Probst for her great support as a supervisor and as a woman. She gave me the opportunity to gain, besides research skills, also an insight into clinical tracers development which opened to me so many opportunities.

I am going to miss you a lot Andrew and Katrin, you both have been an inspiration with your professionalism and your ideas.

I want to thank Prof. Andrea Brancale for always being available, careful and incredibly friendly and Prof. Chris Marshall for his availability and kindness during my time at PETIC. Furthermore, I want to express my gratitude to Prof. Chris McGuigan for being an inspirational guide during this journey.

I also want to thank Stephen Paisey for all the continuous support provided for my experimental work, all members from Andrew's lab, the PETIC staff, Andrea's and Chris's lab for being always helpful and for becoming my friends making the work time incredibly pleasant moments. It's thanks to all of you that I loved every single day of my work in Cardiff University.

I want to thank Prof. Franklin Aigbirhio and Abdul from Wolfson Brain Imaging Centre at Cambridge University and Rohan, Dr. Joachim Bugert and Prof. Arwin Jones for the fruitful collaborations.

I thank the Life Science Research Network of Wales and Cardiff University for their financial support and the opportunity to attend scientific conferences

Finally, I would like to express my sincerest appreciation to my amazing family for always being there for me, for believing in me more than anyone else and for being the best role model I could possibly have. In addition, a huge thank to all my friends in Italy and particularly in Cardiff (luckily you are so many that one page wouldn't fit all your names), and to my special supporter. You guys have been my family in these years. Thanks for the support and the unique moments spent together. I will always keep them in my mind and in my heart.

*Dedicated to mum, dad and Vivi*

## Abstract

Positron Emission Tomography (PET) is a highly sensitive imaging technique used in cancer diagnosis, treatment planning and monitoring of therapy response.  $[^{18}\text{F}]$  is an optimal PET label considering its half-life (110 min) and imaging resolution. One of the major challenges in  $[^{18}\text{F}]$ -PET research is the installation of the weakly nucleophilic  $[^{18}\text{F}]$ fluoride into a precursor molecule to access novel  $[^{18}\text{F}]$ -tracers. Fluorinated nucleosides represent an important class of diagnostic probes for PET imaging as well as anticancer and antiviral therapeutic agents. However drug resistance still represents a major problem. The ProTide approach is a strategy to synthesize prodrugs of the nucleoside monophosphates which overcome their main resistance mechanisms. The challenge of the project is the  $[^{18}\text{F}]$ -fluorination (hot fluorination) of ProTides which may be potential new PET imaging agents and could thus represent a model system to visualize pharmaceutical effects and bioactivation of ProTides directly *in vivo*.

The pro-nucleotide multistep synthetic chemistry has been applied for the synthesis of ProTides. The  $[^{18}\text{F}]$ -radiolabeling of the precursor molecules was performed in an Eckert & Ziegler automated synthetic Modular Lab placed into a shielded hot cell. The radioactive reaction mixtures were analyzed by radio HPLC, and radio TLC. Two different approaches have been followed to access two chemically distinct radiolabelled ProTides. The 3'- $[^{18}\text{F}]$ FLT ProTide was synthesised via a late stage  $[^{18}\text{F}]$ fluorination of *ad hoc* synthesised precursor molecules (Figure 1).

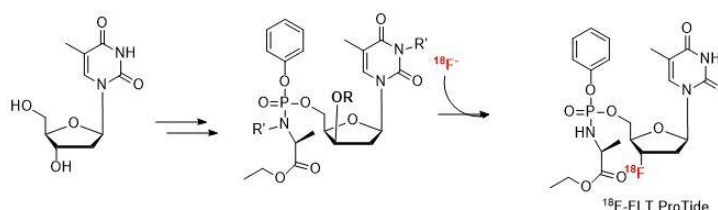


**Figure 1:** Radiochemical synthesis of  $^{18}\text{F}$ - FLT ProTides

The 2'- $[^{18}\text{F}]$ FIAU ProTide was synthesised via an early stage  $[^{18}\text{F}]$ fluorination approach (Figure 2).

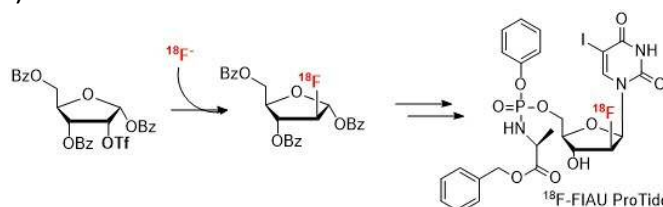


**Figure 2:** Radiochemical synthesis of  $^{18}\text{F}$ -FIAU ProTides

These radiolabelled probes could provide evidence for the *in vivo* behaviour of this class of compounds by answering key questions about their metabolism and uptake directly.

In addition, the project focused on the synthesis of two novel classes of non-radiolabelled fluorinated ProTides. A series of uridine based ProTides (FIAU ProTides) and a series of coumarin based FLT ProTides have been synthesised and evaluated for their antiviral activity and fluorescent properties respectively.

# List of contents

<b>LIST OF ABBREVIATIONS.....</b>	<b>VII</b>
<b>LIST OF FIGURES.....</b>	<b>X</b>
<b>LIST OF TABLES.....</b>	<b>XV</b>
<b>1. INTRODUCTION.....</b>	<b>1</b>
<b>1.1 Positron Emission Tomography (PET).....</b>	<b>1</b>
1.1.1 Physical principles of PET.....	3
1.1.2 [18F]fluorine.....	9
<b>The main properties of [18F]fluorine are summarised in the table below (Table 1.3)<sup>17</sup>.....</b>	<b>9</b>
1.1.2.1 Fluorination.....	11
1.1.2.2 [18F]FDG.....	17
1.1.2.3 [18F]-nucleosides.....	18
1.1.2.4 Other [18F]-labelled PETprobes.....	22
1.1.3 Short lived radioisotopes.....	23
1.1.4 Long-lived radioisotopes: Positron emitting metals.....	24
1.1.5 PET imaging: application in drug discovery.....	26
<b>1.2 Nucleosides.....</b>	<b>27</b>
1.2.1 ProTides.....	29
1.2.2 Fluorinated nucleosides and ProTides.....	32
1.2.2.1 Importance of fluorine in drug molecules.....	33
<b>2. RESEARCH AIMS AND OBJECTIVES.....</b>	<b>47</b>
<b>3. RADIOCHEMICAL SYNTHESIS OF [18F]FLT PROTIDE.....</b>	<b>50</b>
<b>3.1 Introduction.....</b>	<b>50</b>
<b>3.2 [18F]fluorination (Hot): late stage approach.....</b>	<b>51</b>
<b>3.3 Synthesis of the precursor molecules.....</b>	<b>52</b>
3.3.1 Synthesis of cyclised precursor (3.8).....	52
3.3.2 Synthesis of the mesyl, tosyl and nosyl precursors.....	57
<b>3.4 Synthesis of the cold standard.....</b>	<b>64</b>
<b>3.5 Studies of ProTide stability.....</b>	<b>67</b>
<b>3.6 [18F]fluorination.....</b>	<b>67</b>
3.6.1 [18F]-Fluorination of the anhydride precursor (3.8).....	71
3.6.2 [18F]fluorination of the mesyl precursor (3.1).....	72
3.6.3 [18F]fluorination of the tosyl precursor (3.2).....	74

3.6.4 [18F]fluorination of the nosyl precursor (3.3) .....	76
3.6.5 [18F]fluorination of the nosyl BOC protected precursor (3.4).....	81
<b>3.7 Conclusions .....</b>	<b>85</b>
<b>4. RADIOCHEMICAL SYNTHESIS OF [18F]FIAUPROTIDE.....</b>	<b>87</b>
4.1 Introduction .....	87
4.2 [18F]fluorination (Hot): early stage approach.....	88
4.3 Synthesis of the cold standard (4.3) .....	89
4.3 Synthesis of [18F]FIAU (1.16).....	90
4.5 Synthesis of the [18F]FIAUProTide (2.2) .....	97
4.6 Evaluation of the radiotracer [18F]FIAU (1.16) on HSV-TK engineered HEK cell lines.....	99
4.7 Conclusions .....	101
<b>5. SYNTHESIS OF NOVEL 2'-DEOXY-2'-FLUORO-5-IODOURIDINE PROTIDES AS NOVEL ANTIVIRAL AGENTS .....</b>	<b>103</b>
5.1 Introduction .....	103
5.2 Synthesis of novel 2'-deoxy-2'-fluoro-5-iodouridine ProTides .....	106
5.3 Antiviral evaluation .....	113
5.4 Conclusion .....	116
<b>6. SYNTHESIS OF NOVEL FLT CHIMERIC PROTIDES WITH FLUORESCENT PROBES. 117</b>	
6.1 Introduction .....	117
6.2 Synthesis of FLT chimeric ProTides with fluorescent probes.....	120
6.3 Fluorescence data .....	123
6.4 Conclusion .....	124
<b>7. CONCLUSIONS AND FUTURE WORK.....</b>	<b>125</b>
7.1 General conclusions and future perspective .....	125
<b>8. EXPERIMENTAL.....</b>	<b>127</b>
8.1 General information .....	127
8.1.1 Analytics.....	127

8.1.2 Solvents and chemicals .....	127
8.1.3 Radioactive source and equipment .....	128
<b>8.2 Procedures .....</b>	<b>128</b>
8.2.1 Standard procedure A1: synthesis of L-alanine ester hydrochloride salts.....	128
8.2.2 Standard procedure A2: synthesis of L-alanine ester sulfonate salts .....	128
8.2.3 Standard procedure B: synthesis of aryloxy phosphorochloridates .....	129
8.2.4 Standard procedure C: synthesis of phosphoramidates <i>via</i> NMI .....	129
8.2.5 Standard procedure D: synthesis of phosphoramidates <i>via</i> <i>t</i> BuMgCl .....	130
<b>8.3 Spectroscopic data .....</b>	<b>131</b>
8.3.1 Experimental section from Chapter 3 .....	131
8.3.2 Experimental section from chapter 4 .....	149
8.3.3 Experimental section from chapter 5 .....	158
8.3.4 Experimental section from Chapter 6 .....	196
<b>9. APPENDIX.....</b>	<b>204</b>
<b>10. BIBLIOGRAPHY .....</b>	<b>207</b>

## List of abbreviations

Å	Angstrom [ $1\text{Å} = 10^{-10}\text{ m} = 0.1\text{nm}$ ]
BGO crystals	Bismuth Germanium Oxide Crystals
Bq	Bequerel [ 1 Bq= 1 decay/sec ]
BOC	Tert-Butyloxycarbonyl Protecting Group
CAN	Ceric Ammonium Nitrate
CDA	Cytidine deaminase
Ci	Curie [1 Ci = $3.7 \times 10^{10}$ decays/sec =37 GBq]
CsF	Cesium Fluoride
CT	Computed Tomography
DAST	Diethylaminosulfurtrifluoride
dCK	Deoxycytidine Kinase
DCM	Dichloromethane
dFdC	2,2'-Difluoro-2'-Deoxycytidine (Gemcitabine)
DIAD	Diisopropylazodicarboxylate
DMF	Dimethyl Formamide
DNA	Deoxyribonucleic Acid
EPD	Electronic Personal Dosimeters
ESI	Electrospray Ionisation
EtOAc	Ethyl Acetate
eV	Electronvolt [J]
E&Z	Eckert & Zigler Unit
FAC	2'-Fluoro-Deoxy-Arabinocytidine
FDG	2-Fluoro-Deoxy-Glucose
FGI	Functional Group Interconversion
FIAU	2'-Fluoro-Deoxy-Arabino-5-Iodouridine
FLT	3'-Fluoro-Deoxy-L-Thymidine
FMAU	Fluoro-Deoxy-Arabino-5-Methyluridine
GC	Gas Chromatography

GMP	Good Manufacturing Practice
H	Hour
HBV	Hepatitis B Virus
HCl	Hydrogen Chloride
HCV	Hepatitis C Virus
hENT	Human Concentrative Nucleoside Transporter
HIV	Human Immunodeficiency Virus
HPLC	High-Pressure Liquid Chromatography
HSV-TK-1	Herpes Simplex Virus Thymidine Kinase 1
Hz	Hertz [ $1 \text{ Hz} = \text{s}^{-1}$ ]
K222	Kryptofix 222 (Cryptant)
KF	Potassium Fluoride
LC	Liquid Chromatography
M	Molar [Mol/L]
MeCN	Acetonitrile
MeOH	Methanol
mL	Millilitre
MRI	Magnetic Resonance Imaging
MS	Mass Spectrometry
MsCl	Methanesulfonyl (Mesyl) Chloride
NA	Nucleoside Analogues
NaOH	Sodium Hydroxide
NEt <sub>3</sub> /TEA	Triethylamine
NMI	1-Methylimidazole
NMR	Nuclear Magnetic Resonance
NsCl	<i>p</i> -Nitrophenylsulfonyl (Nosyl) Chloride
NTs	Nucleoside Transporters
PET	Positron Emission Tomography
PETIC	Wales Research Diagnostic PET Imaging Centre
pKa	Acid Dissociation Constant

PPh <sub>3</sub>	Triphenylphosphine
ppm	Parts Per Million
pTsOH	<i>p</i> -Toluenesulfonic Acid
QC	Quality Control
R&D	Research and Development
Radio HPLC	Radio High Performance Liquid Chromatography
Radio TLC	Radio Thin Layer Chromatography
RCY	Radiochemical Yield
r.t.	Room Temperature
Rf	Retardation Factor
RNA	Ribonucleic Acid
RR	Ribonucleotidreductase
Rt	Retention Time
SA	Specific Activity
SLC	Solute Carrier Family (Nucleoside Transporter)
SM	Starting Material
SN	Nucleophilic Substitution
SPECT	Single Photon Emission Computed Tomography
Sv	Sievert (1 Sv = 1 joule/kilogram )
t <sub>1/2</sub>	Radiochemical Half-Life
TBAF	Tetrabutyl Ammonium Fluoride
THF	Tetrahydrofuran
TK	Thymidine Kinase 1
TLC	Thin-Layer Chromatography
TMSOTf	Trimethylsilyltrifluoromethanesulfonate
TS	Thymidylate Synthase
TsCl	Toluenesulfonyl (Tosyl) Chloride
US	Ultrasound
UV	Ultraviolet

## List of figures

**Figure 1.1:** Schematic illustration of an annihilation reaction and the subsequent coincidence detection

**Figure 1.2:** Schematic illustration of a cyclotron

**Figure 1.3:** Nuclear reaction short hand

**Figure 1.4:** Eckert& Ziegler automated modular lab

**Figure 1.5:** a) Fastlab from GE healthcare and b) Trasis

**Figure 1.6:** Structure of Kryptofix K[222]

**Figure 1.7:** Synthesis of [18F]FLT via two approaches

**Figure 1.8:** Metal catalyzed allylic fluorination reaction

**Figure 1.9:** Synthesis of the [18F]flutemetamol

**Figure 1.10:** Synthesis of [18F]fluorouracil (**1.9**) via transition-metal-mediated fluorination

**Figure 1.11:** Synthesis of the fluorinating agent Selectfluor

**Figure 1.12:** Electrophilic fluorination with Selectfluor

**Figure 1.13:** Synthesis of Clofarabine (**1.13**)

**Figure 1.14:** Synthesis of [18F]FIAU (**1.16**)

**Figure 1.15:** Structure of the most widely used PET tracer [18F]FDG

**Figure 1.16:** Routine clinical synthesis of the radiotracer [18F]FDG

**Figure 1.17:** [18F] analogues: pyrimidine nucleosides

**Figure 1.18:** Thymidine salvage and *de novo* synthesis pathways

**Figure 1.19:** Structures of some purine nucleoside analogues

**Figure 1.20:** Structures of some [18F]-purine adenosine analogues

**Figure 1.21:** Structure of [18F]FAC

**Figure 1.22:** Structure of the Parkinson's disease PET probe [18F]fluorodopa

**Figure 1.23:** Aprepitant (**1.26**) and a radiomarker of NK1 (**1.27**)

**Figure 1.24:** Structures of ribose and 2'-deoxyribose nucleosides

**Figure 1.25:** Thymidine and cytidine and their analogues

**Figure 1.26:** Pro-nucleotides mechanism of action

**Figure 1.27:** Proposed activation pathway of Protides

**Figure 1.28:** FDA-approved fluorinated anticancer and antiviral nucleoside analogues.

**Figure 1.29:** North and south conformation of two anomers of F-ddA

**Figure 1.30:** Fluorinated anticancer nucleobase, nucleoside and nucleotide analogues in clinical studies

**Figure 1.31:** Fluorinated antiviral nucleoside analogues and derivatives in clinical trials

**Figure 1.32:** Suggested mechanism by which FIAU causes widespread mitochondrial injury, and disturbance in metabolic processes

**Figure 2.1:** Late stage [18F]fluorination of ProTides

**Figure 2.2:** Early stage [18F]fluorination for the synthesis of ProTides

**Figure 2.3:** ProTide approach applied to the 2'-deoxy-2' fluoro- 5-iodouridine

**Figure 2.4:** ProTide approach for the synthesis of hybrid ProTides

**Figure 3.1:** Structure of an [18F]FLT ProTide

**Figure 3.2:** Late stage fluorination approach for the synthesis of the [18F]FLT ProTide

**Figure 3.3:** General scheme for the synthesis of precursor molecules for the synthesis of [18F]FLT ProTide

**Figure 3.4:** Synthesis of the anhydride precursor

**Figure 3.5:** Mitsunobu reaction

**Figure 3.6:** Mechanism of the Mitsunobu reaction

**Figure 3.7:** Synthesis of Phosphorochloridate

**Figure 3.8:** Formation of the anhydride ProTide

**Figure 3.9:** Synthetic procedure for the mesyl, tosyl and nosyl precursors

**Figure 3.10:** Hydrolysis

**Figure 3.11:** ProTide coupling

**Figure 3.12:** Reaction mechanism for the final coupling step in the synthesis of the FLT ProTide

**Figure 3.13 :** Reaction mechanism of the Mesylation

**Figure 3.14:** Mesylation reaction

**Figure 3.15:** Nosylation and Tosylation

**Figure 3.16:** N-Protection using the BOC group

**Figure 3.17:** Fluorination of the Mesyl precursor

**Figure 3.18:** Fluorination of the Nosyl precursor (2.3)

**Figure 3.19:** Synthesis of FLT ProTide using FLT as starting material

**Figure 3.20:** Mechanism of reaction of the Grignard reagent

**Figure 3.21:** Analytical HPLC (UV detector) of the cold [19F]FLT ProTide

**Figure 3.22:** Studies of stability of the FLT ProTide

**Figure 3.23:** Modular Lab Eckert and Ziegler (E&Z) at PETIC centre

**Figure 3.24:** Sketch of EZ Modular Lab

**Figure 3.25:** Flow chart of the synthetic steps in modular lab

**Figure 3.26:** General conditions for the hot fluorination of the precursors

**Figure 3.27:** [18F]fluorination of compound **3.8**

**Figure 3.28:** [18F]fluorination of compound **3.1**

**Figure 3.29:** [18F]fluorination of compound **3.2**

**Figure 3.30:** [18F]fluorination of compound **3.3**

**Figure 3.31:** GE Healthcare TracerlabFxFn

**Figure 3.32:** Sketch of TracerlabFxFn

**Figure 3.33:** Analytical HPLC chromatogram of the cold standard

**Figure 3.34:** [18F]fluorination of compound **3.3** with TracerLabFxFn

**Figure 3.35:** Hot fluorination of the nosyl derivative without the use of Kryptofix as reagent

**Figure 3.36:** Hot fluorination of the BOC protected nosyl derivative (**3.4**)

**Figure 3.37:** [18F]fluorination of compound **3.4**

**Figure 3.38:** Deprotection of the BOC [18F]-intermediate

**Figure 3.39:** Deprotection of compound **3.12**

**Figure 3.40:** Purified [18F]FLT ProTide

**Figure 3.41:** Radio-TLC chromatogram of the purified [18F]FLT ProTide

**Figure 4.1:** Structure of the 2'-[18F]FIAU ProTide target (**2.2**)

**Figure 4.2:** Early stage fluorination approach for the synthesis of the

[18F]FIAU-ProTide (2.2)

**Figure 4.3:** Synthesis of the cold standard FIAU ProTide (4.3)

**Figure 4.4:** Iodination of the starting material (4.4)

**Figure 4.5:** Radiochemical synthesis of [18F]FIAU (1.16)

**Figure 4.6:** Synthesis of the [18F]-sugar (4.2)

**Figure 4.7:** [18F]fluorination of compound 4.1

**Figure 4.8:** Protection of the 5-Iodouracil (4.5)

**Figure 4.9:** Synthesis of protected  $\beta$ -anomer of [18F]FIAU (1.16) and the  $\alpha$ -anomer (4.8)

**Figure 4.10:** Deprotection reaction

**Figure 4.11:** [18F]FIAU purification

**Figure 4.12:** Deprotection reaction when using TMSOTf and SnCl<sub>4</sub> as catalysts

**Figure 4.13:** Synthesis of the [18F]FIAUProTide (2.2)

**Figure 4.14:** Synthesis of [18F]FIAU ProTide

**Figure 4.15:** Proposed retrosynthetic pathway to access the [18F]FIAU ProTide (2.2) via a late stage hot fluorination

**Figure 5.1:** Structures of 2'-deoxy-2'- $\beta$ -fluoro-5-iodouridine (FIAU, 1.66) and its anomer 2'-deoxy-2'- $\alpha$ -fluoro-5-iodouridine (2.3)

**Figure 5.2:** Application of the ProTide strategy to fluorinated uridine based ProTides

**Figure 5.3:** General synthetic scheme for the 2'-deoxy-2'-fluoro-5-iodouridine ProTides

**Figure 5.4:** Iodination of the  $\alpha$ - and  $\beta$ -anomers

**Figure 5.5:** Formation of the naphthyl-phosphorodichloridate

**Figure 5.6:** Synthesis of the L-alanine ester salt via two methods

**Figure 5.7:** Synthesis of the phosphorochloridates

**Figure 5.8:** Synthesis of the ProTides

**Figure 5.9:** Antiviral effect on Zika virus at 10  $\mu$ m on DEPG cells (n=3)

**Figure 5.10:** Antiviral effect of Zika virus at 10  $\mu$ m on HUH7 cells (n=3)

**Figure 5.11:** Cytotoxicity at 10  $\mu$ m on HUH7 cells (n=3)

**Figure 5.12:** Cytotoxicity at 10  $\mu$ m on DBGRT cells (n=3)

**Figure 6.1:** Structure of hybrid coumarin derivatives of FLT ProTides

**Figure 6.2:** Structure of coumarin backbone

**Figure 6.3:** Structures of the coumarin derivatives tipranavir (**6.1**) and (+)-calanolide (**6.2**)

**Figure 6.4:** General synthetic scheme for FLT-coumarin derivatives ProTides

**Figure 6.5:** Synthesis of the phosphorodichloridates

**Figure 6.6:** Synthesis of the phosphorochloridate

**Figure 6.7:** Synthesis of the phosphoramidates

**Figure 6.8:** Fluorescence emission spectrum of compound **6.3**, **6.4** and **6.6**

# List of tables

**Table 1.1:** Selected isotopes used in PET imaging

**Table 1.2:** Nuclear reactions targets and products

**Table 1.3:** Main properties of [18F]fluorine

**Table 1.4:** Common PET Tracers

**Table 1.5:** Fluorinated NAs and their prodrugs in clinical use and clinical development for cancer

**Table 1.5 (cont.):** Fluorinated NAs and their prodrugs in clinical use or clinical development for viral infections

**Table 3.1:** Structures of mesyl, tosyl and nosyl leaving groups and pKa of their equivalent acids

**Table 3.2:** Attempts of cold fluorination of mesyl precursor

**Table 3.3:** [18F]fluorination attempts on the anhydride Precursor

**Table 3.4:** [18F]fluorination attempts on the mesyl precursor

**Table 3.5:** [18F]-fluorination attempts on the tosyl precursor

**Table 3.6:** [18F]fluorination attempts of the nosyl precursor

**Table 4.1:** Attempts for the hot glycosylation reaction

**Table 4.2:** Radiolabelling of wild HEK cells and tk engineered HEK cells

**Table 4.3:** Preliminary radiolabelling experiment results

**Table 5.1:** Structures and yields of **5.6a-5.6e**

**Table 5.2:** Structures and yields of phosphorochloridates synthesised

**Table 5.3:** Structures and yields of **4.3, 5.8a-5**

# 1. Introduction

## 1.1 Positron Emission Tomography (PET)

Positron Emission Tomography (PET) is a highly sensitive non-invasive nuclear imaging technique widely used for cancer diagnosis and treatment planning. It is also used for early detection and treatment of other diseases (i.e. Parkinson's and Alzheimer's disease) by detecting metabolic changes within relevant cells.<sup>1</sup>

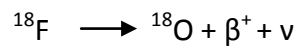
Diagnostic radiology is a field that emerged after the discovery of X-rays by Wilhelm Röntgen in 1895. Nowadays, this technique is still used, together with CT (Computed Tomography), MRI (Magnetic Resonance Imaging) and US (Ultrasound). Although they can be useful in order to provide structural and anatomical information on different medical conditions, their biggest limitation is that they give very poor functional information about biological and metabolic processes.<sup>1</sup>

PET and SPECT (Single-Photon Emission Computed Tomography) instead give the possibility to deeply understand the biological processes in different medical diseases. PET, compared to SPECT, has several advantages such as the possibility of having 3D and 2D physiological and biological information thank to the use of a wider range of positron emitting radioelements and a higher sensitivity.<sup>1</sup> PET, more recently, has also been used for another important and crucial role in the drug discovery industry. Indeed, PET gives the possibility to provide a wide range of useful information on biological and pharmacological properties of several drug candidates through direct radiolabeling of the drug molecule.<sup>2</sup> PET thus represents an important tool for drug discovery and personalized medicine, allowing for several clinical trials and monitoring of patient response to treatments.<sup>3</sup>

Among different positron-emitting isotopes  $^{18}\text{F}$ ,  $^{11}\text{C}$ ,  $^{13}\text{N}$  and  $^{15}\text{O}$  are currently the most widely used in PET.<sup>4</sup> All of them are characterized by a low molecular weight so that no difference in biological activity is observed compared with their non-labelled counterparts.<sup>5</sup> These radioelements decay by positron emission, an anti-electron which encounters an electron and causes an annihilation event leading to the release

of antiparallel gamma-rays<sup>4</sup>. For example, [<sup>18</sup>F]fluorine decays to [<sup>18</sup>O]oxygen, a natural and stable isotope of oxygen, releasing a neutrino ( $\nu$ ) and a positron ( $\beta^+$ ) (Equation 1.1)<sup>6</sup>.

**Equation 1.1: Decay of <sup>18</sup>F**



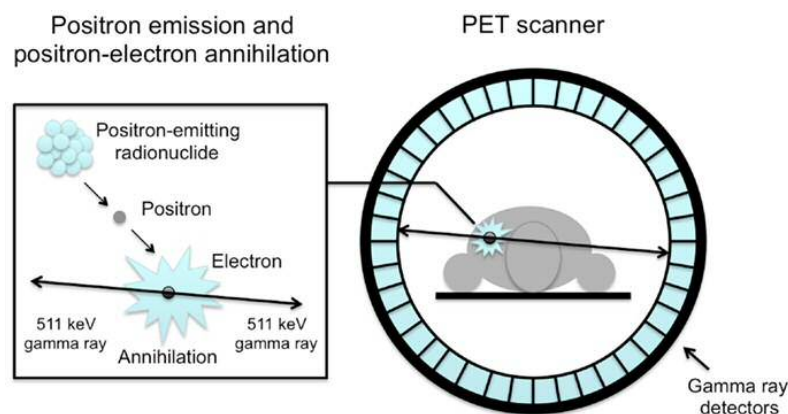
The time frame of  $\beta^+$  emission depends on the half-life of the radioactive nucleus, which varies according to its specific decay constant ( $\lambda$ ) (Equation 1.2)<sup>7</sup>.

**Equation 1.2: Half-life of a radionuclide varies with the decay constant**

$$t_{1/2} = \frac{0.693}{\lambda}$$

The positron ( $\beta^+$ ) can encounter an electron ( $e^-$ ), its antiparticle, by travelling a short distance to the surrounding tissues. An annihilation event thus occurs, and two gamma-ray photons ( $\gamma$ ) of 511 keV are generated from this event (Figure 1.1)<sup>8</sup>.

**Figure 1.1.1: Schematic illustration of an annihilation reaction and the subsequent coincidence detection**



The emitted  $\gamma$ -rays travel in the opposite direction with an angle of  $180^\circ$  and PET scanners, which encircle the patient, detect the pair of photons simultaneously, determining the precise 3D location of the radiolabelled compounds.

Radioelements <sup>13</sup>N and <sup>15</sup>O have very short half-lives (less than 10 minutes), so they require a cyclotron (PET isotope generating particle accelerator) facility on site.

$^{11}\text{C}$  has a half-life of 20.3 min, which is longer, but still often not long enough for a multi-step tracer synthesis<sup>1</sup>.  $^{18}\text{F}$ , on the contrary, is the most widely used radioisotope in PET. With its half-life of 109.77 min, it allows for efficient multi-step synthesis of radiolabelled tracer molecules (Table 1.1)<sup>9</sup>.

**Table 1.1: Selected isotopes used in PET imaging<sup>9</sup>**

Isotope	Half life	$\beta$ -Positron emission
$^{18}\text{O}$	2 min	$\beta^+$ , 1732keV (99.9%)
$^{15}\text{N}$	10 min	$\beta^+$ ,1199 keV (99.8%)
$^{11}\text{C}$	20.39 min	$\beta^+$ ,960 keV (99.8%)
$^{18}\text{F}$	109.8	$\beta^+$ ,633 keV (96.7%)
$^{64}\text{Cu}$	12.7 h	$\beta^+$ ,653 keV (17.9%), $\beta^-$ , 578.7 keV (39%)
$^{124}\text{I}$	4.17 days	$\beta^+$ ,1199 keV (99.8%), $\beta^-$ , 2138 keV (11%)

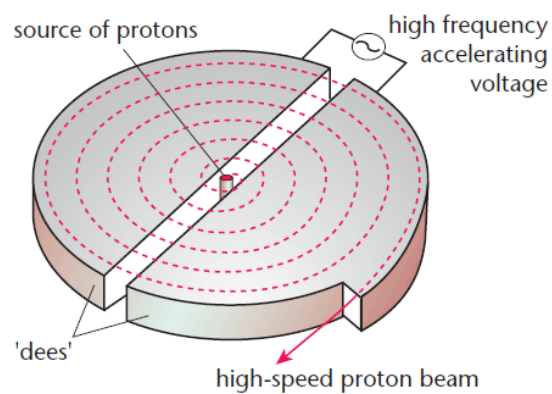
Additionally, the longer half-life allows investigation of biological systems with slower kinetics.<sup>10</sup>

### 1.1.1 Physical principles of PET

#### *From the cyclotron to the PET scan*

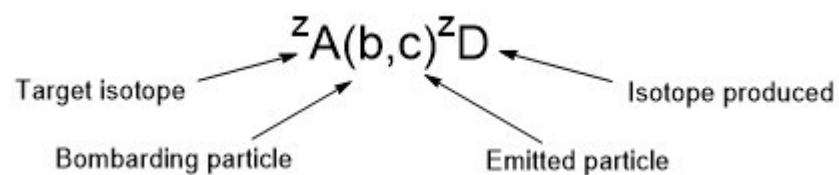
Many steps are required to obtain radiolabelled tracers for PET imaging. The whole process starts with the production of proton rich radioisotopes produced by bombardment of a target by proton sources. This process takes place at very high velocity in cyclic particle accelerators named cyclotrons (Figure 1.2).

The cyclotron uses a combination of electric and magnetic fields. As soon as the positively charged particle enters the gap between the two dees, it is accelerated by the electric field towards one of them. The magnetic field makes the particle do semi-circle movements and then moves it back to the gap. The electric field accelerates the positive particle to the original dee, and this process is repeated with every transition of the particle. Eventually, the particle exits the cyclotron at high speed to bombard the target.<sup>11</sup>

**Figure 1.2: Schematic illustration of a cyclotron**<sup>12</sup>

The positively charged particle, accelerated by the cyclotron, hits the target isotope which emits another particle from its nucleus and thus produces the desired radioisotope. Different targets and nuclear reactions can be used to obtain the desired radioisotope.<sup>11</sup>

Details of a nuclear reaction are normally described as in the short hand in Figure 1.3 where A represent the target isotope, b the bombarding particle, c the emitted particle, D the isotope produced and z the atomic mass.

**Figure 1.3: Nuclear reaction short hand**

Listed below are some nuclear reactions associated with the most common targets (Table 1.2)<sup>11,13</sup>.

**Table 1.2: Nuclear reactions targets and products**<sup>11,13</sup>

TARGET	NUCLEAR REACTION	PRODUCT
<b>N<sub>2</sub> + 0.1% O<sub>2</sub></b>	<sup>14</sup> N(p,α) <sup>11</sup> C	[ <sup>11</sup> C]CO <sub>2</sub>
<b>N<sub>2</sub> + 5% H<sub>2</sub></b>	<sup>14</sup> N(p,α) <sup>11</sup> C	[ <sup>11</sup> C]CH <sub>4</sub>
<b>N<sub>2</sub> + 0.2% O<sub>2</sub></b>	<sup>14</sup> N(d,n) <sup>15</sup> O	[ <sup>15</sup> O]O <sub>2</sub> H <sub>2</sub>
<b><sup>18</sup>O</b>	<sup>18</sup> O(p,n) <sup>18</sup> F	[ <sup>18</sup> F]F <sup>-</sup> (H <sub>2</sub> O) <sub>n</sub>
<b><sup>18</sup>O<sub>2</sub> + 0.6% F<sub>2</sub></b>	<sup>18</sup> O(p,n) <sup>18</sup> F	[ <sup>18</sup> F]F <sub>2</sub>
<b><sup>20</sup>Ne</b>	<sup>20</sup> Ne(d, α) <sup>18</sup> F	[ <sup>18</sup> F]F <sub>2</sub>
<b>H<sub>2</sub>O/ETHANOL</b>	<sup>16</sup> O(p,α) <sup>13</sup> N	[ <sup>13</sup> N]NH <sub>3</sub>
<b>CO<sub>2</sub> (TRACE N<sub>2</sub>)</b>	<sup>12</sup> C(d,n) <sup>13</sup> N	[ <sup>13</sup> N]N <sub>2</sub>

Once a radioisotope is produced, it has to be incorporated into a precursor molecule to obtain the desired radiotracer. Synthesis, purification and quality control (QC) analyses need to be performed in a reasonable short time (typically less than 2 or 3 half-lives).

To achieve this, the radioisotope has to be in a reactive form. Sometimes it is produced directly as its reactive species such as the [<sup>18</sup>F]F<sub>2</sub> gas.<sup>14</sup> Other times, it has to be converted into a more reactive form. This is the case for [<sup>11</sup>C]MeI which can be obtained from [<sup>11</sup>C]-CO<sub>2</sub> or [<sup>11</sup>C]-CH<sub>4</sub>.<sup>15,16</sup> In the case of the [<sup>18</sup>F]fluoride, because of its weak nucleophilicity, its reactivity has to be increased by using crown ethers and azeotropic drying.<sup>17</sup>

The reactive form of the radioisotope has to be introduced into a precursor molecule at a late stage in the multi-step synthesis if possible. Therefore, precursors are usually synthesized to be highly functionalized and activated so that the labeling can be the last step or can be followed by a quick deprotection step only.<sup>10</sup> To speed up the reaction the precursor should be used in super-stoichiometric amounts compared to the radioisotope.<sup>18</sup> Radiotracers are also required to be enantiomerically pure (more than 98%ee) whenever possible.<sup>18</sup>

In order to manipulate the reagents of the reaction when dealing with positron emitting radioisotopes, an automated synthesizer is required so that the chemical reaction can occur in a heavily shielded compartment called a hot cell. The radiotracer

has to be injected into a patient in a short time from the beginning of the synthesis, which means that the reaction has to be reproducible as its failure will lead to severe inconvenience for patients.<sup>18</sup>

Besides these essential requirements, there are some extra desirable ones such as a stable and easily synthesised precursor. A high radiochemical yield (RCY) is also a desirable as more patients can be scanned and the tracer, accordingly to the kind of radioisotope used, could also be transported offsite. To simplify the synthesis, ambient temperature would be ideal as well as a high specific activity (SA).<sup>17</sup>

Specific activity is an important factor when it comes to radiotracers. It is defined as the radioactivity per unit of material (grams or moles of tracers). The higher the SA, the lower the concentration of cold harmful tracer that will be administered.<sup>19</sup> To calculate the specific activity of a tracer, it should be taken into account that [19F]-tracers could be present even if the fluorination was “no carrier-added”.<sup>20</sup> Possible sources of <sup>19</sup>F could be Teflon tubing<sup>21</sup> or ion exchange cartridges<sup>22</sup>. To calculate the exact amount of tracer desired, HPLC with a UV detector can be used for UV sensitive tracers. First, a calibration curve of the cold tracers should be done and then compared with the concentration of the UV signal of the radioactive tracer.<sup>19</sup>

### ***Automated modules for the synthesis***

When dealing with radioactive tracers, the synthetic process is obviously influenced by the short time available for the synthesis, purification and QC analyses (usually not more than 3 half-lives of the radionuclide). For these reasons, for both preclinical and clinical purposes, use of computer controlled synthetic automated modules are required.<sup>22</sup> This will, on one hand, reduce the exposure to radioactivity for operators as modules will be placed into shielded hot cells but will also assure a reproducible synthesis reducing the possibility of human errors and the overall synthesis time. Many companies have developed in recent years automated modules that can be adaptable for many kind of synthesis. The Eckert & Ziegler (E&Z) modular lab (Figure 1.4) is currently one of the most commonly used for the routine synthesis of the gold standard PET tracer [18F]FDG.

**Figure 1.4: Eckert & Ziegler automated modular lab<sup>22</sup>**



Tracers like  $[^{18}\text{F}]\text{FDG}$ , which require a nucleophilic fluorination followed by a single deprotection step, can be synthesised by these automation modules. Other automation modules like Fastlab from GE healthcare and Trasis (Figure 1.5) allow also more complex synthesis with better radiochemical yields (RCY) and radiochemical purity.

**Figure 1.5: a) Fastlab from GE healthcare<sup>23</sup> and b) Trasis<sup>24</sup>**



a.



b.

### ***Analysis and quality control of radiotracers***

Finally, before using the tracer, purification and quality control analyses have to be performed. Again fast purification is required and it can be performed either by preparative HPLC attached to automation modules, ideally just using purification cartridges. Once purified, the tracer is usually isolated in a generally isotonic solution and is passed through sterile filters. One of the samples produced is designated to the

quality control section to make sure all the criteria required are met (this is particularly true when the tracer has to be produced under GMP standards for clinical purposes).<sup>25</sup>

Listed below are some of the routine analyses performed for quality control of radiopharmaceuticals:

- Dose calibration of the radioisotope.
- Filter test to determine its integrity.
- Visual inspection of the product.
- pH measures.
- Endotoxin test.
- Analytical HPLC to determine the radiochemical purity and identity of tracer and side products.
- Radio TLC for RCY, purity and identity calculation.
- Analysis of residual Kryptofix left in the solution.
- GC to determine quantity of residual solvents in the product.<sup>26</sup>

When it comes to the development of novel tracers for R&D purposes, Radio-TLC and Radio-HPLC are the main tools used for high quality analyses. Radio-HPLCs are characterized by a UV, a refractive index or conductivity, and a radioactive detector. This allows straightforward determination of the radioactive profile of the tracer.<sup>26</sup> Real time analyses are provided either by flow-cell radioactivity measures or by the use of microplates scintillation counting. The radioactivity is detected by using NaI or Bismuth Germanium Oxide (BGO) scintillation crystals. They register the annihilation-photons and re-emit low energy photons that are eventually converted into an electrical signal thanks to coupled photomultiplier tubes.<sup>27</sup>

### ***Radiation safety and monitoring***

When dealing with radioactivity, health and safety legislation becomes more stringent when compared to normal organic chemistry synthesis. All the staff must be trained through a radiation safety and monitoring course prior to perform any kind of work according to the current UK Ionisation Radiation Regulations (IRR99).<sup>28</sup> In addition, standard protective clothing and personal radiation film badges must be worn to monitor torso, fingers and head. The IRR99 established a certain annual dose

limit for operators; 200 mSV for the body, 500 mSV for hands, forearms and feet and 150 mSV for the lens of the eye. In order to reduce the risk of exposure, the amount of time spent near to a radiation source must be reduced,<sup>28</sup> the distance from the radioactive material has to be increased as much as possible and lead shields should also be used to minimize the exposure. Lab walls and hot cells should have a width of 4 cm to effectively shield the 511 keV photons.<sup>29</sup> In conclusion, respecting these basic rules as well as using electronic personal dosimeters (EPD) and personal film batch dosimeters will protect the operator as well as the environment in which all the process happens.

### 1.1.2 [18F]fluorine

Often the fluorination occurs in the last synthetic step but several synthetic schemes plan it at an earlier stage since it needs to be followed by a deprotection step. The fluorination, in fact, is often a non-regiospecific reaction, especially under the conditions used in hot chemistry (i.e. high temperature), therefore usually precursor molecules need to be protected in order to avoid degradation of the starting material during the synthesis.<sup>19</sup>

The <sup>18</sup>F half-life of 110 minutes, additionally, permits the [18F]-radiolabelled pharmaceuticals to be transported out of the site of production and also gives the possibility to use them for physiological studies that require scanning times of several hours.<sup>17</sup> Another huge advantage of using [18F]fluorine instead of other radioisotopes, is that it is also characterized by a low percentage of positron emitting energy which is the distance traveled by the positron before the annihilation event. The shorter the distance, the better the image resolution.<sup>10</sup>

The main properties of [18F]fluorine are summarised in the table below (Table 1.3)<sup>17</sup>.

**Table 1.3: Main properties of [18F]fluorine<sup>17</sup>**

PROPERTY	VALUE
half life	110 min
maximum energy of $e^+$	0.64 MeV
mode of decay	$\beta^+$ (97%)
decay product	$^{18}\text{O}$

Besides their advantageous half-life, [18F]-tracers provide high resolution images thanks to the low positron energy emission of the  $^{18}\text{F}$  (0.64 MeV).<sup>17</sup> This implies that, once emitted, the positron has to travel a very short distance ( $\approx 2\text{mm}$ ) before encountering an electron in the surrounding tissue. From this annihilation event two gamma rays of 511 KeV are generated and are detected by the PET scanner.<sup>22</sup>

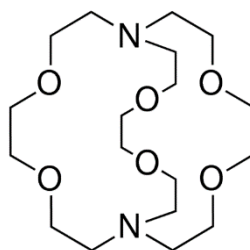
[18F]fluorine is produced from the nuclear reaction  $^{18}\text{O}(p,n)^{18}\text{F}$  in high yields with low energy protons ( $<16\text{ MeV}$ ) and high specific activity (Equation 1.3).<sup>1</sup>

**Equation 1.3: [18F]fluorine production equation**



The high specific activity of [18F]-tracers allows their use in very low concentration (picomolar range).<sup>23</sup> [18F]fluorine can be obtained from the cyclotron or linear charged particle accelerators. Most PET facilities accomplish the generation of [18F]fluorine by irradiation of target molecules in a cyclotron.<sup>10</sup>

To perform a nucleophilic fluorination, the target of proton bombardment is the oxygen-18 enriched water via the nuclear reaction  $^{18}\text{O}(p,n)^{18}\text{F}$ . Once the  $[^{18}\text{F}]\text{F}^-$  is generated, it is entrapped in an ion-exchange cartridge with a base such as KF to afford  $[^{18}\text{F}]\text{KF}$ . The aqueous fluoride thus produced, is a weak nucleophilic agent and, for this reason, a chelator agent like Kryptofix K[222] (Figure 1.6), is used to chelate the potassium and release free [18F]fluoride ion which is thus activated and desolvated ready for the nucleophilic attack.<sup>17</sup>

**Figure 1.6: Structure of Kryptofix K[222]**

If an electrophilic fluorination reaction is required, the target is Neon-20 which is bombarded with deuterons via the nuclear reaction  $^{20}\text{Ne}(d,\alpha)^{18}\text{F}$  generating  $^{18}\text{F}[\text{F}_2]$ , although the nucleophilic reaction is commonly preferred for the introduction of  $^{18}\text{F}$ fluorine into a bioactive molecule.<sup>30</sup>

There are several methodologies used to measure the radiochemical yield of a reaction. Usually the radioactivity of the purified  $^{18}\text{F}$ -labeled compound is compared to the initial radioactivity received from the cyclotron. The unit used for radioactivity in PET is the Becquerel (Bq) or, less frequently, the Curie (Ci). 1Ci is equal to 37 GBq.  $^{18}\text{F}$ -radiolabelled compounds are analyzed by high-performance liquid chromatography (HPLC) or gas chromatography (GC) where they are co-eluted with the standard cold reference with a known mass.<sup>1</sup>

Most radiolabelled compounds are prepared with a no-carrier added method which means that no carrier  $^{19}\text{F}$ fluorine has been added in the generation of the radionuclide, meaning that no cold fluorine has been purposely added.<sup>17</sup> Even though levels of radioactivity produced by a cyclotron run can be very high, the concentration of  $^{18}\text{F}$ fluoride produced will still be lower than the concentration of the precursor used in the synthesis. Even high radioactivity of  $^{18}\text{F}$ fluorine will rarely exceed low micromolar concentration levels.<sup>31</sup>

### 1.1.2.1 Fluorination

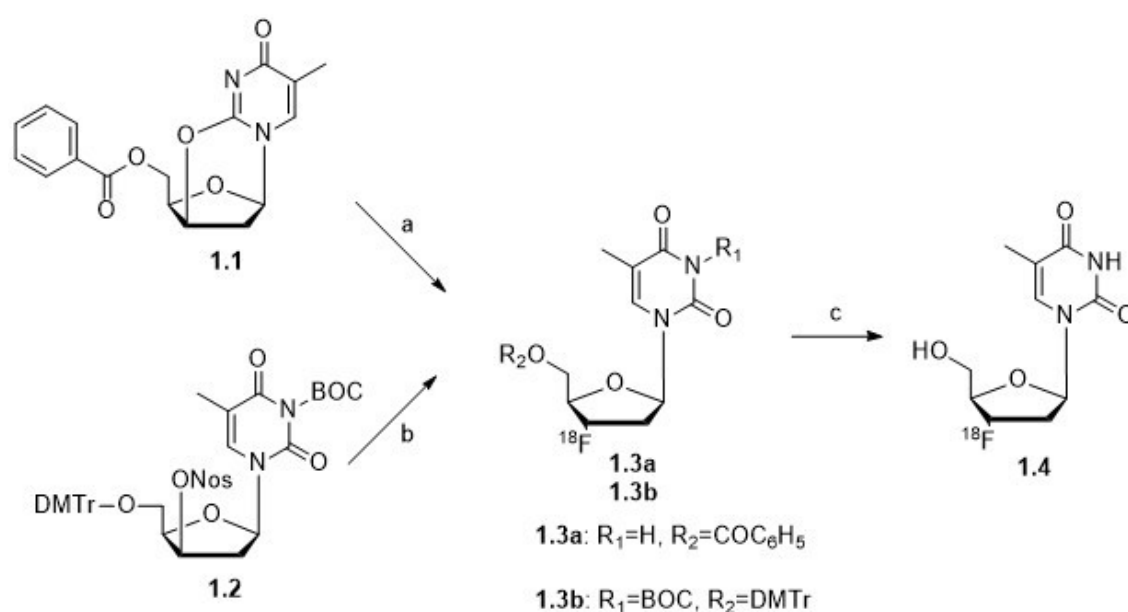
Fluorination reactions are harsh to perform in most cases, so when it comes to synthesise non-radioactive fluorinated molecules, it is usually preferable to start the synthesis with an already fluorinated building block whether possible. On the contrary, when dealing with  $^{18}\text{F}$ fluorine, it is very important to perform the fluorination at a late stage of the multi-step synthesis because of the short half-life of the radioisotope.

In recent years many studies have been carried out to optimise late stage fluorination showing better conditions to enable this step efficiently and rapidly.<sup>1,6,7,18</sup>

### Nucleophilic Fluorination

Nucleophilic fluorinations are the most common kind of [<sup>18</sup>F]-fluorinations (hot fluorination) in use today. The nucleophilic [<sup>18</sup>F]fluoride is produced by the nuclear reaction on enriched water [<sup>18</sup>O]H<sub>2</sub>O through bombardment of protons. The [<sup>18</sup>F]fluoride anion produced is a very weak nucleophile and a strategy has been developed to increase its nucleophilicity. It is first dehydrated through a ion exchange cartridge, and then activated by crown ethers such as Kryptofix K[222] and potassium carbonate.<sup>6,7</sup> Aliphatic nucleophilic fluorinations normally occur with an S<sub>N</sub>2 stereochemistry. Good leaving groups should be used for the precursors and aprotic solvents are suggested because of the low reactivity of the fluoride.<sup>6,32</sup> In Figure 1.7 two synthetic approaches towards [<sup>18</sup>F]FLT, the first in-human approved [<sup>18</sup>F]-labelled nucleoside as a tumour proliferation biomarker, are shown. The two precursors (**1.1** and **1.2**) need to be deprotected to give [<sup>18</sup>F]FLT (**1.4**) after the fluorination step.<sup>33,34</sup>

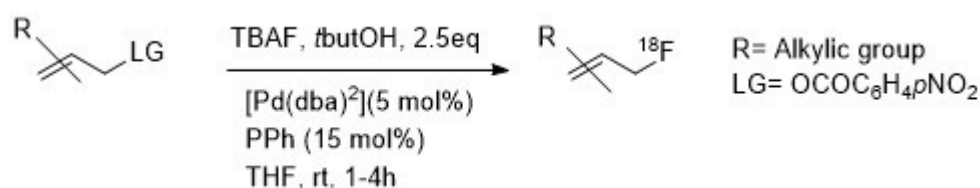
Figure 1.7: Synthesis of [<sup>18</sup>F]FLT via two approaches<sup>34</sup>



**Reagents and conditions:** a) K/(K222)<sup>18</sup>F, anh. DMSO, 160°C, 10min; b) K/(K222)<sup>18</sup>F, anh. CH<sub>3</sub>CN, 135°C, 5min; c) 1N NaOH, 55°C, 10 min or 1N HCl, 105°C, 5 m.

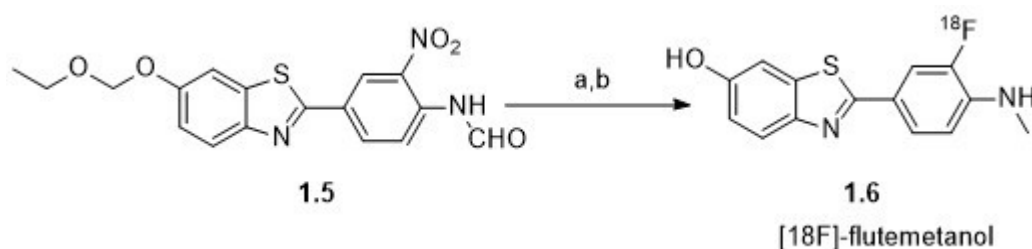
Recently many studies have been carried out to look for improved methods and substrates for these  $[^{18}\text{F}]$ -nucleophilic reactions. Modern organic chemistry technology has been applied to radiochemistry and an example of the results obtained by this combination is the use of a metal-catalyst for allylic fluorination reactions (Figure 1.8).<sup>35,34</sup>

**Figure 1.8: Metal catalysed allylic fluorination reaction**



Nucleophilic aromatic fluorination is more challenging than aliphatic fluorination, and is often used in PET radiochemistry for the synthesis of radiolabelled arenes. Harsh conditions such as high reaction temperature and activated substrates with electron withdrawing groups on the aromatic moieties in the *ortho* or *para* positions relative to the position of fluorination are required. This becomes necessary to overcome the normally disfavoured  $\text{S}_{\text{N}}\text{Ar}$  reaction. When there are electron rich groups on the aromatic ring, a strategy has been developed to circumvent this issue. The electron-donating group is masked as an electron withdrawing one using appropriate protecting groups. An example of this strategy is the synthesis of  $[^{18}\text{F}]$ flutemetamol (**1.6**), a PET imaging agent of the brain used as diagnostic tool for Alzheimer's disease (Figure 1.9).<sup>36,1</sup>

**Figure 1.9: Synthesis of the  $[^{18}\text{F}]$ flutemetamol**

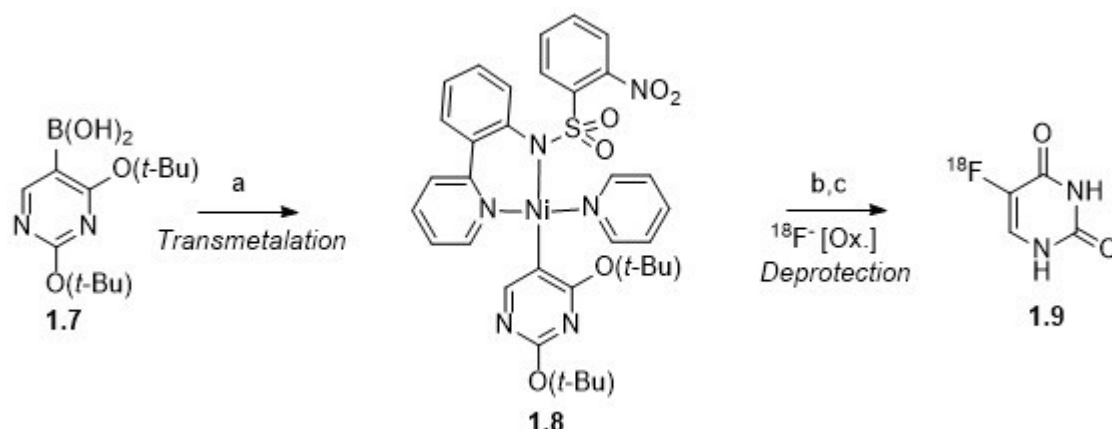


**Reagents and conditions:** a)  $\text{K} / (\text{K222})^{18}\text{F}$ , anh. DMSO,  $150^\circ\text{C}$ , 30min; b) 1N HCl,  $105^\circ\text{C}$ , 5 min.

The radiolabeling of an ortho-nitroaniline was thus enabled by masking the amine group as a formamide group. Therefore the displacement by [ $^{18}\text{F}$ ]fluoride of the nitro group becomes possible.

Often [ $^{18}\text{F}$ ]fluoride is introduced into the aromatic moiety thanks to the use of arylidonium salts, to generate an extremely effective leaving group.<sup>7,37,38</sup> Recently to improve the outcome of these types of fluorination, a number of transition metal catalysed nucleophilic fluorinations have been developed. One of these uses pre-catalysts such as nickel  $\sigma$ -aryl complexes to access [ $^{18}\text{F}$ ]fluorouracil (**1.9**), a PET tracer for cancer imaging (Figure 1.10). This is the first time that a transition-metal-mediated fluorination has been used for clinical application.<sup>34,39</sup>

**Figure 1.10: Synthesis of [ $^{18}\text{F}$ ]fluorouracil (**1.9**) via transition-metal-mediated fluorination<sup>34,39</sup>**



**Reagents and conditions:** a)  $\text{LnNi}^{\text{II}}\text{X}_2$ , pyridine,  $70^\circ\text{C}$ , 1h; b)  $\text{PhI}(4\text{-OMe-pyridine})_2(\text{OTf})_2$ ,  $(18\text{-c-6})\text{K}^{18}\text{F}$ ,  $\text{CH}_3\text{CN}$  (0.5%  $\text{H}_2\text{O}$ ),  $23^\circ\text{C}$ , 1 min; c)  $\text{HCl}$ ,  $\text{EtOH}$ ,  $23^\circ\text{C}$ , 2 min.

### Electrophilic Fluorination

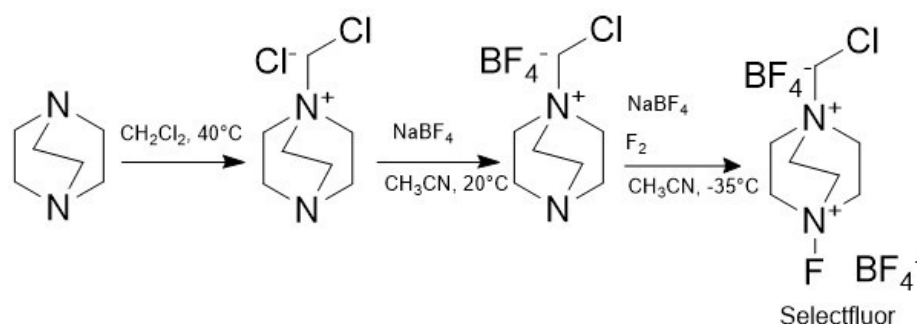
Electrophilic fluorination reactions were commonly used for the preparation of radiopharmaceuticals but they have been mostly replaced nowadays by nucleophilic reactions where possible. Aromatic rings and/or electron rich-double bonds can be readily fluorinated using electrophilic-fluorinating agents.<sup>40</sup> The reason for avoidance of electrophilic fluorination is due to the high reactivity and toxicity of the hazardous fluorine gas ( $[\text{F}_2]$ ), the simplest fluorinated reagent, generated by the nuclear

reaction  $^{20}\text{Ne}(d,\alpha)^{18}\text{F}$ . This kind of reaction is characterized by a low chemical and radiochemical yield and a poor selectivity.

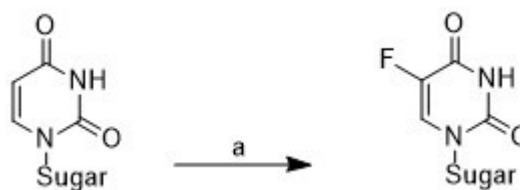
Another method used to produce the fluorine gas ( $[^{18}\text{F}]\text{F}_2$ ) is the bombardment of oxygen-18 ( $^{18}\text{O}(p,n)^{18}\text{F}$ ) and a carrier fluorine gas. Also in this case the specificity and the yields are very low because of the carrier-added production but mostly because of the necessity to isolate by purification the desired radiolabelled compound which can be a difficult procedure.<sup>41,7</sup> To increase both the yields and the selectivity of electrophilic fluorination, several intermediate electrophilic reagents have been produced. Among them  $[^{18}\text{F}]\text{XeF}_2$  and  $[^{18}\text{F}]\text{AcOF}$  are common even though they can never reach a radiochemical yield greater than 50%.<sup>1</sup>

Since most applications preclude the use of fluorine gas, fluorine must bind to an electronegative atom such as nitrogen, activated by a strongly withdrawing group such as the sulfonyl group. An example of a convenient relatively non-toxic electrophilic fluorinated reagent is Selectfluor<sup>®</sup>. It is synthesized using an anion exchange, diazabicyclo[2.2.2]octane, which is chloromethylated, followed by a fluorination with  $\text{F}_2$  or  $[^{18}\text{F}]\text{F}_2$  to furnish the bis(tetrafluoroborate) compounds and the  $[^{18}\text{F}]$  (Figure 1.11). Bis(tetrafluoroborate) salts have been used for the preparation of several fluoroaromatic compounds and have proved to be more selective than  $[^{18}\text{F}]\text{F}_2$ .<sup>42</sup>

**Figure 1.11: Synthesis of the fluorinating agent Selectfluor**



$[^{18}\text{F}]\text{Selectfluor}$  can be used in cases where fluorination of sugar moieties bearing an electron-rich double bond is also required. Besides its application in PET chemistry, Selectfluor is also used for non-radioactive electrophilic fluorinations (Figure 1.12)<sup>42</sup>.

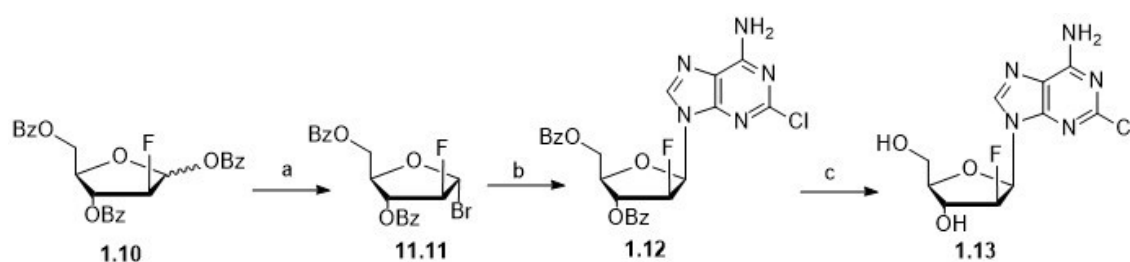
**Figure 1.12: Electrophilic fluorination with Selectfluor**

**Reagents and conditions:** a) Selectfluor, HOAc-H<sub>2</sub>O.

Another electrophilic fluorination agent that has been recently synthesized is the [<sup>18</sup>F]fluoride-derived palladium (IV). This is the first electrophilic agent derived directly from [<sup>18</sup>F]fluoride. Its use has been limited because it involves a two-step sequence reaction and because of the potentially sensitive organometallic reagents.<sup>42</sup>

### ***Other synthetic strategies to access fluorinated molecules***

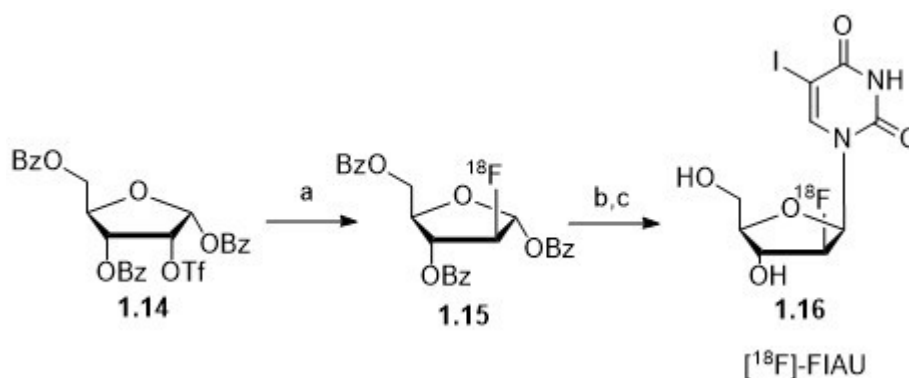
When later-stage fluorination is either not possible or convenient, other synthetic approaches involve the use of already fluorinated building blocks or, in the case of PET chemistry, the early fluorination of a moiety of the molecule. N-glycosylation reaction is for instance used to access some fluorinated nucleosides. It consists of the reaction between already fluorinated nucleobases and sugar moieties. This is considered a convergent approach and is particularly used to access 2'-β-fluoro nucleosides. The fully protected sugar is first brominated to form the 1-α-glycosyl bromide. The β-nucleoside is usually the most favoured product of this reaction as reported in the synthesis of the antineoplastic agent Clofarabine (**1.13**)(Figure 1.13).<sup>43,34</sup>

**Figure 1.13: Synthesis of Clofarabine (1.13)**

**Reagents and conditions:** a) HBr, AcOH, rt; b) 2-chloroadenine, KO<sup>t</sup>-Bu, CH<sub>3</sub>CN, t-AmOH, DCE, 55°C; c) cat. NaOCH<sub>3</sub>, CH<sub>3</sub>OH, rt.

As mentioned before, this synthetic approach is used also in PET chemistry to access a number of [ $^{18}\text{F}$ ]- $\beta$  nucleosides. [ $^{18}\text{F}$ ]FAIU (**1.16**), a reporter gene for the expression of the herpes simplex virus type-1 thymidine kinase (HSV1-tk), is for instance synthesised using the same synthetic convergent approach (Figure **1.14**).<sup>44,45</sup> Schinazi *et al* have recently reviewed synthetic strategies for the convergent approach.<sup>46</sup>

**Figure 1.14: Synthesis of [ $^{18}\text{F}$ ]FAIU (**1.16**)**

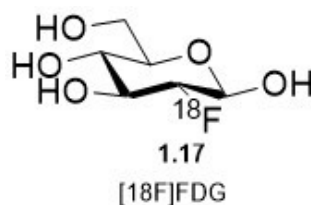


**Reagents and conditions:** a)  $\text{K}/(\text{K}222)^{18}\text{F}$ , anh.  $\text{CH}_3\text{CN}$ ,  $80^\circ\text{C}$ , 30 min; b) 5-iodouridine, HMDS, TMSOTf, anh.  $\text{CH}_3\text{CN}$ ,  $80^\circ\text{C}$ , 1h; c)  $\text{KOCH}_3$ ,  $\text{CH}_3\text{OH}$ ,  $80^\circ\text{C}$ , 10 min.

### 1.1.2.2 [ $^{18}\text{F}$ ]FDG

[ $^{18}\text{F}$ ]FDG (2-[ $^{18}\text{F}$ ]fluoro-2-deoxy-D-glucose) (**1.17**) is the most widely used PET tracer, being used in perhaps as many as 90% of all PET oncology scans.

**Figure 1.15: Structure of the most widely used PET tracer [ $^{18}\text{F}$ ]FDG**



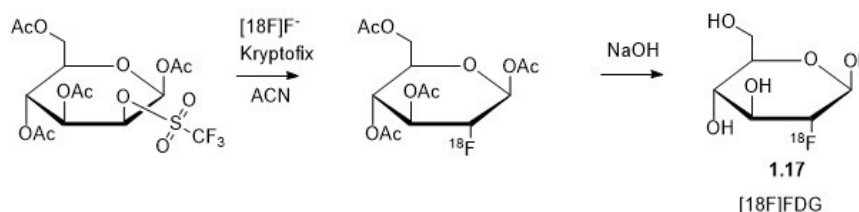
Glucose is a major source of energy for different biological systems. It is first transported by membrane transporters (GLUT) into cells and through the BBB (blood brain barrier). Glucose is there phosphorylated by a hexokinase using ATP as a source of phosphate. [ $^{18}\text{F}$ ]FDG is transported inside the cells with high metabolic activity by

the same transporter as for glucose and it is phosphorylated by the same kinase. But, unlike glucose, it is not metabolized by the glucose-6-phosphate isomerase and it stays entrapped into the cells. Once  $[^{18}\text{F}]$  decays into  $[^{18}\text{O}]$ , the resulting 2- $[^{18}\text{O}]$ -deoxyglucose-6-phosphate is metabolized while the  $[^{18}\text{F}]\text{FDG}$  is excreted.<sup>47</sup>  $[^{18}\text{F}]\text{FDG}$  has many applications in different areas such as oncology, neurology, and cardiology.<sup>48</sup> It can be synthesized using both electrophilic and nucleophilic substitution reactions.

The electrophilic substitution can be performed using either  $[^{18}\text{F}]\text{F}_2$  or  $[^{18}\text{F}]\text{acetyl hypofluorite}$  as the source of  $[^{18}\text{F}]$ -fluorine. The hypofluorite gives better yields than  $[^{18}\text{F}]\text{F}_2$ . The precursor molecule used is 3,4,6-tri-O-acetyl-D-glucan.<sup>49</sup> Another approach for electrophilic substitution used for production of  $[^{18}\text{F}]\text{FDG}$  uses  $[^{18}\text{F}]\text{XeF}_2$  as the source of electrophilic fluoride.<sup>50</sup> Unfortunately none of these methods give very good yields so radiochemical facilities have abandoned them in favour of nucleophilic substitutions.

Nucleophilic reactions can be performed using  $\text{Cs}[^{18}\text{F}]$ ,  $\text{Et}_4\text{N}[^{18}\text{F}]$ , or  $\text{KH}[\text{F}]\text{F}_2$  as source, however  $^{18}\text{F}^-$  in Kryptofix is the most commonly used for everyday routine synthesis, using 1,3,4,6-tetra-O-acetyl-2-O-triflate- $\beta$ -D-mannose as the precursor molecule. Since the first time this synthesis was published, in 1986<sup>51</sup>, several improvements have been made and different modular systems have been used. Taking into account the radioactive decay, radiochemical yields can be even higher than 60 % and the total reaction time can be even less than 26 minutes.<sup>52</sup> Figure 1.16 shows the method mostly used for clinic production of  $[^{18}\text{F}]\text{FDG}$ .

**Figure 1.16: Routine clinical synthesis of the radiotracer  $[^{18}\text{F}]\text{FDG}$**



### 1.1.2.3 $[^{18}\text{F}]$ -nucleosides

#### **$[^{18}\text{F}]\text{fluorouracil}$ (5- $[^{18}\text{F}]\text{FU}$ ) (1.9)**

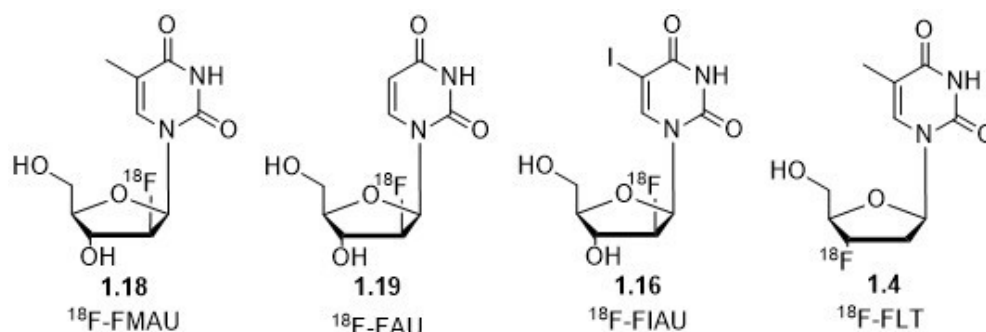
5-FU is a chemotherapeutic agent used in the treatment of solid tumours such as breast and colon cancer, however because of its *in vivo* rapid catabolism, its use for

therapeutic purposes is limited.<sup>53</sup> 5-[<sup>18</sup>F]FU (**1.9**) was synthesized to study the behaviour of 5-FU *in vivo* and 5-ethyluracil, an analogue of 5-FU, was used to block the catabolism of 5-[<sup>18</sup>F]FU. Through this experiment, it was possible to monitor the transport of 5-FU *in vivo* and its anabolism. The study showed very useful information to predict the response of the tumour to 5-FU. However 5-FU is not routinely used for PET imaging because of its rapid catabolism.<sup>10</sup>

### **[<sup>18</sup>F]-analogues of pyrimidine nucleosides**

Several pyrimidine nucleoside analogues were radiolabelled with [<sup>18</sup>F]fluorine for PET research or diagnosis purposes. The most important are [<sup>18</sup>F]FAU (**1.19**), [<sup>18</sup>F]FIAU (**1.16**), [<sup>18</sup>F]FMAU (**1.18**), [<sup>18</sup>F]FFAU, [<sup>18</sup>F]FEAU, [<sup>18</sup>F]FBAU, [<sup>18</sup>F]FCAU and [<sup>18</sup>F]FLT (**1.4**) (Figure 1.17).<sup>54</sup>

**Figure 1.17: [<sup>18</sup>F] analogues: pyrimidine nucleosides**



Among them, the only one that has been well studied as a tumour proliferation marker for PET-imaging and also to understand the response to treatment in cancer patients is [<sup>18</sup>F]FLT (**1.4**).<sup>55</sup> [<sup>18</sup>F]FMAU (**1.18**) has seen limited use in humans but has been widely used in animal models to perform imaging of DNA synthesis. The other pyrimidine analogues [<sup>18</sup>F]FIAU, [<sup>18</sup>F]FFAU, [<sup>18</sup>F]FEAU, [<sup>18</sup>F]FBAU, [<sup>18</sup>F]FCAU, [<sup>18</sup>F]FFAU and also [<sup>18</sup>F]FMAU have also been used as markers for imaging of Herpes simplex virus type 1 thymidine kinase (HSV1-tk) gene expression.<sup>10</sup>

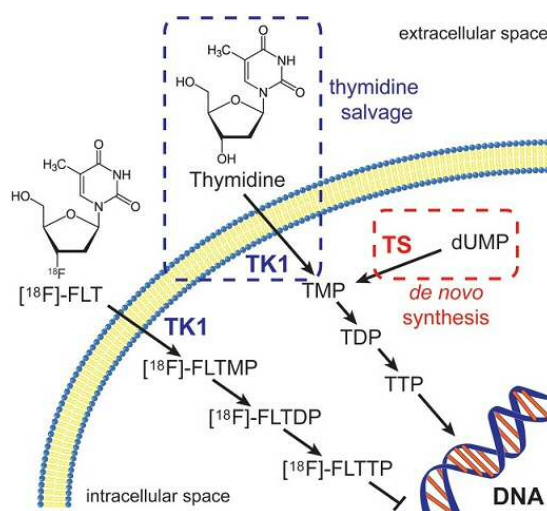
### **[<sup>18</sup>F]FLT**

[<sup>18</sup>F]FLT (**1.4**) is used as a tumour proliferation marker in PET imaging and sometimes to assess response to treatment in cancer patients. [<sup>18</sup>F]FLT has been

widely studied on different types of tumours and is currently the subject of ongoing clinical trials, having been widely investigated since 1998.<sup>10</sup> Indeed it represents a valid alternative to [18F]FDG when assessing tumours with high proliferation rates. Among different types of cancer, it has been used especially for lung, brain (glioma) and colorectal cancer.<sup>10</sup>

As it is an analogue of thymidine, [18F]FLT targets human thymidine kinase (TK1). It is thus phosphorylated into [18F]FLT monophosphate which is trapped into growing cells. The enzyme TK1 takes part in the synthesis of the DNA (deoxyribonucleic acid) and in particular shows a very high activity during the S phase, the synthesis phase of the cell cycle. [18F]FLT thus represents an indicator of cell proliferation rate when accumulated into the cell. Lately it has been shown that [18F]FLT reflects proliferative indices to potentially unreliable extents because it cannot discriminate among high proliferative index tumour, which relies on thymidine salvage pathway, from high proliferation tissues which instead rely especially upon the *de novo* synthesis of thymidine (Figure 1.18).<sup>56</sup>

**Figure 1.18: Thymidine salvage and *de novo* synthesis pathways**<sup>56</sup>

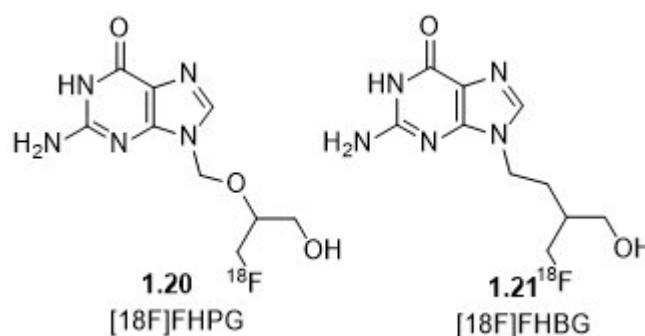


### **[18F]-purine analogue: acycloguanosine**

The first radiolabelled purine analogue nucleoside synthesized was [18F]FHPG (**1.20**).<sup>57</sup> After that, the PCV analogue [18F]FHBG (**1.21**) was developed and has been

widely studied in animal models for a mutated HSV1-tk gene, the sr39-HSV1-tk (Figure 1.19).

**Figure 1.19: Structures of some purine nucleoside analogues**

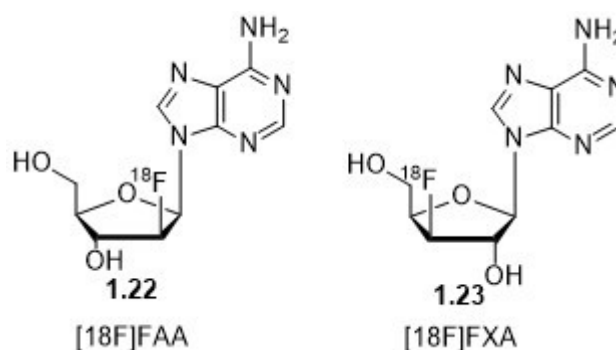


Many imaging studies on the HSV1-tk gene expression have been carried out, but until now just a few clinical studies using [18F]FHBG have been performed on humans.<sup>57</sup>

### **[18F]-purine adenosine analogues**

[18F]FAA (1.22) and [18F]FXA (1.23) (Figure 1.20) are two adenosine analogues that have been tested as substrates of HSV1-tk but their uptake was very low. Nevertheless, as their biodistribution was studied by micro-PET images, [18F]FAA showed a high uptake in tumour visualization, whereas [18F]FXA showed a high uptake in heart. These agents could thus represent respectively a new potential tumour imaging agent and a new potential heart imaging agent. Further studies need to be undertaken to confirm this prospect.<sup>58</sup>

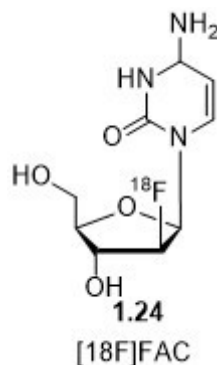
**Figure 1.20: Structures of some [18F]-purine adenosine analogues**



**[18F]FAC**

[18F]FAC (**1.24**) has been studied as a PET tracer for the metabolism of glial cells, being evaluated in rodent models of stroke, glioblastoma, and ischemia-hypoxia. Several studies suggest that it may be used for evaluation of glial cell metabolism associated with neuroinflammation.<sup>59</sup>

**Figure 1.21: Structure of [18F]FAC**

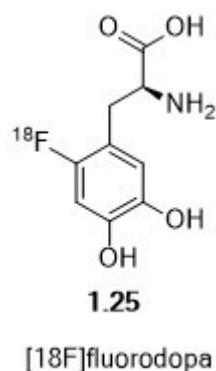


#### 1.1.2.4 Other [18F]-labelled PET probes

##### **[18F]fluorodopa**

[18F]fluorodopa (**1.25**) is a PET probe extensively used in Parkinson's disease to measure progression and the effects of treatments. In particular this agent is used in PET to verify the integrity of the area of the brain damaged by this disease, the nigrostriatal dopaminergic neurons.<sup>60</sup>

**Figure 1.22: Structure of the Parkinson's disease PET probe [18F]fluorodopa**



Other radionuclides are used in PET imaging and their biological applications vary according to their affinity to different classes of biomolecules. Detailed discussion

of further types [18F]-labelled PET tracers is beyond the scope of this introductory chapter.

### 1.1.3 Short lived radioisotopes

#### ***Carbon – 11***

Another commonly used radioisotope in PET imaging is [11C]carbon. The nuclear reaction most widely used for its production is  $^{14}\text{N}(p,\alpha)^{11}\text{C}$ . When this reaction happens in the presence of oxygen, the product is [11C]CO<sub>2</sub>, whereas [11C]CH<sub>4</sub> is obtained in the presence of hydrogen. These two radiolabelled compounds can be used as reagents for many other chemical reactions.<sup>61</sup>

[11C]CO<sub>2</sub> is used as intermediate to synthesise [11C]CH<sub>3</sub>I, the most widely used reagent to perform methylation of heteroatoms to obtain a large number of [11C]-tracers. [11C]CH<sub>3</sub>I can be produced by two methods known as wet or dry methods. The wet method uses a reducing agent such as LiAlH<sub>4</sub> to reduce [11C]CO<sub>2</sub>. This step is followed by an iodination step with HI to finally obtain the methylating reagent [11C]CH<sub>3</sub>I.<sup>60</sup> The dry method uses instead high temperature to perform iodination with I<sub>2</sub> using as a substrate [11C]CH<sub>4</sub>.<sup>16,62</sup> The 'dry or gas' method is nowadays the method of choice for the synthesis of [11C]CH<sub>3</sub>I because of the high SA of the radiolabelled product obtained.<sup>63</sup>

#### ***Nitrogen – 13***

Because of its very short half life (9.96 min), [13N]nitrogen has a limited application in PET chemistry and, together with [15O]oxygen and other short lived radioisotopes, is commonly used for perfusion studies. However, many attractive applications of [13N]-tracers have incentivised the development of many synthetic strategies for its incorporation into drug molecules. This is due to the fact that nitrogen is present in a large number of natural and synthetic molecules with biologically interesting activities.

[13N]nitrogen is normally incorporated into molecules using the reagent [13N]NH<sub>3</sub>. The radioisotope is commonly produced by the nuclear reaction  $^{16}\text{O}(p,\alpha)^{13}\text{N}$  using water as a target. A mixture of [13N]NO<sub>3</sub>, [13N]NO<sub>2</sub> and [13N]NH<sub>3</sub> are thus produced. By using DeVarda's alloy, nitrate and nitrite are reduced to ammonia.<sup>64</sup>

[<sup>13</sup>N]NH<sub>3</sub> is used in nucleophilic reactions using substrates such as acyl chloride derivatives, or for enzymatic aminoacids synthesis.<sup>65,13</sup> [<sup>13</sup>N]NH<sub>3</sub> has also been used to study blood flow and to measure perfusion in myocardium and brain. Under the form of [<sup>13</sup>N]N<sub>2</sub>, produced by the <sup>12</sup>C(d,n)<sup>13</sup>N nuclear reaction, it has been used for studies of nitrogen fixation and ventilation.<sup>66,67</sup>

### **Oxygen – 15**

The most challenging radioisotope in terms of time constraints is [<sup>15</sup>O]oxygen with its 2 mins radiochemical half-life. It is normally used just for simple reactions such as production of [<sup>15</sup>O]H<sub>2</sub>O and [<sup>15</sup>O]O<sub>2</sub> to study blood flow and monitor levels of oxygen.<sup>68</sup>

### **1.1.4 Long-lived radioisotopes: Positron emitting metals**

Long-lived radiometals such as [<sup>89</sup>Zr], [<sup>68</sup>Ga] and [<sup>64</sup>Cu] have been and still are commonly used for PET imaging studies.<sup>69–71</sup> Unlike short-lived radioisotopes, they are not incorporated into molecules directly but, thanks to coordination chemistry and click chemistry, they are attached to ligands which are then coupled to the biomolecules of interest such as antibodies.<sup>72,70</sup>

In the table below (Table 1.4) a summary of the most common PET tracers in clinical use and in clinical development is shown.

**Table 1.4: Common PET Tracers<sup>73</sup>**

TRACER	BIOLOGICAL TARGET
<b>Carbon 11</b>	
[ <sup>11</sup> C]methionine	Amino-acid transport
[ <sup>11</sup> C]leucine	Protein synthesis
[ <sup>11</sup> C]methyl- spiperone	Dopamine and serotonin receptors
[ <sup>11</sup> C]PK-11195	Peripheral benzodiazepine receptors
[ <sup>11</sup> C]diprenorphine	Non-selective opiate receptors
[ <sup>11</sup> C]carfentanil	μ-Opioid receptor
[ <sup>11</sup> C]flumazenil (FMZ)	Central benzodiazepine receptors

---

[11C]raclopride	Dopamine type 2 (D2) receptor
[11C]Schering-23390	Dopamine type 1 (D1) receptor
[11C]nomifensine	Dopamine transporter (DAT)
[11C]deprenyl	Monoamine oxidase type-B (MAO-B)
[11C]McNiel 5652	Serotonin transporter (SERT/5-HTT)
[11C]WAY 100635	Serotonin 5-HT1A receptor
[11C]FBL 457	Dopamine (D2/3) receptors
L-1-[11C]tyrosine	Brain tumor protein synthesis
[11C]MDL 100907	Serotonin 5-HT2A receptor
[11C] $\beta$ -CIT-FE	Dopamine transporter (DAT)
[11C]PMP	Acetylcholinesterase (ACE)
[11C]verapamil P-	glycoprotein (P-gp) substrate
[11C]MP4A	Acetylcholinesterase (ACE)
[11C]NNC112	Dopamine (D1) receptor
[11C] $\alpha$ -methyl-l-tryptophan	Tryptophan activity
[11C]DASB	Serotonin transporter (SERT/5-HTT)
[11C]Ro5-4513	GABA-benzodiazepine receptors
[11C]temozolomide	Temozolomide pharmacokinetics
[11C]PIB	$\beta$ -Amyloid
[11C]harmine	Monoamine oxidase type-A (MAO-A)
[11C]methylreboxetine (MRB)	Norepinephrine transporter (NET)
[11C]ABP688	Glutamate receptor 5 (mGluR5)
<b>Fluorine 18</b>	
[18F]FDG	Glucose utilisation
[18F]F-DOPA	Dopamine synthesis
[18F]A-85380	Nicotine acetylcholine receptors
[18F]fallypride	Dopamine (D2) receptor
[18F]SPA-RQ	Neurokinin-1 receptor
[18F]fluoroethyl-L-tyrosine	Brain tumour protein synthesis
[18F]fluorothymidine	Brain tumour proliferation
[18F]MK-9470	Cannabinoid receptor type 1 (CBR-1)
[18F]fluoromisonidazole	Brain tumour hypoxia

---

---

 Oxygen

[15O]oxygen

Oxygen utilisation

[15O]water

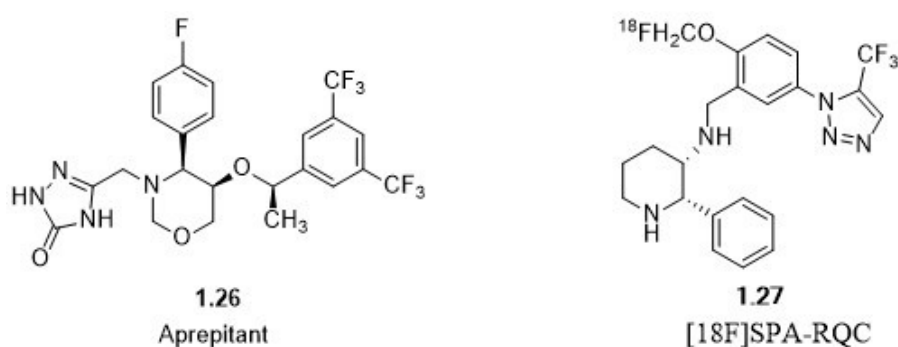
Blood flow

### 1.1.5 PET imaging: application in drug discovery

PET Imaging has been used not just as a diagnostic tool but more recently as a means to answer key questions in drug discovery on biological and pharmacological behaviour of certain compounds *in vivo*. Matthews and co-workers have recently reviewed this area of study.<sup>74</sup> By radiolabelling certain drug candidates, it is possible to gain useful information on their biodistribution *in vivo* such as whether or not they reach the target tissue primarily in rodents and primates, and secondarily in humans. This technique is also useful to understand whether some compounds can cause side effects by accumulating at non-target sites and additionally biodistribution studies can give information on dose-limiting toxicity. These kinds of studies can also give the possibility, through PET scans, to have data on pharmacokinetics and pharmacodynamics of drug candidates by comparing radio-TLC and radio-HPLC of the parent compound to the metabolism products.<sup>1</sup>

PET imaging can also give knowledge of receptor occupancy. Bergstrom *et al.* have studied in particular the substance P (NK1) antagonist Aprepitant (**1.26**). This agent was evaluated as an antidepressant and for chemotherapy-induced nausea. They used [<sup>18</sup>F]SPA-RQC (**1.27**), a selective radiomarker of NK1, to understand the minimal dose necessary to have the required anti-emetic effects<sup>75</sup> (Figure 1.23).

Figure 1.23: Aprepitant (1.26) and a radiomarker of NK1(1.27)

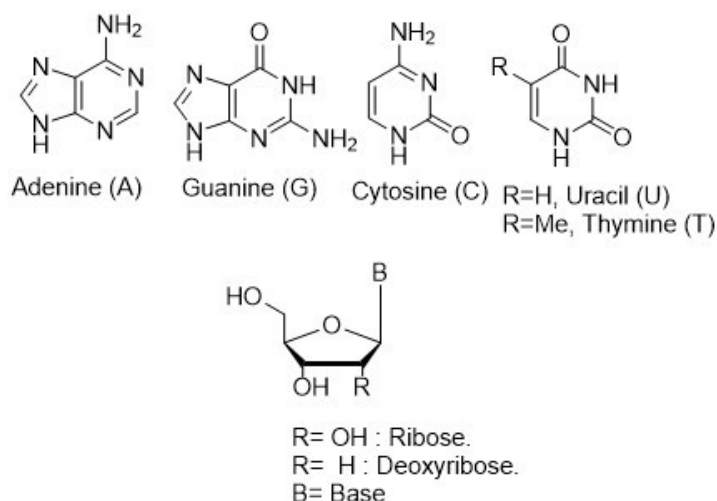


Bergstrom *et al.* understood that 100 mg/day was an effective dose for its antiemetic purpose but that this dose was not effective as an antidepressant. Indeed Merck was evaluating Aprepitant's application as an anti-depressive in Phase III clinical trial where the dose of 300 mg/day was still a not effective dose to have the anti-depressive effect. The PET studies, which demonstrated that that dose was definitely enough to achieve the occupancy of the target receptor, saved Merck several million dollars through interruption of the ongoing Phase III clinical trial on this compound.<sup>1</sup>

## 1.2 Nucleosides

Nucleosides are endogenous compounds critically involved in DNA and RNA synthesis but also in enzyme regulation, metabolism and cell signaling.<sup>76,77</sup> Several nucleoside and nucleotide analogues have been synthesized to act as antimetabolites of their physiological counterparts in several biochemical pathways. They inhibit viral replication and cellular metabolism by incorporation into DNA and RNA and thus they represent cornerstones in the treatment of patients with cancer and viral infections. Nucleosides can inhibit several essential enzymes like kinase, pyrimidine and purine nucleoside phosphorylase, several viral and human polymerases, DNA methyl transferase, thymidylate synthase, and ribonucleotidreductase. Chemically they consist of a purine or pyrimidine nucleobase, which is linked to a sugar moiety<sup>78</sup> (Figure 1.24).

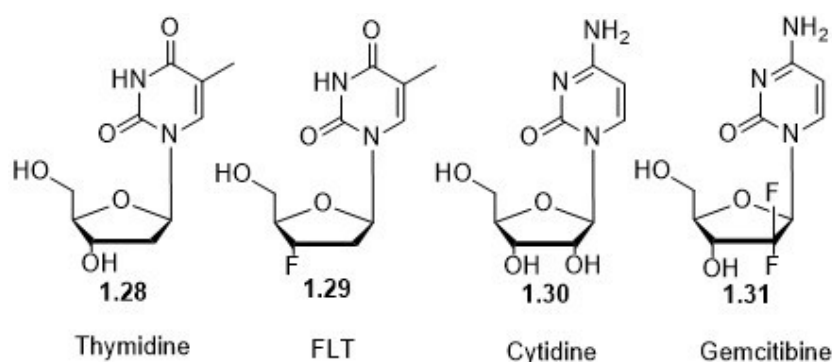
**Figure 1.24: Structures of ribose and 2'deoxyribose nucleosides**



When nucleosides have a phosphate group in the 5' position of the sugar moiety they are named nucleotides. Their activity depends on certain modifications on the nucleobase that gives them different specific properties. Nucleosides can act as antimetabolites, where the metabolic pathway of these synthetic nucleosides and nucleotides is the same one of their endogenous counterparts.<sup>79</sup> After cellular uptake performed by nucleoside-transporter systems, NAs become substrates for specific nucleo(s)tide kinase enzymes which convert them to the 5'-mono, -di and triphosphate forms.<sup>26</sup> The active triphosphate form can interfere with the *de novo* synthesis of DNA/RNA precursors, leading to the inhibition of DNA and RNA synthesis and to suppression of cell growth and division.<sup>26</sup>

The first phosphorylation is the rate-limiting phosphorylation step of their activation pathway. Thymidine kinase (TK1) or deoxycytidine kinase (dCK) can carry out this phosphorylation according to the substrate. For instance, TK1 is specific for thymidine (**1.28**) and its analogues, while dCK is specific for cytidine (**1.30**) and its analogues (e.g. gemcitabine **1.31**).

**Figure 1.25: Thymidine and cytidine and their analogues**

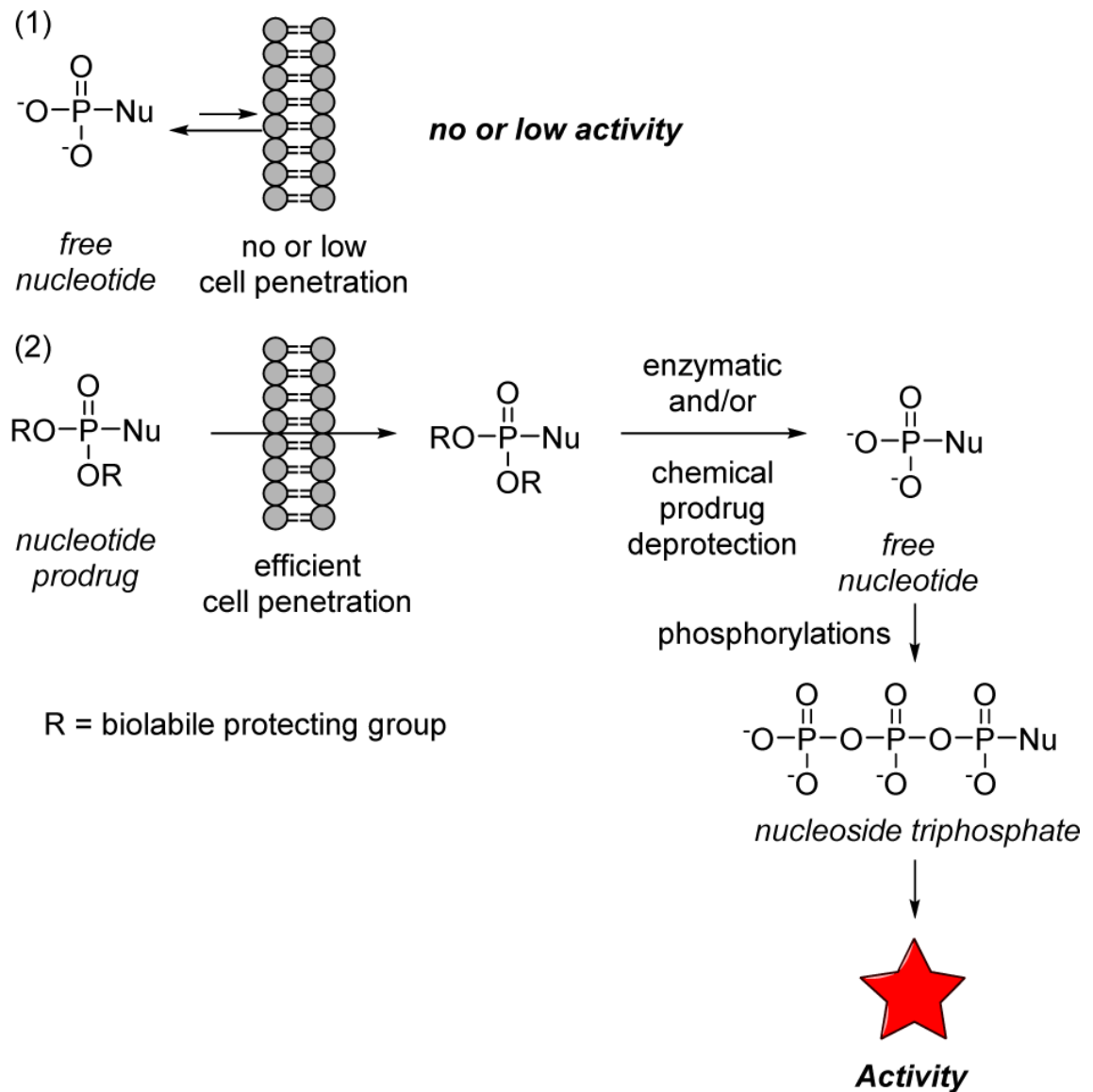


When nucleosides are monophosphorylated, they are effectively entrapped inside the cellular cytoplasm as charged nucleotides. Nucleosides are hydrophilic molecules that diffuse slowly across cell membranes, therefore cells have developed a complex transport system to facilitate membrane transport. This system consists of multiple carrier proteins, the nucleoside transporters (NTs), which facilitate their cellular uptake for nucleotide biosynthesis. The monophosphorylated nucleosides are therefore further phosphorylated by other kinases to form the diphosphates and the triphosphates which finally take part in the biosynthesis of DNA and RNA.<sup>80</sup>

### 1.2.1 ProTides

Despite the enormous importance of nucleoside analogues as both antiviral and anticancer agents, drug resistance still represents a major issue for their clinical application. As already described above, to exert their therapeutic activity, nucleoside analogues need to be phosphorylated by intracellular kinases to the 5'-mono-, di- and triphosphate forms. Many synthetic strategies have been developed to access directly the active 5'-triphosphate form, but these compounds are not viable drug candidates because of their chemical instability and high polarity which disallow their effective crossing through cell membranes. Nevertheless, the first phosphorylation is considered to be rate-limiting step of their activation pathway, therefore many approaches to develop prodrugs of nucleoside monophosphate forms have been developed.<sup>81</sup>

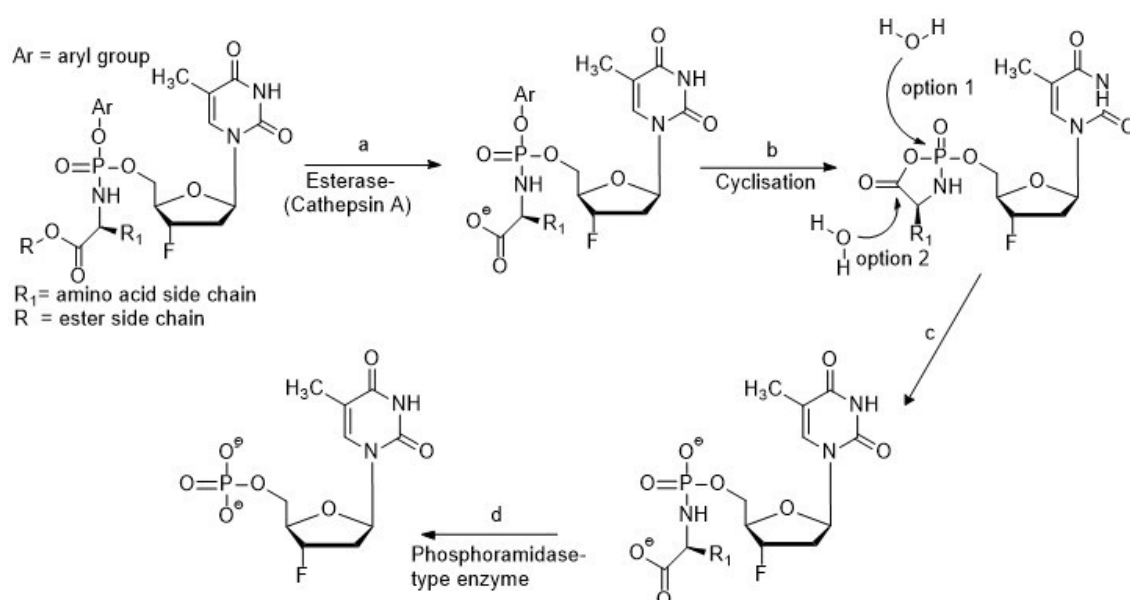
The phosphoramidate-based technology, also known as the ProTide (PronucleoTide) approach, developed by McGuigan and co-workers in 1995 is considered one of the most effective pro-nucleotide strategies currently used in the clinic.<sup>82,83</sup> It consists in masking the negatively charged 5'-O-monophosphate form as a phosphoramidate. This masked derivative, after passive diffusion through cell membrane and subsequent intracellular metabolism, delivers the 5'-O-monophosphate form<sup>84</sup> which is thus trapped into the cell and available for further phosphorylations (Figure **1.26**).<sup>82,83</sup>

Figure 1.26: Pro-nucleotides mechanism of action<sup>81</sup>

Chemically ProTides are aryloxyphosphoramidate prodrugs synthesized through a coupling reaction between a phosphorochloridate and the 5'-OH of the nucleoside. The phosphorus atom is attached to an amino acid alkyl ester and to an aryloxy group enabling passive transmembrane transport and masking the negative charge.<sup>84,85</sup>

Figure 1.27 below shows a proposed activation pathway for this class of compounds that leads to the intracellular delivery of active nucleoside monophosphates. Once crossed the cell membrane the monophosphate is firstly deprotected by an esterase or cathepsin A producing the carboxylate intermediate. A spontaneous cyclization occurs forming a five-member ring and releasing a phenol or a naphthol. The cyclic intermediate then undergoes through chemical opening by water producing the phosphoramidate diester. The diester is finally cleaved by an intracellular phosphoramidase or by an histidine triad nucleotide-binding protein 1 (HINT-1) releasing the active nucleoside monophosphate.<sup>83</sup>

**Figure 1.27: Proposed activation pathway of Protides**



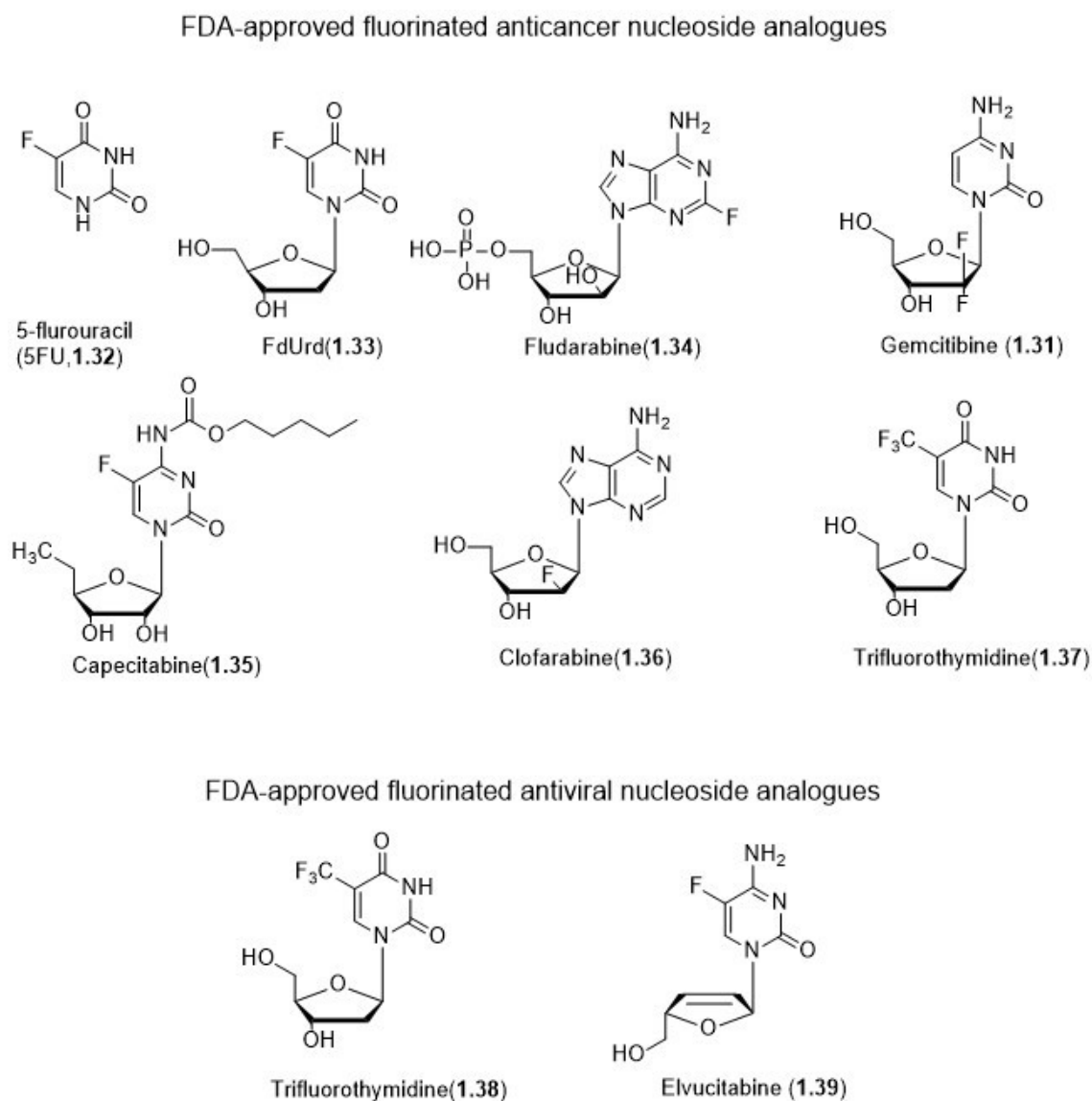
Other phosph(on)ate prodrugs strategies comprise the carbonyloxymethyl, including POM and POC groups, that have shown to increase oral bioavailability and systemic exposure when compared to the parent phosphonic acids. This class includes the FDA approved adefovir and tenofovir.

S-Acyl-2-thioethyl (SATE) is another pronucleotide strategy developed in 1990 where the phosphotriesters incorporate a thioethyl chain with the thiol masked as a thioester (Sate group). CycloSal phosphate and phosphonate prodrugs developed by Chris Meier, use instead salicylic alcohols to mask the NA- monophosphate form. It was

successfully applied to some antiviral nucleotides such as AZT, d4t and acyclovir. All these and other pronucleotide strategies have been recently reviewed by Scinazi *et al.*

### **1.2.2 Fluorinated nucleosides and ProTides**

An important class of antiviral and anticancer drugs is represented by fluorinated 2'- and 3'-substituted nucleosides where one or more hydrogens on the sugar moiety are substituted by fluorine atoms. Figure **1.28** shows all the FDA-approved fluorinated anticancer and antiviral nucleoside analogues.<sup>34</sup>

**Figure 1.28: FDA-approved fluorinated anticancer and antiviral nucleoside analogues.**

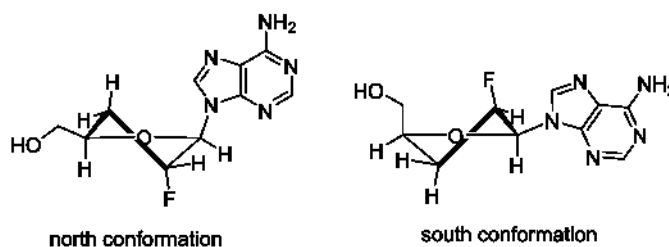
### 1.2.2.1 Importance of fluorine in drug molecules

Despite the widespread occurrence of fluorine as an element on earth, organofluorine compounds are almost absent in nature. Nevertheless, 20-25% of synthetic drugs are thought to contain in their structure at least one fluorine.<sup>86,87,34</sup> Fluorine plays a crucial role in the optimisation of clinical candidates. It increases the lipophilicity (logP) which is a major factor, together with the molecular size, that influences membrane permeability that can lead to an optimization of drug candidates' oral bioavailability. Modulation of pKa can also have a huge impact on compounds bioavailability as well as on their absorbance. Fluorine is the most

electronegative element (3.98 on the Pauling scale) and, when included into a molecule, can strongly affect the acidity or the basicity of the surrounding functional groups in the molecule.<sup>34,88,89</sup>

Additionally, when the fluorine is bonded to the carbon, the highly polarised bond formed can provide a remarkable stability to the molecule itself. All these factors can have a positive impact on selectivity, toxicity, potency, and on pharmacokinetic and pharmacodynamic properties of the molecule. The size of fluorine (van der Waals radius of 1.47Å) is also very similar to that of hydrogen (1.20 Å), therefore it is frequently used to replace the H or the hydroxyl group in drug molecules without causing steric perturbation. However, from the chemical point of view its replacement does not lead to dramatic changes whereas from the biological point of view it can block oxidative metabolism and therefore block the formation of unwanted metabolites. Drug molecules are indeed usually metabolised by enzymes such as Cytocrome P450 (CYP450) monooxygenases that decrease compounds lipophilicity and therefore increase their clearance. Fluorine substitution bypasses that problem by blocking these sites from enzymatic cleavage and, therefore, increases the metabolic stability of many drug molecules.<sup>34,88,89</sup>

Fluorine has a major impact on nucleosides and when placed on the ribose ring of nucleoside analogues, it can significantly affect the conformation of nucleosides. It causes changes in the dipole-dipole and gauche interactions, on the F-base interactions and influences the anomeric effect. Generally, when placed in the 2'- $\beta$ -position of the ribose, fluorine favours a south conformation of the molecule, which has often conferred to the molecule an enhanced anti-HIV activity, whereas the fluorine in the 2'- $\alpha$ -position favours a north conformation (Figure 1.29). Nevertheless, a general rule that correlates the position of the fluorine with the biological activity of the molecule is difficult to define. A research group working on pro-nucleotide CycloSal triesters of 2'-fluorinated-2',3'-dideoxyadenosines (F-ddA) studied the effects induced by two opposite  $\alpha$  and  $\beta$  configurations of the fluorine at C2' of the dideoxyribose moiety. They showed that 2'- $\beta$ -F-ddA is active as an anti-HIV agent, whereas the - $\alpha$  analogue did not show any antiviral activity. Interestingly, when the  $\alpha$ -configured phosphotriesters of the inactive 2'- $\alpha$ -F-ddA were tested, they showed a higher anti-HIV activity compared to 2'- $\beta$ -F-ddA (Figure 1.29).<sup>34,90</sup>

**Figure 1.29: North and south conformation of two anomers of F-ddA**

### ***Fluorinated anticancer nucleosides and ProTides***

Nowadays many fluorinated nucleosides are used in the clinic as anticancer and antiviral drugs. 5-fluorouracil (**1.32**) was one of the first to be approved by the FDA and, along with FdUrd (its nucleoside analogue)(**1.33**) is currently used for the treatment of patients with solid tumours such as gastric, breast, colon and pancreatic carcinoma (Table **1.5**). Both compounds are metabolised by FdUMP to the 5'-monophosphate form to exert their biological activity. FdUMP forms a complex together with thymidylate synthase (TS) and the reduced co-factor 5,10-methylenetetrahydrofolate (5,10-CH<sub>2</sub>-THF) which is the source of the methyl group. Herein the fluorine exerts an essential role in the metabolism of the molecule. As it is more tightly bound to carbon in the 5-position compared to the hydrogen in FdUMP, it prevents the  $\beta$ -elimination reaction and the consequent release of TS enzyme. The complex TS/FdUMP/mTHF causes the irreversible inhibition of enzymatic function. Therefore, the formation of TMP which is the building block for the DNA synthesis decreases.<sup>34,91,92</sup> Nevertheless, inherent and acquired resistance is commonly associated with the nucleoside analogue 5-FU (such as diminished cellular uptake, and a decreased activation to the 5'-monophosphate form by thymidine kinase or overexpression of TS). Many prodrugs of 5-FU and of other nucleosides have been developed and are currently in use in the clinic to address these key resistance mechanisms.<sup>93</sup>

The application of the ProTide strategy to FdUrd led to development of L-alanine-based 5'-ProTide NUC-3373 (**1.43**). Compared to its parent nucleoside, NUC-3373 showed cytostatic activity independently of thymidine kinase (TK) in TK-deficient cell lines.<sup>85</sup> Moreover, NUC-3373 is resistant to the degradation by catabolic enzymes

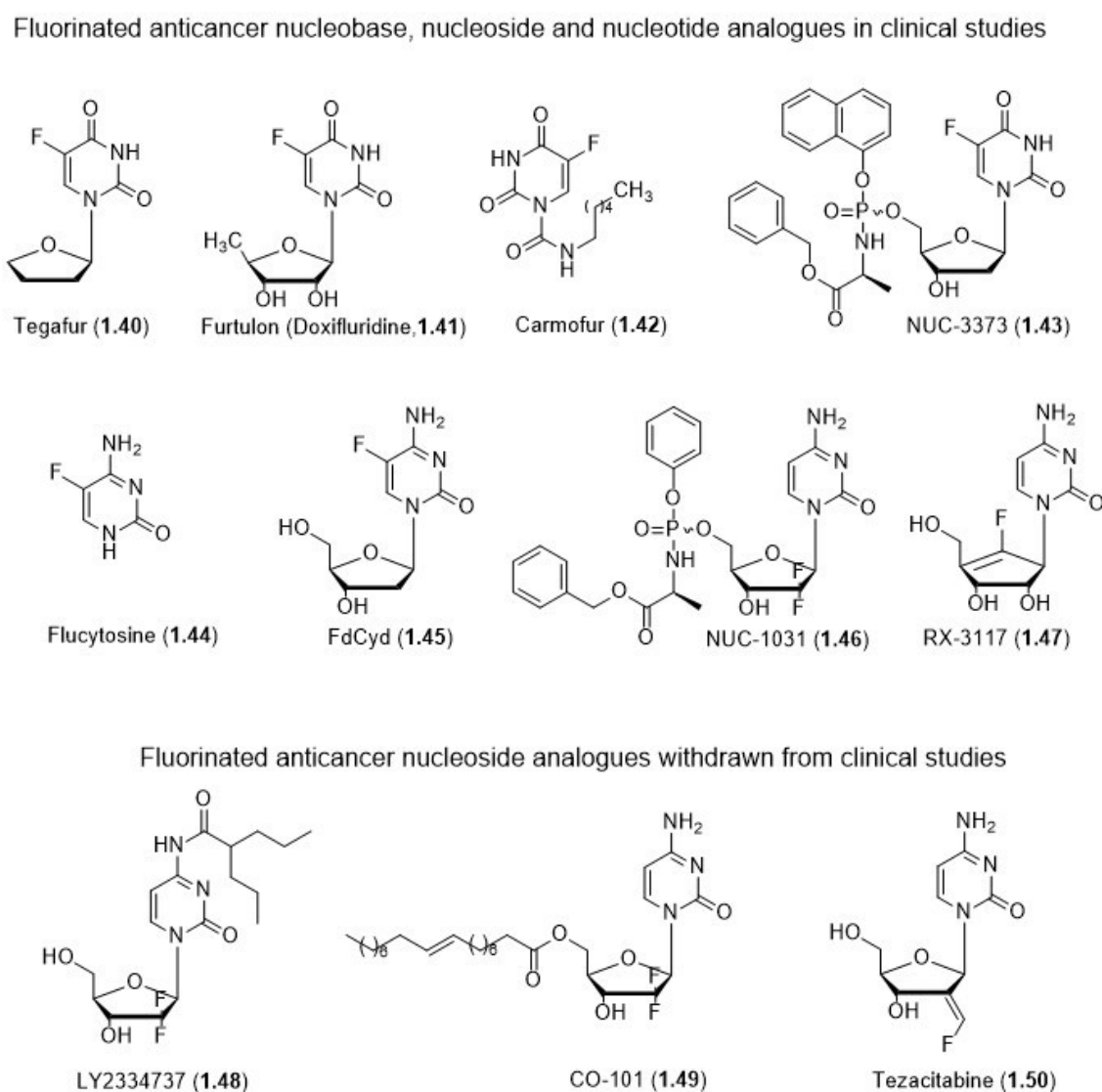
such as thymidine phosphorylase (TP), which is often upregulated in tumour cells, and dihydropyrimidine dehydrogenase (DPD), an enzyme overexpressed in the liver. In addition, within *in vitro* models, NUC-3373 generates up to 363-fold higher intracellular levels of FdUMP compared to 5-FU in the human colorectal cancer cell line HT29.<sup>94</sup> *In vivo* studies showed greater tumour volume reduction in the human colorectal cancer HT29 mouse xenograft model when NUC-3373 was tested compared to 5-FU.<sup>95</sup> A Phase I clinical study of NUC-3373 started in 2016 on patients with advanced solid tumours (Table 1.5).<sup>34,96</sup>

Another clinically widely used fluorinated anticancer agent is gemcitabine (2'-deoxy-2',2'-difluorocytidine, dFdC) (**1.31**) which has been approved for the treatment of pancreatic, non-small cell lung, ovarian and breast cancers.<sup>97,98</sup> Again its clinical effectiveness is reduced because of resistance mechanisms such as poor cellular uptake and poor conversion of gemcitabine into active metabolites by deoxycytidine kinases, plus rapid deamination by cytidine deaminase into the inactive and toxic by-product dFdU.<sup>99-101</sup> The triphosphate metabolite (dFdC-TP), which is the active form of dFdC, is thus incorporated into the growing DNA chain in the S-phase of cell cycle and therefore causes chain termination of DNA synthesis leading eventually to cell death. The diphosphate form (dFdC-DP) of dFdC also contributes significantly to its anticancer activity by inhibiting ribonucleotide reductase (RNR). As a result dFdC-TP is incorporated as a substrate for DNA polymerase instead of natural deoxynucleotides.<sup>34,102</sup>

To improve the clinical efficacy of gemcitabine many modifications have been applied to its original chemical structure. Novel gemcitabine-based prodrugs such as LY2334737 (**1.48**), CO-101 (**1.49**) and more interestingly the phosphoramidate NUC-1031 (**1.46**) have therefore been developed. NUC-1031 is a phosphoramidate L-alanine-based ProTide of gemcitabine designed to overcome the resistance mechanisms of the parent nucleoside. Its cellular uptake is indeed independent of nucleoside transporters compared to the parent lead. Once into the cell, it releases the 5'-monophosphate form via consecutive steps which are mediated by a carboxyesterase-type enzyme and phosphoramidase-type enzyme that catalyses the P-N bond cleavage.<sup>34,103</sup> Phase I clinical studies conducted in patients with advanced solid tumours in 2012 showed promising pharmacokinetics and a favourable safety profile

and efficacy. NUC-1031 demonstrated the ability to achieve 217x higher intracellular dFd-CTP levels compared to the parent compound. The plasma half-life of this ProTide was also much more favourable (7.3 h) than the one reported with gemcitabine (1.5 hours). In conclusion these studies indicated that NUC1031 was able to achieve a durable disease control in a high number of patients including the ones who were refractory to, or who relapsed on prior gemcitabine treatment. NUC-1031 is currently investigated in several clinical trials for the treatment of patients with ovarian, biliary and pancreatic cancers.<sup>104,34</sup> Figure 1.30 shows all anticancer fluorinated nucleobase, nucleoside and nucleotide analogues in clinical development.

**Figure 1.30: Fluorinated anticancer nucleobase, nucleoside and nucleotide analogues in clinical studies<sup>34</sup>**



### ***Purine-based anticancer fluorinated nucleoside analogues***

Fludarabine (FAMP) (**1.34**) is the 5'-monophosphate form of the purine nucleoside analogue 2'-fluoro-arabinofuranosyladenine used for the treatment of B-cell chronic lymphocytic leukaemia (B-CLL). It is also used in chemoimmunotherapy in combination with the monoclonal antibody rituximab and the DNA-alkylating agent cyclophosphamide, to treat CLL patients.<sup>34,105</sup> As it is a monophosphate, it is negatively charged at physiological pH, therefore is unable to enter cells. To reach the active 5'-triphosphate form (F-ara-ATP), it is therefore first dephosphorylated to F-ara-A, incorporated into the cell by nucleoside transport systems, and re-phosphorylated by deoxycytidine kinase to the original 5'-monophosphate form. Subsequently the adenylate kinase and nucleoside diphosphate kinase catalyse the phosphorylation to the 5'-di and 5'-triphosphate forms, respectively. F-ara-ATP thus inhibits DNA polymerases by acting as an alternative substrate to the natural deoxynucleotide (dATP).<sup>34,106,107</sup> Interestingly here the fluorine is essential as it increases the relative resistance of F-ara-A to the deamination performed by adenosine deaminase.<sup>34,107</sup> Nevertheless, some clinical trials of fludarabine showed severe central nervous toxicity, somnolence and an increase of liver enzyme levels. This is probably due to the phosphorolytic cleavage of F-ara-A which releases the metabolite 2-fluoroadenine (F-Ade) that can accumulate as the toxic triphosphate F-AdeTP. Many resistance mechanisms have been associated with the nucleoside analogue fludarabine. Mainly they are related to alterations in membrane nucleoside transporters, deoxycytidine kinase and cytoplasmic 5-nucleotidase cN-II activities, and to changes in the expression of miR-34a, a small non-coding RNA molecule which mediates post-transcriptional gene silencing.<sup>34,107,109</sup>

Clofarabine (Cl-F-ara-A)(**1.36**) is a second-generation chemotherapeutic agent similar in structure to fludarabine, which compared to fludarabine, shows resistance to phosphorolytic cleavage and deamination. Clofarabine is currently approved for clinical use in the treatment of relapsed and refractory paediatric acute lymphoblastic leukaemia. Clofarabine triphosphate is the active form of the nucleoside analogue and it exerts its anticancer activity by inhibition of ribonucleotidoreductase and inhibition of DNA synthesis after incorporation into the DNA chain thus inducing apoptosis.<sup>34,107,109</sup> The fluorine atom in clofarabine has also an essential role as it has

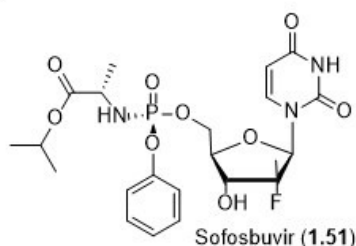
been postulated that, because of the electron-withdrawing properties, it modifies the reactivity of the 3'-OH group and the three-dimensional structure of DNA so that incorporation of other nucleotide analogues and extension of the DNA chain is inhibited.<sup>34,107,109</sup> The resistance mechanisms associated with the other nucleoside analogues have also been reported for clofarabine. However, recent studies showed that this agent, besides its anticancer activity, has also been reported to inhibit DNA polymerase activity of HIV-1 reverse transcriptase and to limit the dNTP substrates pool for the synthesis of viral DNA.<sup>34,110,111</sup>

### ***Antiviral fluorinated nucleosides and ProTides***

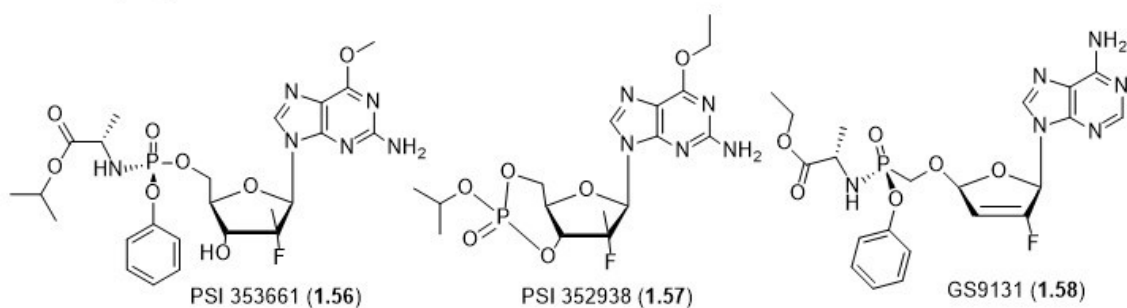
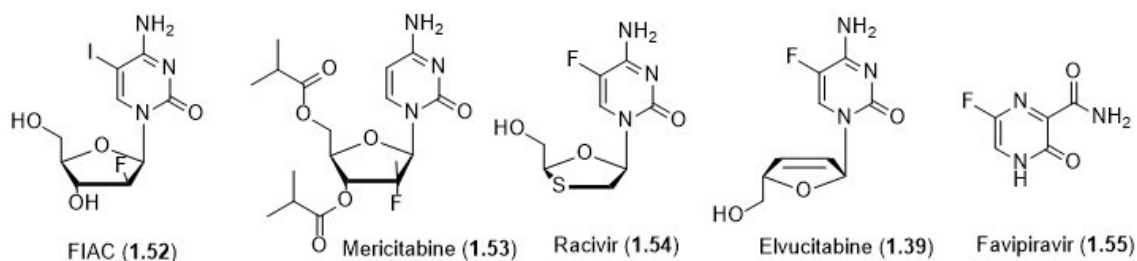
Nucleoside analogues also represent a significant class of antiviral therapeutic agents. They are currently used in the clinic for the treatment of hepatitis b virus (HBV), hepatitis c virus (HCV), human immunodeficiency virus (HIV), human respiratory syncytial virus (HRSV), human cytomegalovirus (HCMV), and Varicella zoster virus (VZV). Compared to the anticancer nucleoside analogues, they are chemically more diverse and they are characterised by a better tolerance profile due to low levels of activity on mammalian enzymes.<sup>34,110</sup> The active antiviral form is again the 5'-triphosphate nucleoside analogue. They are classified as nucleoside reverse transcriptase inhibitors (NRTis) including both compounds mimicking the endogenous natural nucleosides and those that need to be phosphorylated to their 5'-triphosphate form to be active. Their targets are the catalytic residues of the viral polymerase that interact with the template, the primer and the incoming nucleoside 5'-triphosphates. The introduction of fluorine in their chemical structure helped to improve their biological profiles and to provide an improved metabolic stability.<sup>110</sup> Figure **1.31** reports the fluorinated antiviral nucleoside analogues and derivatives available in the clinic as well as some that are currently undergoing clinical trials.<sup>34</sup>

**Figure 1.31: Fluorinated antiviral nucleoside analogues and derivatives in clinical trials<sup>34</sup>**

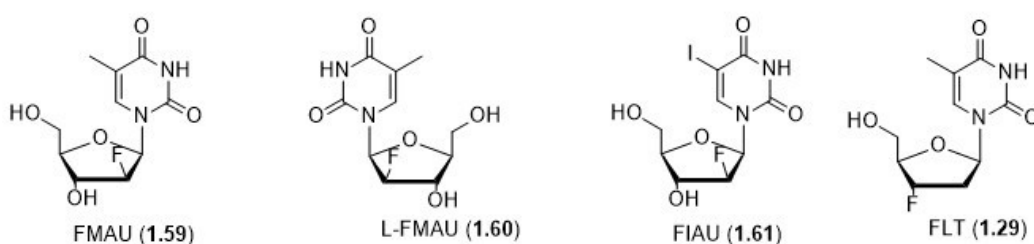
FDA-approved antiviral fluorinated nucleotide analogue



Fluorinated antiviral nucleoside and nucleotide analogues in clinical studies



Fluorinated antiviral nucleoside analogues withdrawn from clinical studies

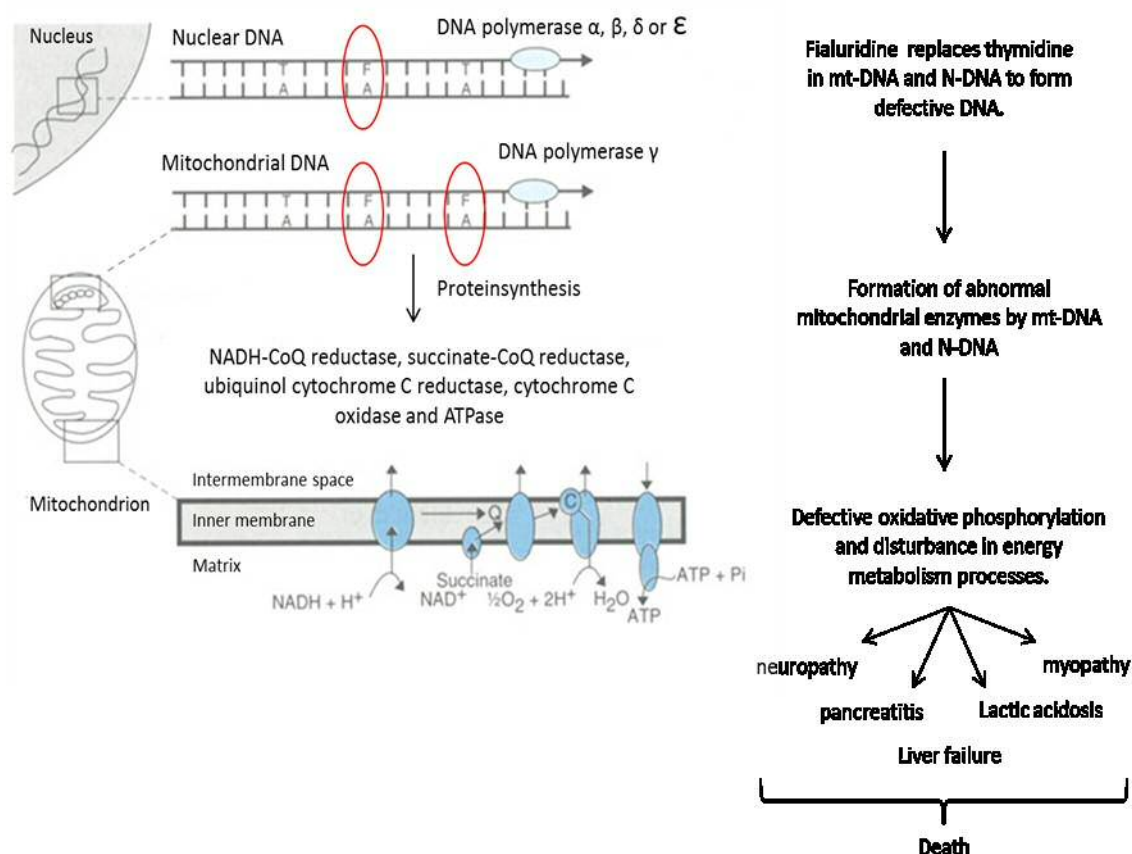


### ***Pyrimidine-based antiviral fluorinated nucleosides and prodrugs***

One of the first antiviral fluorinated nucleoside analogue synthesised in 1971 was the 3'-fluoro-3'-deoxythymidine (FLT)(**1.29**), known as Alovudine. Its anti-HIV activity was only discovered in 1988, when studies showed that this agent had a major potency when compared to the established anti-HIV agent azidothymidine (AZT).<sup>34,112</sup> *In vitro* studies proved that FLT inhibits replication of highly resistant nucleoside reverse transcriptase inhibitor (NRTI) HIV strains. However FLT did not

progress further in clinical trials because of dose-dependent safety concerns.<sup>113</sup> ProTides of FLT have also been synthesised and early *in vitro* studies showed potent inhibition of HIV-1 and HIV-2 replication, although they showed less potency when compared to the parent nucleoside therefore did not proceed to the clinical stage.<sup>34,114</sup> FIAU (Fialuridine) (**1.61**) was another 2'-F-nucleoside analogue that was selected as a Phase I clinical trial candidate for the treatment of HBV, but it showed mitochondrial toxicity resulting in lactic acidosis and hepatic failure (Figure 1.32).<sup>113</sup>

**Figure 1.32: Suggested mechanism by which FIAU causes widespread mitochondrial injury, and disturbance in metabolic processes**<sup>115</sup>



After its failure in a Phase II clinical trial in 1993, [<sup>18</sup>F]FIAU (**1.16**) has been used in PET imaging as a reporter-gene of HSV1-TK.<sup>116</sup> Emtricitabine (FTC) is an anti HIV agent included into the list of the essential medications compiled by the World Health Organization. Chemically emtricitabine is a 5-fluorodeoxycytidine derivative characterised by an oxathiolane ring as sugar. Its active triphosphate form acts by inhibiting the reverse transcriptase (NRTI). Compared to the antiviral agent Lamivudine, the presence of the fluorine atom boosts its bioavailability and its half-

life.<sup>117-119</sup> Mericitabine (RG-7128)(**1.53**) is another potent anti-HCV agent that has recently successfully completed Phase I and II clinical trials. Chemically mericitabine is a 3',5'-diisobutyrate prodrug of the well studied 2'-deoxy-2'-fluorocytidine (FdC).<sup>120</sup>

Sofosbuvir (Sovaldi<sup>®</sup>, GS7977)(**1.51**) is an anti-HCV phosphoramidate prodrug of  $\beta$ -D-2'-deoxy-2'- $\alpha$ -fluoro-2'- $\beta$ -C-methyluridine. It is an inhibitor of the NS5B RNA polymerase, a protein responsible for the synthesis of both positive and negative-strand genomic RNA. Sofosbuvir mimics the natural substrate of NS5B polymerase, is incorporated into the growing RNA strand and thus induces chain termination. It was initially synthesized and commercialised as a diastereoisomeric mixture (GS-9851), which comprised Sofosbuvir (GS-7977, S<sub>p</sub> isomer) and GS-491241 (R<sub>p</sub> isomer). Cathepsin A (CatA) and carboxyl esterase 1 (CES1) convert GS-9851 into an inactive and achiral intermediate that is then hydrolysed by a histidine triad nucleotide-binding protein 1 (Hint1) into the 5'-monophosphate form. A second phosphorylation performed by uridine-monophosphate-cytidine-monophosphate kinase (UMP-CMP) leads to the 5'-diphosphate form which is eventually converted into the active 5'-triphosphate form by nucleoside diphosphate kinase.<sup>34,121,122</sup> The single stereoisomer drug Sofosbuvir, compared to the diastereoisomeric mixture, is characterised by a more specific metabolism that leads to a lower potential for cytochrome P450-mediated drug-drug interactions. Compared to other anti-HCV agents, Sofosbuvir showed a high genetic barrier to resistance and remarkable sustained virological response rates (SVR) (over 90% of patients). Sofosbuvir was approved by FDA 2013 in the USA for the treatment of chronic HCV infection in patients with genotypes 1, 2, 3 or 4. In combination with Ribavirin, it showed effects also in co-infected subjects with HIV. In addition, Sofosbuvir prevented a recurrence of HCV infection in most of the patients awaiting liver transplant.<sup>34,122,123</sup> Recently, Sofosbuvir has been also evaluated for the treatment of Zika virus and first *in vitro* studies showed promising results but further studies need to be undertaken.<sup>124</sup>

### ***Purine-based fluorinated antiviral nucleosides and prodrugs***

Many fluorinated purine-based nucleosides and prodrugs have also been synthesised and, among them, PSI-353661 (**1.56**) and PSI-352938 (**1.57**) (prodrugs of  $\beta$ -D-2'-deoxy-2'- $\alpha$ -fluoro-2'- $\beta$ -C-methylguanosine-5'-monophosphate), have shown a promising *in vitro* anti-HCV activity. Both of them showed a unique resistance profile

making them good candidates for a combination therapy with other anti-HCV agents including other nucleosides analogues.<sup>125</sup> The phosphoramidate agent GS9131 (**1.58**) is another 2'-F'-purine based prodrug which has been shown to inhibit HIV-1 reverse transcriptase (RT) together with a remarkable resistance profile toward N(t)RTI resistance mutations. GS9131 is currently under clinical evaluation.<sup>34,126</sup>

**Table 1.5: Fluorinated NAs and their prodrugs in clinical use and clinical development for cancer<sup>34</sup>**

Drug Name	Originator/Developer	Phase	Disease	Target
<b>Fluorouracil (5-FU, 1.32)</b>	Roche	Approved (1962)	Colorectal, breast, pancreatic, stomach cancer	TS
<b>Floxuridine (FdUrd, 1.33)</b>	Roche	Approved (1970)	Liver metastasis	TS
<b>Capecitabine (1.35)</b>	Roche	Approved (1998)	Metastatic breast, colorectal cancer	TS
<b>Tegafur (1.40) + Uracil</b>	Taiho Pharmaceutical	Used in Japan, Taiwan II II/III	Advanced GI cancers Colon, combination therapy for hepatocellular carcinoma Gastric cancer	TS, DNA synthesis inhibition
<b>Tegafur (1.40) + Gimeracil + Oteracil</b>	Taiho Pharmaceutical	III	Advanced gastric cancer in combination with cisplatin	TS
<b>Doxifluridine (1.41)</b>	Aida Pharmaceuticals	III	Combination therapy for GI cancer	TS
<b>FdCyd(1.45) + THU</b>	National Cancer Institute	I and II	Neoplasms	DNA methyltransferase
<b>Flucytosine (1.44)</b>	Tocagen	I/II I	Combination therapy for solid tumours Brain tumours	TS
<b>NUC-3373 (1.43)</b>	NuCana	I	Colorectal and breast cancer	TS

<b>Gemcitabine (1.31)</b>	Eli Lilly	Approved (1996)	Non-small cell lung, breast, pancreatic, ovarian, soft tissue sarcoma	DNA polymerase RNR, dCMP deaminase
<b>LY2334737 (1.48)</b>	Eli Lilly	Discontinued	Malignant and metastatic solid tumours	DNA synthesis inhibition
<b>CO-101 (1.49)</b>	Clavis Pharma	Discontinued	Advanced solid tumours Metastatic pancreatic dual adenocarcinoma	DNA synthesis inhibition
<b>NUC-1031 (1.46)</b>	NuCana	III II I	Pancreatic cancer Ovarian cancer Combination therapy for ovarian and biliary tract cancers	DNA synthesis inhibition
<b>RX-3117 (1.47)</b>	Rexahn Pharmaceuticals/TEVA Pharmaceuticals	I/II I	Solid tumours Combination therapy for ovarian cancer	DNA methyltransferase
<b>Tezacitabine (1.50)</b>	Aventis/Chiron Corporation	Discontinued	Hematological malignancies	RNR
<b>Trifluorothymidine (1.37) + Tipiracil HCl (TAS-102)</b>	Taiho Pharmaceutical	Approved (2015)	Metastatic colorectal cancer	TS
<b>Fludarabine (1.34)</b>	Southern Research Institute/Bayer HealthCare Pharmaceuticals	Approved (1991)	Hairy cell leukemia, B-cell CLL	DNA polymerase, RNR, DNA primase
<b>Clofarabine (1.36)</b>	Bioenvision	Approved (2004)	Pediatric refractory ALL	DNA polymerase, RNR

---

Information about status of clinical trials available from [www.clinicaltrials.gov](http://www.clinicaltrials.gov).

**Table 1.5 (cont.): Fluorinated NAs and their prodrugs in clinical use or clinical development for viral infections<sup>34</sup>**

<b>Drug Name</b>	<b>Originator/Developer</b>	<b>Phase</b>	<b>Disease</b>	<b>Viral Target</b>
<b>Trifluorothymidine (1.38) Viroptic</b>	GlaxoSmithKline	Approved (1998)	Herpes Simplex Virus (HSV)	DNA polymerase
<b>Emtricitabine Emtriva</b>	Emory University/Gilead	Approved (2003)	Human Immunodeficiency Virus (HIV)	Nucleoside reverse transcriptase
<b>Sofosbuvir (1.51) Sovaldi</b>	Gilead	Approved (2013)	Hepatitis C (HCV)	NS5B RNA-dependent RNA polymerase
<b>Mericitabine (1.53)</b>	Pharmasset/Hoffmann-LaRoche	II	HCV	NS5B RNA-dependent RNA polymerase
<b>Favipiravir (1.55)</b>	Toyama Chemical/MediVector	Approved in Japan (2014) III JIKI trial	As stockpiling against Influenza Pandemics Influenza Ebola	RNA-dependent RNA polymerase
<b>Fiacitabine (1.52, FIAC)</b>	Memorial Sloan-Kettering Cancer Center/Oclassen Pharmaceuticals	II	Cytomegalovirus and HIV infections	DNA polymerase RNR
<b>Elvucitabine (1.39)</b>	Yale University/Achillion Pharmaceuticals	II	Chronic HIV infections	Nucleoside reverse transcriptase
<b>Racivir (1.54)</b>	Emory University/Pharmasset	II	HIV	Nucleoside reverse transcriptase
<b>Fialuridine (1.61, FIAU)</b>	Oclassen Pharmaceuticals/Eli Lilly	Discontinued	HSV, HIV, and Hepatitis B (HBV)	DNA polymerase
<b>Clevudine (1.60,</b>	Bukwand/Pharmasse	Discontinued	HBV	DNA

<b>L-FMAU)</b>	t	d		polymerase
<b>Alovudine (1.29, FLT)</b>	Medivir/Beijing Mefuvir Medicinal Technology	Discontinued	HIV	DNA polymerase
<b>PSI 353661 (1.56)</b>	Pharmasset	Preclinical development	HCV	NS5B RNA-dependent RNA polymerase
<b>PSI 352938 (1.57)</b>	Pharmasset	I	HCV	NS5B RNA-dependent RNA polymerase
<b>GS9131 (1.58)</b>	Gilead	I	HCV	Nucleoside reverse transcriptase

---

Information about status of clinical trials available from [www.clinicaltrials.gov](http://www.clinicaltrials.gov).

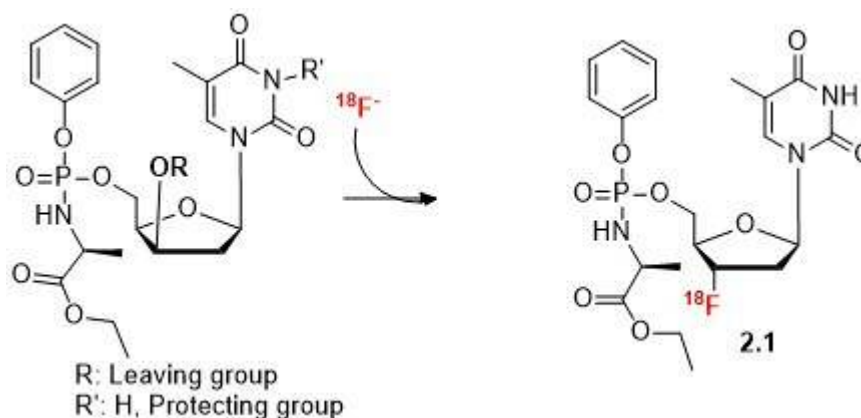
## 2. Research aims and objectives

As a proof of concept, this project aims to develop [ $^{18}\text{F}$ ]-radiolabelled ProTides that will be used as PET imaging agents and a model system to visualize pharmaceutical and biological effects of ProTides directly *in vivo*. Although many synthetic routes towards [ $^{18}\text{F}$ ]-radiolabelled nucleosides have been accomplished in the past,<sup>127</sup> to our knowledge the synthesis of [ $^{18}\text{F}$ ]-radiolabelled ProTides has never been achieved until now. Two different ProTides will be synthesised as model standards of two classes of fluorinated ProTides, the 2' and the 3'-fluorinated ProTides.

The 3'-[ $^{18}\text{F}$ ]FLT ProTide (**2.1**) and the 2'-[ $^{18}\text{F}$ ]FIAU ProTide(**2.2**) will be synthesised exploring different synthetic routes using both late stage and early stage fluorination following different synthetic pathways.

In order to obtain the [ $^{18}\text{F}$ ]FLT ProTide, suitable precursor molecules will first be synthesised using cold chemistry methods.<sup>128</sup> The main goal will consist in finding good leaving groups that could be easily replaced by the weak anhydrous nucleophile [ $^{18}\text{F}$ ]fluoride. Several leaving groups will thus be explored and tested for radiofluorination compatibility under different reaction conditions. (Figure **2.1**)

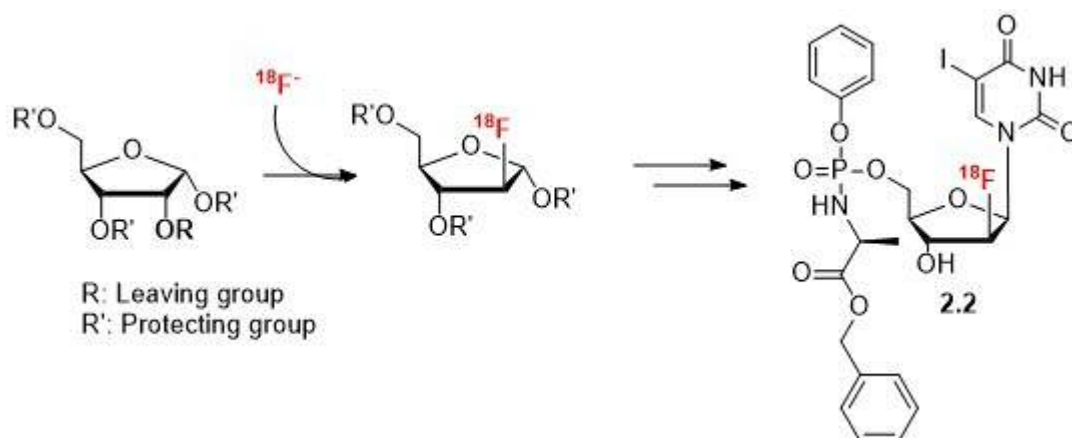
**Figure 2.1: Late stage [ $^{18}\text{F}$ ]fluorination of ProTides**



A second approach could consist in synthesising the 2'-[ $^{18}\text{F}$ ]FIAU ProTide through an early stage hot fluorination. Although more challenging because of the short half-life of the  $^{18}\text{F}^-$  allowing a limited time to perform the multistep synthesis, this

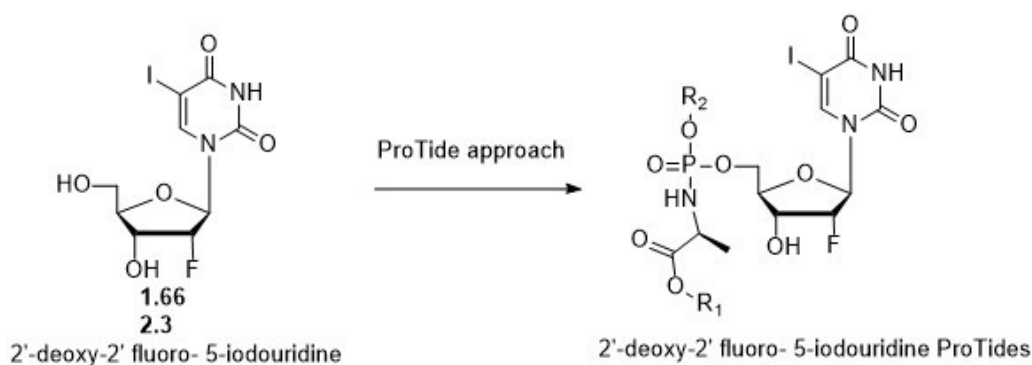
last approach could lead to the desired product avoiding the formation of undesired radiolabelled by-products (Figure 2.2).

**Figure 2.2: Early stage [ $^{18}\text{F}$ ]fluorination for the synthesis of ProTides**

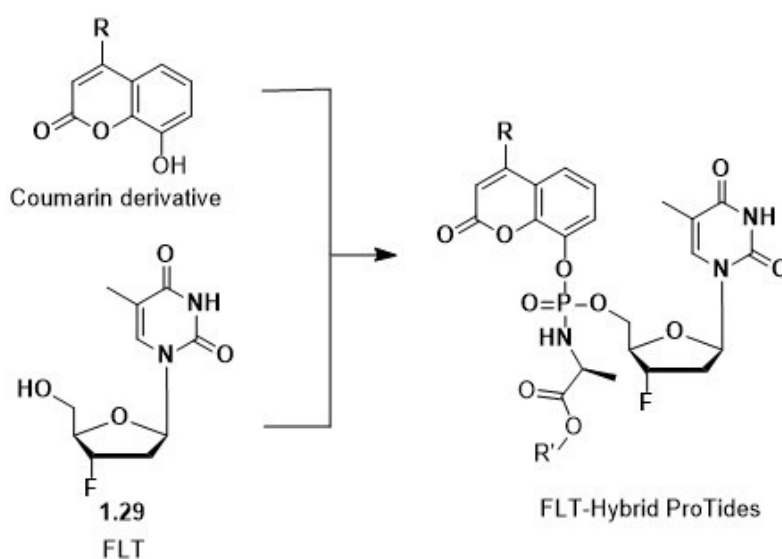


Once a [ $^{18}\text{F}$ ]-radiolabeled ProTide will be synthesised in reasonable chemical and radiochemical yields, it could finally be used for early *in vivo* experiments to study absorption, distribution, metabolism, excretion and toxicity (ADMET) properties of this class of compounds as well as investigate their potential as a novel class of PET diagnostic probes.

Besides the aim of translating fluorinated ProTides into PET tracers, a secondary objective of this project, is to synthesise a novel class of non-radiolabelled 2'-fluoro- 5-iodo uridine based ProTides as potential antiviral drugs. Starting from the observation that many uridine based nucleosides, and particularly fluorinated ones, showed promising antiviral properties against many DNA and RNA viruses,<sup>34</sup> it was speculated that the application of ProTide strategy will lead to a new more potent and less toxic class of antiviral compounds. A series of 2'-deoxy-2' fluoro- 5-iodouridine ProTides will therefore be synthesised, and studies of cytotoxicity will be performed on Zika and Dengue viruses strands (Figure 2.3).

**Figure 2.3: ProTide approach applied to the 2'-deoxy-2' fluoro- 5-iodouridine**

Lastly, a further goal of this research project, is to synthesise FLT non-radiolabelled hybrid fluorescent ProTides. These compounds, compared to conventional ProTides, will be characterised by a coumarin residue that could provide fluorescent properties to further develop our knowledge on their metabolism for future *in vitro* studies. Besides the fluorescent properties, the substitution of the common aromatic moiety with a coumarin derivative ring, could possibly lead to less toxic metabolic products and potentially increase their antiviral activity through a co-drug approach, given the known biological activity associated with coumarin derivatives<sup>129</sup> (Figure 2.4).

**Figure 2.4: ProTide approach for the synthesis of hybrid ProTides**

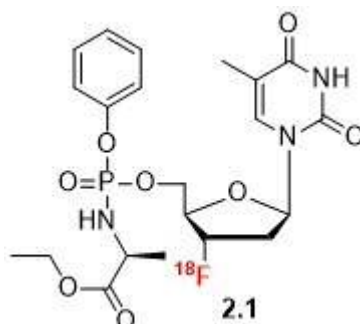
## 3. Radiochemical synthesis of [18F]FLT ProTide

### 3.1 Introduction

The main goal of this research project is the synthesis of [18F]-radiolabeled ProTides as a proof of concept for the ProTide strategy through future *in vivo* biodistribution studies. Several ProTides are currently either approved therapies or under clinical evaluation and have proved to be more active than their parent nucleoside analogues by circumventing their main resistance mechanisms.<sup>83</sup> Radiolabelling these compounds with a radioisotope with a relatively short half life, such as [18F]fluorine, would enable their use as PET imaging probes in order to have a deeper understanding of their ADMET properties directly *in vivo*. Eventually, this could be a first step towards the future of a Protide based personalized medicine.

Two [18F]-radiolabelled ProTides have been chosen as targets for this project, the [18F]FLT ProTide (**2.1**) and the [18F]FIAU ProTide (**2.2**), as a model standard of 3'-fluorinated and 2'-fluorinated ProTides respectively, following two different synthetic approaches. In this chapter the late stage fluorination approach for the synthesis of the [18F]FLT ProTide (**2.1**) will be discussed.

**Figure 3.1: Structure of an [18F]FLT ProTide**



[18F]FLT ProTide has been chosen as a model standard for the class of the 3'-fluorinated ProTides for the reasons listed below:

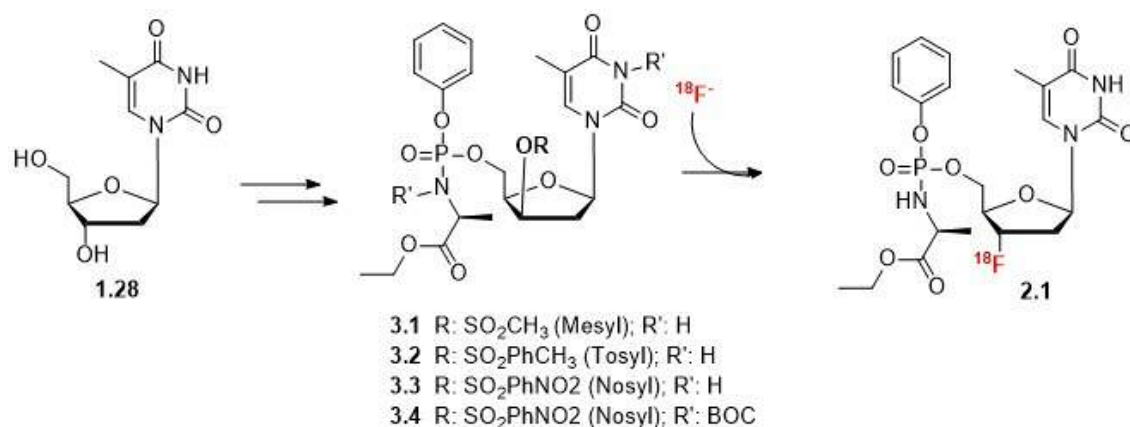
- It already contains a fluorine in its original structure hence radiolabelling this Protide with [18F]fluorine comes as a natural and convenient choice.

- [18F]FLT (**1.4**) is an established PET imaging agent (proliferation biomarker), therefore convenient strategies for its synthesis have already been extensively studied and can be a guide for the synthesis of **2.1**.<sup>130</sup>
- It is a thymidine based ProTide, thus the absence of other reactive sites on the nucleosidebase moiety of the molecule (i.e. the amino group on the cytidine based Gemcitabine (**1.31**)) will avoid further protection and deprotection steps that will make the radiosynthesis longer and more difficult to perform.
- A series of FLT ProTides have already been synthesised showing a safe toxicological profile and a moderate anti HIV activity.<sup>114</sup>

### 3.2 [18F]fluorination (Hot): late stage approach

As stated before, convenient syntheses to access [18F]FLT (**1.4**) have extensively been studied. In the examples reported above (Figure 1.6, Chapter 1), the [18F]fluorination occurred at a late stage in the synthesis. Wherever possible, this approach should always be the one of choice considering the limited time available when dealing with [18F]fluorine. Similarly, a late stage approach has also been chosen for the synthesis of the [18F]FLT ProTide following the synthetic scheme below (Figure 3.2), starting with commercially available thymidine and making use of a preformed ProTide intermediate (**3.1-3.4**) containing a good leaving group such as mesyl, tosyl or nosyl.

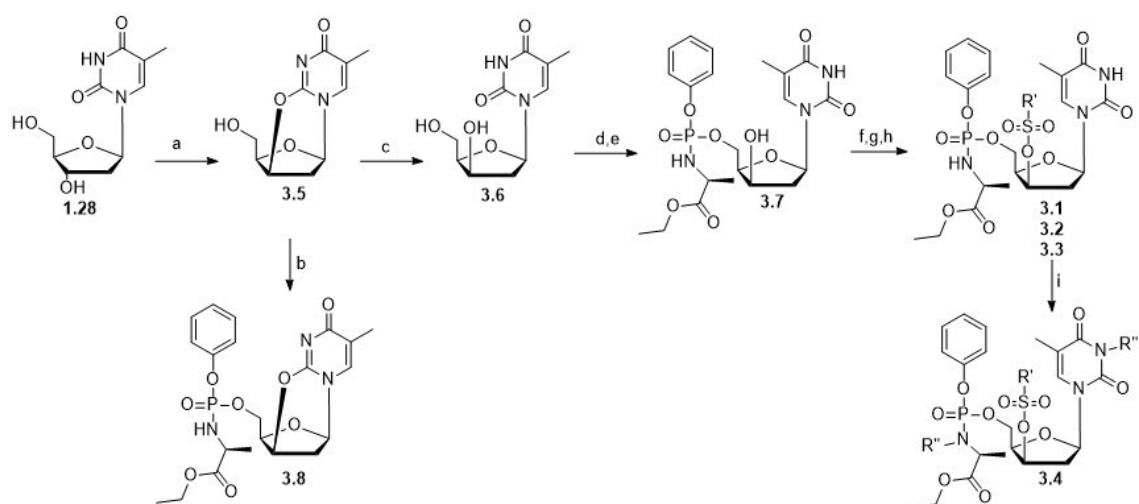
**Figure 3.2: Late stage fluorination approach for the synthesis of the [18F]FLT ProTide**



### 3.3 Synthesis of the precursor molecules

Keeping in mind what was stated in the introduction regarding the use of precursors with good leaving groups to allow the weak nucleophile [<sup>18</sup>F]fluoride to perform the nucleophilic substitution (Chapter 1, pg 11), five possible precursor molecules of the [<sup>18</sup>F]FLT ProTide (**2.1**) have been synthesised following the general synthetic scheme reported in Figure 3.3.

**Figure 3.3: General scheme for the synthesis of precursor molecules for the synthesis of [<sup>18</sup>F]FLT ProTide**



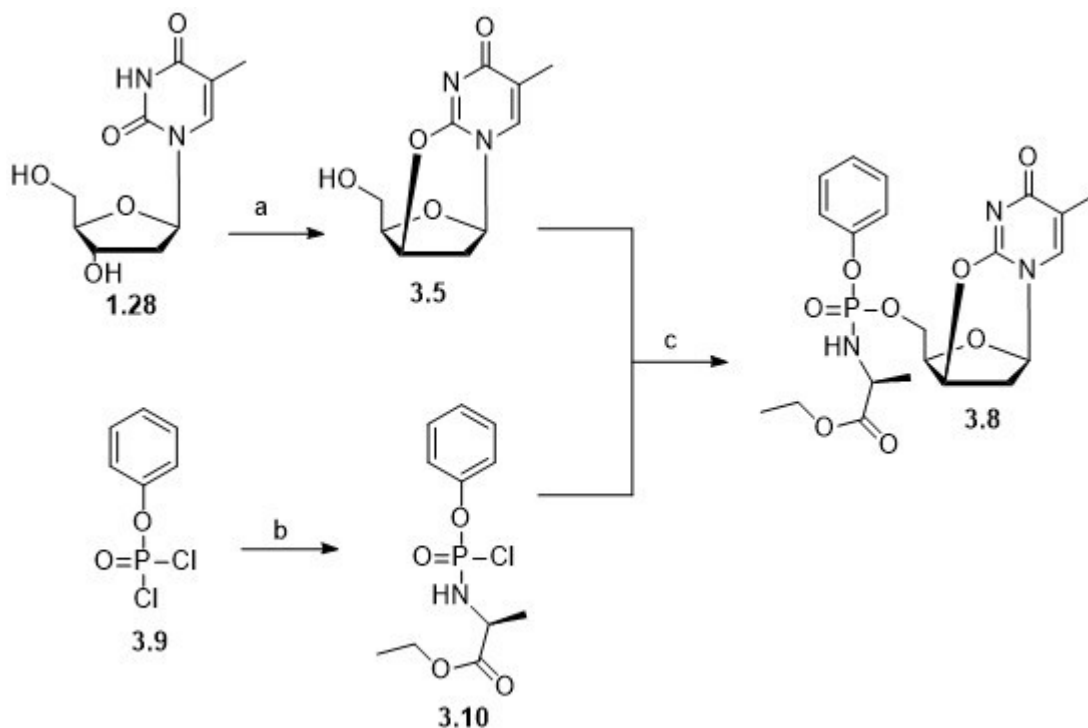
**Reagents and conditions:** a) PPh<sub>3</sub>, DIAD, anh. CH<sub>3</sub>CN, -20°C to 0°C, 5h, 65%; b) Phosphorochloridate, NMI, anh. THF, 25°C, 18h, nitrogen atm., 0.6%; c) NaOH[1.5M], CH<sub>3</sub>OH, 90°C, 3h, 64%; d) L-alanine ethyl ester hydrochloride salt, Et<sub>3</sub>N, -78°C to rt, anh. CH<sub>2</sub>Cl<sub>2</sub>, 3h, 95%; e) Phosphorochloridate, NMI, anh. THF, 25°C, 18h, nitrogen atm., 21%; f) Mesyl chloride, Et<sub>3</sub>N, anh. CH<sub>2</sub>Cl<sub>2</sub>, nitrogen atm., 0°C to 25°C, 1.5hr, 29,5%; g) Tosyl chloride, pyridine, AgOTf, 0°C to rt, 2h, 60%; h) Nosyl chloride, pyridine, AgOTf, 0°C to rt, 2h, 30%; i) di-tert-butyl dicarbonate, pyridine, rt, 16h, 56%.

#### 3.3.1 Synthesis of cyclised precursor (3.8)

The synthesis of the first anhydride ProTide precursor for fluorination was performed according to the scheme shown below (Figure 3.4), making use of Mitsunobu reaction<sup>131</sup> on the commercially available starting material thymidine. The

“anhydro” intermediate (**3.5**) was then reacted with the ProTide precursor phosphoryl chloride (**3.10**) according to a previously reported ProTide protocol.<sup>128</sup>

**Figure 3.4: Synthesis of the anhydride precursor**

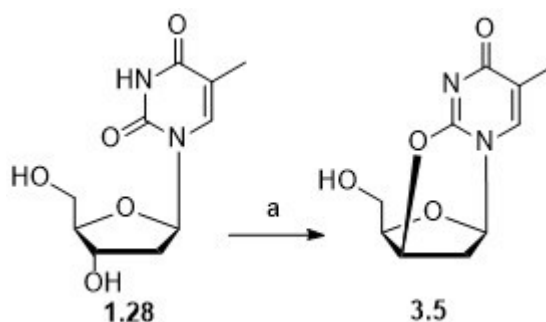


**Reagents and conditions:** a)  $\text{PPh}_3$ , DIAD, anh.  $\text{CH}_3\text{CN}$ ,  $-20^\circ\text{C}$  to  $0^\circ\text{C}$ , 5h, 65%; b) L-alanine ethyl ester hydrochloride salt,  $\text{Et}_3\text{N}$ ,  $-78^\circ\text{C}$  to rt, anh.  $\text{CH}_2\text{Cl}_2$ , 3h, 95%; c) Phosphorochloridate, NMI, anh. THF,  $25^\circ\text{C}$ , 18h, nitrogen atm., 0.6%.

Firstly it was investigated whether 2' and 3' fluorinated nucleoside analogues can be accessed via fluorination of anhydrous precursors with applications also in radiochemistry.<sup>132</sup> For this reason a Mitsunobu reaction was performed using thymidine (**1.28**) as starting material in order to obtain the six membered 2,3'-anhydride derivative via an intramolecular cyclisation. For this purpose DIAD (diisopropylazodicarboxylate) and  $\text{PPh}_3$  (triphenylphosphine) were used (Figure 3.5).<sup>133</sup>  $\text{PPh}_3$  combines with DIAD to form a zwitterionic phosphonium intermediate which deprotonates the 3'-OH on the thymidine to form the anionic nucleophile. This intermediate binds to the zwitterionic phosphonium ion to perform an  $\text{S}_{\text{N}}2$  attack

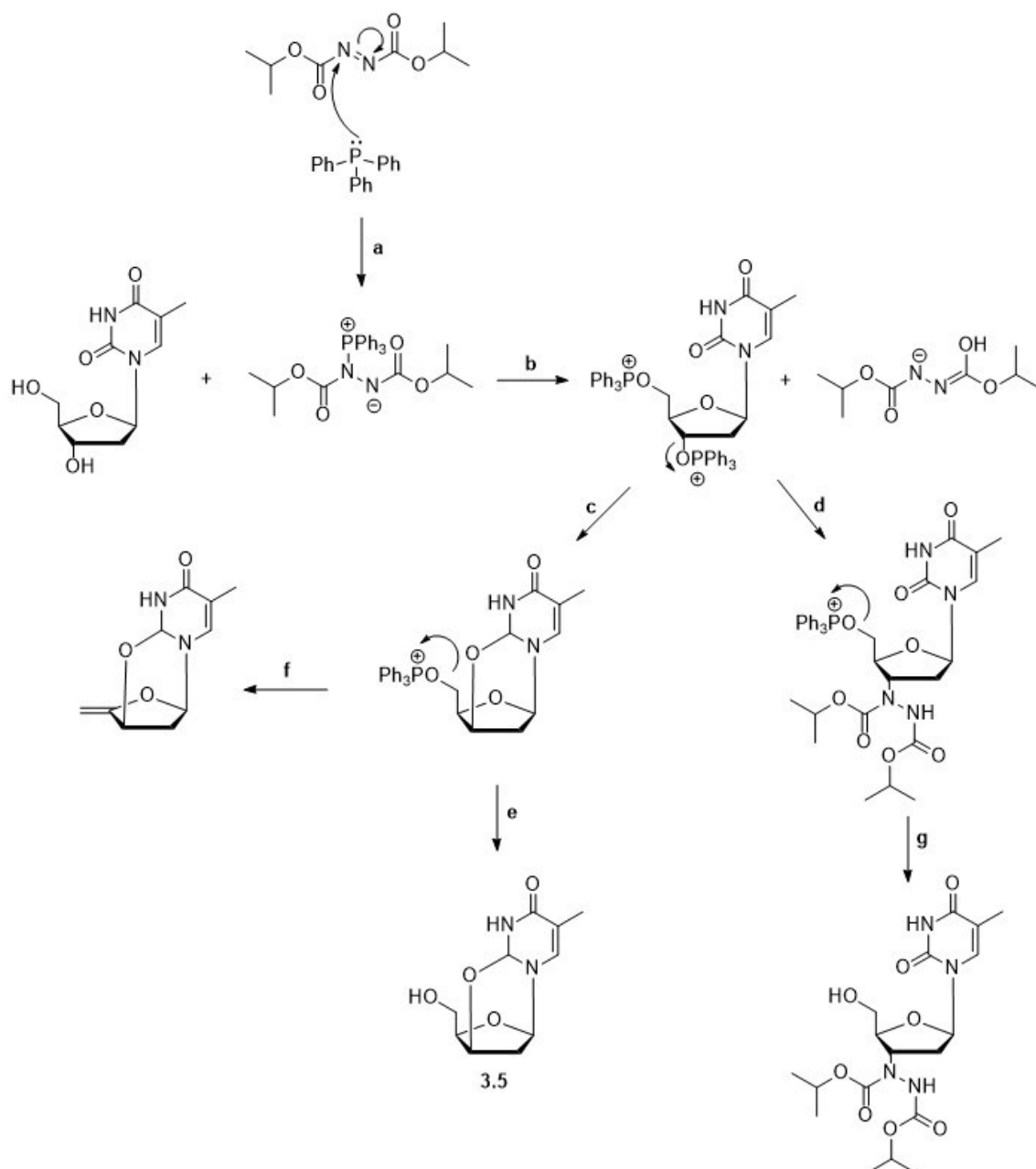
leading to the 2,3'-anhydrothymidine, that is now characterised by an inverted stereochemistry at C-3' position. The reaction is driven forward also by the formation of the strong P=O bond in the byproduct triphenylphosphine oxide-Figure 3.6 shows formation of **3.5** together with other side products.

**Figure 3.5: Mitsunobu reaction**



**Reagents and conditions:** a) PPh<sub>3</sub>, DIAD, anh. CH<sub>3</sub>CN, -20°C to 0°C, 5h, 65%.

**Figure 3.6: Mechanism of the Mitsunobu reaction**<sup>134</sup>

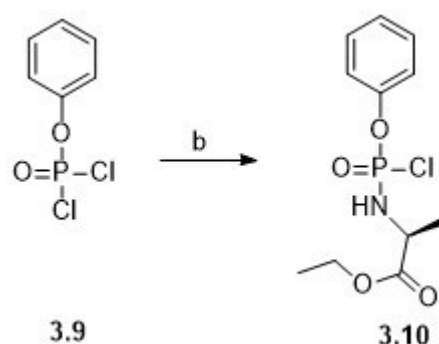


The formation of the desired product was confirmed by NMR spectroscopy. In particular the disappearance of the proton signal at 9.5 ppm of the NH of the pyrimidine ring, confirmed the positive outcome of the reaction. Column chromatography on silica gel using a gradient elution of  $\text{CH}_2\text{Cl}_2$  and  $\text{CH}_3\text{OH}$  has been used for the purification. A moderate yield of 65% was obtained as also reported in the literature;<sup>133</sup> comparison of NMR data with this previously published compound confirmed the identity of product **3.5**.

In the meantime a phosphorochloridate was synthesized following the standard procedure of McGuigan *et al.* for the synthesis of ProTides.<sup>84</sup> The ethyl ester of the L-

alanine hydrochloride salt was used under anhydrous conditions to react with the commercially available phenyl dichlorophosphate. Triethylamine was used as a base necessary to trigger the nucleophilic attack of the L-alanine amine moiety on the phosphorus of the phosphorochloridate. The formation of the desired product was monitored by  $^{31}\text{P}$  NMR. To avoid the oxidation of the phosphorodichloridate and phosphorochloridate, the reaction and the work up were performed under nitrogen atmosphere (Figure 3.7).

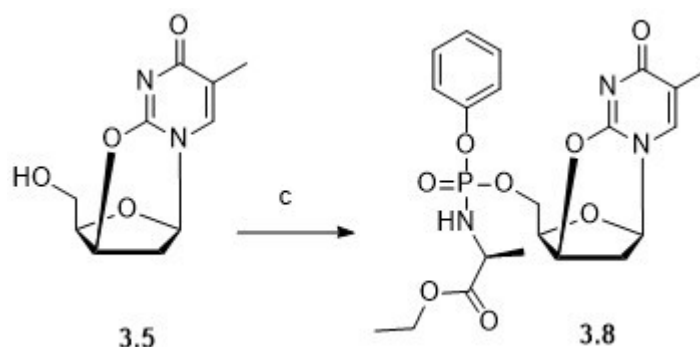
**Figure 3.7: Synthesis of Phosphorochloridate**



**Reagents and conditions:** b) L-alanine ethyl ester hydrochloride salt,  $\text{Et}_3\text{N}$ ,  $-78^\circ\text{C}$  to rt, anh.  $\text{CH}_2\text{Cl}_2$ , 3h, 95%.

Due to the formation of the chiral phosphorus center, two diastereoisomers have been produced from this reaction in a ratio of 1:1.  $^{31}\text{P}$  NMR in fact shows two distinctive peaks for the phosphorus of the two diastereoisomers. These products were used for the next coupling reaction with the nucleoside moiety without further purification. No separation of the diastereoisomers was performed as this is outside the remit of this project.

The first precursor molecule, the anhydride derivative (**3.8**), was then synthesized by coupling the product of the Mitsunobu reaction (**3.5**) with the phosphorochloridate using NMI as per the previously reported procedure<sup>128</sup> (Figure **3.8**).

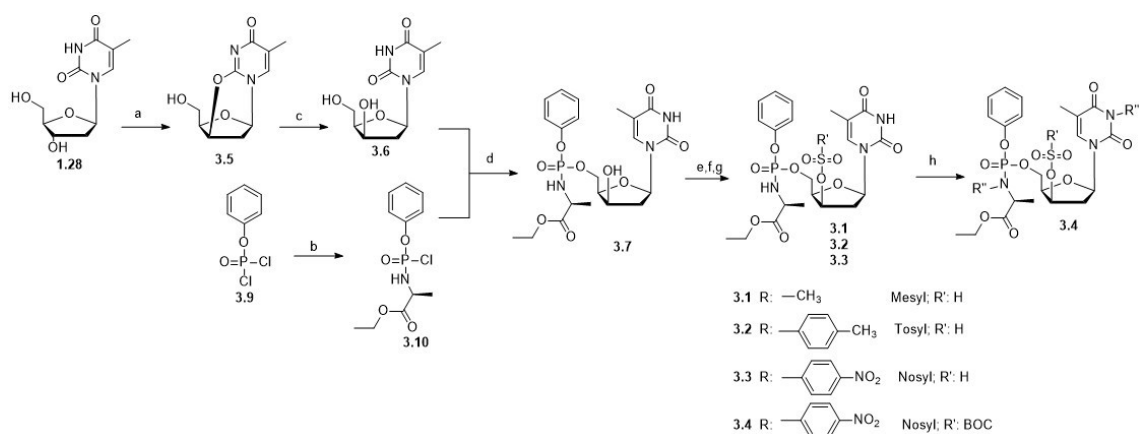
**Figure 3.8: Formation of the anhydride ProTide**

**Reagents and conditions:** c) Phosphorochloridate, NMI, anh. THF, 25°C, 18h, nitrogen atm., 0.6%.

The product was obtained in very poor yields and the first purification of the product by column chromatography on silica gel did not give the clean product because of the formation of several by-products with similar polarity. A second purification by preparative TLC was then performed to furnish eventually a clean diastereoisomeric mixture of **3.8** as a yellowish oil. This precursor molecule was then used for both [19F]fluorination (**cold fluorination**) and [18F]fluorination (**hot fluorination**) attempts.

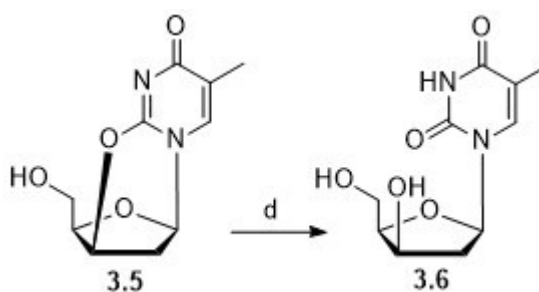
### 3.3.2 Synthesis of the mesyl, tosyl and nosyl precursors

All the other precursor molecules were synthesised following the scheme below (Figure 3.9).

**Figure 3.9: Synthetic procedure for the mesyl, tosyl and nosyl precursors**

**Reagents and conditions:** a) PPh<sub>3</sub>, DIAD, anh. CH<sub>3</sub>CN, -20°C to 0°C, 5h, 65%; b) L-alanine ethyl ester hydrochloride salt, Et<sub>3</sub>N, -78°C to rt, anh. CH<sub>2</sub>Cl<sub>2</sub>, 3h, 95%; d) NaOH[1.5M], CH<sub>3</sub>OH, 90°C, 3h, 64%; e) Phosphorochloridate, NMI, anh. THF, 25°C, 18h, nitrogen atm, 60%; e) Mesylchloride, Et<sub>3</sub>N, anh. CH<sub>2</sub>Cl<sub>2</sub>, nitrogen atm., 0°C to 25°C, 1.5hr, 29.5%; f) Nosyl chloride, pyridine, AgOTf, 0°C to rt, 2h, 30%; g) Tosyl chloride, pyridine, AgOTf, 0°C to rt, 2h, 60%; h) Di-tert-butyl dicarbonate, pyridine, rt, 16h, 56%.

The first two steps (a, b) are the same as shown for the synthesis of the first precursor. The Mitsunobu product (**3.5**) was then hydrolysed to obtain the free hydroxyl group in 3'-β position of the sugar moiety.<sup>135</sup> The hydrolysis was carried out in basic conditions to obtain the 1-(2-deoxy-β-lyxofuranosyl thymidine) (**3.6**) with a good yield (Figure **3.10**).

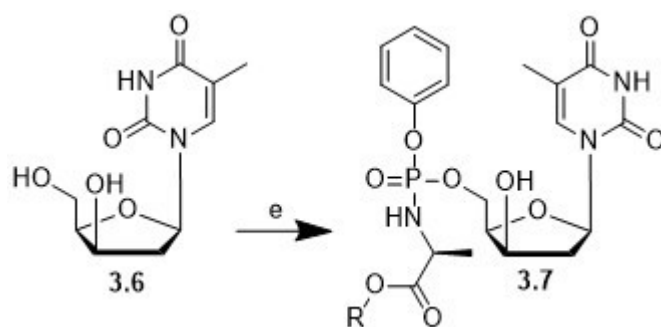
**Figure 3.10: Hydrolysis**

**Reagents and conditions:** d) NaOH[1.5M], CH<sub>3</sub>OH, 90°C, 3h, 64%.

The phosphorochloridate (**3.10**) was again synthesised as a diastereoisomeric mixture following the standard procedure.<sup>84</sup>

These products were used for the next coupling reaction with the nucleoside moiety without further purification. A coupling reaction was then performed between the phosphorochloridates and the nucleobase moiety (Figure **3.11**).

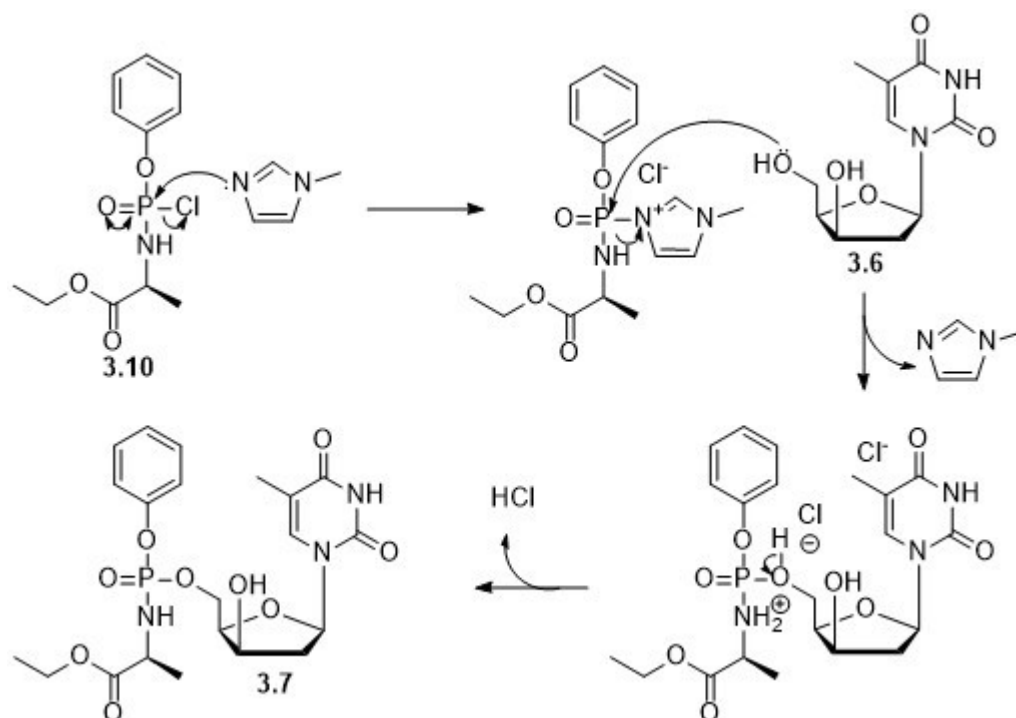
**Figure 3.11: ProTide coupling**



**Reagents and conditions:** e) Phosphorochloridate, NMI, anh. THF, 25°C, 18h, nitrogen atm., 18%.

For this synthetic step 1-methylimidazole (NMI) was used as a base to form an imidazolium intermediate with the phosphorochloridate that can then readily react with the nucleoside. Below is shown the mechanism of action of this reaction when using the base NMI (Figure **3.12**).

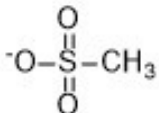
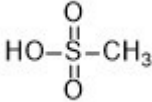
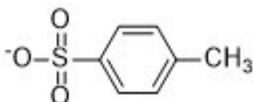
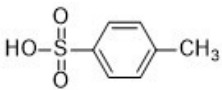
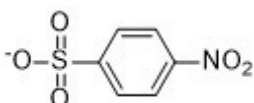
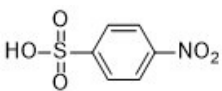
**Figure 3.12: Reaction mechanism for the final coupling step in the synthesis of the FLT ProTide<sup>135</sup>**



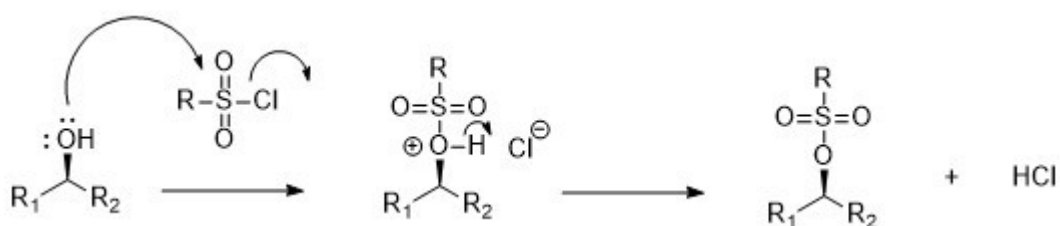
The hydroxylic group in the 5' position of the sugar moiety is a primary alcohol therefore it is more prone to act as a nucleophile compared to the secondary hydroxyl group in the 3' position. For this reason, no protecting groups were necessary at this stage of the synthesis.

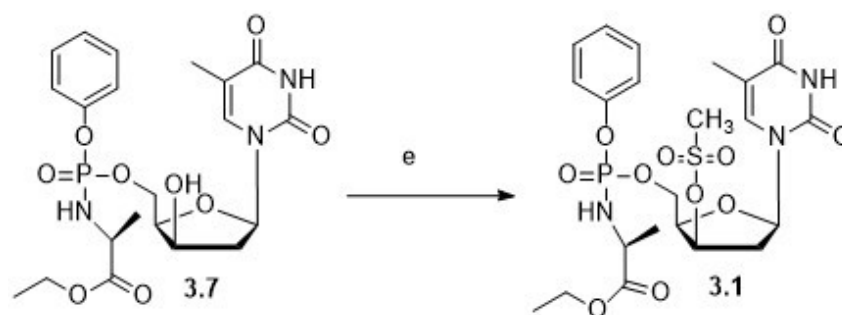
The successful formation of the ProTide was confirmed by  $^1\text{H}$  NMR,  $^{13}\text{C}$  NMR and  $^{31}\text{P}$  NMR, and mass spectrometry. Again, two diastereoisomers were formed showing two separate characteristic peaks of the phosphoramidate group around 3ppm on the  $^{31}\text{P}$  NMR. As the hydroxylic group is a poor leaving group,<sup>135</sup> and the fluoride is a weak nucleophilic agent (even when rigorously dried and complexed with the crown ether Kryptofix to enhance nucleophilicity), the hydroxylic group was converted into better leaving groups. In particular three organosulfonates, the methanesulfonate (mesyl), the *p*-toluenesulfonate (tosyl) and the *p*-nitrobenzenesulfonate (nosyl) have been chosen as leaving groups because of their ability to be easily replaced by the fluoride via an  $\text{S}_{\text{N}}2$  reaction<sup>19</sup> (Table 3.1).

**Table 3.1: Structures of mesyl, tosyl and nosyl leaving groups and pKa of their equivalent acids**

STRUCTURE	NAME	ABBREVIATION	PKA OF THE CONJUGATE BASE
	Methanesulfonate	( <sup>-</sup> OMs)	Mesylate pKa-2 
	<i>p</i> -Toluenesulfonate	( <sup>-</sup> OTs)	Tosylate pKa-3 
	<i>p</i> -Nitrobenzenesulfonate	( <sup>-</sup> ONs)	Nosylate pKa-6 

From this series of precursors the first synthesised product was the mesyl derivative (**3.1**). Figure **3.13** shows the reaction mechanism of the mesylation of the 3'-alcohol with mesyl chloride as reagent. The presence of a base such as pyridine or Et<sub>3</sub>N can be used to speed up the reaction rate.<sup>136</sup>

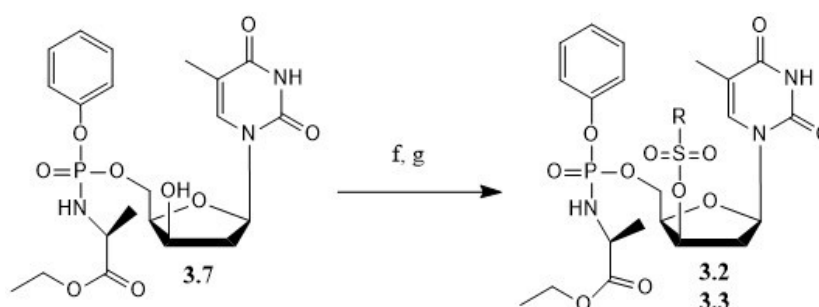
**Figure 3.13: Reaction mechanism of the Mesylation**

**Figure 3.14: Mesylation reaction**

**Reagents and conditions:** e) Mesylchloride, Et<sub>3</sub>N, anh. CH<sub>2</sub>Cl<sub>2</sub>, nitrogen atm., 0°C to 25°C, 1.5hr, 29,5%.

An excess of triethylamine (10 eq) was used as a base to activate the hydroxyl group to react with an excess of mesyl chloride (4 eq). The reaction was monitored by TLC and was stopped when all the starting material was converted into the product. The crude product was then purified by silica gel column chromatography to afford the desired clean compound.

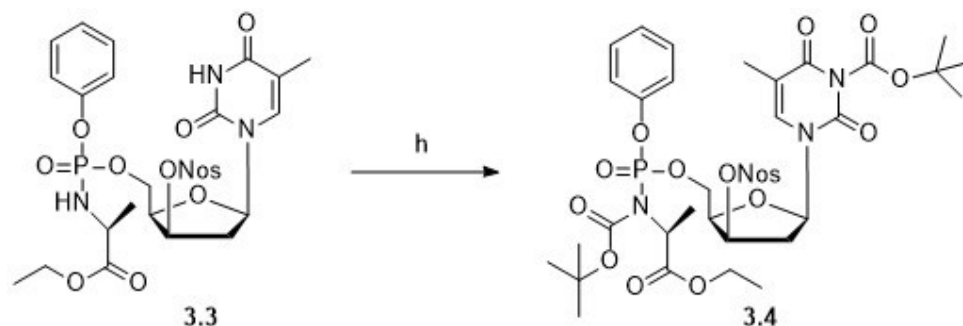
For the synthesis of the tosylate (3.2) and nosylate (3.3) precursors the same procedure was used but a very low and slow conversion was noted, hence the use of a different base combined with the use of a catalyst helped to speed up the reaction and have a better conversion rate.

**Figure 3.15: Nosylation and Tosylation**

**Reagents and conditions:** f) Nosyl chloride, pyridine, AgOTf, 0°C to rt, 2h, 30%; g) Tosyl chloride, pyridine, AgOTf, 0°C to rt, 2h, 60%.

In both cases the reaction was carried out in the presence of pyridine and silver triflate (AgOTf), a halide-abstrating reagent that could increase the reaction rate.<sup>137</sup> Both compounds were purified by silica gel column chromatography to furnish the final products in yields ranging from 30 to 60%. The fifth precursor molecule synthesized was a derivative of the nosyl precursor. The nosyl derivative (**3.3**), as discussed later on in the [18F]fluorination section, proved to be a very good potential precursor for the [18F]fluorination but its lack of stability led to a partial decomposition of the starting material before the radiolabelling step could happen. For this reason a new more stable version of the nosylate precursor was synthesised. The aim was originally to protect the NH moiety on the pyrimidine ring in order to avoid the formation of the undesired byproducts during the fluorination step.<sup>138</sup> The diprotected ProTide (on both the NH of the pyrimidine ring and the NH of the phosphoramidate moiety) was instead the major product of the reaction.

**Figure 3.16: N-Protection using the BOC group**



**Reagents and conditions:** h) Ditert-butyl dicarbonate, pyridine, rt, 16h, 56%.

Although the product obtained was not the expected one, it anyway proved to be the perfect candidate as a precursor for the [18F]fluorination enhancing stability on both the pyrimidine ring and on the phosphoramidate moiety. Its fluorination is discussed later on in the [18F]fluorination section.

### 3.4 Synthesis of the cold standard

For the synthesis of the cold standard (**3.11**) a few attempts to perform cold fluorination of the mesyl precursor (**3.1**) have been carried out but none of them gave the desired product. Tetrabutyl ammonium fluoride tri-hydrate (TBAF.3H<sub>2</sub>O), KF or CsF were used as source of fluorine. Kryptofix was used to enhance the weak nucleophilicity of the fluorine. None of the reactions gave the desired fluorinated compound returning only unreacted starting material and other by-products (Table 3.2).<sup>1</sup>

Figure 3.17: Fluorination of the Mesyl precursor

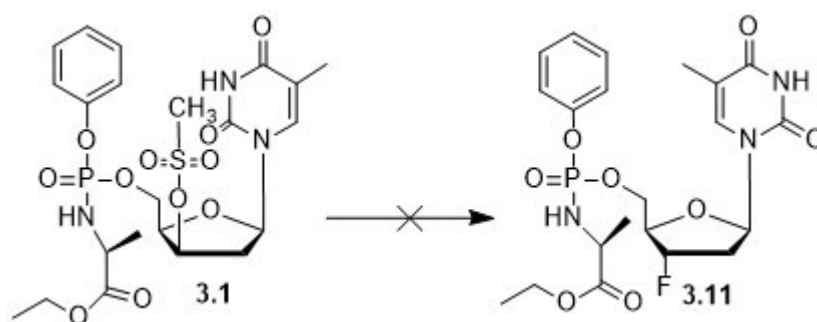
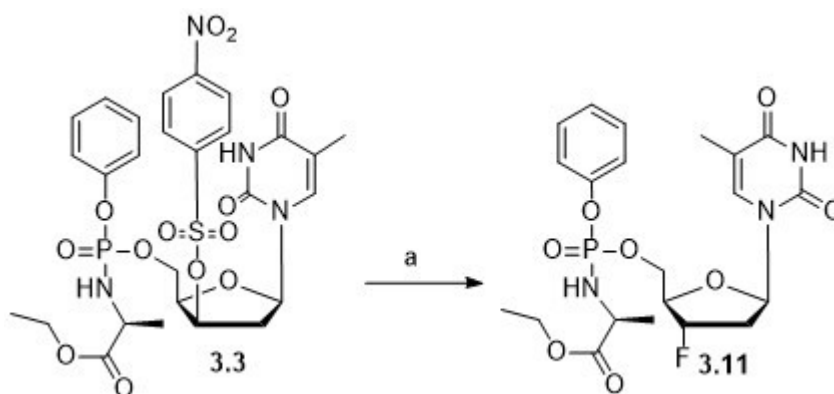


Table 3.2: Attempts of cold fluorination of mesyl precursor (**3.1**)

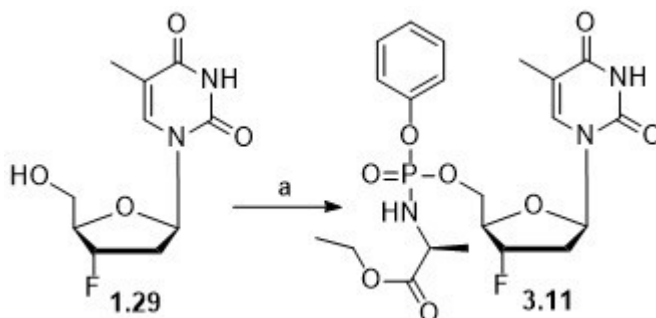
Starting material	T °C	Fluorine source	Solvent	Reaction time	Product
<b>3.1</b>	70 °C	TBAF	THF	1h	No
<b>3.1</b>	120 °C	KF	DMF	1h	No
<b>3.1</b>	120 °C	CsF	DMF	1h	No

When the fluorination was performed on the nosyl derivative (**3.3**), the formation of the FLT ProTide (**3.11**) was observed even if the yield was low.

**Figure 3.18: Fluorination of the Nosyl precursor (3.3)**

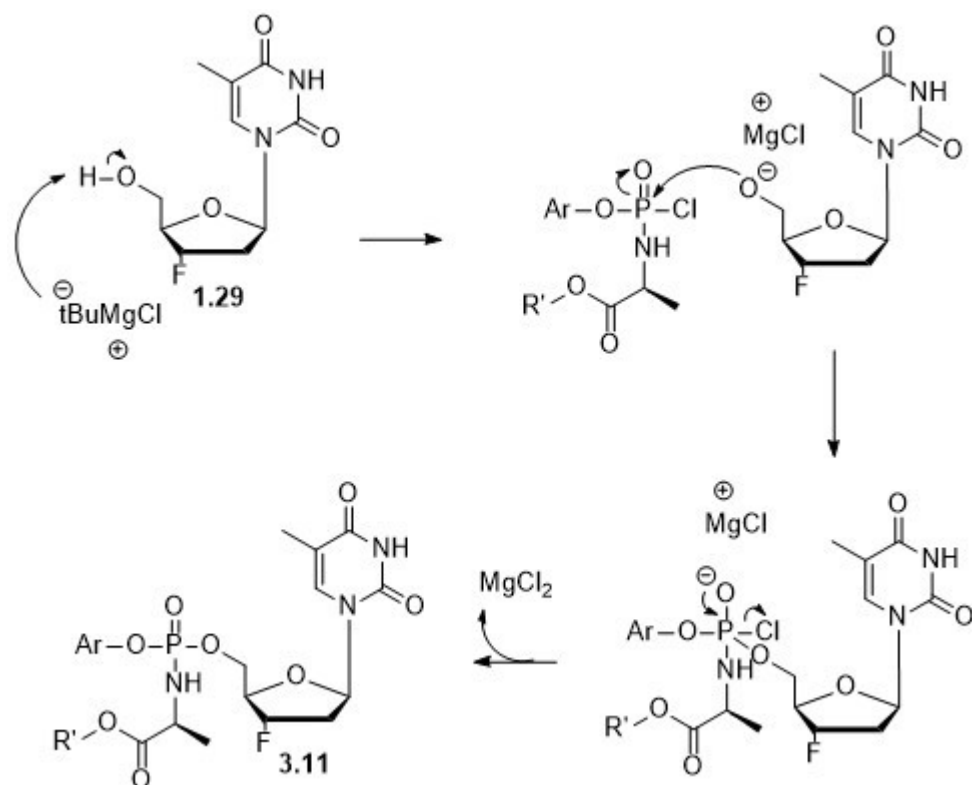
**Reagents and conditions:** a) TBAF 1M in THF, anh.DMF, rt, 1h, 3%.

The poor yield of this reaction was due to the formation of many by-products. Another synthetic strategy was also used to access the FLT ProTide (**3.11**) in better yields (Figure **3.19**).

**Figure 3.19: Synthesis of FLT ProTide using FLT as starting material**

**Reagents and conditions:** a) Phosphorochloridate, t-BuMgCl, anh. THF, 18h, 23.5%.

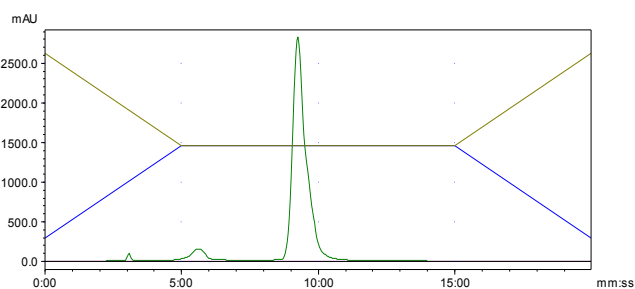
The commercially available FLT (**1.29**) was used as starting material and the Grignard reagent t-BuMgCl was used to perform the coupling reaction with the phosphorochloride (Figure **3.19**, **3.20**) giving the desired compound in better yields.<sup>114,128</sup>

**Figure 3.20: Mechanism of reaction of the Grignard reagent**

This compound was eventually used as cold standard for the [18F]fluorination step. It has indeed to be co-spiked with the radiolabelled compound on an HPLC system in order to compare the retention time of the cold and the hot FLT ProTide. The same HPLC gradient elution ( $\text{H}_2\text{O}-\text{CH}_3\text{CN}$  99%-1% to 50%-50%) was used for the analyses of the [18F]fluorination reactions.

**Figure 3.21: Analytical HPLC (UV detector) of the cold [19F]FLT ProTide.**

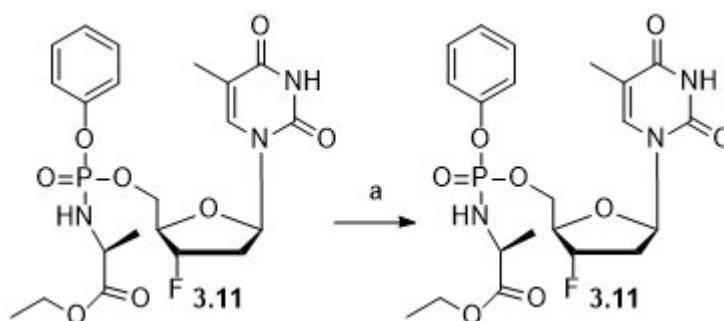
( $\text{H}_2\text{O}-\text{CH}_3\text{CN}$  99%-1% to 50%-50%).  $R_T$ : 9.7 min



### 3.5 Studies of ProTide stability

Studies of stability of the FLT-ProTide (**3.11**) were then performed in order to prove that, once formed, the [18F]FLT ProTide is stable under the harsh conditions used in radiochemistry (i.e high temperature, excess of a fluoride source and Kryptofix).

**Figure 3.22: Studies of stability of the FLT ProTide**



**Reagents and conditions:** a) KF(10eq), Kryptofix(10 eq), anh.solvent, 40-120 °C.

To a stirring solution of FLT-ProTide in anhydrous DMF, a solution of KF and Kryptofix in DMF anhydrous was added at rt. The reaction mixture was heated for 1h at 40°C, 80°C, 100°C and 120°C. Each reaction was monitored by TLC, <sup>31</sup>P NMR, and <sup>19</sup>F NMR to observe the potential degradation of the starting material and eventually the formation of side products. No decomposition was observed up to 120°C which is the maximum temperature that was going to be used for the [18F]fluorination step.

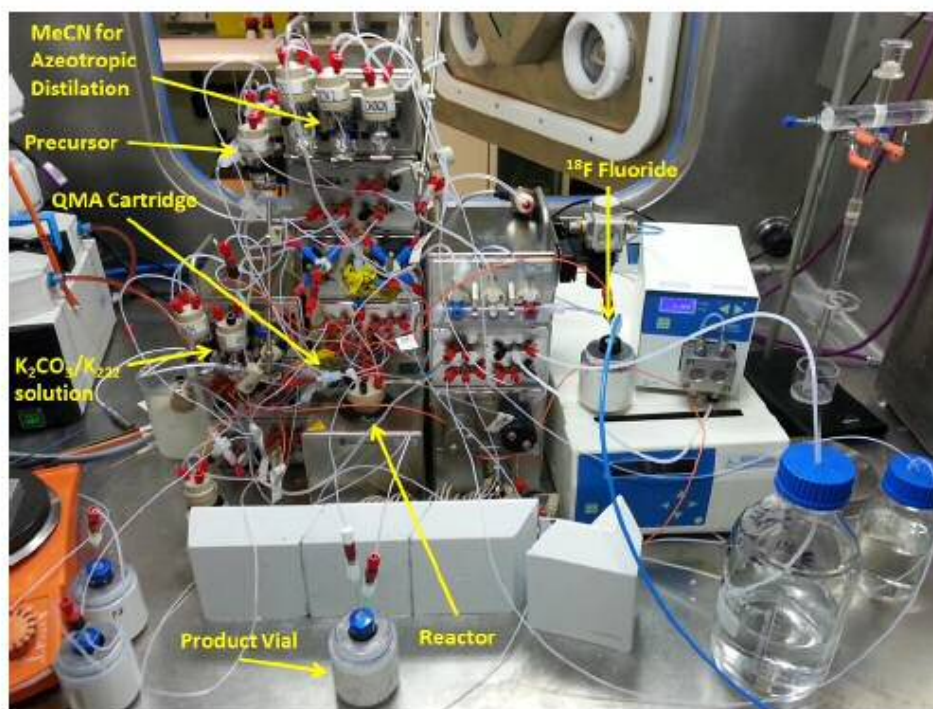
The reaction mixture was then purified by silica gel column chromatography and the starting material was recovered and was analyzed by <sup>1</sup>H NMR, <sup>13</sup>C NMR, <sup>19</sup>F NMR, <sup>31</sup>P NMR, which all confirmed its stability and purity.

### 3.6 [18F]fluorination

Before starting attempts of hot fluorination of the precursor molecules synthesised, the fully automated synthetic system (Eckert and Ziegler Nuclear Interface Module) for the introduction of <sup>18</sup>F<sup>-</sup> into the precursor molecule had to be been configured. This system, located into a shielded hot cell, was set up as shown in Figure

**3.23.** The process consists mainly in the entrapment of the  $^{18}\text{F}^-$ , which comes in a water solution (2 mL) directly from the cyclotron, into a QMA cartridge (a silica-based, hydrophilic, anion-exchanger designed for the extraction of anionic analytes such as  $^{18}\text{F}^-$ ). A Kryptofix solution passes through it to form the complex KF-K222. An azeotropic distillation of this aqueous solution is performed two times with 1 mL of anhydrous acetonitrile at  $120^\circ\text{C}$ . Finally the precursor molecule dissolved in 1 mL of anhydrous solvent is added and the reaction mixture is allowed to stir. Temperature and time of the reaction can be modified for each experiment.<sup>139</sup>

**Figure 3.23: Modular Lab Eckert and Ziegler (E&Z) at PETIC centre**



The module set up consists of 9 elements (Figure 3.24):

(A) Reaction vial.

(B) QMA cartridge preconditioned with 5 mL of an 8.4% aqueous solution of  $\text{NaHCO}_3$  solution followed by 10 mL of water, to trap  $^{18}\text{F}^-$  from the cyclotron.

(C) Kryptofix [2.2.2] vial.

(D) Anhydrous acetonitrile vial for the azeotropic evaporation.

(E) Precursor vial filled with the precursor dissolved in the reaction solvent.

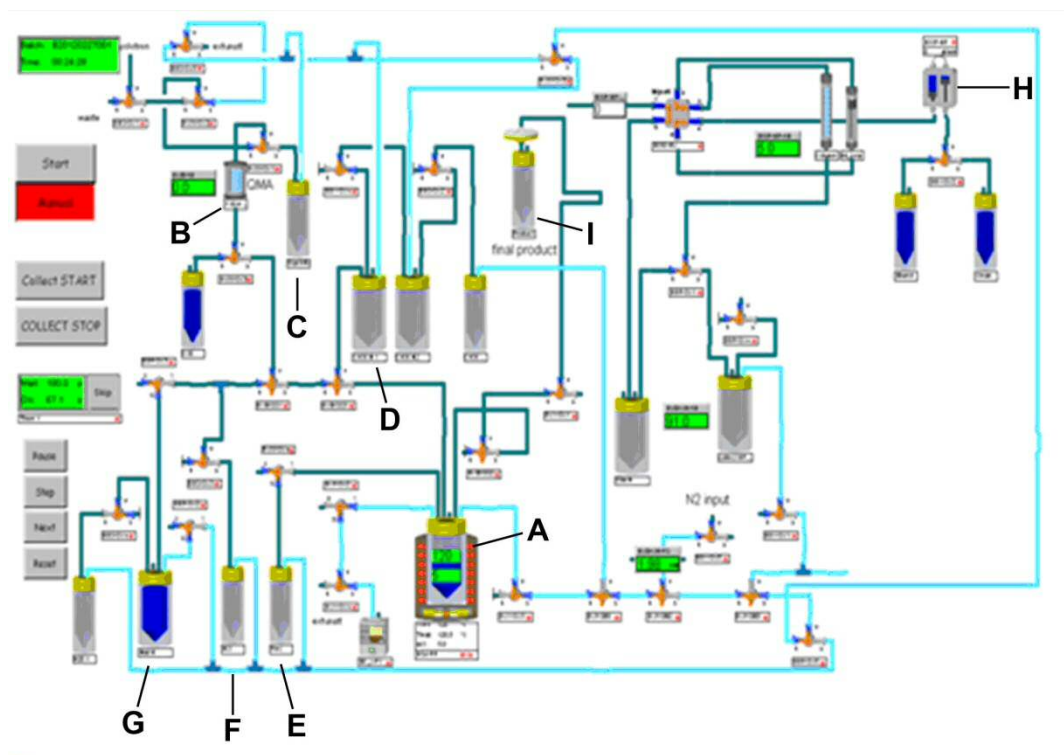
(F) Acid vial filled with 0.05M HCl for eventual deprotection.

(G) Base vial filled with 0.25M NaOH for eventual neutralization.

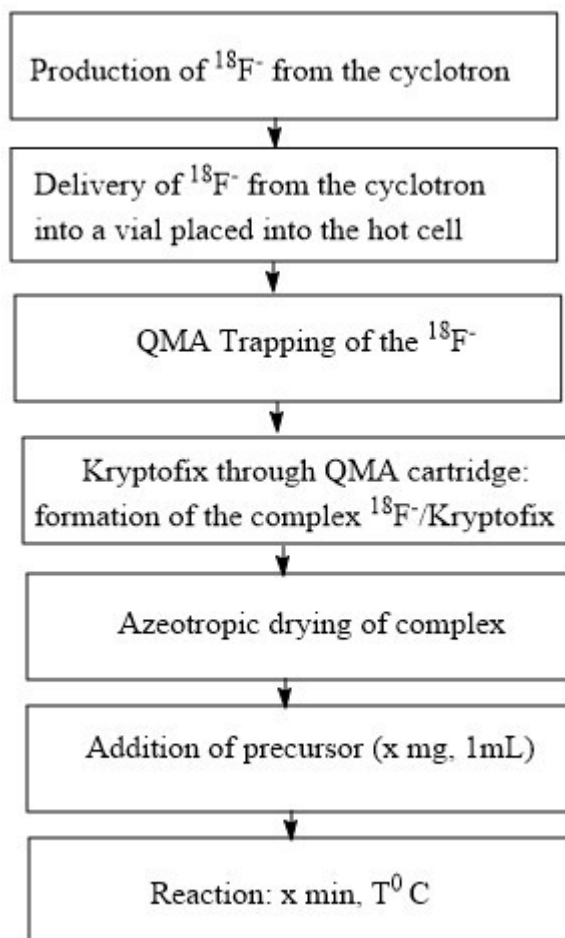
(H) Vacuum pump for solvent removal.

(I) Final product vessel for product isolation.

**Figure 3.24: Sketch of EZ Modular Lab**

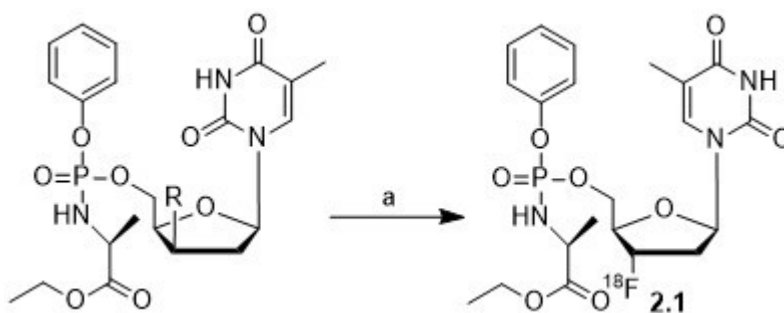


A flow chart of the process performed by the software program is shown in Figure 3.25.

**Figure 3.25: Flow chart of the synthetic steps in modular lab**

Several conditions have been explored for the hot fluorination. In particular the three essential requirements that can deeply influence the outcome of the radiolabelling are the time of the reaction (15-30 mins), the absolute anhydrous conditions (i.e absence of water and use of anhydride solvents) and the high temperature (90-120°C).

Reaction mixtures were analyzed by using a radio TLC and a radio HPLC. The reaction mixture was co-eluted with the cold reference standard in order to compare the retention time of the cold standard (detected with the UV detector) and of the radiolabelled compound (detected with the radioactive detector) on the HPLC system.<sup>52,140</sup>

**Figure 3.26: General conditions for the hot fluorination of the precursors**

**Reagents and conditions:** a) <sup>18</sup>F<sup>-</sup>, Kryptofix [K222], anh. solvent, x mins, T °C.

### 3.6.1 [<sup>18</sup>F]-Fluorination of the anhydride precursor (3.8)

The first attempts of [<sup>18</sup>F]-Fluorination have been carried out on the anhydride precursor (3.8) because of the easily accessible intermediate 3.5. Several reaction conditions have been explored as reported in Table 3.3.

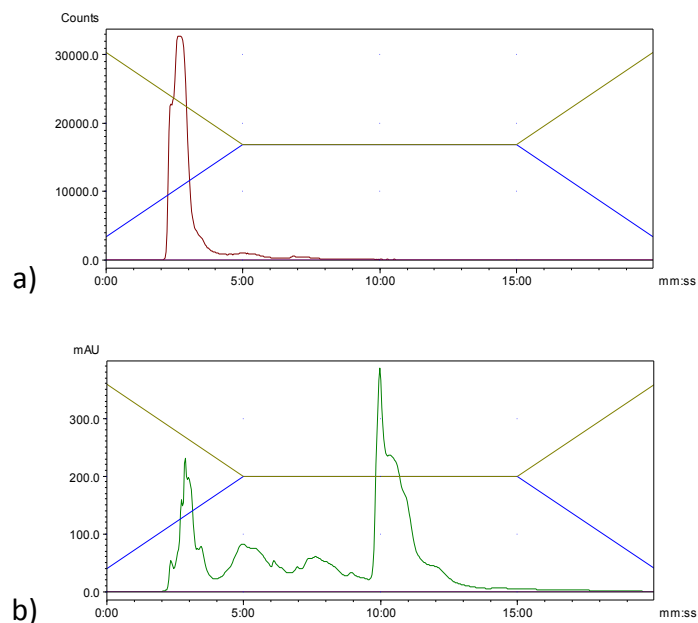
**Table 3.3: [<sup>18</sup>F]fluorination attempts on the anhydride precursor**

Precursor	Solvent	mg	T(°C)	Time	( <sup>18</sup> F)	<sup>18</sup> F-FLTProtide	<sup>18</sup> F-by-products
3.8	CH <sub>3</sub> CN	10	90°C	15min	3.1 GBq	No	No
3.8	CH <sub>3</sub> CN	10	90°C	20min	2.4 GBq	No	No
3.8	CH <sub>3</sub> CN	10	90°C	30min	1.3GBq	No	No
3.8	DMF	10	120°C	15min	876MBq	No	No
3.8	DMF	10	120°C	20min	2.1GBq	No	No
3.8	DMF	10	120°C	30min	2.9 G Bq	No	No

None of the reactions gave the desired radiolabelled product or any other radiolabelled by-products, returning just unreacted [<sup>18</sup>F]fluorine as shown also from the radio HPLC chromatograms (Figure 3.27).

**Figure 3.27: [18F]fluorination of compound 3.8**

a) Radioactive chromatogram of the reaction mixture showing free  $^{18}\text{F}^-$  at 3min; b) UV chromatogram of the reaction mixture co-spiked with the cold standard (**3.11**). (Rt of compound **3.11**: 10 min)



No other attempts have been performed as this precursor didn't show any reactivity towards the [18F]fluorination. This could be due to the poor reactivity of the 3'-position suggesting that the use of better leaving groups such as the mesyl, tosyl or nosyl is required for this type of reaction.

### 3.6.2 [18F]fluorination of the mesyl precursor (3.1)

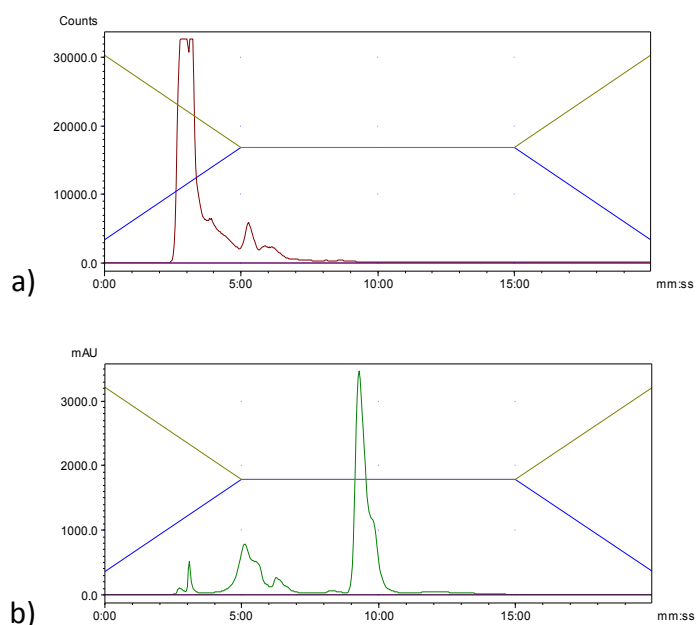
The second precursor tested was the mesyl precursor (**3.1**) because of its synthetic accessibility and because of its balance between reactivity and stability as leaving group. Similar reaction conditions to the ones used for the anhydride derivative have been tested for this step (Table **3.4**).

**Table 3.4: [ $^{18}\text{F}$ ]fluorination attempts on the mesyl precursor**

Precursor	Solvent	Mg	T(°C)	Time	( $^{18}\text{F}$ )	$^{18}\text{F}$ -FLTProtide	$^{18}\text{F}$ -by-products
<b>3.1</b>	DMF	10mg	120°C	15min	810 MBq	No	No
<b>3.1</b>	DMF	10mg	120°C	20min	2.35 GBq	No	No
<b>3.1</b>	DMF	10mg	120°C	30min	910 MBq	No	No
<b>3.1</b>	DMF	20 mg	120°C	15min	580 MBq	No	No
<b>3.1</b>	DMF	20 mg	120°C	20min	970 MBq	No	No
<b>3.1</b>	DMF	20 mg	120°C	30min	780 MBq	No	No

**Figure 3.28: [ $^{18}\text{F}$ ]fluorination of compound 3.1**

a) Radioactive chromatogram of the reaction mixture showing a major peak of free  $^{18}\text{F}$ - at 3min; b) UV chromatogram of the reaction mixture co-spiked with the cold standard (**3.11**). (Rt of compound **3.11**: 10 min)



As again no radiolabelled products were formed and only [ $^{18}\text{F}$ ]fluorine was returned unreacted, a larger amount of starting material was used (20 mg) to test whether this variable could influence the outcome of the reaction. In this case, the

reaction also did not give the desired product indicating that the amount of ProTide used as starting material was not a limiting factor for the successful outcome of the reaction.

### 3.6.3 [<sup>18</sup>F]fluorination of the tosyl precursor (3.2)

The third precursor used was the tosyl precursor (3.2) because of its reactivity towards fluorination but also better stability compared to the nosyl derivative (3.3) (Table 3.5).<sup>141</sup>

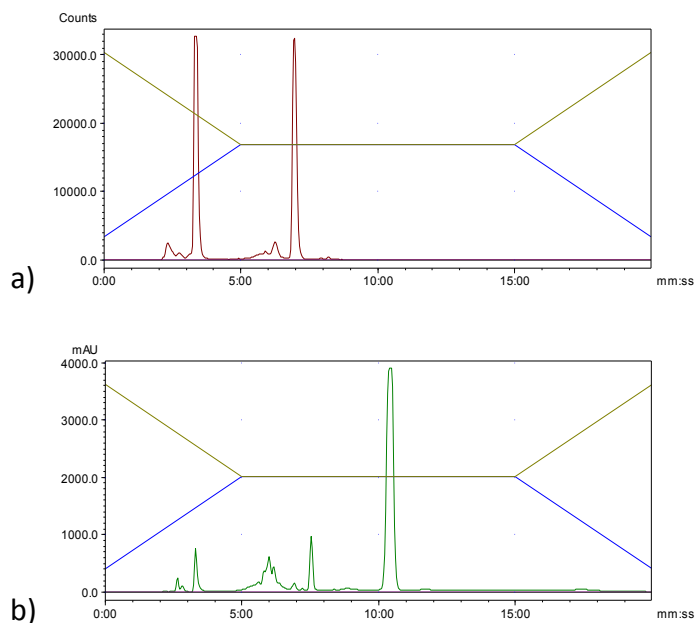
**Table 3.5: [<sup>18</sup>F]fluorination attempts on the tosyl precursor**

Precursor	Solvent	Mg	T(°C)	Time	( <sup>18</sup> F)	<sup>18</sup> F-FLTProtide	<sup>18</sup> F-by-products
<b>3.2</b>	CH <sub>3</sub> CN	10 mg	90°C	15min	2GBq	No	Yes
<b>3.2</b>	CH <sub>3</sub> CN	10 mg	90°C	20min	1.2 GBq	No	Yes
<b>3.2</b>	CH <sub>3</sub> CN	10 mg	90°C	30min	2.5 GBq	No	Yes
<b>3.2</b>	DMF	10 mg	120°C	15min	2.3 GBq	No	No

The tosyl precursor, compared to the previous anhydro and mesyl substituted precursors, finally gave, together with unreacted [<sup>18</sup>F]fluorine, a unique radiolabelled compound (Rt:7min) when the reaction was stirred for 30 mins at 90°C using acetonitrile as solvent.

**Figure 3.29: [ $^{18}\text{F}$ ]fluorination of compound **3.2****

a) Radioactive chromatogram of the reaction mixture showing free  $^{18}\text{F}$ - at 3.5min and a  $^{18}\text{F}$ -product at 7 min; b) UV chromatogram of the reaction mixture co-spiked with the cold standard (**3.11**). (Rt of compound **3.11**: 10.6 min)



Unfortunately the radiolabelled product did not have the expected retention time on the HPLC (Rt cold standard: 10 min) but the product proved to be slightly more polar than the cold standard, suggesting that the reaction time was a key factor and, that  $90^\circ\text{C}$  was enough as no precursor was left at the end of the reaction. In order to understand the identity of the product formed, a step back to cold chemistry was required. An attempt of cold fluorination on the tosyl derivative was performed and similar reaction conditions were tested. The reaction was indeed stirred at  $90^\circ\text{C}$  for 30 mins using KF as source of fluorine. Purification was performed by silica gel column chromatography but no clear  $^1\text{H}$  NMR and  $^{13}\text{C}$  NMR spectra were obtained because of the formation of many by-products and the challenging purification. Nevertheless, the  $^{19}\text{F}$  NMR showed two peaks at  $-200\text{ppm}$  as for the FLT ProTide (**3.11**).  $^{31}\text{P}$  NMR was also performed and showed the two characteristic peaks of the phosphoramidate moiety at around 3 ppm. This suggested that probably, the slight change in retention time was due to a loss of a moiety such as the ester on the L-alanine. Mass spectrometry did not

confirm this hypothesis showing a major peak at 453 that does not correspond to any of the substructures hypothesised.

### 3.6.4 [<sup>18</sup>F]fluorination of the nosyl precursor (3.3)

The fourth precursor, the nosyl derivative (3.3), was then used for the [<sup>18</sup>F]fluorination attempt. Among all precursors synthesised, although the nosyl is supposed to be the more reactive one, it is likely characterised by a lack of stability that could be a deterrent for its usage. All the conditions explored for this reaction are reported in Table 3.6.

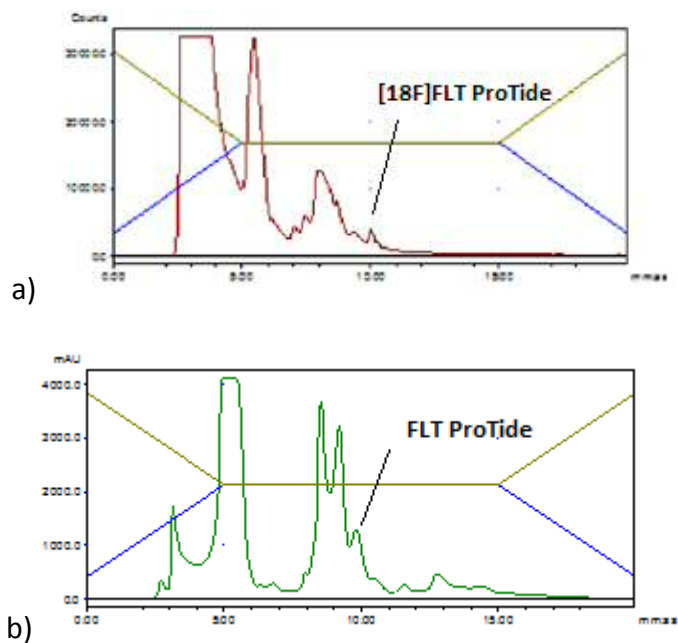
**Table 3.6: [<sup>18</sup>F]fluorination attempts of the nosyl precursor**

Precursor	Solvent	Mg	T(°C)	Time	( <sup>18</sup> F)	<sup>18</sup> F-FLTProtide	<sup>18</sup> F-by-products
<b>3.3</b>	CH <sub>3</sub> CN	10 mg	90°C	15min	1.2 GBq	No	Yes
<b>3.3</b>	CH <sub>3</sub> CN	10 mg	90°C	20min	1.5 GBq	Yes	Yes
<b>3.3</b>	CH <sub>3</sub> CN	10 mg	90°C	30min	2.3 GBq	Yes	Yes
<b>3.3</b>	CH <sub>3</sub> CN	10 mg	90°C	40min	2.2 GBq	Yes	Yes
<b>3.3</b>	DMF	10 mg	120°C	15min	734 MBq	No	Yes
<b>3.3</b>	DMF	10 mg	120°C	20min	1.1 GBq	No	Yes

Similarly, to the fluorination of the tosyl derivative, the major radiolabelled products had retention times of 5 and 8 mins as the major products of the reaction, together with many other more polar by-products. However, when the reaction was performed at 90°C for 30 mins in acetonitrile, also the desired [<sup>18</sup>F]FLT ProTide (2.1) was formed although in poor yields (Figure 3.30).

**Figure 3.30: [18F]fluorination of compound 3.3**

a) Radioactive chromatogram of the reaction mixture showing free  $^{18}\text{F}$ - at 3min, [18F]-by-products at 5 and 8 min and [18F]FLT ProTide at 10 min; b) UV chromatogram of the reaction mixture co-spiked with the cold standard (**3.11**). (Rt of compound **3.7**: 10 min)



To re-confirm this positive result, the same reaction was performed also on another automated synthetic modular lab (the GE FxFnTracerlab), at the Molecular Imaging Chemistry Laboratory (MICL) in the Wolfson Brain Imaging Centre of Cambridge University to prove the reproducibility of this reaction with different automated synthesisers (Figure 3.31).

**Figure 3.31: GE Healthcare TracerlabFxFn<sup>142</sup>**



The set up of this synthesiser was similar to the one of the E&Z one (Figure 3.32):

(A) Reaction vial.

(B) QMA cartridge preconditioned with 5 mL of a 8.4% aqueous solution of NaHCO<sub>3</sub> solution followed by 10 mL of water, to trap <sup>18</sup>F<sup>-</sup> from the cyclotron.

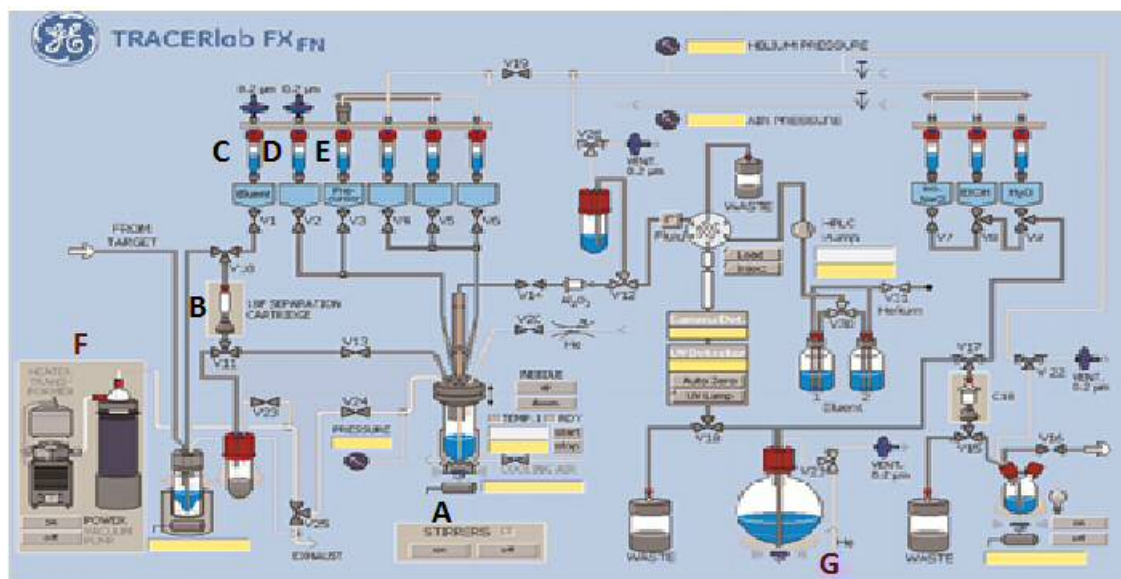
(C) Kryptofix [2.2.2] vial.

(D) Anhydrous acetonitrile vial for the azeotropic evaporation.

(E) Precursor vial filled with the precursor dissolved in the reaction solvent.

(F) Vacuum pump for solvent removal.

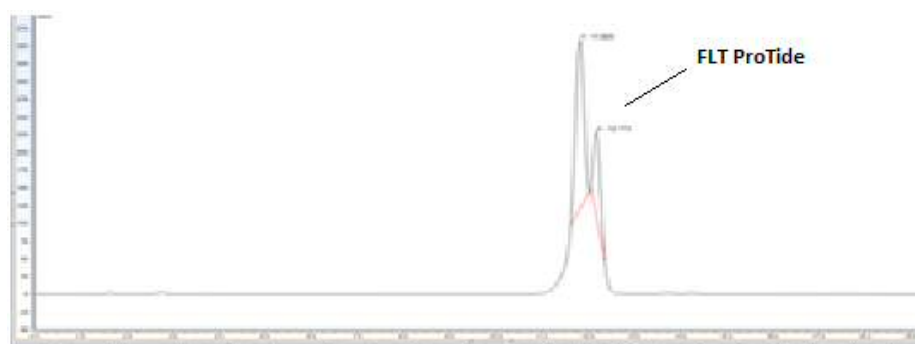
(G) Final product vessel for product isolation.

Figure 3.32: Sketch of Tracerlab Fx<sub>FN</sub>

For QC control the cold standard (**3.11**) was again run on a C18 column on an HPLC system this time using an isocratic elution (Figure 3.33).<sup>140</sup>

Figure 3.33: Analytical HPLC chromatogram of the cold standard

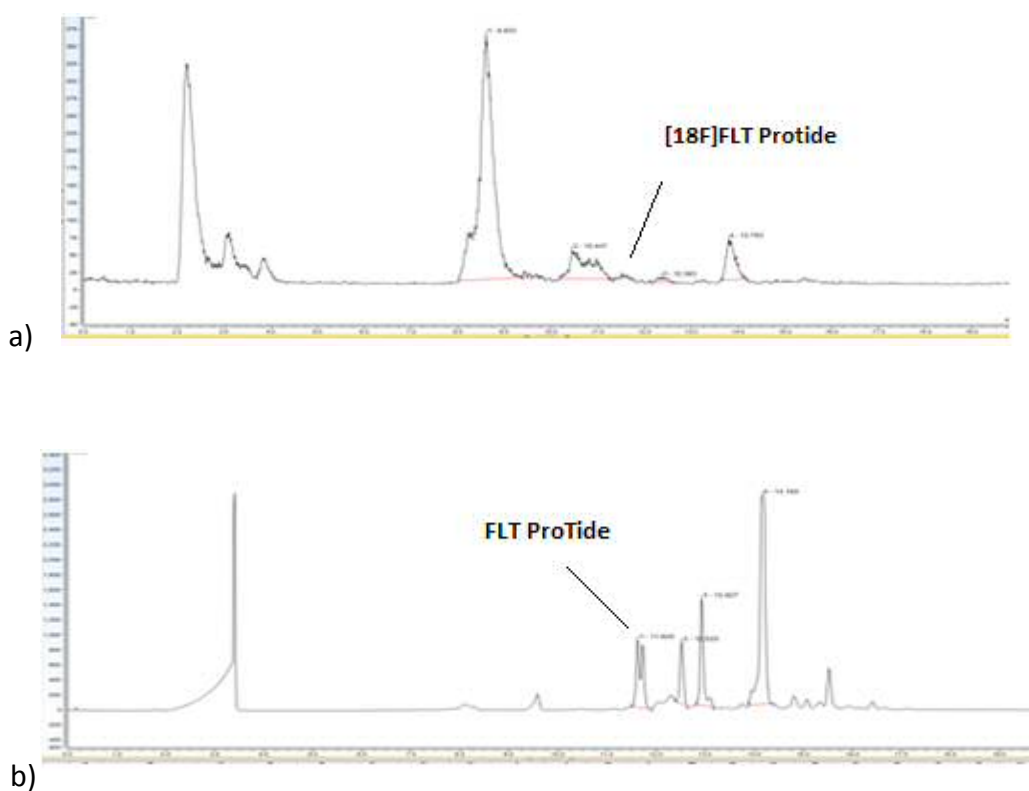
Isocratic system: 65% $\text{H}_2\text{O}$ -35% $\text{CH}_3\text{CN}$ ,  $R_t$  of the two diastereoisomers: 11.8 and 12.2 min.



Again the results of the hot fluorination were the same obtained as with the E&Z modular lab. A slight decrease in the yield of the reaction was observed but results obtained with the E&Z synthesiser were generally confirmed (Figure 3.34).

**Figure 3.34: [18F]fluorination of compound 3.3 with TracerLabFxFn**

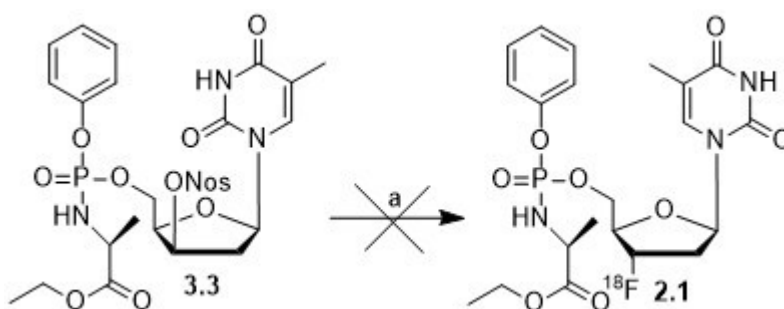
- a) Radioactive chromatogram of the reaction mixture showing many  $^{18}\text{F}$ -by-products and [18F]-FLT ProTide at 12 min; b) UV chromatogram of the reaction mixture co-spiked with the cold standard (3.11). (Rt of compound 3.11: 11.8-12.2 min)



Bearing in mind the future desired clinical application of the tracer, another variable was then introduced in the system to understand whether the reaction could be performed even without the use of Kryptofix which, despite being a good enhancer for the nucleophilicity of the [18F]-fluorine, is considered to be toxic when used in high quantity.<sup>143</sup>

This method replaces Kryptofix with the base tetraethylammoniumhydrogen carbonate that is dissolved in a polar aprotic solvent (MeCN, DMF, DMSO) containing up to 5% of water and it can be used to efficiently elute [18F]-fluoride from an anion-exchange cartridge (QMA, carbonate form) to produce tetraethylammonium [18F]fluoride. This method has been widely applied for different aliphatic and aromatic radiosyntheses allowing [18F]-nucleophilic substitution by avoiding the use of Kryptofix and eliminating the long azeotropic drying procedures<sup>144</sup> (Figure 3.35).

**Figure 3.35: Hot fluorination of the nosyl derivative without the use of Kryptofix as reagent**



**Reagents and conditions:** a)  $^{18}\text{F}$  (2.3 GBq),  $\text{Et}_3\text{NHCO}_3$ , anh.  $\text{CH}_3\text{CN}$ ,  $90^\circ\text{C}$ , 30 min.

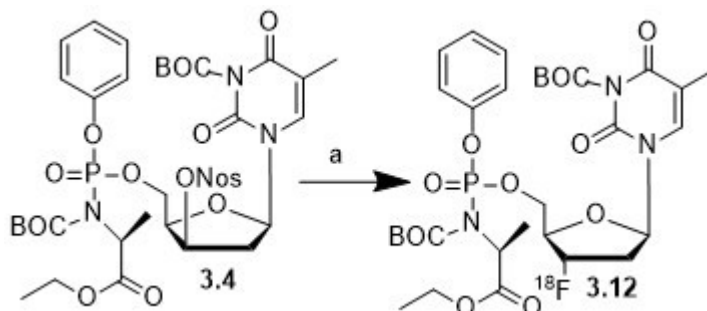
As no positive increase in the yield was observed, the next step was the protection of the two NH moieties of the nosyl derivative that could interfere with the reaction outcome thus decreasing the percentage of formation of the desired product.

### 3.6.5 [18F]fluorination of the nosyl BOC protected precursor (3.4)

The addition of the two BOC protecting groups should avoid the formation of some of the by-products hypothesised and in particular of the anhydride derivative and of the cyclised ProTide. In this case the fluorination does not represent the last step but it has to be followed by a short deprotection step.<sup>145,146</sup> In order to perform this reaction, the E&Z modular lab was re-programmed in order to add a deprotection step to the reaction. When the reaction was tested, the first attempt eventually gave

the desired radiolabelled [ $^{18}\text{F}$ ]-BOC protected FLT ProTide under the following conditions (Figure 3.36).

**Figure 3.36: Hot fluorination of the BOC protected nosyl derivative (3.4)**

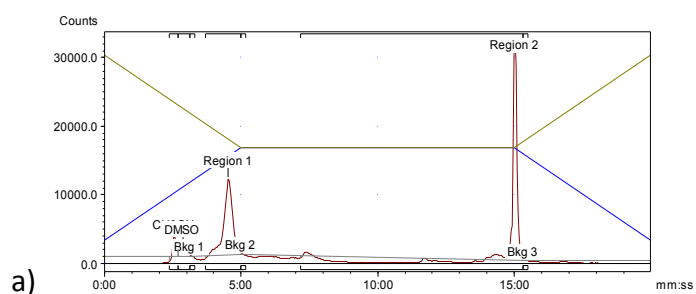


**Reagents and conditions:** a)  $^{18}\text{F}^-$  (2.5GBq), Kryptofix, anh.  $\text{CH}_3\text{CN}$ ,  $90^\circ\text{C}$ , 30 min.

After 30 mins of radiolabelling at  $90^\circ\text{C}$ , the reaction mixture was passed through an Al cartridge to remove the excess unreacted  $^{18}\text{F}^-$ . An aliquot of the reaction mixture was then taken and injected into the HPLC showing a major product with a retention time at around 15 mins. This suggested that the desired BOC radiolabelled product was formed therefore supporting the hypothesis that the BOC protection provides a better stability to the nosyl precursor.

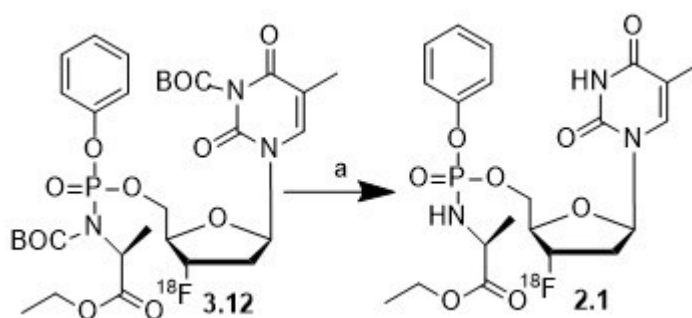
**Figure 3.37: [ $^{18}\text{F}$ ]fluorination of compound 3.4**

a) Radioactive chromatogram of the reaction mixture showing BOC-protected [ $^{18}\text{F}$ ]FLT ProTide at 15 min



The solvent was then removed from the reaction mixture at 95 °C under a stream of nitrogen in a separate heating module. The deprotection step was carried out by adding product **3.12** to the stirring reaction mixture of 1mL of 2N HCl for 10 mins at 95°C.<sup>1</sup>

**Figure 3.38: Deprotection of the BOC [18F]-intermediate**

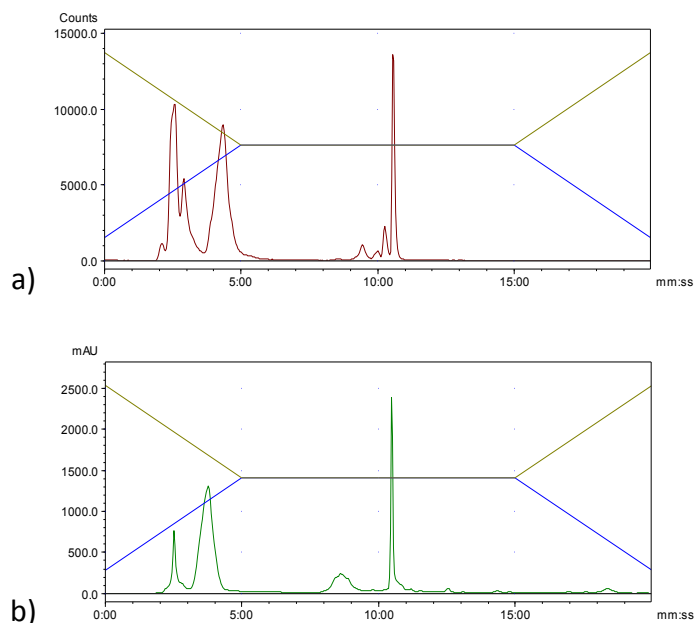


**Reagents and conditions:** a) 2M HCl, 95°C, 10 min.

Neutralisation was then performed with a 2M NaOH solution. An aliquot of the reaction mixture was taken and co-injected with the cold standard into the HPLC. Gratifyingly the major product of this reaction was the [18F]FLT ProTide with few other minor by-products

**Figure 3.39: Deprotection of compound 3.12**

a) Radioactive chromatogram of the reaction mixture showing [18F]FLT ProTide as major peak at 10.8 min; b) UV chromatogram of the reaction mixture co-spiked with the cold standard (**3.11**). (Rt of compound **3.11**: 10.7 min)

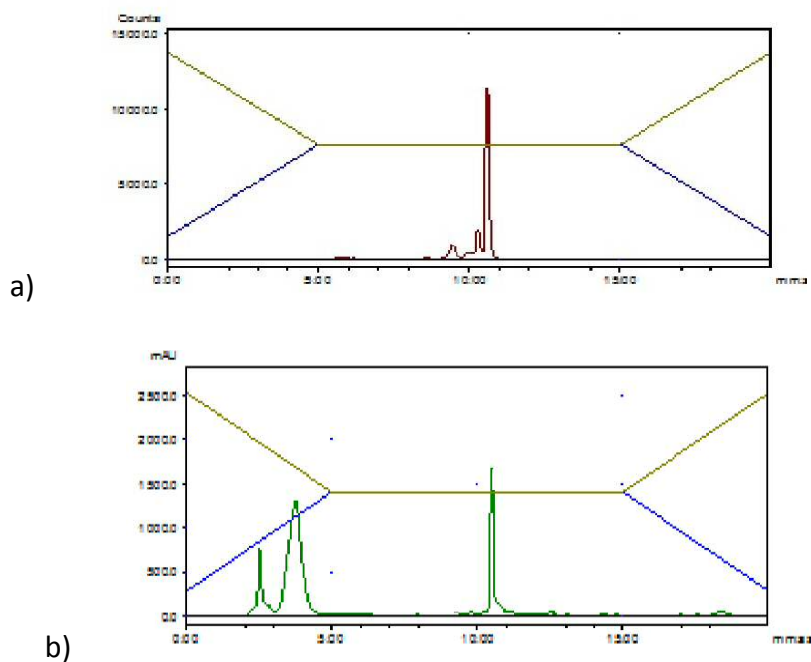
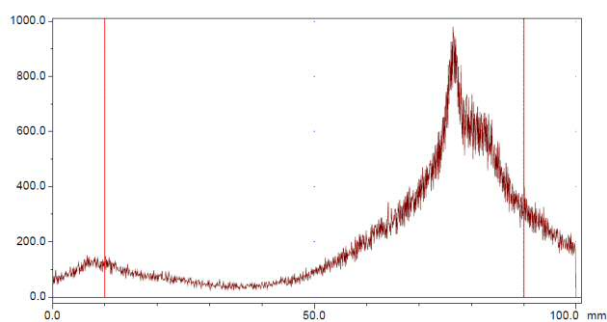


The compound was then purified by semi-preparative HPLC and was eluted after 35 minutes at a flow rate of 3.5 mL/min using 30% CH<sub>3</sub>CN/70% H<sub>2</sub>O as the mobile phase. The HPLC solvent was then removed from the mixture under a stream of nitrogen. The radioactive product was taken up in saline and subsequently flushed through a sterility filter to obtain a sterile and clean aqueous solution of [18F]FLT ProTide.

An aliquot of the purified sample was analysed by HPLC (Figure 3.39) via co-elution with the cold standard. Radiochemical reactions were carried out using starting activities between 1.5-8 GBq, leading to final product activities of 240-480MBq in a highly respectable RCY of 15-30% (n=5, decay-corrected from end of bombardment (EoB)), with high radiochemical purities (97%) and specific activities 1800 mCi/μmol. The total synthesis time was 130 min after the end of bombardment (EoB).

**Figure 3.40: Purified [18F]FLT ProTide**

- a) Radioactive chromatogram of the purified [18F]FLT ProTide with Rt: 10.8 min ,  
 b) UV chromatogram of the reaction mixture co-spiked with the cold standard  
 with Rt: 10.7 min.

**Figure 3.41: Radio-TLC chromatogram of the purified [18F]FLT ProTide**

### 3.7 Conclusions

Five potential precursor molecules of the [18F]FLTProTide (**2.1**) and a cold reference standard, the [19F]FLT ProTide (**3.11**), have been synthesised using cold

chemistry methods. Late stage [18F]fluorination was performed on all the precursors synthesised exploring different reaction conditions. The nosyl derivate (**3.3**) furnished the desired product in poor yield therefore protection of the NH moieties of the molecule was performed in order to minimize the formation of undesired side products. This protection markedly increased the yield of the reaction furnishing the desired radiolabelled BOC protected compound. This compound was then deprotected to finally furnish the desired target compound **2.1**. This is the first time to our knowledge that a radiolabelled ProTide has been synthesised.

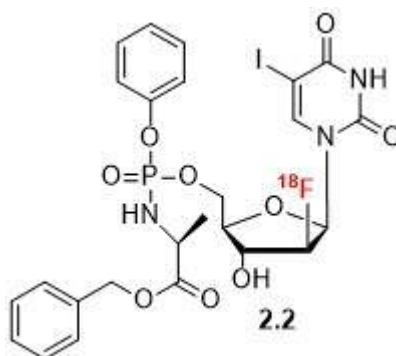
However, the results here presented should be regarded as first trials of the synthesis of [18F]radiolabelled ProTides. Further investigations with different set-ups (e.g. different automated synthetic modules, microwave-assisted synthesis) should be carried out to validate the reproducibility and clinical potential application of this radiosynthesis.<sup>9,45,145</sup>

## 4. Radiochemical synthesis of [18F]FIAU ProTide

### 4.1 Introduction

Besides the late stage [18F]fluorination approach discussed in Chapter 3, another synthetic pathway involving an early stage [18F]fluorination has been followed to access a different class of radiolabelled compounds, the 2'-[18F]FIAU ProTides (Figure 4.1).

Figure 4.1: Structure of the 2'-[18F]FIAU ProTide target (2.2)



[18F]FIAU (**1.16**) is already a well known PET imaging probe used as a biomarker for imaging HSV1-*tk* gene expression.<sup>146</sup> Reporter gene imaging is a non invasive technique used in live subjects to determine location, duration and extent of expression of the gene of interest.<sup>147-150</sup> In particular Herpes simplex virus-1 thymidine kinase (HSV1-*tk*) is one of the genes most widely used as a reporter in molecular imaging to visualise and monitor many biological processes including lymphocyte migration<sup>151</sup>, transcriptional regulation<sup>152</sup>, and stem-cell tracking.<sup>153,154</sup> Radiolabelled nucleoside analogues, such as [18F]FIAU, can be used for monitoring HSV1-*tk* gene expression using PET imaging.<sup>54</sup>

[18F]FIAU ProTide has been chosen as a model standard for the class of the 2'-fluorinated ProTides for the following reasons:

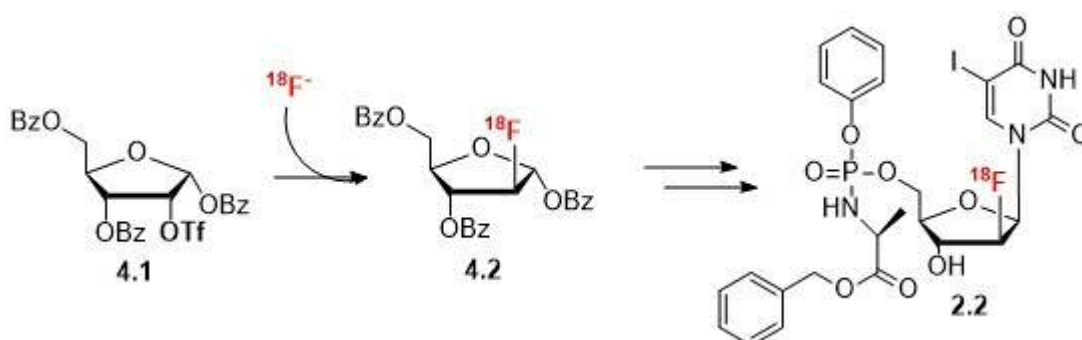
- Fluorine is placed in position 2' on the sugar moiety therefore it can be used as model standard for the radiochemical synthesis of other 2'-[18F]ProTides.

- [18F]FIAU (**1.16**) is a PET imaging probe and many synthetic strategies have already been extensively explored<sup>45,116,132,155</sup> and can be used as a guide for the synthesis of its ProTide. Additionally studies of retention of [18F]-FIAU on HEK (human equilibrative kidney) cells engineered to express HSV- *tk1* can be useful to prove the successful synthesis of this tracer.
- It is a uridine based ProTide, thus the absence of other reactive sites on the nucleobase moiety of the molecule will avoid further protection and deprotection steps.

## 4.2 [18F]fluorination (Hot): early stage approach

Among many synthetic approaches, the only one reported in the literature which gives [18F]FIAU in good yields consists of an early stage hot fluorination of the sugar moiety followed by a multi-step synthesis<sup>155</sup> that has to be performed in a relative short time taking into account the half life of the [18F]fluorine (an ideal synthesis should not exceed three half lives)<sup>1</sup>. A similar synthetic pathway to that of [18F]FIAU will be applied for the synthesis of its ProTide according to the scheme outlined in Figure 4.2.

**Figure 4.2: Early stage fluorination approach for the synthesis of the [18F]FIAU ProTide (2.2)**



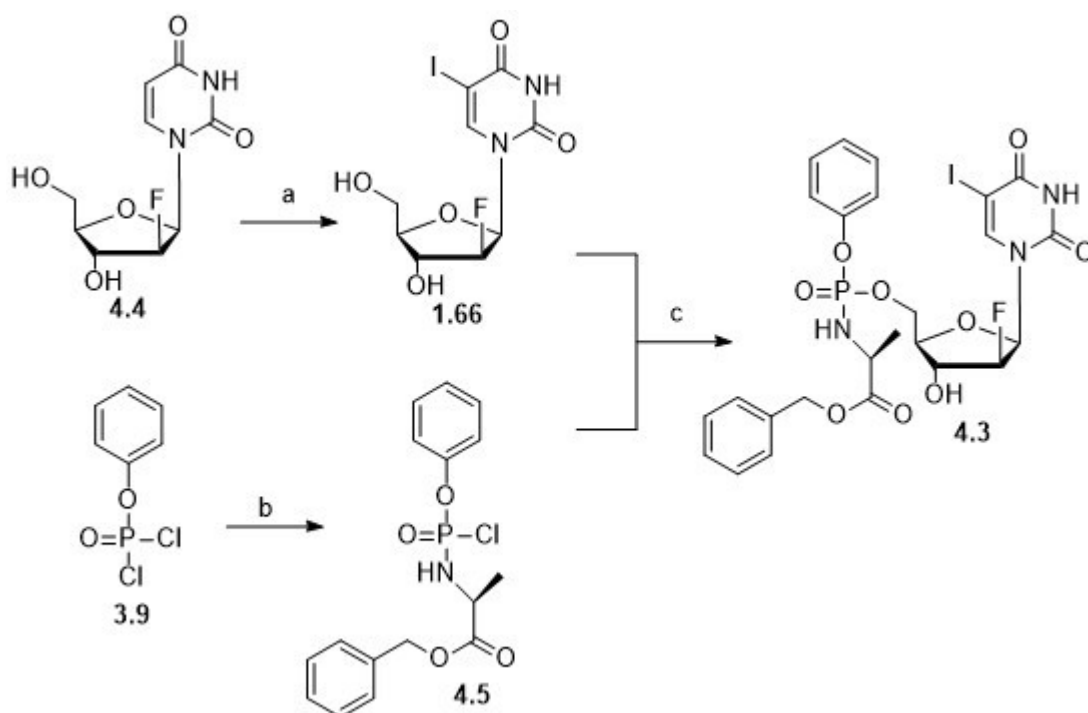
Although the early stage hot fluorination is considered not to be ideal when a multi-step synthesis has to be performed, the advantage consists in the radiolabelling

step that does not give any by-products thus providing a compound that can be used for the next steps without further purification.

### 4.3 Synthesis of the cold standard (4.3)

Again a cold standard, the FIAU ProTide (**4.3**), was synthesised in order to have a reference compound to co-inject into the analytical HPLC together with the radiolabelled compound as a proof of the successful outcome of the reaction.<sup>140</sup> As the synthesis of [18F]FIAU is well known, no attempts at cold fluorination were performed to test the reactivity towards nucleophilic substitution performed by the fluoride on the triflate group of the precursor molecule **4.1**. Therefore the synthesis of the cold standard was accomplished following the synthetic scheme in Figure **4.3**.

**Figure 4.3: Synthesis of the cold standard FIAU ProTide (4.3)**

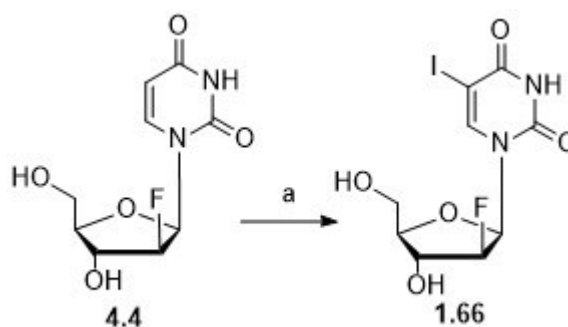


**Reagents and conditions:** a) I<sub>2</sub>, Ceric ammonium nitrate, CH<sub>3</sub>CN, 75°C, 1h, 60%; b) L-alanine benzyl ester hydrochloride salt, Et<sub>3</sub>N, -75°C to rt, anh. CH<sub>2</sub>Cl<sub>2</sub>, 3h, 88%; c) NMI, anh. THF, 0°C to rt, 16h, 12%.

The commercially available 2'-deoxy-2'-β-fluoro-uridine (**4.4**) was used as starting material of the synthesis (Figure **4.4**). I<sub>2</sub> was used as reagent to perform the iodination reaction in position 5 of the pyrimidine ring and ceric ammonium nitrate

was used as catalyst and oxidant to speed up the reaction rate.<sup>156,157</sup> After 1 hour of refluxing at 75°C the starting material was all converted into the product. The reaction was then quenched with a saturated solution of Na<sub>2</sub>S<sub>2</sub>O<sub>3</sub> to remove any unreacted highly toxic iodine, and the product was extracted into ethyl acetate and used for next step without any further purification.

**Figure 4.4: Iodination of the starting material (4.4)**

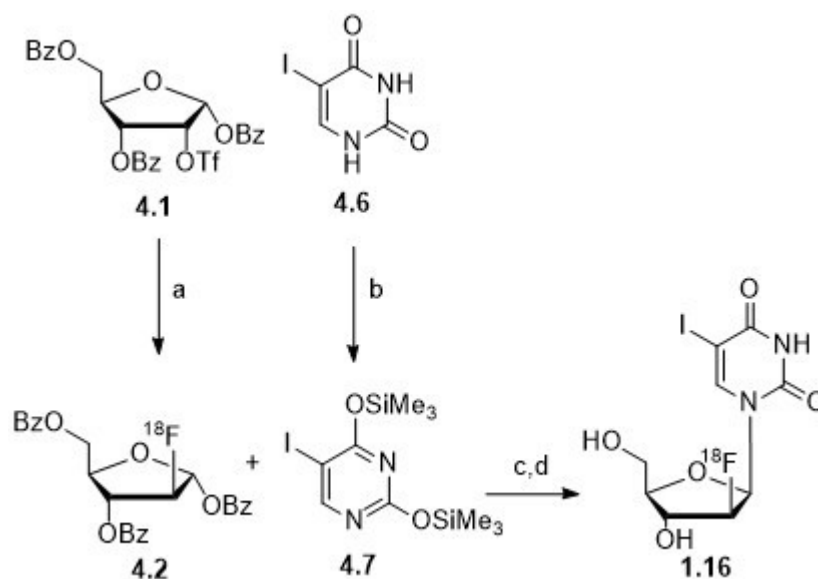


**Reagents and conditions:** a) I<sub>2</sub>, Ceric ammonium nitrate, CH<sub>3</sub>CN, 75°C, 1h, 60%.

Step b and c were performed according to the standard procedure for the synthesis of ProTides<sup>128</sup> to furnish the final compound 4.3 with a yield of 11%.

### 4.3 Synthesis of [18F]FIAU (1.16)

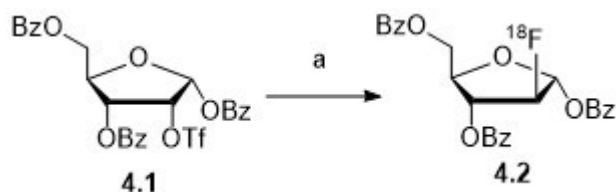
For the synthesis of the [18F]FIAU the following synthetic procedure reported in literature has been followed (Figure 4.5).<sup>45</sup>

**Figure 4.5: Radiochemical synthesis of [18F]FAIU (1.16)**

**Reagents and conditions:** a)  $^{18}\text{F}^-$ , Kryptofix, anh.  $\text{CH}_3\text{CN}$ ,  $95^\circ\text{C}$ , 30 min; b) Hexamethyldisilaxane, TMSOTf, anh. dichloroethane,  $85^\circ\text{C}$ , 2h; c) anh.  $\text{CH}_3\text{CN}$ ,  $85^\circ\text{C}$ , 1h; d)  $\text{NaOCH}_3/\text{CH}_3\text{OH}$ ,  $80^\circ\text{C}$ , 10 min.

Compared to the other reported radiosyntheses of this tracer, this one has the advantage of avoiding the bromination step in position 2 of compound **4.2** before the coupling with **4.7**.<sup>54,155</sup> Therefore a shorter synthesis is obtained with also the advantage of avoiding the usage of the highly toxic  $\text{Br}_2$  reagent.

The first step consists of the hot fluorination of the commercially available starting material sugar **4.1**. In this case the leaving group is the triflate, one of the best leaving groups amongst the organosulfonates.<sup>158</sup> The reaction was carried out using the E&Z modular lab following the same procedure described in Chapter 3. The conditions for the radiolabelling are reported below.

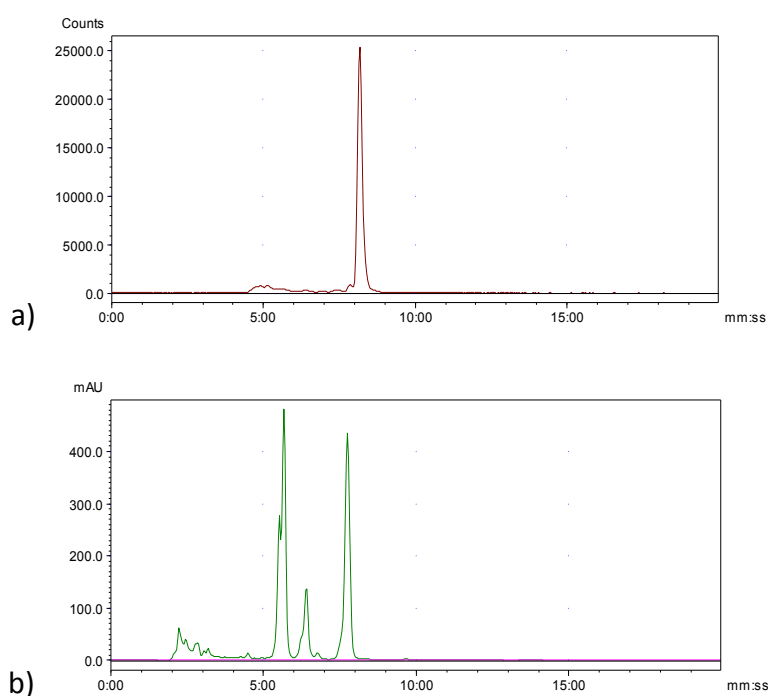
**Figure 4.6: Synthesis of the [18F]-sugar (4.2)**

**Reagents and conditions:** a)  $^{18}\text{F}^-$ , Kryptofix, anh.  $\text{CH}_3\text{CN}$ ,  $95^\circ\text{C}$ , 30 min.

After purification with an alumina cartridge (characterized by an extremely polar surface for analyte retention) to eliminate the excess of free  $^{18}\text{F}^-$ ,<sup>41</sup> the radiolabelled sugar (**4.2**) was produced and used for next step without further purification. When an aliquot of the hot mixture was co-spiked with the cold standard (commercially available), it showed the same retention time at around 8 min as shown in Figure 4.7.

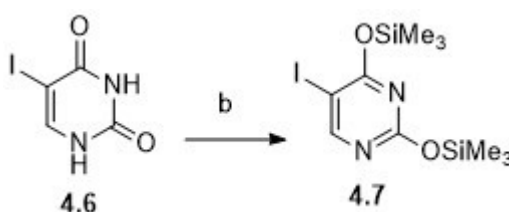
**Figure 4.7: [18F]fluorination of compound 4.1**

- a) Radioactive chromatogram of the reaction mixture showing the [18F]-sugar **4.2** as the unique product of the reaction with Rt of 8.2 min; b) UV chromatogram of the reaction mixture co-spiked with the cold standard. (Rt of commercially available cold standard: 7.9 min). b) HPLC system: 98%  $\text{CH}_3\text{CN}$ , 2%  $\text{H}_2\text{O}$ .



The second step consists in the protection of the base moiety that was freshly synthesised while the hot fluorination was ongoing in a second heating module placed into the hot cell next to E&Z modular lab. Hexamethyldisilaxane was used as protecting reagent and trimethylsilyltrifluoromethanesulfonate (TMSOTf) was used as catalyst to activate the following glycosylation reaction<sup>45</sup>(Figure 4.8). To confirm that the reaction was complete, HPLC and LC-MS were performed.

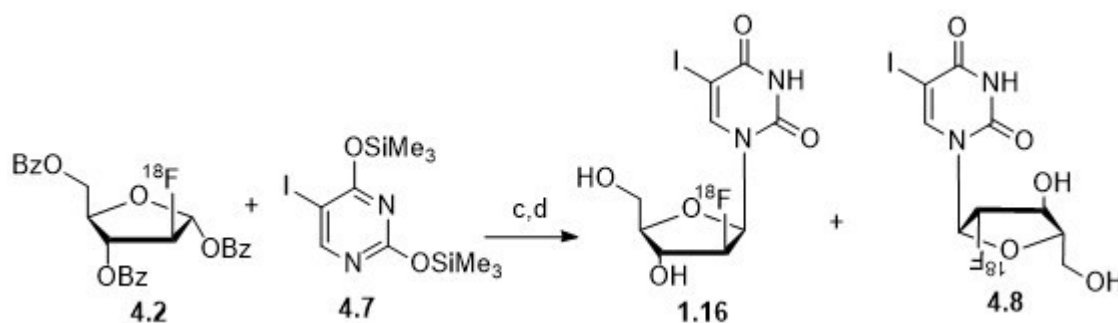
**Figure 4.8: Protection of the 5-Iodouracil (4.5)**



**Reagents and conditions:** b) Hexamethyldisilaxane, TMSOTf, anh. DCE, 85°C, 2h.

Compound **4.7** was dried at 90°C under compressed air to remove the dichloroethane solvent, obtaining a yellowish oil. The radiolabelled sugar (**4.2**) (in CH<sub>3</sub>CN solution) was then delivered directly from the E&Z unit to the vial containing the protected uracil (**4.7**) to perform the glycosylation reaction followed by a quick deprotection step as shown in Figure 4.9. The glycosylation is known to be a non-stereoselective reaction because of the formation of a new stereogenic centre.<sup>159</sup> Indeed two anomers were formed from this reaction, the β-anomer (the [18F]FIAU (**1.16**) and the α-anomer (**4.7**).<sup>155</sup>

**Figure 4.9: Synthesis of protected  $\beta$ -anomer of [18F]FIAU (1.16) and the  $\alpha$ -anomer (4.8)**

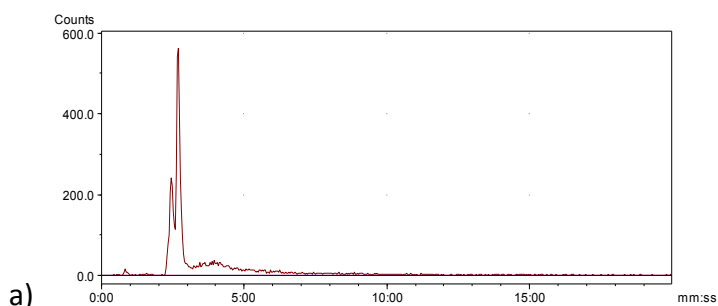


**Reagents and conditions:** c) anh. CH<sub>3</sub>CN, 85°C, 1h ; d) NaOCH<sub>3</sub>/CH<sub>3</sub>OH, 80°C, 10 min.

An aliquot of the reaction mixture was taken for analytical evaluation. The  $\alpha$  and the  $\beta$  anomers were formed in a ratio 1 to 2 as also reported in literature.<sup>45,132,155</sup>

**Figure 4.10: Deprotection reaction**

a) Radioactive chromatogram of the reaction mixture showing the two anomers at 2.1 min ( $\alpha$  anomer, 4.8) and at 2.9 min ( $\beta$  anomer, [18F]FIAU, 1.16). HPLC system: 98% H<sub>2</sub>O, 2% CH<sub>3</sub>CN.

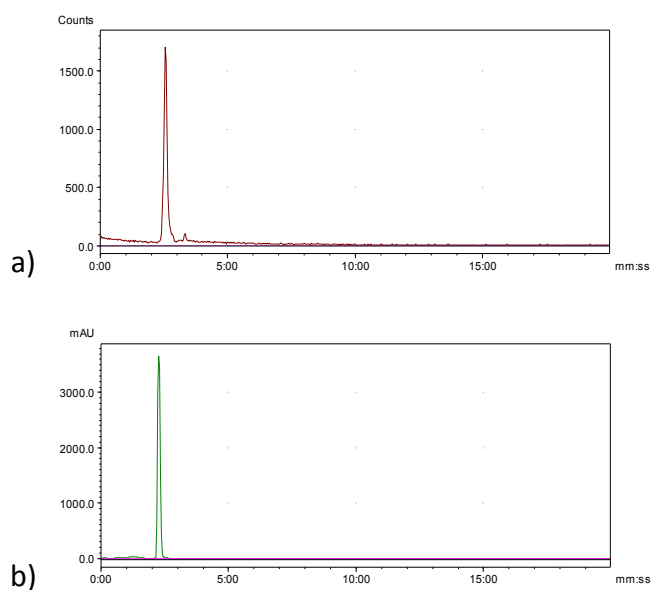


The anomeric mixture was then purified by semi-preparative HPLC and was eluted after 7.3 minutes at a flow rate of 3.5 mL/min using 20% CH<sub>3</sub>CN/80% H<sub>2</sub>O as the

mobile phase. An aliquot of the purified compound was taken for analytical HPLC evaluation and co-spiked with the cold standard.

**Figure 4.11: [18F]FIAU purification**

a) Radioactive chromatogram of the [18F]FIAU (**1.16**) showing the product with Rt of 2.3 min; b) UV chromatogram of the reaction mixture co-spiked with the cold standard (**1.61**). (Rt of cold standard: 2.1 min). HPLC system: 98% H<sub>2</sub>O, 2% CH<sub>3</sub>CN.



The radiolabelled compound showed the same retention time as the standard and also literature strongly supports that the elution time of the  $\beta$ -anomer is longer than the  $\alpha$ .<sup>45</sup> Nevertheless an additional biological evaluation of the tracer was performed to support the isolation of the correct anomer (see section 4.6).

In order to optimise and speed up the glycosylation step, several conditions and combination of catalysts were explored (Table 4.1).<sup>10,45</sup>

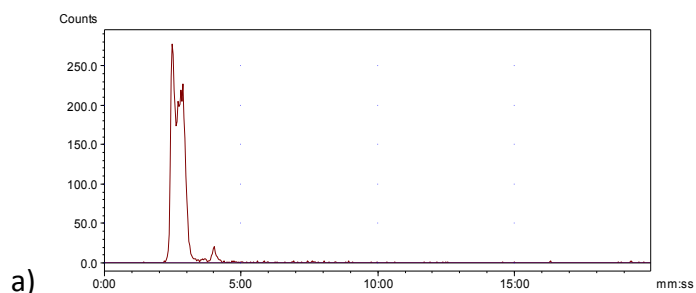
**Table 4.1: Attempts for the hot glycosylation reaction**

Solvent	Temperature	Time	Catalyst	Ratio $\beta$ : $\alpha$
CH <sub>3</sub> CN	85°C	30min	TMSOTf	Incomplete
CH <sub>3</sub> CN	85°C	45min	TMSOTf	Incomplete
CH <sub>3</sub> CN	85°C	1h	TMSOTf	2:1
CH <sub>3</sub> CN	95°C	30 min	TMSOTf	Incomplete
CH <sub>3</sub> CN	85°C	15 min	TMSOTf+SnCl <sub>4</sub> <sup>1</sup>	1:1.3

However, despite improving the rate of the synthesis when using a combination of catalysts, also the ratio changed favouring the formation of the  $\alpha$ -anomer (Figure 4.12).

**Figure 4.12: Deprotection reaction when using TMSOTf and SnCl<sub>4</sub> as catalysts**

a) Radioactive chromatogram of the reaction mixture showing the two anomers at 2.2 min ( $\alpha$  anomer, **4.8**) and at 2.4 min ( $\beta$  anomer, [18F-FIAU], **1.6**). HPLC system: 98% H<sub>2</sub>O, 2% CH<sub>3</sub>CN.

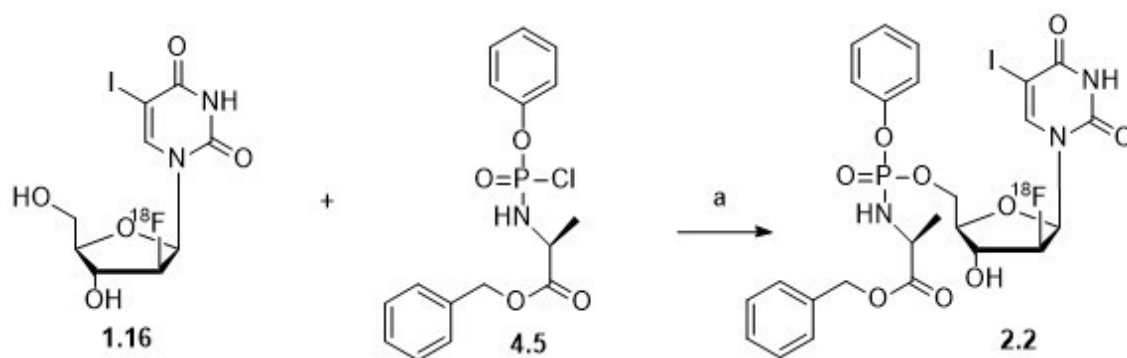


Therefore, based on these attempts at optimisation of reaction conditions, the synthetic pathway in Figure 4.9 was established as the more suitable for synthesis of [18F]FIAU.

## 4.5 Synthesis of the [18F]FIAUProTide (2.2)

Finally the last step consisted in the coupling between the [18F]FIAU (**1.16**) and the phosphorochloridate (**4.5**) previously synthesised according to the standard procedure described in Chapter 3.<sup>128</sup>

**Figure 4.13: Synthesis of the [18F]FIAUProTide (2.2)**



**Reagents and conditions:** a) NMI, anh. THF, 50°C, 20 min.

This step, as reported in literature, normally takes 16h or more to be completed. Therefore, preliminary studies to optimise the duration of this step were performed *via* cold chemistry. The cold reaction was carried out at rt, 30°C, 40°C and 50°C to reduce the reaction time as much as possible. When this step was performed at 50°C, the coupling was completed after 20 mins. Hence these conditions were applied for the radiochemical synthesis.

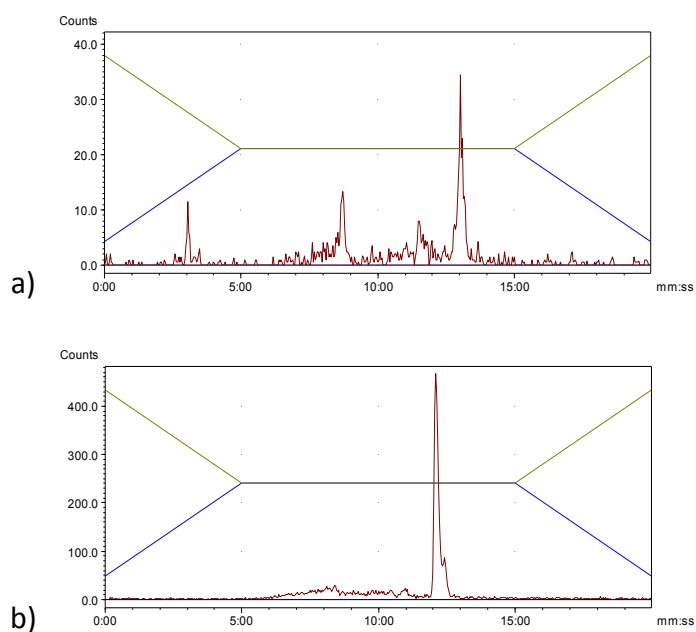
A solution of the phosphorochloridate (**4.5**) in anhydrous THF was added manually to the vial containing [18F]FIAU (**1.16**) which was previously dried under compressed air to eliminate the solvent residue from the semi-preparative HPLC separation. The reaction was allowed to stir for 20 min at 50°C and then dried under a flow of nitrogen, re-dissolved in CH<sub>3</sub>CN and an aliquot was taken to perform an analytical HPLC run. [18F]FIAU ProTide (**2.2**) was the main product of the reaction as shown in Figure 4.14. The major peak was isolated *via* semi preparative HPLC and was eluted after 23 minutes at a flow rate of 3.5 mL/min using 50% CH<sub>3</sub>CN/50% H<sub>2</sub>O as the mobile phase. The HPLC solvent was removed from the mixture under a stream of

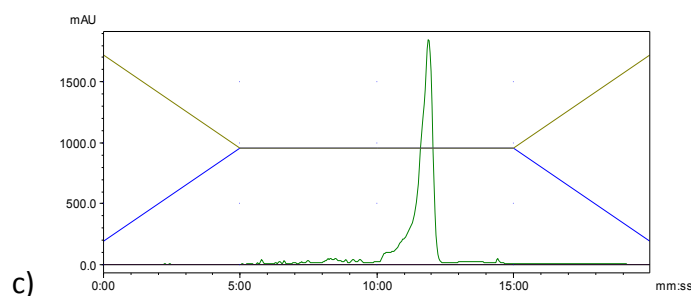
nitrogen. The radioactive product was taken up in saline and subsequently flushed through a sterility filter to obtain a sterile and clean aqueous solution of [18F]FIAU ProTide.

An aliquot of the purified sample was analysed by analytical HPLC via co-elution with the cold standard as shown in Figure 4.14. Radiochemical reactions were carried out using starting activities between 7-15 GBq, leading to final product activities of 8-56 MBq in a RCY of 1-5% (n=7, decay-corrected from end of bombardment (EoB)), with high radiochemical purities (98%) and specific activities of 1800 mCi/ $\mu$ mol. The total synthesis time was 240 min after the end of bombardment (EoB).

**Figure 4.14: Synthesis of [18F]FIAU ProTide**

a) Radioactive chromatogram of the [18F]FIAU ProTide reaction mixture showing a major peak with Rt of 13 min; b) Radioactive chromatogram of the [18F]FIAU ProTide purified with Rt of 12.3 min; c) UV chromatogram of the [18F]FIAU ProTide co-spiked with the cold standard (4.3). (Rt of cold standard: 12.2 min). HPLC system: 90% H<sub>2</sub>O-10% CH<sub>3</sub>CN to 50% H<sub>2</sub>O-50% CH<sub>3</sub>CN.





## 4.6 Evaluation of the radiotracer [18F]FIAU (1.16) on HSV-TK engineered HEK cell lines

Human embryonic kidney cells 293, also referred to as HEK 293 or simply HEK cells, are specific cell lines originally derived from human embryonic kidney cells grown in tissue culture. They have been widely used in cell biology because of their reliable growth and propensity for transfection. Additionally, they are used in the biotechnology industry and gene therapy.<sup>160</sup>

This series of experiments was carried out alongside Dr. Stephen Paisey of the Positron Emission tomography Imaging Centre (PETIC) at Cardiff University. The hypothesis of these experiments is that HEK cells engineered to express the herpes simplex thymidine kinase will retain higher levels of radioactivity, than the wild type cells, after radiolabelling with [18F]FIAU ( $H_1$ ).

$$H_0 : \mu_{TK} \leq \mu_{HeK}$$

$$H_1 : \mu_{TK} > \mu_{HeK}$$

This will be additional proof for the successful synthesis of the correct anomer ( $\beta$ ) ([18F]FIAU, **1.16**) discussed in section 4.4 because of the known affinity of HSV-tk cells towards this tracer.<sup>138</sup>

HEK 293 cells were previously transfected to contain PC-DNA expressing the herpes simplex virus thymidine kinase (TK-HEK), ampicillin resistance and neomycin were also used. The [18F]FIAU synthesised was used for the radiolabelling. 8.1 MBq of activity of [18F]FIAU in 1mL of water were diluted in 30ml of phosphate buffered saline solution and split into 6 samples of 5 mL. The radioactive FIAU PBS solution was then used to re-suspend the 6 cell pellets (3 regular and 3 thymidine kinase HEK populations) and samples were incubated with shaking for 30 minutes. The cells were

then centrifuged at 1500rpm for 5 minutes with isolation of the supernatant and a 1mL sample collected for activity measurement. The cells were then re-suspended in 5mL of regular phosphate buffered saline solution and centrifuged at 1500rpm for 5 minutes. The supernatant was again decanted with a 1mL sample collected for activity measurement. The cells were then re-suspended in 2mL PBS with 15 $\mu$ L taken for counting and 2 x 1ml aliquots taken for activity measurement for each sample.<sup>151,161</sup> Counts per minute were recorded using an automatic gamma counter.

Table 4.2 shows the results of the radiolabelling procedure. The cells were radiolabelled using [18F]FIAU with the KBq of radioactivity retained calculated using the <sup>18</sup>F standard curve in Appendix 1. KBq retained per 10<sup>4</sup> cells was calculated using the raw data in Appendix 2. The T-test (performed assuming group means have equal variance) clearly show that the TK cells retained significantly more [18F]FIAU (Appendix 4).

**Table 4.2: Radiolabelling of wild HEK cells and tk engineered HEK cells**

Sample	Live cells/mL (x10 <sup>4</sup> )before	Live cells/mL (x10 <sup>4</sup> )after	KBq retained/ 10 <sup>4</sup> cells labelled	Cell % survival after radiolabelling
HEK 1	17	3	0.1057	17.6
HEK 2	14	1.5	0.1172	10.7
HEK 3	22.5	2	0.1263	8.9
TK-HEK 1	4.5	0.5	1.4355	11.1
TK-HEK 2	5.5	1	1.2698	18.2
TK-HEK 3	5	0.5	1.3134	10.0

In conclusion the evidence strongly supports the claim that the TK-HEK cells retain more [18F]FIAU than the wild type cells (Table 4.3).

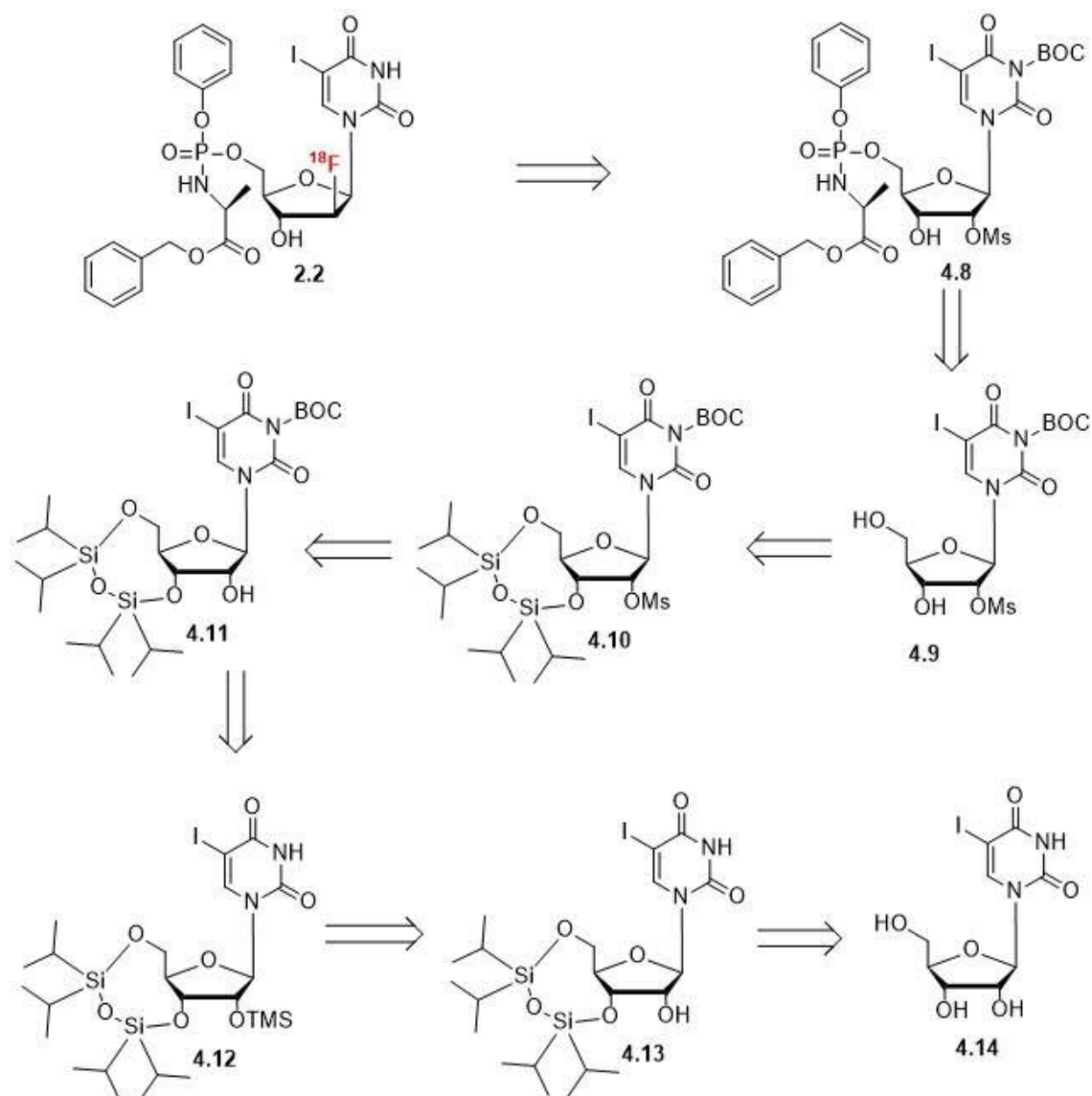
**Table 4.3: Preliminary radiolabelling experiment results**

Cell type	Cell count ( x 10 <sup>4</sup> )	CPM	KBq	KBq retained per 10 <sup>4</sup> cells labelled
HEK	53.0	170190.8	16.2713	0.307
TK	32.5	433802.4	38.5619	1.18

## 4.7 Conclusions

In conclusion [18F]FIAU ProTide (**2.2**) was synthesised via an early stage hot fluorination with an overall synthesis time of 4h. Although this approach cannot currently find any clinical application in PET imaging because of the duration of the radiosynthesis, it can be used for preliminary studies to monitor the behaviour of the 2'-fluorinated ProTides in animal models. In order to increase the yield of the reaction and reduce its duration, the use of microfluidic systems would be advisable.<sup>6</sup> Another synthetic approach that could be pursued to access the [18F]FIAU ProTide (**2.2**) would involve the synthesis of a suitable precursor molecule to perform a late stage fluorination as shown in the retrosynthesis suggested in Figure **4.15**.

**Figure 4.15: Proposed retrosynthetic pathway to access the [18F]FAIU ProTide (2.2) via a late stage hot fluorination**



Additionally studies of retention of [18F]FAIU on HEK cells engineered to express HSV-TK1 were performed and further evidenced the successful synthesis of this tracer showing a major retention compared to wild type cells.

## 5. Synthesis of novel 2'-deoxy-2'-fluoro-5-iodouridine ProTides as novel antiviral agents

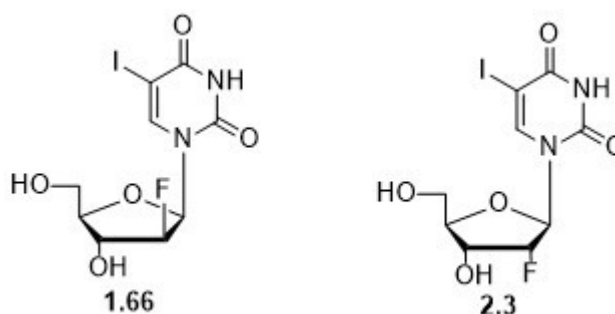
### 5.1 Introduction

Viral infections can be classified into three main groups. The first class includes life-threatening chronic viruses like the Human Immunodeficiency Virus (HIV), the Hepatitis B virus (HBV), and Hepatitis C Virus (HCV). The second class comprises acute viral infections that are generally non-lethal and self-resolving in otherwise healthy patients such as influenza viruses. The third class includes non-lethal viral infections but with a significant economic impact, such as the common cold caused by rhinoviruses.<sup>162</sup> In the last two decades important achievements have been made in the treatment of these viral infections. Nevertheless the spread of new viral diseases such as Zika, Ebola and new strains of hepatitis and herpes viruses has characterised recent years with potential for a pandemic outbreak,<sup>163–165</sup> therefore there is significant unmet medical need for new antiviral agents.

Nucleoside analogues (NA), particularly fluorinated nucleosides, represent an important class of antiviral agents and act as inhibitors of nucleoside reverse transcriptase (NRTIs). Their active form is the 5'-triphosphate form and their targets are the catalytic residues of the viral polymerase that interact with the template, the primer and the incoming nucleoside 5'-triphosphates.<sup>34,166–169</sup> Uridine based nucleosides and ProTides have been of particular interest for the treatment of viral infections.<sup>34,81,122,170</sup>

For example, Sofosbuvir (**1.72**), the ProTide of  $\beta$ -D-2'-deoxy-2'- $\alpha$ -fluoro-2'- $\beta$ -C-methyluridine, is a recently approved anti-HCV agent characterised by a uridine backbone, and a fluorine in the 2'- $\alpha$ -C position of the ribose moiety.<sup>122,123,171</sup> FIAU (Fialouridine) was another 2'-F-nucleoside analogue (Figure 5.1) that was selected as a Phase I clinical trial candidate for the treatment of HBV, however it showed mitochondrial toxicity resulting in lactic acidosis and hepatic failure.<sup>172,173</sup>

**Figure 5.1: Structures of 2'-deoxy-2'- $\beta$ -fluoro-5-iodouridine (FIAU, 1.66) and its anomer 2'-deoxy-2'- $\alpha$ -fluoro-5-iodouridine (2.3)**



After a successful Phase I clinical trial, Fialouridine (**1.66**) was selected to progress to Phase II in order to assess its safety and efficacy using a 24-week treatment course in 15 patients.<sup>172</sup> After 4 weeks of treatment, a decrease in HBV-DNA levels of more than 90% was shown proving a clear virological response of HBV to this agent. Nevertheless, during the 13<sup>th</sup> week of treatment, one patient was found with an unexpected and sudden onset of severe hepatotoxicity and lactic acidosis leading to an immediate termination of the ongoing trial. Despite the termination of the trial, 7 out of 15 patients continued to develop a severe form of lactic acidosis and severe declining hepatic synthetic function and some others also showed pancreatitis, neuropathy and myopathy. Five patients eventually died because of these persistent side effects and the other two survived after an emergency liver transplant.<sup>174</sup>

It was observed that the organs that were affected by these toxicities were the ones that are largely dependent on mitochondrial function. A tissue biopsy was then performed for further investigation, showing abnormally enlarged and irregularly shaped mitochondria as well as an abnormal accumulation of macrovesicular and microvesicular fat droplets. All these features of the multisystem toxicity can be somehow connected to a widespread mitochondrial injury and a disturbance in energy metabolism processes.<sup>115,175</sup>

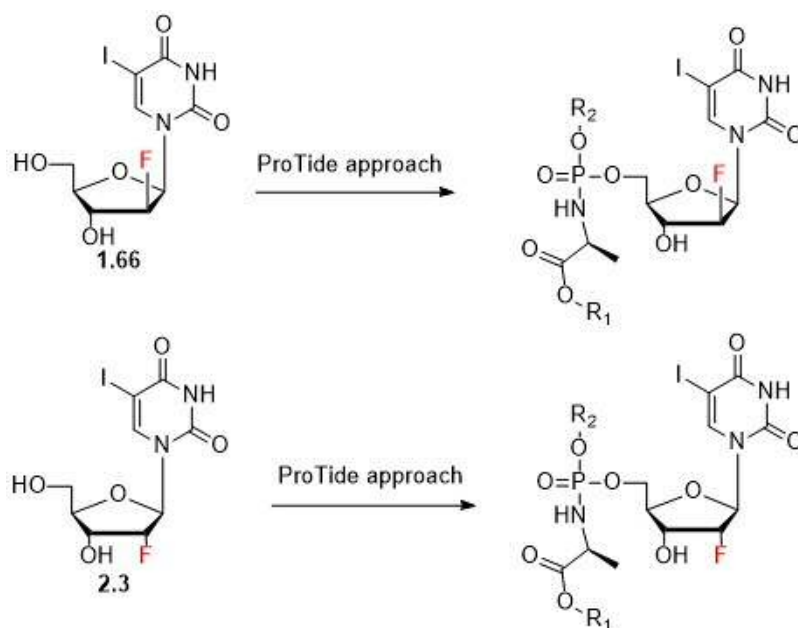
After Fialouridine trials were halted due to this unexpected and severe toxicity, an *in-vitro* study was conducted by Colacino *et al.* showing how Fialouridine is efficiently incorporated into mitochondrial-DNA (mt-DNA) by DNA polymerase- $\gamma$  replacing thymidine therefore leading to an increased cellular toxicity.<sup>176,177</sup> Its incorporation into nascent mt-DNA chains is due to the unblocked hydroxy group in the 3' position of

the deoxyribose moiety that allows the addition of nucleotides to the growing mt-DNA chain (and to a lesser extent on the nuclear-DNA (N-DNA)). This results in the formation of non-functional mt-DNA and N-DNA thus affecting gene expression, essential for the cells survival and correct functioning.<sup>176</sup>

After the failure in 1993 of Fialouridine in Phase II clinical trial no further studies were conducted on its therapeutic activity or its toxicity. It was instead investigated as a diagnostic probe leading to the PET tracer agent [18F]FIAU (**1.16**) discussed in Chapter 4. Furthermore, no studies have been conducted on its isomer 2'-deoxy-2'- $\alpha$ -fluoro-5-iodouridine that therefore represents a novel and interesting chemical entity. As the uridine backbone represents an already validated starting point to design antiviral agents, uridine based Protides and particularly fluorinated ones, could represent novel antiviral agents for the treatment of new viral diseases such as Zika, Ebola and new strains of hepatitis and herpes viruses for which there is no established treatment.<sup>163,178</sup>

The aim of this project is to synthesise a novel class of 2'-deoxy-2'-fluoro-5-iodouridine ProTides and evaluate them as antiviral agents for the treatment of newly arising viral diseases. It is expected that the application of the ProTide strategy could potentially lead to potent antiviral agents with an increased antiviral activity compared to their parent NA and reduced toxicity. It will be also discussed how the fluorine in the  $\alpha$ - or  $\beta$ -2'-C position of the ribose can play a role in the activity of these NAs and their prodrugs.<sup>90</sup> The synthesis of a series of 2'-deoxy-2'- $\alpha$ -fluoro-5-iodouridine ProTides will be the main target of the project as the  $\alpha$ -anomer (**2.3**) represents a novel and more convenient starting material for the synthesis compared to the  $\beta$ -anomer (FIAU, **1.66**). Nevertheless a ProTide of the  $\beta$ -anomer (FIAU, **1.66**), will also be synthesised to understand whether the position of the fluorine can lead to any change in their antiviral activity (Figure **5.2**).

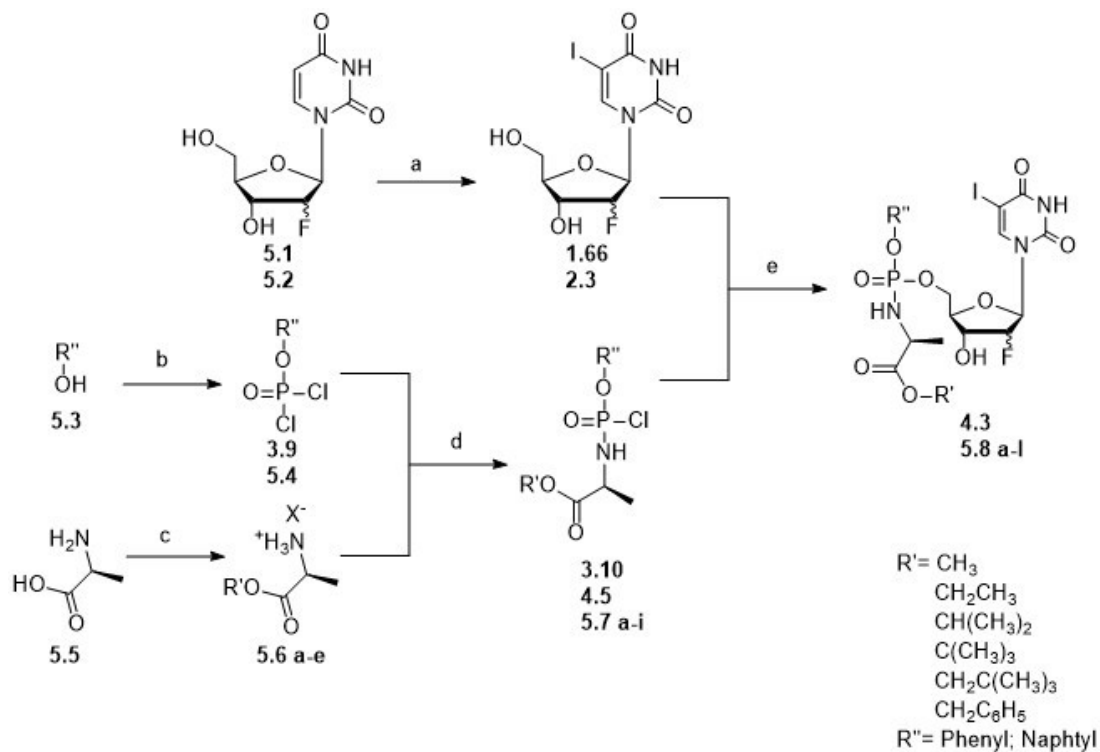
**Figure 5.2: Application of the ProTide strategy to fluorinated uridine based ProTides**



## 5.2 Synthesis of novel 2'-deoxy-2'-fluoro-5-iodouridine ProTides

The synthesis of 2'-deoxy-2'-fluoro-5-iodouridine ProTides was based on standard ProTide chemistry<sup>84</sup> discussed earlier in the thesis, via five major steps as shown in Figure 5.3.

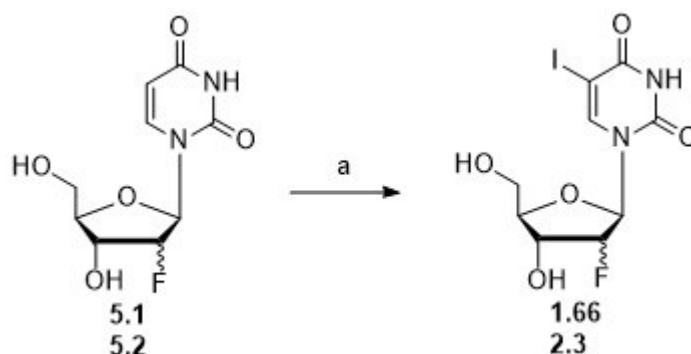
**Figure 5.3: General synthetic scheme for the 2'-deoxy-2'-fluoro-5-iodouridine ProTides**



**Reagents and conditions:** a)  $\text{I}_2$ , ceric ammonium nitrate,  $\text{CH}_3\text{CN}$ ,  $75^\circ\text{C}$ , 1h, 57-60%; b)  $\text{POCl}_3$ ,  $\text{Et}_3\text{N}$ ,  $-78^\circ\text{C}$  to rt, 3h, 91%; c) Alcohol, thionyl chloride or p-toluensulfonic acid,  $90^\circ\text{C}$ , 3-5h, 78-89%; d)  $\text{Et}_3\text{N}$ ,  $-78^\circ\text{C}$  to rt, anh.  $\text{CH}_2\text{Cl}_2$ , 3h, 80-91%; e) NMI, anh. THF,  $0^\circ\text{C}$  to rt, 16h, 3-12%.

The first step consisted in the iodination of both the  $\alpha$ - and  $\beta$ -anomers of the 2'-fluoro-2'-deoxyuridine with  $\text{I}_2$  and ceric ammonium nitrate as catalyst (Figure 5.4) as described in Chapter 3.<sup>156</sup> The purified compounds were analysed via MS and NMR.  $^1\text{H}$ -NMR showed a singlet at  $\delta=8.53\text{ppm}$  for the proton in the 6-position of the pyrimidine confirming the successful outcome of the reaction.

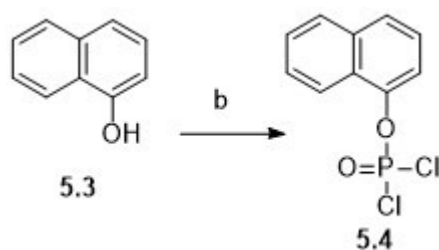
**Figure 5.4: Iodination of the  $\alpha$ - and  $\beta$ -anomers**



**Reagents and conditions:** a)  $I_2$ , ceric ammonium nitrate,  $CH_3CN$ ,  $75^\circ C$ , 1h, 57-60%.

Whereas phenylphosphorochloride is commercially available, the naphthyl derivative is not. Therefore compound **5.4** ( $R'' =$  naphthyl) was synthesised by coupling naphthol with phosphorus oxychloride using triethylamine as the base and salt scavenger. Anhydrous solvent and nitrogen atmosphere were essential for the positive outcome of the reaction. The crude reaction mixture was reduced *in vacuo* and used without further purification for next step (Figure 5.5).<sup>128</sup>

**Figure 5.5: Formation of the naphthyl-phosphorodichloridate**



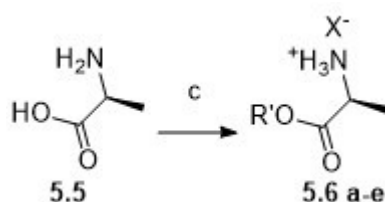
**Reagents and conditions:** b)  $POCl_3$ ,  $Et_3N$ ,  $-78^\circ C$  to rt, 3h, 91%.

L-alanine was chosen as the amino acid for the phosphoramidate moiety because, as widely reported in literature, the replacement of natural amino acids with other amino acids such as the D-alanine<sup>179</sup>, or simple amines leads to a slight or complete loss of activity of these derivatives in most ProTide cases.<sup>180</sup> L-alanine is the

most commonly used natural amino acid used in ProTide chemistry.<sup>181</sup> Several esters of the L-alanine were used and, among them, methyl, ethyl and tert-butyl L-alanine esters were commercially available therefore were used directly for the coupling with the phosphorodichloridate.<sup>182</sup> Isopropyl, neopentyl and benzyl L-alanine ester were instead synthesised via an esterification reaction of the L-alanine.

Two methods were used to access two kinds of salts, the chloride and sulfonate salts of the L-alanine esters (Figure 5.6).<sup>103</sup> The first method consisted in the reaction between the alcohols with L-alanine and thionyl chloride to obtain the chloride salts. However, sulfonate salts are considered to be more stable than the chloride salts<sup>183</sup> therefore the alcohols were also reacted with L-alanine and *para*-toluene sulfonic acid (*p*-TSA) to access also the equivalent L-alanine ester sulfonate salts (Figure 5.6). In this second method, to shift the equilibrium to the right and therefore to push the reaction to completion, Dean-stark apparatus was used to condense and thus collect the water produced during the reaction. To monitor the reaction, thin layer chromatography (TLC) was used. To confirm the formation of the product, a ninhydrin solution capable of detecting the amino groups of the amino acid, was sprayed on the TLC plate eluted in a system of 2-propanol/water (7:3). A different R<sub>f</sub> between the L-alanine and the ester salt was observed. All the L-alanine ester salts were thereafter used for the next step without further purification.

**Figure 5.6: Synthesis of the L-alanine ester salt via two methods**

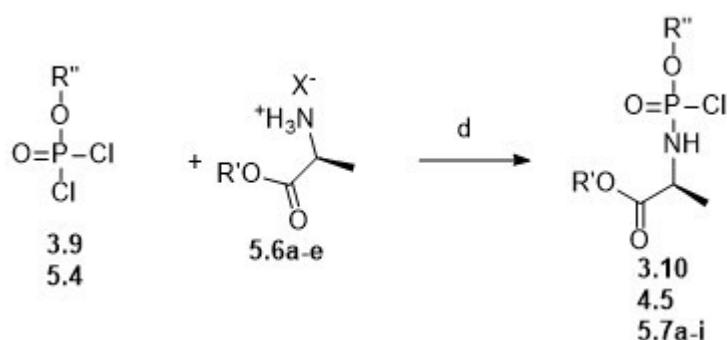


**Reagents and conditions:** c) Alcohol, thionyl chloride or *p*-toluenesulfonic acid, 90°C, 3-5h, 75-89%.

**Table 5.1: Structures and yields of 5.6a-e**

ID	R'-X	Yield
<b>5.6a</b>	Neopentyl chloride	75%
<b>5.6b</b>	Neopentyl sulfonate	83%
<b>5.6c</b>	Isopropyl chloride	89%
<b>5.6d</b>	Isopropyl sulfonate	78%
<b>5.6e</b>	Tert-butyl chloride	84%

The phosphorochloridates were synthesised according to the standard procedure by the reaction of the L-alanine ester salts with aryl dichlorophosphonates at low temperatures under nitrogen atmosphere with TEA used as a base<sup>84</sup> (Figure 5.7). Formation of phosphorochloridates was confirmed by <sup>31</sup>P-NMR. Once the reaction was complete, the solvent was evaporated under reduced pressure and the resulting solid was re-dissolved in anhydrous diethyl ether and filtered under nitrogen. The filtrate was then evaporated *in vacuo* to obtain yellowish oils that were used for the next step without further purification.

**Figure 5.7: Synthesis of the phosphorochloridates**

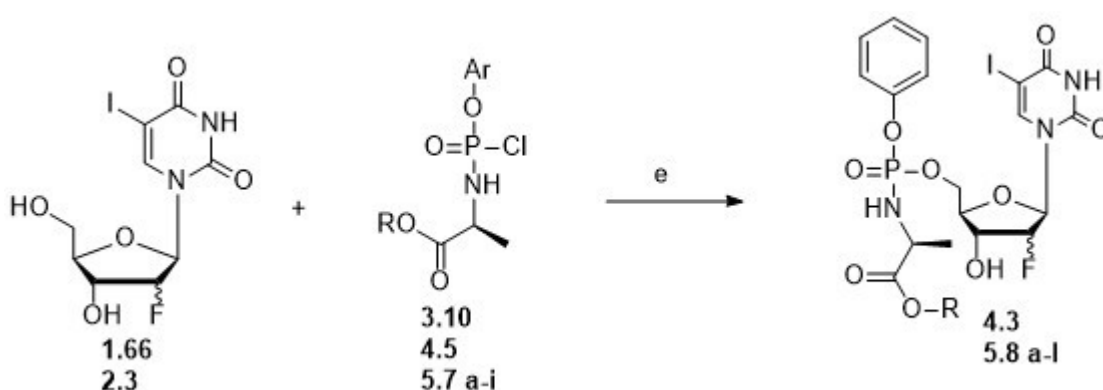
**Reagents and conditions:** d) L-alanine ester salt, Et<sub>3</sub>N, -78°C to rt, anh. CH<sub>2</sub>Cl<sub>2</sub>, 3h, 80- 95%.

**Table 5.2: Structures and yields of Phosphorochloridates synthesised**

ID	R	R'	Yield
<b>3.10</b>	Ethyl	Phenyl	95%
<b>4.5</b>	Benzyl	Phenyl	88%
<b>5.7a</b>	Methyl	Phenyl	80%
<b>5.7b</b>	Isopropyl	Phenyl	83%
<b>5.7c</b>	Neopentyl	Phenyl	91%
<b>5.7d</b>	Tert-butyl	Phenyl	82%
<b>5.7e</b>	Methyl	Phenyl	85%
<b>5.7f</b>	Ethyl	Naphtyl	94%
<b>5.7g</b>	Isopropyl	Naphtyl	82%
<b>5.7 h</b>	Neopentyl	Naphtyl	80%
<b>5.7i</b>	Tert-butyl	Naphtyl	81%

Finally, the methyl, ethyl, isopropyl, benzyl, neopentyl and tert-butyl phosphorochloridates were reacted with 2'-deoxy-2'- $\alpha$ -fluoro-5-iodouridine in anhydrous THF using N-methylimidazole to form an imidazolium intermediate with the phosphorochloridates that can readily react with 2'-deoxy-2'-fluoro-5-iodouridine to form the ProTides (Figure 5.8).

After 24 h the reactions were stopped and the solvent was evaporated *in vacuo*. The residues were extracted with CH<sub>2</sub>Cl<sub>2</sub> and 0.5N HCl necessary to neutralise the base used in the reaction. The organic layer was then concentrated under reduced pressure to obtain yellowish oils. All ProTides were purified by column chromatography using a gradient system of CH<sub>2</sub>Cl<sub>2</sub>/CH<sub>3</sub>OH (100% to 95% CH<sub>2</sub>Cl<sub>2</sub>) and, where necessary, also by the use of preparative TLC plates.

**Figure 5.8: Synthesis of the ProTides**

**Reagents and conditions:** e) NMI, anh. THF, 0°C to rt, 16h, 3-12%.

**Table 5.3: Structures and yields of 4.3, 5.8a-5.8i**

ID	Nucleoside	R	R'	Yield
<b>4.3</b>	$\beta$	Benzyl	Phenyl	9%
<b>5.8a</b>	$\alpha$	Methyl	Phenyl	7%
<b>5.8b</b>	$\alpha$	Ethyl	Phenyl	12%
<b>5.8c</b>	$\alpha$	Isopropyl	Phenyl	3%
<b>5.8d</b>	$\alpha$	Neopentyl	Phenyl	3%
<b>5.8e</b>	$\alpha$	Tert-butyl	Phenyl	6%
<b>5.8f</b>	$\alpha$	Benzyl	Phenyl	11%
<b>5.8g</b>	$\alpha$	Methyl	Naphtyl	4%
<b>5.8h</b>	$\alpha$	Ethyl	Naphtyl	7%
<b>5.8i</b>	$\alpha$	Isopropyl	Naphtyl	5%
<b>5.8l</b>	$\alpha$	Benzyl	Naphtyl	3%

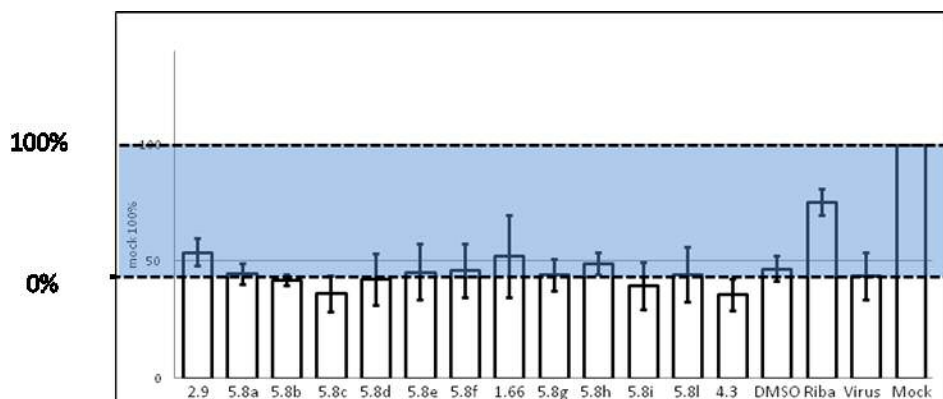
The yields of the ProTides were poor for several reasons. Firstly synthesis and purification consisted of several steps that normally lead to an expected loss of products. Secondly, some intermediates were used as crude compounds without any purification resulting in the formation of several by-products. Finally, the hydroxyl group in the 3' position of the ribose can compete with the one in 5' position when

reacting with the phosphorochloridates causing the formation of several by-products. The use of NMI in this final step can reduce the formation of by-products. Indeed the Grignard reagent *t*-BuMgCl has proved to be very successful for the phosphorylation of many nucleoside analogues,<sup>85</sup> but its use can lead to phosphorylation of the other free hydroxyl groups in the molecule. This can result in the formation of mixtures of 5'-mono and 3',5'-bisphosphorylated by-products, thereby reducing the overall yield of the reaction. Although mixtures can be separable by column chromatography, the isomeric mixtures can be very difficult to separate resulting in a loss of pure product.

### 5.3 Antiviral evaluation

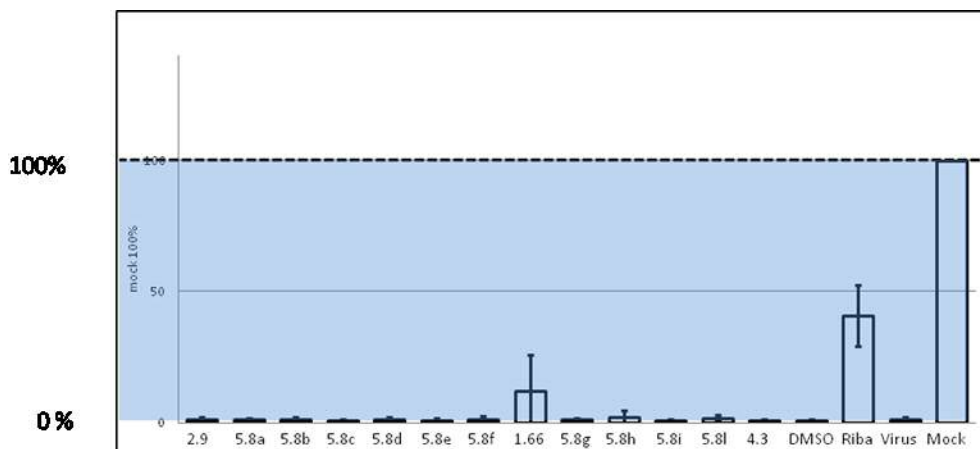
Initially antiviral evaluation was performed against Zika virus within the facility of Dr. Joachim Bugert at the Institut für Mikrobiologie der Bundeswehr, in Munich. Zika is a mosquito-borne flavivirus transmitted primarily by *Aedes* mosquitoes. It was first identified in 1947 in monkeys and later in humans in 1952 in Uganda and the United Republic of Tanzania. Recent outbreaks of Zika virus disease have been recorded in Africa, the Americas, Asia and the Pacific. Typical symptoms are similar to other arbovirus infections such as dengue, and include mild fever, skin rash, conjunctivitis, muscle and joint pain, malaise or headache. It can also lead to microcephaly and Guillain-Barré syndrome, and other neurological complications are also being investigated. There is currently no vaccine available.<sup>184</sup>

Zika antiviral effect was first tested on DBGRT cells, glioma cells derived from an adult female with glioblastoma multiforme who had been treated with local brain irradiation and multidrug chemotherapy<sup>184,185</sup>. When the Zika antiviral effect was tested on DBGRT cells, none of the compounds tested (**1.66**, **2.29**, **2.9**, **4.3**, **5.8a-l**) reached the threshold of 50% protection at 10 µM. Lead compounds of this series were interestingly the two nucleosides **2.29** and **1.66**. Ribavirin (Riba) was used as positive control at 100 µM (Figure 5.9).

**Figure 5.9: Antiviral effect on Zika virus at 10  $\mu\text{m}$  on DEPG cells (n=3)**

HUH7 cells have been chosen as second line for the antiviral testing of compounds **1.61**, **2.29**, **4.3**, **5.8a-l**. They are well differentiated hepatocyte-derived carcinoma cell lines, originally taken from a liver tumour in a 57-year-old Japanese male in 1982.<sup>184,186</sup> They are extensively used in hepatitis C and dengue virus and more recently in Zika virus research conducted by Bluemling *et al.*<sup>187-189</sup> When tested in HUH7 cells, none of the compounds synthesised reached the threshold of 50% protection at 10 $\mu\text{M}$ . The lead compound was again FIAU (**1.66**). Ribavirin (Riba) was again used as control at a concentration of 100 $\mu\text{M}$  (Figure **5.10**).

**Figure 5.10: Antiviral effect of Zika virus at 10µm on HUH7 cells (n=3)**



Cytotoxicity essays have also been performed on both cell lines. When the toxic effect was tested at 10µM in HUH7cells, none of the compounds showed toxicity (Figure 5.11) but, when tested on DBGRT at 10µM, some of the compounds showed toxicity although the CC<sub>50</sub> was >10µM (Figure5.12).

**Figure 5.11: Cytotoxicity at 10µm on HUH7 cells (n=3)**

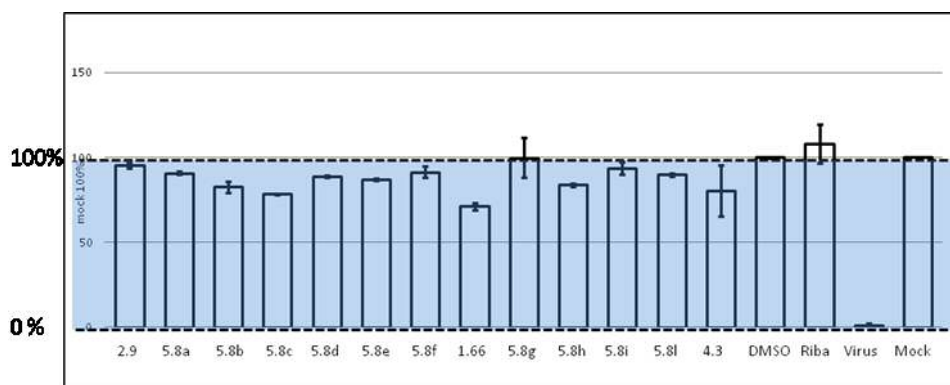
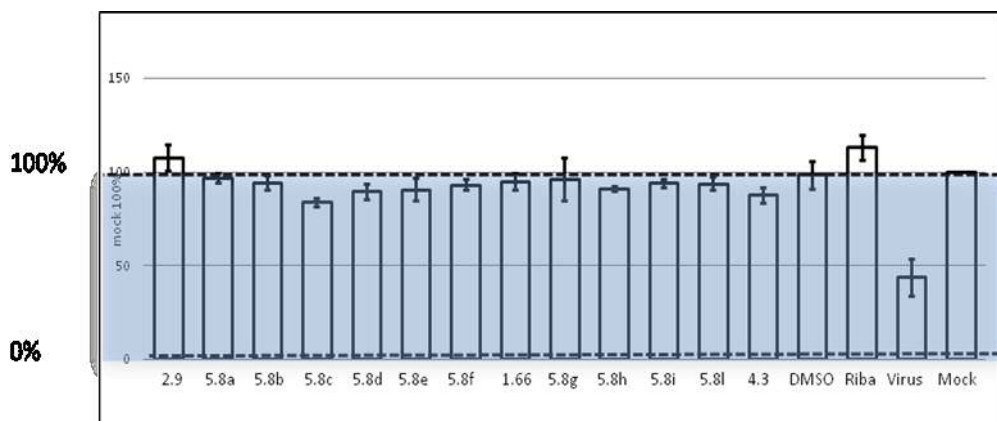


Figure 5.12: Cytotoxicity at 10 $\mu$ m on DBGRT cells (n=3)

## 5.4 Conclusion

In conclusion a novel class of 2'-deoxy-2'-fluoro-5-iodouridine ProTides has been synthesised. The yields of the final ProTides were low because of purification issues associated with the intermediates and because of the presence of the hydroxyl group in the 3'-position of the sugar that can compete with the hydroxyl in the 5'-position when reacting with the phosphorochloridates leading to the formation of by-products.

Initial antiviral tests show no activity against Zika virus when compared to the antiviral agent Ribavirin. No particular difference in activity has been noticed between the  $\alpha$ - and  $\beta$ -anomers showing that position of fluorine in this particular case does not influence either the cytotoxicity or the antiviral activity of these compounds and interestingly, no increase in activity has been observed in the ProTides when compared to the parent lead nucleosides. Future plans will consist of performing antiviral tests against HSV and Dengue viruses that could be other potential targets of these novel fluorinated uridine based pro-nucleotides.<sup>189</sup>

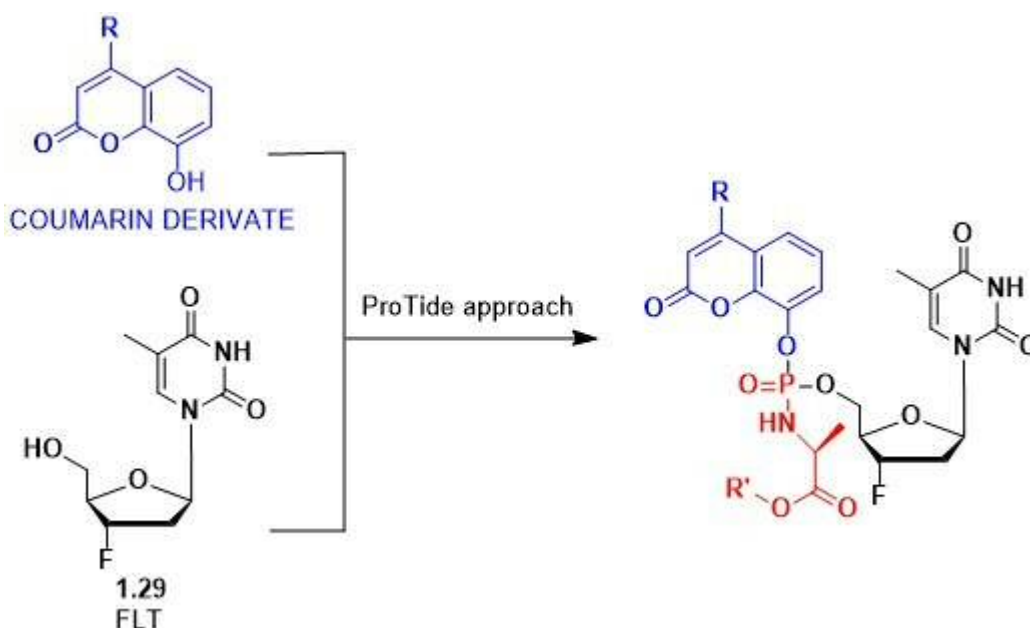
## 6. Synthesis of novel FLT chimeric ProTides with fluorescent probes

### 6.1 Introduction

The scientific importance of ProTide technology in the anticancer and antiviral drug discovery setting has already been discussed in Chapter 1.<sup>82</sup> Nevertheless questions remain surrounding the mechanism of *in vivo* ProTide activation, biodistribution and the potential toxicity of their metabolites. Although PET would be the most sophisticated and sensitive imaging tool to answer these questions, other imaging techniques could be used as a short-term approach that would give a first insight of the ProTide activation pathway and metabolism within *in vivo* models.<sup>190–192</sup>

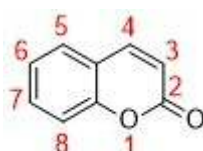
Fluorescence spectroscopy is a widely used technique that analyzes the fluorescence of molecules by using a beam of light, typically ultraviolet light, to excite the electrons in molecules and cause them to emit light. Measurement of fluorescence is taken by devices called fluorimeters.<sup>193</sup> With the rapid development of fluorescence analysis technology, small-molecule fluorescent probes have been widely applied to track biological changes with many advantages such as high sensitivity and selectivity compared to other imaging tools.<sup>193,194</sup>

The aim of this project is indeed to synthesise a small series of ProTides as fluorescent probes by replacing the normally used and potentially toxic phenyl and naphthyl groups with aromatic moieties known to have characteristic fluorescent as well as therapeutic properties. In particular the fluorescent probes chosen as targets for this project were the coumarin derivatives of FLT ProTides (Figure 6.1).

**Figure 6.1: Structure of hybrid coumarin derivatives of FLT ProTides**

Coumarins, naturally occurring fluorophores from the benzopyrone family,<sup>195</sup> have been chosen for this co-drug approach<sup>196</sup> for several reasons:

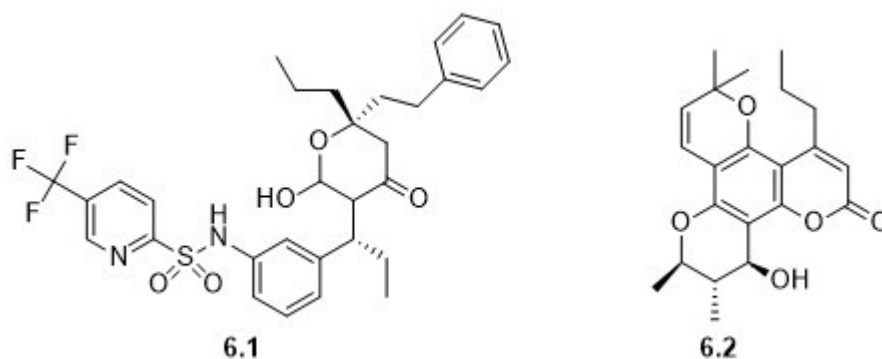
- They are non-polar cell permeable molecules with drug-like properties.<sup>197,198</sup>
- The coumarin backbone is particularly advantageous because of its stability, synthetic accessibility and light emitting properties. When substituted in position 7 with electron-donating groups the intensity of blue fluorescence emitted increases remarkably<sup>197,199</sup> (Figure 6.2).

**Figure 6.2: Structure of coumarin backbone**

- The 4-hydroxycoumarin pharmacophore has been shown to be a potent inhibitor of HIV protease leading to the approval of tipranavir (**6.1**),<sup>198</sup> an anti-HIV agent.<sup>198,200,201</sup> Synthetic (+)-calanolide (**6.2**), a non-nucleoside reverse transcriptase inhibitor (NNRTI) of HIV-1, has also completed phase I/II clinical trials as combination therapy for HIV infection (Figure 6.3).<sup>202,203</sup> Many other

coumarin derivatives are currently under clinical investigation as anti-HIV agents.<sup>204,205</sup>

**Figure 6.3: Structures of the coumarin derivatives tipranavir (6.1) and (+)-calanolide (6.2)**



FLT (**1.29**) has been selected as the nucleoside to be incorporated into this novel hybrid ProTide for the following reasons:

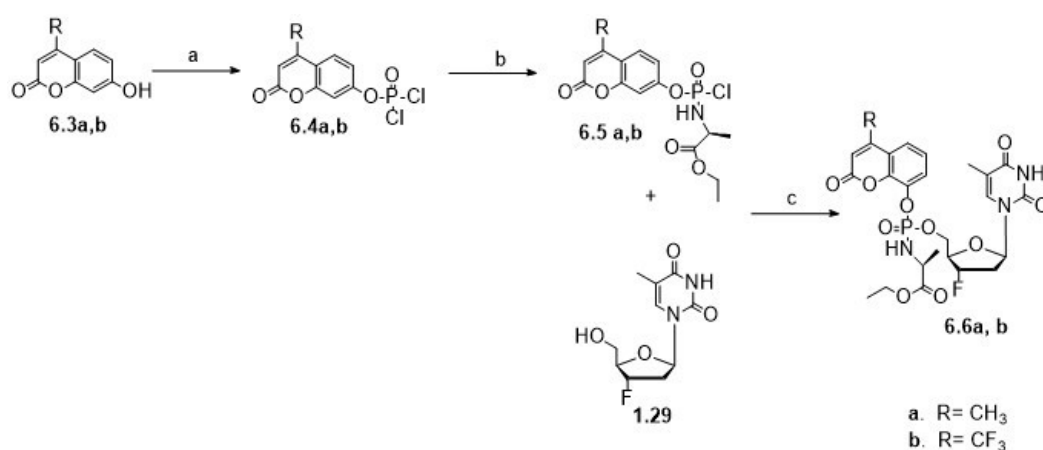
- It was one of the first fluorinated nucleosides synthesised that showed a potent inhibition of reverse transcriptase in HIV strains. However it did not progress further in clinical trial because of dose-dependent safety concerns.<sup>53</sup>
- ProTides of FLT have been synthesised showing also potent inhibition of HIV-1 and HIV-2 replication.<sup>114</sup>
- The absence of hydroxyl groups on the 2' and 3' position of the ribose sugar ensures a selective 5'- O-phosphorylation thus preventing the formation of side products.<sup>128</sup>

This co-drug approach could represent an exciting opportunity to boost the antiviral activity of FLT and its ProTides by working synergistically with the coumarin derivative, as well as providing a novel class of fluorescent ProTide probes. It is proposed that coumarin-containing FLT ProTides will be characterised by an absence of toxicity and will have potentially a better anti-HIV activity compared to the parent nucleoside overcoming their resistance mechanisms.

## 6.2 Synthesis of FLT chimeric ProTides with fluorescent probes

The synthesis of coumarin-derivatives of FLT ProTides was accomplished according to the general scheme shown in Figure 6.4.

**Figure 6.4: General synthetic scheme for FLT-coumarin derivative ProTides**



**Reagents and conditions:** a) POCl<sub>3</sub>, Et<sub>3</sub>N, -78°C to rt, 1h, 86-86%; b) L-alanine ester salt, anh. CH<sub>2</sub>Cl<sub>2</sub>, Et<sub>3</sub>N, -78°C to rt, 2h, 71-81%; c) Phosphorochloridate, *t*BuMgCl, anh. THF, 0°C to rt, 16 h, 5-11%.

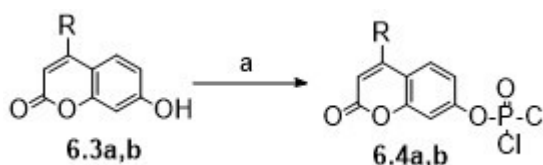
Two coumarin derivatives have been chosen as starting materials to form the phosphorochloridate, the 4-methylumbelliferone (4-MU) (**6.3a**, R = Me) and the 7-hydroxy-4-(trifluoromethyl)coumarin (4-TF) (**6.3b**, R = CF<sub>3</sub>).

4-MU (**6.3a**), besides being a pH-sensitive fluorescent indicator, is also currently used for the treatment of biliary spasm. It inhibits hyaluronic acid synthesis that is a factor often associated with diseases such as tumour progression.<sup>205–207</sup> 4-MU is indeed under investigation as an anticancer agent because of its ability to inhibit proliferation, migration and invasion of cancer cells.<sup>207,208</sup> It also showed activity against chronic hepatitis C and B and is currently in Phase II clinical trials under the registered name of Heparvit.<sup>209</sup> Recent studies also suggest its potential for future HIV-1 reservoir eradication strategies.<sup>210</sup>

4-TF (**6.3b**) is used as fluorescent probe for the imaging of enzymes such as endoplasmic reticulum carboxylesterases, enzymes involved in the cleavage of ester-containing prodrugs.<sup>211,212</sup> Although 4-TF has not shown any therapeutic activity, its application to ProTide strategy could be useful for *in vivo* imaging of the ProTide activation pathway into cells.

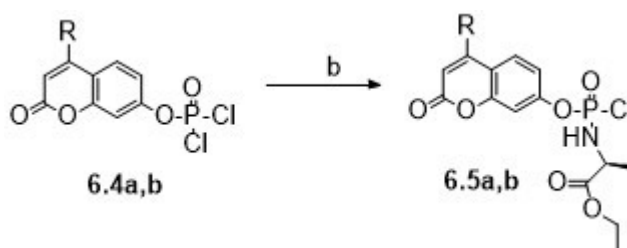
The first step consisted of the synthesis of phosphorochloridates according to the standard procedure shown in Chapter 3 and 5.<sup>128</sup> In this case the appropriate coumarin derivative was coupled with phosphorus oxychloride using triethylamine as the base, and HCl scavenger. Anhydrous conditions were again essential for the successful outcome of the reaction therefore all the synthetic procedures have been conducted under nitrogen atmosphere. Compounds were obtained in good yields and were used for the next step without further purification (Figure 6.5).

**Figure 6.5: Synthesis of the phosphorodichloridates**



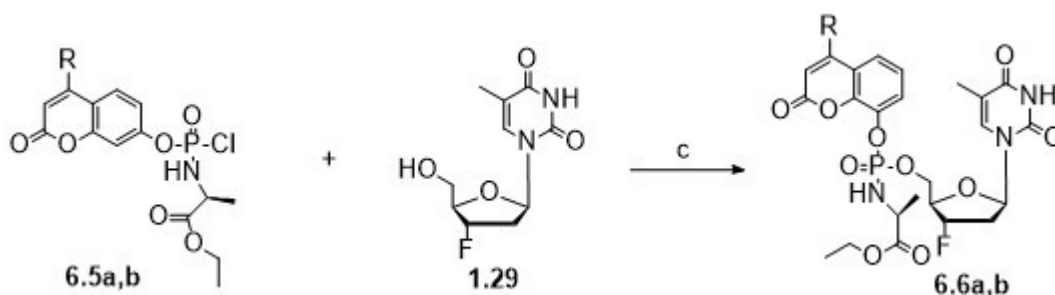
**Reagents and conditions:** a) POCl<sub>3</sub>, Et<sub>3</sub>N, -78°C to rt, 1h, 86-88%.

Step b consisted of the formation of the phosphorochloridates by reacting the phosphorodichloridates with the appropriate L-alanine esters using TEA as the base and anhydrous conditions as per the previously reported standard procedure.<sup>128</sup> The reaction mixture was monitored by <sup>31</sup>P NMR and after 1h at rt the conversion of the starting material into the product was complete, therefore the reaction was stopped, reduced under *vacuum* and stored in the freezer under a strict nitrogen atmosphere (Figure 6.6).

**Figure 6.6: Synthesis of the phosphorochloridate**

**Reagents and conditions:** b) L-alanine ester salt,  $\text{CH}_2\text{Cl}_2$ ,  $\text{Et}_3\text{N}$ ,  $-78^\circ\text{C}$  to rt, 2h, 71-81%.

Step c consisted of the coupling between the commercially available FLT with the freshly synthesised phosphorochloridate. Tert-butyl magnesium chloride ( $t\text{BuMgCl}$ ) was used as base following the standard procedure showed in Chapter 3.<sup>22</sup> The reaction mixture was dried under *vacuum* and purified using silica gel column chromatography. (Figure 6.7)

**Figure 6.7: Synthesis of the phosphoramidates**

**Reagents and conditions:** c) Phosphorochloridate,  $t\text{BuMgCl}$ , anhydrous THF,  $0^\circ\text{C}$  to rt, 16 h, 5-11%.

Attempts to synthesise other coumarin derivatives of FLT ProTides bearing a benzyl, isopropyl or neopentyl L-alanine ester were performed but all intermediate reactions (step a and b) led to the formation of numerous by-products. Attempts at purification using silica gel column chromatography were performed leading to further decomposition of the intermediates because of their instability and sensitivity to air.

Attempts to synthesise their equivalent ProTides by using the non-purified reaction mixtures led to formation of ProTides in very poor yield (0.1-0.3%) so that the isolation by gradient flash column chromatography was not successful due to the

formation of side products with similar Rf values. Despite many attempts at further purification via preparative TLC, no successful isolation of these compounds was achieved.

ProTides **6.6a** and **6.6b** were instead isolated as diastereisomeric mixtures in the ratio of roughly 1:1 as yellowish solids with yield ranging from 5-11%. All ProTides and intermediates were characterised by MS,  $^{31}\text{P}$ -NMR,  $^1\text{H}$ -NMR,  $^{19}\text{F}$ -NMR, COSY-NMR,  $^{13}\text{C}$ -NMR and HSQC-NMR.

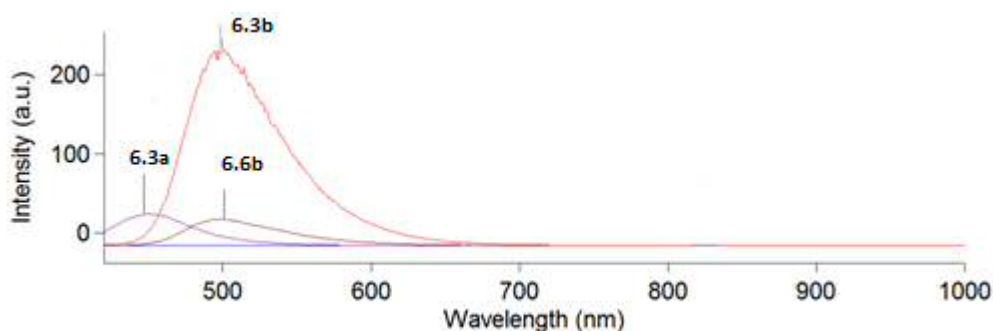
As mentioned before,  $^{31}\text{P}$ -NMR was used to monitor formation of most products and intermediates. Despite using stringent anhydrous and inert conditions,  $^{31}\text{P}$ -NMR revealed the presence of side products in most of the crude mixtures of intermediates that were synthesised.

The use of non-purified mixtures has probably contributed to the formation of many side products. To increase the yield and prevent the formation of too many by-products, it is suggested for the future to purify the crude phosphorochloridate mixtures by preparative HPLC.

### 6.3 Fluorescence data

Measures of fluorescence emission of the Protides synthesised has been taken to compare them with the parent coumarin derivatives.<sup>213</sup> Compound **6.6a** emitted no fluorescence, however the 4-MU (**6.3a**) emitted at short wavelengths. Compound **6.6b** showed a weak fluorescence emission at the same wavelength as the parent 4-FT (**6.3.b**) (500 nm).

Figure 6.8: Fluorescence emission spectrum of compound 6.3a, 6.3b and 6.6b



These preliminary data suggest that these ProTides could be used as fluorescent Probes as they possess different UV absorption fluorescence wavelengths and intensity compared to their parent coumarin derivatives. Therefore, a change in UV fluorescence could be observed during metabolism *in vivo* when the coumarin is cleaved off the ProTide. This change could be useful to visualise ProTide uptake *in vivo*, and thus confirm whether ProTides are activated inside the cells as speculated.

## 6.4 Conclusion

In conclusion two novel ProTides of FLT containing coumarin derivatives and L-alanine esters as masking groups (**6.6a**, **6.6b**), have been synthesised as models of a new class of ProTide fluorescent probes. These novel compounds are characterised by fluorescence properties that may allow the visualisation of their uptake thus demonstrating their activation mechanism. This co-drug approach with coumarin derivatives could also boost the anti-HIV properties of the parent NA FLT. Another six ProTides were synthesised but couldn't be isolated because of the formation of numerous side products, instability issues, poor yield and difficult purification process. All ProTides and by-products have been characterised by MS and NMR spectroscopy.

It is recommended for the future to test these compounds in *in vitro* models to assess their efficacy and potency as anti-HIV and more generally as antiviral agents. If efficacious, they could be optimised by altering the coumarin moiety with other coumarins known to have anti-HIV activity or simply by increasing the lipophilicity of the parent coumarin to facilitate their cell permeability. This could increase the anti-HIV efficacy of FLT ProTides even further. The drawback of this co-drug approach, as for any other co-drug approaches, could be the issue with dosing.<sup>196,214</sup> Therapeutic doses for FLT and for the coumarin derivative could be different so that the administration of both drugs as one co-drug may not be feasible. Nevertheless, UV absorbance and fluorescence data could still be used to visualise uptake and activation mechanism of this class of novel FLT chimeric ProTides with fluorescent probes in *in vivo* models.

## 7. Conclusions and future work

### 7.1 General conclusions and future perspective

The phosphoramidate (ProTide) technology developed by McGuigan and co-workers from 1995 onwards is considered to be the most effective pro-nucleotide approach currently used in the clinic.<sup>17</sup> Fluorinated nucleosides and ProTides represent a significant class of anticancer and antiviral agents used in the clinic and in clinical development. Fluorine plays a crucial role in the optimization of these clinical agents and candidates by improving their selectivity, toxicity, potency, and pharmacokinetic and pharmacodynamic properties.<sup>34</sup>

In order to visualize pharmaceutical and biological effects of fluorinated ProTides directly *in vivo*, [18F]-radiolabelled ProTides have been synthesised for the first time as PET imaging probes. These imaging biomarkers represent a proof of concept for the ProTide strategy and a model system to visualize their pharmaceutical and biological effects directly *in vivo*. Two [18F]-radiolabelled ProTides have been synthesised as model standards for two classes, the 2'- and the 3'-fluorinated ProTides. The 3'-[18F]FLT ProTide (**2.1**) was synthesised *via* a convenient late stage [18F]fluorination of *ad hoc* designed precursor molecules. Among the five precursor molecules synthesised, the nosyl derivative furnished the desired product in poor yields therefore protection of the NH moieties of the molecule with BOC protecting groups was performed to minimize the formation of undesired by-products. This protection increased remarkably the yield of the reaction furnishing the desired radiolabelled BOC protected compound that was then deprotected to finally furnish the desired target compound **2.1** in good radiochemical yield and radiochemical purity. The 2'-[18F]FIAU ProTide (**2.2**) was synthesised following a different synthetic approach involving an early stage [18F]-fluorination of the sugar moiety with an overall synthetic time of 4h.

This was the first time that [18F]-radiolabelled ProTides have ever been synthesised. Although these results have to be regarded as first trials of their synthesis, these radiolabelled probes could provide evidence for the *in vivo* behaviour of this

class of compounds answering key questions about their metabolism and uptake directly.

For the future it is recommended to investigate different set-ups such as the use of different automated synthetic modules, microwave-assisted synthesis and microfluidic systems in order to validate the potential clinical application of these radiosyntheses. These radiolabelled ProTides not only could represent a first step towards ProTide personalised medicine but, on the other hand, could also represent a novel class of PET imaging diagnostic probes.

Other imaging techniques could also be used to provide insight into ProTide activation pathways *in vivo*.<sup>215</sup> For this reason novel ProTides of FLT containing coumarin derivatives (**6.6a**, **6.6b**), have been synthesised as new potential fluorescent probes and therapeutic agents. By incorporating the coumarin moiety, these new FLT ProTides are characterised by fluorescence properties, which should allow the visualisation of their uptake thus demonstrating their activation mechanism. As some coumarin derivatives are also characterised by interesting antiviral therapeutic properties, this could also be considered as a co-drug approach that could boost the anti HIV properties of the parent NA FLT. Future work will investigate their efficacy and potency as anti-HIV and more generally as antiviral agents. Where efficacious, optimization of the coumarin moiety with respect to anti-HIV properties could be performed in order to boost their therapeutic activity. UV absorbance and fluorescence data will be used to visualise uptake and the activation mechanism of this class of novel FLT chimeric ProTides with fluorescent probes within *in vivo* models.

Besides the use of imaging techniques to study the mechanism of action of ProTides, a novel class of cold, non-fluorescent 2'-deoxy-2'-fluoro-5-iodouridine ProTides (**2.9**, **4.3**, **5.8a-l**) have been synthesised and tested as antiviral agents in response to the high demand of novel antiviral agents against the outbreak of new viral diseases or against novel strains of well-known viruses.<sup>178</sup> Initial antiviral tests against Zika virus did not show any activity of these fluorinated uridine based ProTides when compared to Ribavirin, but further investigation on other viruses such as Dengue and HSV are currently ongoing.

## 8. Experimental

### 8.1 General information

#### 8.1.1 Analytics

$^1\text{H}$  NMR spectra were measured on a Bruker Avance Ultra Shield spectrometer (500 MHz) at ambient temperature. Data were recorded as follows: chemical shift in  $\delta$ ppm from internal standard tetramethylsilane; multiplicity (*s* = singlet; *d* = doublet; *t* = triplet; *m* = multiplet); coupling constant (Hz), integration and assignment.  $^{13}\text{C}$  NMR spectra were measured on a Bruker Avance Ultra Shield spectrometer (125 MHz) at ambient temperature. Chemical shifts were recorded in ppm from the solvent resonance employed as the internal standard (e.g.  $\text{CDCl}_3$  at 77.00 ppm).  $^{31}\text{P}$  NMR spectra were recorded on a Bruker Avance Ultra Shield spectrometer (202 MHz) at ambient temperature.  $^{19}\text{F}$  NMR spectra were recorded on a Bruker Avance Ultra Shield (474 MHz) spectrometer at ambient temperature. Highperformance liquid chromatography (HPLC) analysis was conducted on an Agilent Technology 1200 Series System with an analytical reversed phase column (Phenomenex Synergi 4 $\mu$  Hydro- RP 80, C-18, 4.6 $\times$ 250 mm) and with a semi-preparative reversed phase column (Phenomenex Synergi 4 $\mu$  Hydro-RP 80, C-18, 10 $\times$ 250 mm) both coupled with a RAM/RAM Model 4 detector (Lablogic System, Ltd.) for radio-HPLC purposes. Thin-layer chromatography (TLC) was conducted on pre-coated silica gel 60 GF<sub>254</sub> plates. Preparative TLC plates (20 $\times$ 20 cm, 500-2000 silica) were purchased from Merck. Radio-TLC was performed on a Canberra UNISPEC 125. Mass spectrometry analysis (LC-ESI-MS) was performed on a Bruker micro-TOF or on an Agilent 6430 T-Quadrupole spectrometer. High-resolution mass spectrometry (ESI-HRMS) was performed at the EPSRC National Mass Spectrometry facility at Swansea University.

#### 8.1.2 Solvents and chemicals

All the anhydrous solvents and reagents were purchased from Sigma-Aldrich and they were used without further purification. Some nucleosides used as starting materials were purchased from Carbosynth Ltd. UK. Fluka silica gel (35-70 mm) was

used as stationary phase for column chromatography. Radioactive material was purified with QMA and Al cartridges (Waters corp., Milford, MA, USA).

### 8.1.3 Radioactive source and equipment

$^{18}\text{F}$ -Fluoride was produced in an IBA Cyclon 18/9 cyclotron using the  $^{18}\text{O}(\text{p},\text{n})^{18}\text{F}$  nuclear reaction.  $^{18}\text{O}$ -Enriched water (enrichment grade 98%, 2.2 mL, Nukem GmbH Germany) was irradiated with 18MeV protons. An Eckert & Ziegler module system was used to perform the radiofluorinations. A vacuum pump N820 (Neuberger, Freiburg, Germany) was used for the drying process. Smartline pump 100 126 was used for the semi-preparative HPLC attached to the Eckert & Ziegler module system.

## 8.2 Procedures

Described below are the standard procedures followed in the synthesis of L-alanine ester salts, phosphorochloridates and the ProTides.<sup>128</sup>

### 8.2.1 Standard procedure A1: synthesis of L-alanine ester hydrochloride salts

Thionyl chloride (2.0 mol/eq) was added dropwise to a stirring solution of the appropriate alcohol (15.0 mol/eq) at 0°C under nitrogen atmosphere. The reaction was allowed to stir at 0°C for 0.5 hr then slowly allowed to warm to room temperature (r.t). L-alanine (1.0 mol/eq) was added dropwise and the mixture was heated under reflux overnight. The reaction was monitored by TLC using 2-propanol/water (7:3) and ninhydrin solution. The solvent was removed *in vacuo* with last traces of solvent removed by azeotropic co-evaporation to give a solid crude product.

### 8.2.2 Standard procedure A2: synthesis of L-alanine ester sulfonate salts

A mixture of L-alanine (1.0 mol/eq), the appropriate alcohol (15.0 mol/eq) and para-toluene sulfonic acid (p-TSA) monohydrate (1.1 mol/eq) in toluene was heated

under reflux overnight using the Dean-Stark apparatus. The reaction was monitored by TLC using 2-propanol/water (7:3) and ninhydrin solution. The solvent was then removed *in vacuo* with last traces of solvent removed by azeotropic co-evaporation to give a solid crude product.

### **8.2.3 Standard procedure B: synthesis of aryloxy phosphorochloridates**

To a solution of an appropriate amino acid ester salt (1.0molequivalent) and phenyl dichlorophosphate (1.0 mol/eq) in anhydrous  $\text{CH}_2\text{Cl}_2$ , anhydrous triethylamine (TEA) (2.0 mol/eq) was added dropwise at  $-78^\circ\text{C}$  under a nitrogen atmosphere. The reaction mixture was then stirred at  $-78^\circ\text{C}$  for 1h, then at r.t for 3h. The reaction was monitored by  $^{31}\text{P}$ -NMR. The solvent was removed under reduced pressure and the residue triturated with anhydrous diethyl ether. The precipitate was filtered under nitrogen and the filtrate was concentrated to produce the product as an oil.

### **8.2.4 Standard procedure C: synthesis of phosphoramidates *via* NMI**

To a stirring solution of an appropriate nucleoside (1.0 mol equivalent) in anhydrous tetrahydrofuran (THF) at  $0^\circ\text{C}$  under nitrogen atmosphere, N-methylimidazole (NMI) (5.0mol equivalent) was added and the reaction was stirred for 30 min. A solution of an appropriate phosphorochloridate (3.0mol equivalent) dissolved in THF was then added dropwise and the reaction was stirred at r.t for 18h. The reaction was monitored by TLC with  $\text{CH}_2\text{Cl}_2/\text{CH}_3\text{OH}$  (9:1). The solvent was then removed *in vacuo* to give a residue that was re-dissolved in  $\text{CH}_2\text{Cl}_2$  and washed twice with 0.5N HCl. The organic phase was dried over  $\text{MgSO}_4$ , filtered and reduced to dryness to give a crude product that was purified by flash column chromatography eluting with  $\text{CH}_2\text{Cl}_2/\text{CH}_3\text{OH}$  in different proportions depending on the specific analogue being synthesised.

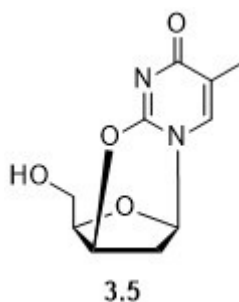
### 8.2.5 Standard procedure D: synthesis of phosphoramidates *via* **tBuMgCl**

To a stirring solution of the appropriate nucleoside (1 mol/eq) in anhydrous THF under a nitrogen atmosphere, tBuMgCl (1.1 mol/eq) was added, and stirred for 10 min. The appropriate phosphorochloridate (1.2 mol/eq) dissolved in anhydrous THF was added to the reaction mixture dropwise. The reaction mixture was left stirring at rt for 24 h, then anhydrous THF solvent removed by evaporation *in vacuo* at rt. The crude product was purified by flash column chromatography eluting with CH<sub>2</sub>Cl<sub>2</sub>/CH<sub>3</sub>OH in different proportions depending on the specific analogue being synthesised.

## 8.3 Spectroscopic data

### 8.3.1 Experimental section from Chapter 3

(3R,5R)-3-(hydroxymethyl)-8-methyl-2,3-dihydro-5H,9H-2,5-methanopyrimido[2,1-b][1,5,3]dioxazepin-9-one. (3.5)



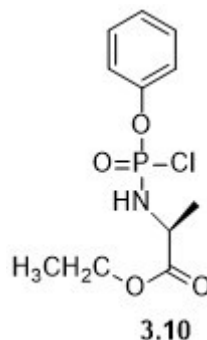
**MF:** C<sub>10</sub>H<sub>12</sub>N<sub>2</sub>O<sub>4</sub>

**MW:** 224.22

A mixture of thymidine (**1.28**) (1eq, 0.250g, 1.032mmol) and triphenylphosphine (Ph<sub>3</sub>P) (2eq, 0.541g, 2.064mmol) was suspended in anhydrous acetonitrile (20mL) and cooled down to -15°C. To this mixture diisopropylazodicarboxylate (DIAD) (2eq, 0.406mL, 0.417g, 2.64 mmol) was added dropwise maintaining the temperature below -5°C with vigorous stirring. After the addition the reaction was left to stir for 5h at 0°C. Following this, the mixture was again cooled down to -20°C and ethyl acetate (20mL) was added at the same temperature and stirred for other 15min. The white precipitate formed, was collected by Buchner filtration and washed with cold ethyl acetate. The filtrate solution was reduced to dryness and the resulting compound was purified by silica gel column chromatography using 90% CH<sub>2</sub>Cl<sub>2</sub>-10%CH<sub>3</sub>OH as eluent to obtain the product **3.5** as a white solid. Yield: 52%. Rf: 0.5.

**<sup>1</sup>H-NMR** (500 MHz, DMSO-d<sub>6</sub>): δppm 7.55 (*d*, *J*=1.2Hz, 1H, ArH), 5.80 (*d*, *J*=3.9Hz, 1H, H-1'), 5.23 (*brs*, 1H, H-3'), 5.01 (*t*, 1H, C-5'OH), 4.20 (*m*, 1H, H-4'), 3.51 (*m*, 2H, H-5', H-5''), 2.55 (*d*, *J*=1.2Hz, H-2', 1H), 2.47 (*ddd*, *J*<sub>1,8</sub>=19Hz, *J*<sub>1,4</sub>=6.7Hz, *J*<sub>1,2</sub>=3Hz, 1H, H-2''), 1.76 (*d*, *J*=1.1Hz, 3H, CH<sub>3</sub>).

Note: Data agrees with previously published papers.<sup>216</sup>

**(2S)-ethyl-2-((chloro(phenyl)phosphoryl)amino)propanoate. (3.10)****MF:** C<sub>11</sub>H<sub>15</sub>ClNO<sub>4</sub>P**MW:** 291.6

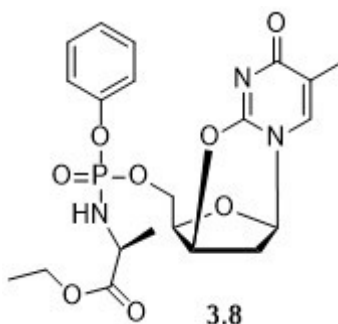
Compound **3.10** was prepared according to standard procedure B. Anhydrous triethylamine (2eq; 0.662mL; 0.480g; 4.74mmol), phenyldichlorophosphate (**3.9**) (1eq; 0.354 mL; 0.500 g; 2.37 mmol) and L-alanine ethyl ester hydrochloride salt (1eq; 0.364g; 2.37mmol) in anhydrous CH<sub>2</sub>Cl<sub>2</sub> (5mL) were used to obtain the final compound (**3.10**) as a yellowish oil which wasn't further purified. Yield: 92%.

<sup>1</sup>H-NMR (500 MHz, CDCl<sub>3</sub>): δ ppm 7.35-7.41 (*m*, 2H, Ar-H), 7.21-7.30 (*m*, 3H, Ar-H), 4.53 (*m*, 1H, NH), 4.21 (*m*, 1H, CH), , 3.95 (*m*, 2H, CH<sub>2</sub>), 1.51 (*m*, 3H, CH<sub>3</sub>), 1.23 (*m*, 3H, CH<sub>3</sub>).

<sup>31</sup>P-NMR (202 MHz, CDCl<sub>3</sub>): δppm 7.71, 8.05.

Note: Data agrees with previously published papers.<sup>85,103,156</sup>

**Ethyl((((3R,5R)-8-methyl-9-oxo-2,3-dihydro-5H,9H-2,5-methanopyrimido[2,1-b][1,5,3]dioxazepin-3-yl)methoxy)(phenoxy)phosphoryl)-L-alaninate. (3.8)**



**MF:** C<sub>21</sub>H<sub>26</sub>N<sub>3</sub>O<sub>8</sub>P

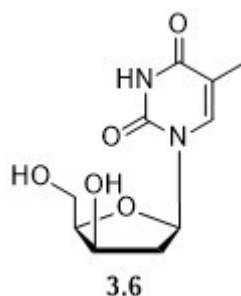
**MW:** 691.3

Compound **3.8** was synthesised according to standard procedure C. 2'-3'-anhydrothymidine (**3.5**) (1eq; 0.175g; 0.780mmol), NMI (5eq; 0.331mL; 0.320g; 3.9mmol) and ethyl(2chloro(phenyl)phosphorylamino)propanoate (**3.10**) (3 eq; 0.684g; 2.34mmol) were reacted to obtain a residue that was purified by silica gel column chromatography (CH<sub>2</sub>Cl<sub>2</sub>/CH<sub>3</sub>OH gradient from 100%CH<sub>2</sub>Cl<sub>2</sub> to 95%CH<sub>2</sub>Cl<sub>2</sub>) to furnish the desired product (**3.8**) as a yellowish oil. Yield: 0.6%.

**<sup>1</sup>H-NMR** (500 MHz, CDCl<sub>3</sub>): δppm7.40 (*d*, *J*=3.9Hz, 1H, H6), 7.23 (*td*, *J*=7.8, 2.8Hz, 2H, CH-phenyl), 7.13 (*d*, *J*=7.6Hz, 2H, CH-phenyl), 7.09 (*t*, *J*=7.6Hz, 1H, CH-phenyl), 5.89 (*ddd*, *J* = 31.8, 16.5, 1.9 Hz, 1H, 1'-CH), 4.39 (*d*, *J*= 7.0 Hz, 2H, 5'-CH<sub>2</sub>), 4.22 (*m*, 1H,2'-CH), 4.1 (*m*, 1H, 3'-CH), 4.09 (*m*, 1H, 4'-CH), 3.86 (*d*, *J*=10.7Hz, 1H, NH-ala), 3.76 (*m*, 2H, CH<sub>2</sub>-ester), 3.29 (*dd*, *J*=7.0, 4.9Hz, 1H, CH-ala), 1.21 (*dd*, *J*=10.3, 6.4Hz, 3H, CH<sub>3</sub>-ala), 1.15 (*t*, *J*=7.0Hz, 3H, CH<sub>3</sub>-ester). **<sup>13</sup>C-NMR** (125 MHz, CDCl<sub>3</sub>): δppm174.70 (C=O, ala), 171.41 (C-4), 169.00 (C-2), 151.51 (C-6), 139.86, 128.13 (Ar-C and Ar-CH), 100.87, 94.73 (C-5), 91.20, 90.21 (C-4'), 89.12, 88.41 (C-3'), 85.7, 84.31 (C-1'), 63.41(C-5'),62.17, 62.12 (CH<sub>3</sub>-ester), 59.21 (CH-ala), 55.75 (C-3'), 43.12 (C-2'), 30.01, 28.76 (CH<sub>3</sub>-ala). **<sup>31</sup>P-NMR** (202 MHz, CDCl<sub>3</sub>): δppm3.71, 3.43. **MS (ESI)<sup>+</sup>**: 692.3 [M+H<sup>+</sup>]. **HPLC**: Rt: 10.03 min

(95%). [Gradient: (0') 95% $\text{H}_2\text{O}$ /5% $\text{CH}_3\text{CN}$  - (5') 50%  $\text{H}_2\text{O}$ /50% $\text{CH}_3\text{CN}$ - (15') 50%  $\text{H}_2\text{O}$ /50%  $\text{CH}_3\text{CN}$ - (20') 95%  $\text{H}_2\text{O}$ /5%  $\text{CH}_3\text{CN}$ ].

**1-((2R,4R,5R)-4-hydroxy-5-(hydroxymethyl)tetrahydrofuran-2-yl)-5-methylpyrimidine- 2,4(1H,3H)-dione. (3.6)**



**MF:** C<sub>10</sub>H<sub>14</sub>N<sub>2</sub>O<sub>5</sub>

**MW:** 242.2

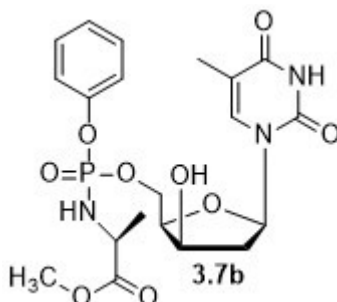
A mixture of 2'-3'-anhydrothymidine (**3.5**) (0.200g; 0.892mmol) and aq. 1.5M NaOH (3.33mL) was stirred in methanol (30mL) under reflux for 3h. The clear solution changed colour to gold brown upon heating. The reaction was monitored by TLC analysis. Once the reaction was complete, the solvent was removed by evaporating under reduced pressure. The crude compound was purified by silica gel column chromatography (CH<sub>2</sub>Cl<sub>2</sub>/CH<sub>3</sub>OH gradient from 100% to 90% of CH<sub>2</sub>Cl<sub>2</sub>) to obtain the product (**3.6**) as a white powder. Yield: 64%. (R<sub>f</sub>: 0.4 in 90%CH<sub>2</sub>Cl<sub>2</sub>/10%CH<sub>3</sub>OH TLC system).

**<sup>1</sup>H-NMR** (500 MHz, DMSO-d<sub>6</sub>): δppm 11.24 (s, 1H, NH), 7.78 (s, 1H, H-6), 6.07 (dd, *J* = 8.5, 2.44 Hz, 1H, H-1'), 5.25 (d, *J*=3.35Hz, 1H, 3'-OH), 4.67 (t, *J*= 5.49Hz, 1H, 5'-OH), 4.23 (m, 1H, H-3'), 3.60-3.84 (m, 3H, H-4', H-5' and H-5''), 2.55-2.59 (m, 1H, H-2''), 1.84 (dd, *J*=14.95Hz, *J*=2.14Hz, 1H, H-2'), 1.76 (s, 3H, CH<sub>3</sub>).

Note: Data agrees with previously published papers.<sup>216</sup>

**(2S)-methyl-2-((((2R,3R,5R)-3-hydroxy-5-(5-methyl-2,4-dioxo-3,4-dihydropyrimidin-1(2H)-yl)tetrahydrofuran-2-yl)methoxy)(phenoxy)phosphoryl)amino)propanoate.**

**(3.7b)**



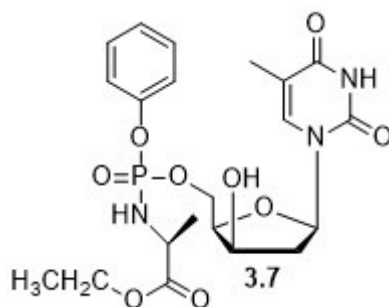
**MF:** C<sub>20</sub>H<sub>26</sub>N<sub>3</sub>O<sub>9</sub>P

**MW:** 483.4

Compound **3.7b** was synthesised according to the standard procedure C. 1-(2-deoxy-β-lyxofuranoxyl thymidine) (**3.6**) (1eq; 0.109g; 0.45mmol), NMI (5eq; 0.177mL; 0.183g, 2.23mmol) and methyl-(2-chloro(phenyl)phosphorylamino)propanoate (**5.7a**) (3eq; 0.350g; 1.34mmol) were reacted to obtain a residue that was purified by silica gel column chromatography (CH<sub>2</sub>Cl<sub>2</sub>/CH<sub>3</sub>OH gradient from 100% CH<sub>2</sub>Cl<sub>2</sub> to 95% CH<sub>2</sub>Cl<sub>2</sub>) to afford the product **3.7b** as a white solid. Yield: 9.3%.

**<sup>1</sup>H NMR**(500 MHz, CDCl<sub>3</sub>): δppm 7.56 (*d*, *J* = 7 Hz, 1H, H-6), 7.33-7.41 (*m*, 2H, Ar- H), 7.22-7.31 (*m*, 3H, Ar-H), 6.24-6.31 (*m*, 1H, H-1'), 5.25 (*m*, 1H, 3'-OH), 4.98 (*m*, 1H, H-3'), 4.30-4.51 (*m*, 2H, NH, H-4'), 3.94-4.02 (*m*, 1H, CH), 3.67 (*s*, 3H, OCH<sub>3</sub>), 3.38 (*d*, *J* = 16 Hz, 2H, H-5', H-5''), 2.45-2.47 (*m*, 1H, H-2''), 2.07-2.23 (*m*, 1H, H-2'), 1.850 (*d*, *J* = 10 Hz, 3H, CH<sub>3</sub> -Thy), 1.15-1.38 (*m*, 3H, CH<sub>3</sub> -Ala). **<sup>31</sup>P NMR**: (202 MHz, CDCl<sub>3</sub>): δppm 5.34, 4.89

**(2S)-ethyl2-((((2R,3R,5R)-3-hydroxy-5-(5-methyl-2,4-dioxo-3,4-dihydropyrimidin-1(2H)-yl)tetrahydrofuran-2-yl)methoxy)(phenoxy)phosphoryl)amino)propanoate**



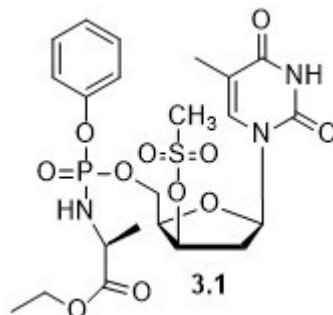
**MF:** C<sub>21</sub>H<sub>28</sub>N<sub>3</sub>O<sub>9</sub>P

**MW:** 497.4

Compound **3.7** was prepared according to standard procedure C. 1-(2-deoxy-β-lyxofuranoxyl thymidine) (**3.6**) (1eq; 0.175g; 0.721mmol), NMI (5eq; 0.287mL; 0.297g, 3.62mmol) and ethyl-(2-chloro(phenyl)phosphorylamino)propanoate (**3.10**) (3eq; 0.633g; 2.17mmol) were reacted to obtain a residue that was purified by silica gel column chromatography (97% CH<sub>2</sub>Cl<sub>2</sub>/3% CH<sub>3</sub>OH) to afford the product as a white solid. Yield: 18.4 %. Rf: 0.4

**<sup>1</sup>H-NMR** (500 MHz, CDCl<sub>3</sub>): δppm7.58 (*d*, *J*=7 Hz, 1H, H-6), 7.35-7.43 (*m*, 2H, Ar-H), 7.20-7.29 (*m*, 3H, Ar-H), 6.25-6.32 (*m*, 1H, H-1'), 5.22 (*m*, 1H, 3'-OH), 4.94 (*m*, 1H, H-3'), 4.31-4.52 (*m*, 2H, NH, H-4'), 3.95-4.03 (*m*, 1H, CH), 3.68 (*d*, *J*=7Hz, 2H, CH<sub>2</sub>-ester), 3.35 (*d*, *J*=16Hz, 2H, H-5', H-5''), 2.48-2.51 (*m*, 1H, H-2''), 2.09-2.25 (*m*, 1H, H-2'), 1.85 (*d*, *J*=10Hz, 3H, CH<sub>3</sub>-thy), 1.16-1.23 (*m*, 6H, CH<sub>3</sub>-ester). **<sup>31</sup>P-NMR** (200 MHz, CDCl<sub>3</sub>): δppm5.34, 4.98.

**(2S)-ethyl2-((((2R,3R,5R)-5-(5-methyl-2,4-dioxo-3,4-dihydropyrimidin-1(2H)-yl)-3-((methylsulfonyl)oxy)tetrahydrofuran-2-yl)methoxy)(phenoxy)phosphoryl)amino)propanoate. (3.1)**



**MF:** C<sub>22</sub>H<sub>30</sub>N<sub>3</sub>O<sub>11</sub>PS

**MW:** 575.5

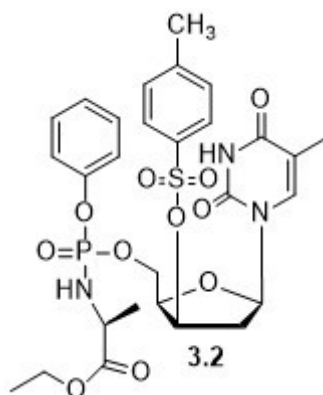
Triethylamine (10eq; 1.06mL; 0.769g; 7.6mmol) and mesyl chloride (4 eq; 0.235mL; 0.348g; 3.04mmol) were added to a solution of the compound **3.7** (1eq; 0.378g; 0.76mmol) in dry CH<sub>2</sub>Cl<sub>2</sub> (20mL) at 0°C. The mixture was stirred at this temperature for additional 10 minutes before it was allowed to warm up to rt and it was stirred for 1.5 h. After full conversion of the starting material, the mixture was diluted with sat. NaHCO<sub>3</sub>-solution and extracted with CH<sub>2</sub>Cl<sub>2</sub> (2x 20mL). After drying over Na<sub>2</sub>SO<sub>4</sub>, the solution was reduced *in vacuo* and the resulting compound was purified by silica gel column chromatography (CH<sub>2</sub>Cl<sub>2</sub>/CH<sub>3</sub>OH gradient from 100% CH<sub>2</sub>Cl<sub>2</sub> to 95% CH<sub>2</sub>Cl<sub>2</sub>) to afford the product (**3.1**) as a white solid. Yield: 29.5%. Rf: 0.45 in 90%CH<sub>2</sub>Cl<sub>2</sub>/10%CH<sub>3</sub>OH TLC system.

**<sup>1</sup>H NMR** (500 MHz, CDCl<sub>3</sub>): δppm 8.93-8.96(s, 1H, NH, thy), 7.33-7.32 (*d*, *J*=7 Hz, 1H, H-6), 7.24-7.28 (*m*, 2H, Ar-H), 7.10-7.15 (*m*, 3H, Ar-H), 6.23-6.21 (*m*, 2H, H-1'), 5.19-5.15 (*s*, 1H, NH-ala), 3.84-4.37 (*m*, 1H, H-3'; 1H, H-4'; 1H, CH; 2H, H-5', H-5''; 4H, CH<sub>2</sub>-ala), 2.96-3.01 (*s*, 3H, SO<sub>2</sub>CH<sub>3</sub>), 2.72-2.75 (*m*, 1H, H-2''), 2.38-2.42 (*m*, 2H, H-2'), 1.87 (*d*, *J*=1Hz, 3H, CH<sub>3</sub>-thy), 1.28-1.33 (*m*, 3H, CH<sub>3</sub>-ala), 1.19-1.16 (*m*, 3H, CH<sub>3</sub>-ala). **<sup>13</sup>C NMR** (125 MHz, CDCl<sub>3</sub>) δppm 173.7-173.4 (C=O, acetyl), 163.6 (C-2), 150.42 (C-1), 135.1 (C-4), 129.8 (C-2; C-6Ar), 125.2 (C-4Ar), 120.2 (C-3; C-5Ar), 111.6 (C-3), 83.5 (C-1'), 79.9(C-

3'), 77.3 (C-4'), 63.7 (C-5'), 61.7 (CH<sub>2</sub>-Ala), 50.8 (CH-ala), 39.2 (C-2'), 38.8 (CH<sub>3</sub>-mesyl), 21.34 (CH<sub>3</sub>-ethyl), 14.04 (CH<sub>3</sub>-ala), 12.76 (CH<sub>3</sub>-thy). **<sup>31</sup>P NMR** (202MHz, CDCl<sub>3</sub>): δppm 2.92, 2.63. **MS(ESI<sup>+</sup>)**: 576.2 [M+H<sup>+</sup>]. **HPLC**: Rt: 13.2 min (98%). [Gradient: (0') 95%H<sub>2</sub>O/5%CH<sub>3</sub>CN - (5') 50% H<sub>2</sub>O/50%CH<sub>3</sub>CN- (15') 50% H<sub>2</sub>O/50% CH<sub>3</sub>CN- (20') 95% H<sub>2</sub>O/5% CH<sub>3</sub>CN].

(2S)-ethyl-2-((((2R,3R,5R)-5-(5-methyl-2,4-dioxo-3,4-dihydropyrimidin-1(2H)-yl)-3-(tosyloxy) tetrahydrofuran-2-yl)methoxy)(phenoxy)phosphoryl)amino)propanoate.

(3.2)



MF: C<sub>28</sub>H<sub>34</sub>N<sub>3</sub>O<sub>11</sub>PS

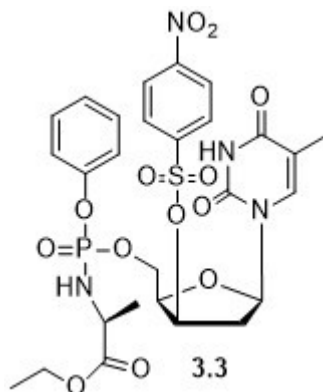
MW: 651.6

The ProTide **3.7** (1 eq; 0.181g; 0.364mmol) was dissolved in pyridine (5mL) at 0°C and tosylchloride (2eq; 0.138g; 0.727mmol) and silvertrifluoromethanesulfonate (AgOTf) (2eq; 0.186g; 0.727mmol) were added. The reaction mixture was stirred for 1h at 0°C and then it was allowed to slowly warm down to rt. It was then stirred at rt for other 2h. After, the reaction mixture was diluted with EtOAc, it was filtered, and the filtrate was washed with H<sub>2</sub>O and brine. The organic layer was dried over Na<sub>2</sub>SO<sub>4</sub> anhydrous and the solvent was evaporated under reduced pressure. The residue was purified by silica gel column chromatography (95% CH<sub>2</sub>Cl<sub>2</sub>/5% CH<sub>3</sub>OH) to give the product **3.2** as a yellowish solid. Yield: 35%; Rf: 0.55.

**<sup>1</sup>H NMR** (500 MHz, CDCl<sub>3</sub>) δppm 7.76-7.75 (*d*, *J*=1.9Hz, 1H, H6 Ar), 7.34 (*dd*, *J*=15.7, 8.6Hz, 4H, Ar-H tosyl), 7.27-7.17 (*m*, 5H, Ar), 6.19-5.20 (*td*, *J*=7.8, 2.9Hz, 1H, H-1') , 4.45-3.74 (*m*, 12H), 2.72-2.61 (*m*, 1H, CH-ala), 2.46 (*s*, 3H, CH<sub>3</sub>, tosyl), 1.85 (*s*, 3H, CH<sub>3</sub>, thym), 1.39 (*t*, *J*=7.2 Hz, CH<sub>3</sub>, ethyl), 1.31 (*m*, 3H, CH<sub>3</sub>-ala). **<sup>13</sup>C NMR** (126 MHz, CDCl<sub>3</sub>) δppm 173.65, 173.59 (C-ala), 163.52 (C1-thy), 150.58, 150.53 (C3-thy), 150.25, 150.19(C1-tosyl), 145.99, 145.98 (C1-phenyl), 135.04, 134.95 (CH-thy), 133.05, 132.90 (C4-tosyl), 130.27, 130.21(CH, C2, C6-tosyl), 129.75, 129.70 (CH, C2, C6-

phenyl), 127.64, 127.58 (CH,C4-phenyl), 125.10, 120.35 (CH, C3, C5-phenyl), 120.31, 120.21 (CH, C3, C5-tosyl), 111.15, 110.98 (C3-thy), 84.22, 83.99 (CH, C1'), 80.96, 80.90 (CH, C3'), 80.72, 80.66 (CH, C4'), 63.89, 63.85 (CH<sub>2</sub>, C6'), 63.33, 63.29(CH<sub>2</sub>, ethyl), 50.39, 50.38(CH, ala), 39.03 (CH<sub>2</sub>, C3'), 21.69, 21.00 (CH<sub>3</sub>-ethyl), 20.96, 20.95 (CH<sub>3</sub>-tosyl), 14.12 (CH<sub>3</sub>, ala), 12.49, 12.44 (CH<sub>3</sub>-thy). **<sup>31</sup>P NMR** (202 MHz, CDCl<sub>3</sub>) δppm 2.78, 2.66. **MS (ESI)<sup>+</sup>**: 652.2 [M +H<sup>+</sup>]; 674.1 [M + Na<sup>+</sup>]. **HPLC**: Rt: 16.03 min (98%). [Gradient: (0') 95%H<sub>2</sub>O/5%CH<sub>3</sub>CN - (5') 50% H<sub>2</sub>O/50%CH<sub>3</sub>CN- (15') 50% H<sub>2</sub>O/50% CH<sub>3</sub>CN- (20') 95% H<sub>2</sub>O/5% CH<sub>3</sub>CN].

**2S)-ethyl2-((((2R,3R,5R)-5-(5-methyl-2,4-dioxo-3,4-dihydropyrimidin-1(2H)-yl)-3-(((4-nitrophenyl)sulfonyl)oxy)tetrahydrofuran-2yl)methoxy)(phenoxy)phosphoryl)amino)propanoate. (3.3)**



**MF:** C<sub>27</sub>H<sub>31</sub>N<sub>4</sub>O<sub>13</sub>PS

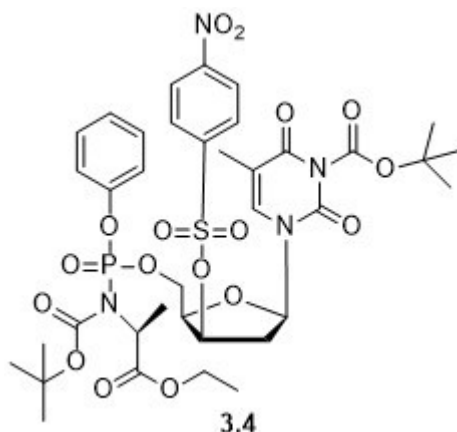
**MW:** 682.5

The ProTide **3.7** (1eq; 1.16g; 2.34 mmol) was dissolved in pyridine (20mL) at 0°C and 4-nitrobenzenesulfonylchloride (nosyl chloride) (2eq; 1.06g; 4.79mmol) and silvertrifluoromethanesulfonate (AgOTf) (2eq; 1.23g; 4.79 mmol) were added. The reaction mixture was stirred for 1h at 0°C and then it was allowed to slowly warm down to rt. It was then stirred at rt for other 2h. After the reaction mixture was diluted with EtOAc, it was filtered, and the filtrate was washed with H<sub>2</sub>O and brine. The organic layer was dried over Na<sub>2</sub>SO<sub>4</sub> anhydrous and the solvent was evaporated under reduced pressure. The residue was purified by silica gel column chromatography (95% CH<sub>2</sub>Cl<sub>2</sub>/5% CH<sub>3</sub>OH) to give compound **3.3** as yellowish solid. Yield: 60%. Rf: 0.6.

**<sup>1</sup>H NMR** (500 MHz, CDCl<sub>3</sub>) δppm 8.77-8.67 (s, 1H, NH, thy), 8.41-8.39 (d, J=2.2Hz, 2H-Ar, nosyl), 8.14-8.08 (m, 2H-Ar, nosyl), 7.71(ddd, J=7.6, 4.7, 1.7 Hz, 1H, H6-Ar), 7.42-7.30 (m, 5H-Ar), 6.28-5.28 (m, 1H-H-1'), 4.51-3.75 (m, 6H), 2.79-2.46 (m, 1H, CH-ala), 1.96-1.86 (m, 2H, H2'), 1.37 (t, J=7.6 Hz, 3H, CH<sub>3</sub> ester), 1.31-1.25 (m, 6H, CH<sub>3</sub>-thy, CH<sub>3</sub>-ala).  
**<sup>13</sup>C NMR** (126 MHz, CDCl<sub>3</sub>) δppm 173.66, 173.36 (C-ala), 163.48(C2, thy), 151.13, 151.10 (C1, thy), 150.29, 150.25 (C1,nosyl), 141.45, 141.35 (C1, phenyl), 134.73, 134.67 (CH, thy), 129.86, 129.81 (CH, C2-6, nosyl), 129.15, 129.13 (CH, C2, C6, phenyl), 125.28 (CH,

C4, phe), 124.84, 124.77 (CH, C3, C5, phenyl), 120.15, 120.11 (CH, C3, C5, nosyl), 120.06, 120.02, 111.36, 111.23 (C, C3, thy), 84.14, 84.00 (CH, C1'), 80.58, 80.52 (CH, C3'), 80.25, 80.18 (CH, C4'), 63.17, 63.14 (CH<sub>2</sub>, C5'), 62.82, 62.79 (CH<sub>2</sub>, ethyl), 50.41, 50.20 (CH, ala), 39.18, 39.16 (CH<sub>2</sub>, C2'), 20.94, 20.90 (CH<sub>3</sub>, ethyl), 14.12, 14.11 (CH<sub>3</sub>, ala), 12.58, 12.56 (CH<sub>3</sub>, thy). **<sup>31</sup>P NMR** (202 MHz, CDCl<sub>3</sub>) δppm 2.75, 2.48. **MS (ESI)<sup>+</sup>**: 705.1 [M + Na<sup>+</sup>]. **HPLC**: Rt: 15.88 min (99%). [Gradient: (0') 95% H<sub>2</sub>O/5% CH<sub>3</sub>CN - (5') 50% H<sub>2</sub>O/50% CH<sub>3</sub>CN - (15') 50% H<sub>2</sub>O/50% CH<sub>3</sub>CN - (20') 95% H<sub>2</sub>O/5% CH<sub>3</sub>CN].

**Tert-butyl 3-((2R,4R,5R)-5-((((tert-butoxycarbonyl)((S)-1-ethoxy-1-oxopropan-2-yl)amino)(phenoxy)phosphoryl)oxy)methyl)-4-(((4-nitrophenyl)sulfonyl)oxy)tetrahydrofuran-2-yl)-5-methyl-2,6-dioxo-3,6-dihydropyrimidine-1(2H)-carboxylate. (3.4)**



**MF:** C<sub>37</sub>H<sub>47</sub>N<sub>4</sub>O<sub>17</sub>PS

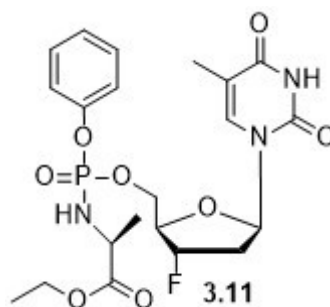
**MW:** 882.83

The nosylate precursor (**3.3**) (1eq, 0.050g, 0.073mmol) was dissolved in pyridine (6mL) at rt under nitrogen atmosphere. Diterbutyl dicarbonate (BOC<sub>2</sub>O) (1.3eq, 0.021ml, 0.020g, 0.095mmol) was added dropwise and the reaction was allowed to stir for 3 days. The crude product was then evaporated *in vacuo* and was purified by silica gel column chromatography (CH<sub>2</sub>Cl<sub>2</sub>/CH<sub>3</sub>OH gradient from 100% CH<sub>2</sub>Cl<sub>2</sub> to 95% CH<sub>2</sub>Cl<sub>2</sub>) to obtain the product **3.4** as a yellowish oil. Yield: 56%. Rf: 0.67 in 90% CH<sub>2</sub>Cl<sub>2</sub>/10% CH<sub>3</sub>OH as TLC system.

**<sup>1</sup>H NMR** (500 MHz, CDCl<sub>3</sub>) δppm 8.47–8.36 (*d*, 2H, *J*=2.2Hz, Ar, nosyl), 8.17–8.08 (*m*, 2H, Ar, nosyl), 7.38 (*m*, 1H, Ar), 7.32–7.24 (*m*, 4H), 7.17 (*s*, 1H, Ar), 6.31–6.24 (*m*, 1H-H-1'), 4.51–3.75 (*m*, 7H), 2.78–2.43 (*m*, 1H, CH-Ala), 2.31–2.23 (*m*, 1H-H-2'), 2.01 (*m*, 3H, CH<sub>3</sub>,thy), 1.53–1.49 (*m*, 9H, CH<sub>3</sub>, tert-butyl), 1.44 (*m*, 9H, CH<sub>3</sub>, tert-butyl), 1.38 (*t*, *J*=7.6Hz, 3H, CH<sub>3</sub>, ester), 1.31 (*m*, 3H, CH<sub>3</sub>,ala). **<sup>13</sup>C NMR** (126 MHz, CDCl<sub>3</sub>) δppm 175.50, 174.29 (C,ala), 161.32 (C2, thy), 150.13, 150.08 (C1, thy), 150.02, 150.00 (C1, nosyl) 143.51, 142.21 (C1, phenyl), 132.71, 132.23 (CH, thy), 130.68, 129.99 (CH, C2-C6, nosyl), 129.34, 129.5 (CH, C2,C6, phenyl), 126.28 (CH, C4, phe), 125.79,

124.85 (CH, C3, C5, phe), 120.15, 120.13 (CH, C3,C5, nosyl), 120.06, 120.02, 111.36, 111.23 (C, C3, thy), 84.13, 84.10 (CH, C1'), 80.78-80.77 (C-tert-butyl), 80.58, 80.52 (CH, C3'), 80.25, 80.18 (CH, C4'), 63.21, 63.20 (CH<sub>2</sub>, C5'), 62.79, 62.77 (CH<sub>2</sub>, ethyl), 50.39, 50.30 (CH, ala), 39.18, 39.15 (CH<sub>2</sub>, C2'), 28.41-28.23 (CH<sub>3</sub>, tert-butyl), 20.94, 20.90 (CH<sub>3</sub>, Ethyl), 14.12, 14.11 (CH<sub>3</sub>, ala), 12.58, 12.56 (CH<sub>3</sub>, thy). **<sup>31</sup>P**NMR: (202 MHz, CDCl<sub>3</sub>): δppm 2.61-2.53. **MS** (ESI<sup>+</sup>): 905.83 [M + Na<sup>+</sup>]. **HPLC**: Rt: 17.1 min (99%). [Gradient: (0') 95% H<sub>2</sub>O/5% CH<sub>3</sub>CN - (5') 50% H<sub>2</sub>O/50% CH<sub>3</sub>CN- (15') 50% H<sub>2</sub>O/50% CH<sub>3</sub>CN- (20') 95% H<sub>2</sub>O/5% CH<sub>3</sub>CN].

**2S)-ethyl2-((((((2R,3S,5R)-3-fluoro-5-(5-methyl-2,4-dioxo-3,4-dihydropyrimidin-1(2H)-yl)tetrahydrofuran-2-yl)methoxy)(phenoxy)phosphoryl)amino)propanoate. (3.11)**



**MF:** C<sub>21</sub>H<sub>27</sub>FN<sub>3</sub>O<sub>8</sub>P

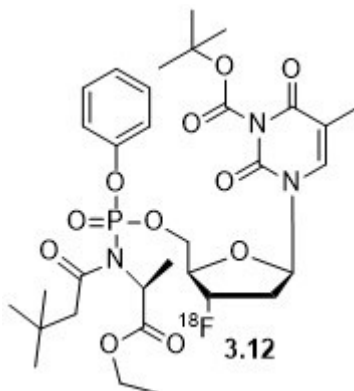
**MW:** 499.4

To a stirring solution of FLT (**1.29**) (1eq; 0.100g; 0.41mmol) in anhydrous THF, was added under nitrogen atmosphere *t*ButMgCl (1.5eq; 0.08mL) and the reaction mixture was stirred at rt for 30min. Then a solution of the phosphorochloridate **3.10** (2eq; 0.239g; 0.82mmol) in anhydrous THF was added dropwise to the reaction mixture and was left to stir overnight. The solvent was evaporated under reduced pressure and the resulting residue was purified by silica gel column chromatography (CH<sub>2</sub>Cl<sub>2</sub>/CH<sub>3</sub>OH from 100% CH<sub>2</sub>Cl<sub>2</sub> to 95% CH<sub>2</sub>Cl<sub>2</sub>) to afford the product **3.7** as a yellowish oil. Yield: 23.5 %. (Rf: 0.44 in 90%CH<sub>2</sub>Cl<sub>2</sub>-10%CH<sub>3</sub>OH TLC system).

**<sup>1</sup>H NMR** (500 MHz, CDCl<sub>3</sub>): δppm 8.60 (br s, 1H, NH), 7.55 (s, 1H, H-6), 7.33-7.41 (m, 2H, Ar-H), 7.20-7.29 (m, 3H, Ar-H), 6.23-6.30 (m, 1H, H-1'), 5.33 (m, 1H, H-3'), 4.43-4.53 (m, 1H, NH, H-4'), 4.21 (m, 1H, CH), 3.95 (m, 2H, CH<sub>2</sub>), 3.35-3.51 (m, 2H, H-5', H-5''), 2.48-2.51 (m, 1H, H-2''), 2.55-2.33 (m, 2H, H<sub>2</sub>''), 1.93-1.74 (m, 3H, CH<sub>3</sub>, thy), 1.30-1.18 (d, *J*=6.9Hz, CH<sub>3</sub>-ala). **<sup>19</sup>F-NMR** (479 MHz, CDCl<sub>3</sub>): δppm -173.70, -175.20. **<sup>31</sup>P NMR** (202 MHz, CDCl<sub>3</sub>): δppm 4.34, 4.12. **MS (ESI<sup>+</sup>)**: 498.1 [M + H<sup>+</sup>]. **HPLC**: Rt: 10.8 min (96%). [Gradient: (0') 95% H<sub>2</sub>O/5% CH<sub>3</sub>CN - (5') 50% H<sub>2</sub>O/50% CH<sub>3</sub>CN- (15') 50% H<sub>2</sub>O/50% CH<sub>3</sub>CN- (20') 95% H<sub>2</sub>O/5% CH<sub>3</sub>CN].

Note: Data agrees with previously published papers.<sup>114</sup>

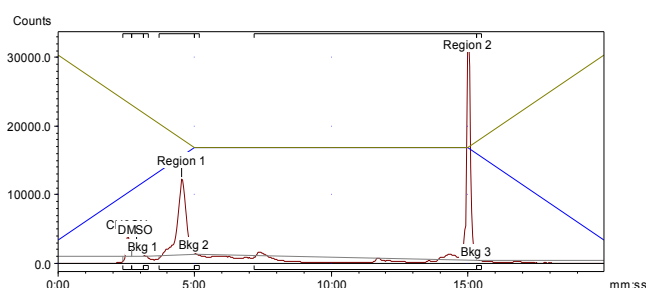
**Tert-butyl-3-((2R,4S,5R)-5-(((N-((S)-1-ethoxy-1-oxopropan-2-yl)-3,3-dimethylbutanamido)(phenoxy)phosphoryl)oxy)methyl)-4-(fluoro-<sup>18</sup>F)tetrahydrofuran-2-yl)-5-methyl-2,6-dioxo-3,6-dihydropyrimidine-1(2H)-carboxylate. (3.12)**



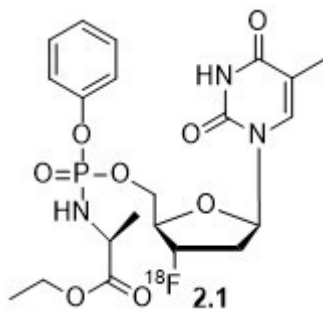
**MF:** C<sub>32</sub>H<sub>45</sub><sup>18</sup>FN<sub>3</sub>O<sub>11</sub>P

**MW:** 696.70

Aqueous <sup>18</sup>F (2.5 GBq), produced by the cyclotron by the nuclear reaction, was trapped in a QMA cartridge before it was eluted with an aqueous solution of KHCO<sub>3</sub> and Kryptofix in CH<sub>3</sub>CN. The resulting <sup>18</sup>F/KHCO<sub>3</sub>/Kryptofix complex was dried by co-evaporation with CH<sub>3</sub>CN anhydrous (2x 1 mL) under reduced pressure and a stream of nitrogen. A solution of the precursor **3.4** (20mg) in CH<sub>3</sub>CN anhydrous (1mL) was added and the reaction was stirred for 30 mins at 95°C. The resulting mixture was passed through an alumina cartridge to finally obtain the radiolabelled product **3.12**. The reaction mixture was analyzed by analytical HPLC and radio TLC. (Analytical HPLC: (0') 95%H<sub>2</sub>O/5%CH<sub>3</sub>CN - (5') 50% H<sub>2</sub>O/50%CH<sub>3</sub>CN- (15') 50% H<sub>2</sub>O/50%CH<sub>3</sub>CN- (20') 95%H<sub>2</sub>O/5%CH<sub>3</sub>CN); Rt: 15 min.



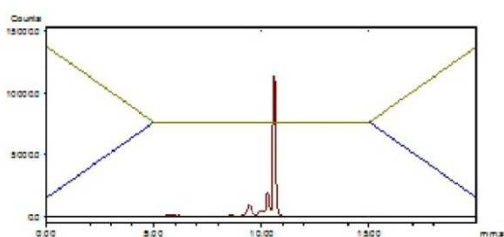
**Ethyl (((((2R,3S,5R)-3-(fluoro-18F)-5-(5-methyl-2,4-dioxo-3,4-dihydropyrimidin-1(2H)-yl)tetrahydrofuran-2-yl)methoxy)(phenoxy)phosphoryl)-L-alaninate. (2.1)**



**MF:** C<sub>21</sub>H<sub>27</sub><sup>18</sup>FN<sub>3</sub>O<sub>8</sub>P

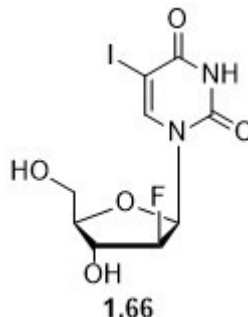
**MW:** 498.43

The BOC protected [18F]-radiolabelled ProTide (**3.12**) was transferred into a V-vial. A solution of 2N HCl (1mL) was added and it was allowed to stir for 10 mins. It was then neutralised with NaOH 2N. The compound was then purified by semi-preparative HPLC and was eluted after 35 minutes at a flow rate of 3.5 mL/min using 70% H<sub>2</sub>O/30% MeCN as the mobile phase. The HPLC solvent was then removed from the mixture under a stream of nitrogen. The radioactive product was taken up in saline and subsequently flushed through a sterility filter to obtain a sterile and clean aqueous solution of [18F]FLT ProTide (**2.1**). RCY of 15-30% (n=5, decay-corrected from end of bombardment (EoB)), with high radiochemical purities (97%) and specific activities of 1800 mCi/μmol. The total synthesis time was 130 min after the end of bombardment (EoB). The reaction mixture was analyzed by analytical HPLC and radio TLC. (Analytical HPLC: (0') 95%H<sub>2</sub>O/5%CH<sub>3</sub>CN - (5') 50% H<sub>2</sub>O/50%CH<sub>3</sub>CN- (15') 50% H<sub>2</sub>O/50%CH<sub>3</sub>CN- (20') 95%H<sub>2</sub>O/5%CH<sub>3</sub>CN); Rt: 10.8 min).



### 8.3.2 Experimental section from chapter 4

#### 2'-deoxy-2'- $\alpha$ -F-5-iodouridine. (**1.66**)



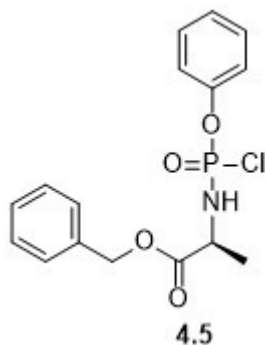
**MW:** 372.1

**MF:** C<sub>9</sub>H<sub>10</sub>FIN<sub>2</sub>O<sub>4</sub>

To a solution of 2'- $\beta$ -fluoro-2'-deoxyuridine (**4.4**) (2eq; 2g; 8.12mmol) in anhydrous acetonitrile (50mL), iodine (1.2eq; 1.24g; 4.87mmol) and ceric ammonium nitrate (CAN) (1eq; 2.23g; 4.062mmol) were added. The reaction mixture was stirred at 75°C for 1h and it was then quenched with a saturated solution of Na<sub>2</sub>S<sub>2</sub>O<sub>3</sub> and concentrated. The residue was re-dissolved in ethyl acetate and washed twice with brine. The organic layer was dried under MgSO<sub>4</sub>, filtered and concentrated *in vacuo* to give compound **1.66** as a pale yellow solid. Yield: 60%. **HPLC:** Rt: 2.3 min (95%). 98%H<sub>2</sub>O/2%CH<sub>3</sub>CN.

**<sup>1</sup>H-NMR** (500 MHz, DMSO-*d*<sub>6</sub>):  $\delta$ ppm 11.69 (*s*, 1H, NH), 8.53 (*s*, 1H, 6-CH), 5.86 (*d*, *J*=15.8Hz, 1H, 1'-CH), 5.60 (*d*, *J*=6.4Hz, 1H, 3'-OH), 5.39 (*t*, *J*=4.5Hz, 1H, 3'-CH), 5.04 (*dd*, *J*=53.2, 4.1Hz, 1H, 2'-CH), 4.18 (*ddd*, *J*=23.4, 11.4, 7.2Hz, 1H, 4'-CH), 3.90 (*d*, *J*=8.2Hz, 1H, 5'-OH), 3.85–3.79 (*m*, 1H, 5'-CH), 3.63–3.58 (*m*, 1H, 5'-CH). **<sup>13</sup>C-NMR** (125 MHz, DMSO-*d*<sub>6</sub>):  $\delta$ ppm 167.88 (C=O), 165.01 (C=O), 145.02 (C-6), 125.19 (C-2'), 121.26 (C-1'), 115.81 (C-4'), 61.11 (C-5), 57.30 (C-3'), 45.87 (C-5'). **<sup>19</sup>F-NMR** (470 MHz, DMSO-*d*<sub>6</sub>):  $\delta$ ppm -202.09.

Note: Data agrees with previously published papers.<sup>155</sup>

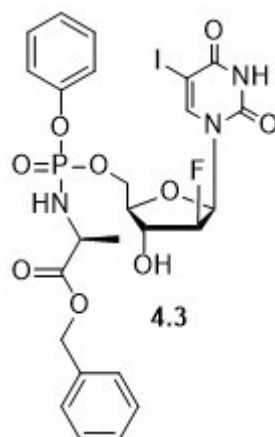
**Benzyl(chloro(phenoxy)phosphoryl)-L-alaninate. (4.5)****MW:** 353.73**MF:** C<sub>16</sub>H<sub>17</sub>ClNO<sub>4</sub>P

Compound **4.5** was prepared according to the standard procedure B. Anhydrous triethylamine (2eq; 1.26mL; 0.918g; 9.08mmol), phenyl dichlorophosphate (**3.9**)(1eq; 0.678mL; 0.958 g; 4.54 mmol) and L-alanine benzyl ester hydrochloride salt ( 1eq; 1.50g; 4.54mmol) were reacted to afford compound **4.5** as a yellowish oil which wasn't further purified. Yield: 88%.

**<sup>1</sup>H NMR** (500MHz, CDCl<sub>3</sub>): δppm7.54–7.47 (*m*, 7H, Ar-H), 7.46–7.40 (*m*, 3H, Ar-H), 5.27 (*d*, *J*=8.4Hz, 2H, CH<sub>2</sub>-ester), 4.69 (*d*, *J*=9.9Hz, 1H, NH), 4.13 (*dd*, *J*=34.4, 29.8 Hz, 1H, CH-ala), 1.52 (*m*, 3H, CH<sub>3</sub>-ala). **<sup>31</sup>P NMR** (202 MHz, CDCl<sub>3</sub>): δppm8.03-7.75.

Note: Data agrees with previously published papers.<sup>85,103,156</sup>

**Benzyl (((((2R,3R,4S,5R)-4-fluoro-3-hydroxy-5-(5-iodo-2,4-dioxo-3,4-dihydropyrimidin-1(2H)-yl)tetrahydrofuran-2-yl)methoxy)(phenoxy)phosphoryl)-L-alaninate. (4.3)**



**MF:** C<sub>25</sub>H<sub>26</sub>FIN<sub>3</sub>O<sub>9</sub>P

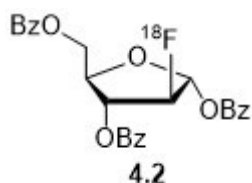
**MW:** 689.3

Compound **4.3** was prepared according to the standard procedure C. 1-(3-fluoro-4-hydroxy-5-(hydromethyl)tetrahydrofuran-2-yl)-5-iodopyrimidine-2,4(1H,3H)-dione (**1.66**) (1eq; 0.400g; 1.07mmol), NMI (5eq; 0.424mL; 0.439g; 5.35mmol), benzyl-2-(chloro(phenoxy)phosphorylamino)propanoate (**4.5**)(3eq; 1.05g; 3.22mmol) were reacted to obtain a residue that was purified by silica gel column chromatography (CH<sub>2</sub>Cl<sub>2</sub>/CH<sub>3</sub>OH from 100% CH<sub>2</sub>Cl<sub>2</sub> to 95% CH<sub>2</sub>Cl<sub>2</sub>) to obtain the product **4.3** as a yellowish oil. Yield: 10%.

**<sup>1</sup>H NMR** (500 MHz, CDCl<sub>3</sub>): δppm 10.59 (s, 1H, 3-NH), 7.89 (s, 1H, 6-CH), 7.53–7.48 (m, 2H, CH-phenyl), 7.45 (t, *J*=8Hz, 2H, CH-phenyl), 7.41-7.38 (m, 2H, CH-benz), 7.17-7.15 (m, 2H, CH-benz), 7.13 (t, 8Hz, 1H, CH-benzyl), 7.12 (t, *J*=7.4 Hz, 1H, CH-phenyl), 5.99 (m, 1H, 1'-CH), 5.79 (dd, *J*=47.6, 4.6 Hz, 1H, 2'-CH), 5.14 (m, 2H, CH<sub>2</sub>-benz), 4.90 (m, 2H, 5'-CH<sub>2</sub>), 4.39 (m, 1H, 4'-CH), 4.27 (m, 1H, 3'-CH), 4.19 (m, 1H, 3'-OH), 4.02 (m, 1H, NH-ala), 3.99 (m, 1H, CH-ala), 1.29 (d, *J*=7.0Hz, 3H, CH<sub>3</sub>-ala). **<sup>13</sup>C NMR** (125 MHz, CDCl<sub>3</sub>): δppm 171.9 (C=O, ala), 168.12 (C-4), 144.18 (C-2), 149.0 (C-phenyl), 147.91 (C-benzyl), 145.5, 145.1 (C-6), 128.31-121.48 (Ar-C), 94.3 (C-5), 92.10 (C-4'), 89.13 (C-2'), 83.6, 82.97 (C-1'), 81.08, 80.97 (C-ester), 69.61, 68.14 (C-3'), 67.23 (C-5'), 52.8 (CH-ala), 21.98 (CH<sub>3</sub>-ala). **<sup>19</sup>F NMR** (470 MHz, CDCl<sub>3</sub>): δ -200.91, -201.15. **<sup>31</sup>P NMR** (202 MHz,

$\text{CDCl}_3$ ):  $\delta$ ppm 3.90, 3.86. **MS** (ESI)<sup>+</sup>: 690.3 [M + H<sup>+</sup>]. **HPLC**: Rt: 13.4 min (97%). [Gradient: (0') 95% H<sub>2</sub>O/5% CH<sub>3</sub>CN - (5') 50% H<sub>2</sub>O/50% CH<sub>3</sub>CN- (15') 50% H<sub>2</sub>O/50% CH<sub>3</sub>CN- (20') 95% H<sub>2</sub>O/5% CH<sub>3</sub>CN].

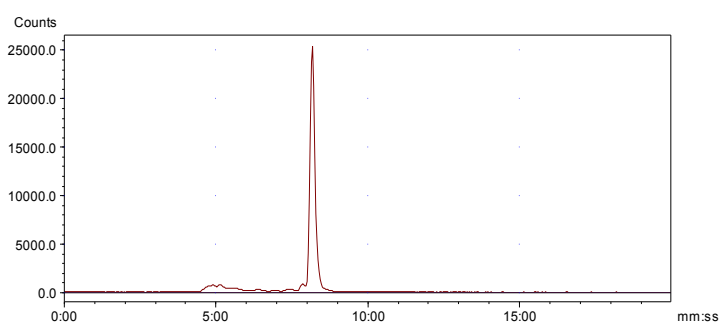
**(2R,3S,4R,5R)-5-((benzoyloxy)methyl)-3-(fluoro-<sup>18</sup>F)tetrahydrofuran-2,4-diyl  
dibenzoate. (4.2)**



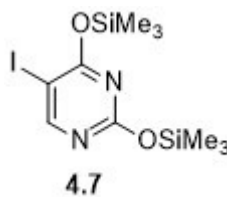
**MF:** C<sub>26</sub>H<sub>21</sub><sup>18</sup>F<sub>7</sub>

**MW:** 463.4

Aqueous <sup>18</sup>F (4.11 GBq), produced by the cyclotron by the nuclear reaction, was trapped in a QMA cartridge before it was eluted with an aqueous solution of KHCO<sub>3</sub> and Kryptofix in CH<sub>3</sub>CN. The resulting <sup>18</sup>F/KHCO<sub>3</sub>/Kryptofix complex was dried by co-evaporation with CH<sub>3</sub>CN anhydrous (2x 1mL) under reduced pressure and a stream of nitrogen. A solution of the triflate precursor of the sugar (**4.1**) (20 mg) in CH<sub>3</sub>CN anhydrous (1 mL) was added and the reaction was stirred for 30 mins at 95°C. The resulting mixture was passed through an alumina cartridge to finally obtain the radiolabelled product that was used for next step without any further purification. The reaction mixture was analyzed by analytical HPLC and radio TLC. (Analytical HPLC: 100% CH<sub>3</sub>CN; Rt: 8.3 min).

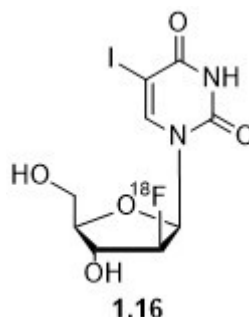


Note: Data agrees with previously published papers.<sup>155</sup>

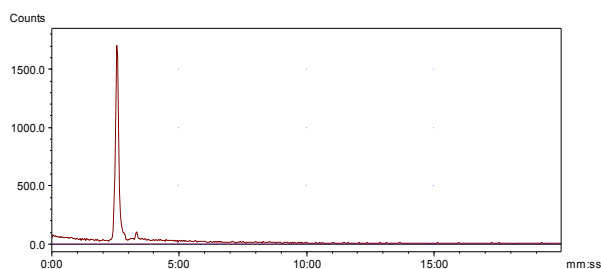
**5-iodo-2,4-bis((trimethylsilyl)oxy)pyrimidine. (4.7)****MF:** C<sub>10</sub>H<sub>19</sub>IN<sub>2</sub>O<sub>2</sub>Si<sub>2</sub>**MW:** 382.3

To a solution of 5-iodouracil (**4.6**) (1eq; 10mg; 0.042mmol) in dichloroethane (500μL), hexamethyldisilazane (11.4eq; 100μL; 0.0774mg; 0.479mmol) and TMSOTf (13.1eq; 100μl, 0.123mg; 0.549mmol) were added into a 4mL vial on a hot plate placed into a hot cell. The mixture was stirred for 2h at 85°C. The crude mixture was used directly for next step without further purification. The purity of the compound was proved by analytical HPLC (88% H<sub>2</sub>O/12% CH<sub>3</sub>CN, Rt= 6.9 min) and LC-MS ([M+H<sup>+</sup>]: 383.2).

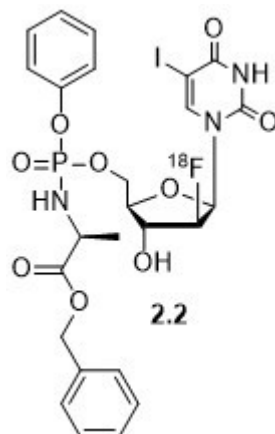
Note: Data agrees with previously published papers.<sup>155</sup>

**<sup>18</sup>FIAU****1-((2R,3S,4R,5R)-3-(fluoro-<sup>18</sup>F)-4-hydroxy-5-(hydroxymethyl)tetrahydrofuran-2-yl)-5-iodopyrimidine-2,4(1H,3H)-dione. (1.16)****MF:** C<sub>9</sub>H<sub>10</sub><sup>18</sup>FN<sub>2</sub>O<sub>5</sub>**MW:** 371.0

Compound synthesised with the E&Z modular lab (**4.2**), was delivered directly from the unit to the vial containing 2-4-bis(trimethyl silyl)-5-iodo uracil (**4.7**). The mixture was then heated at 85°C for 60 min. To this mixture, 0.5M of NaOMe in CH<sub>3</sub>OH (1mL) was added and the reaction was stirred at 85°C for other 5 min. The precipitate was reconstituted in water (1mL) and neutralized with 6N HCl. The reaction mixture was then analyzed by analytical HPLC showing the formation of the 2 anomers α and β of the 2'-deoxy-2'-fluoro-5-iodouridine. (Analytical HPLC: 98% H<sub>2</sub>O/2% CH<sub>3</sub>CN; R<sub>t</sub> : α anomer 2.1 min; β anomer 2.9 min). The anomeric mixture was then purified by semi-preparative HPLC and the target compound (**1.16**) was eluted after 7.3mins at a flow rate of 3.5mL/min using 20% CH<sub>3</sub>CN/ 80% H<sub>2</sub>O as the mobile phase to obtain the final compound which was analysed by analytical HPLC. (Analytical HPLC: 98% H<sub>2</sub>O/2% CH<sub>3</sub>CN; R<sub>t</sub>: 2.1min).



Note: Data agrees with previously published papers.<sup>155</sup>

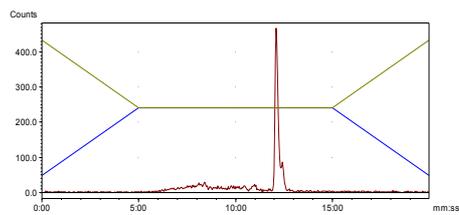
**[<sup>18</sup>F]FIAU ProTide. (2.2)**

**MF:** C<sub>25</sub>H<sub>26</sub><sup>18</sup>FIN<sub>3</sub>O<sub>9</sub>P

**MW:** 688.3

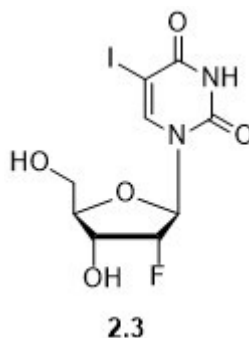
To the vial containing [<sup>18</sup>F]FIAU (**1.16**) under nitrogen atmosphere, NMI (0.1mL) was added dropwise and the solution of benzyl-2-(chloro(naphthoxy)phosphorylamino)propanoate (**4.5**) (0.050g) dissolved in anhydrous THF (0.5ml) was added dropwise. The reaction mixture was stirred at 50°C for 20 mins and then dried under a flow of nitrogen, re-dissolved in CH<sub>3</sub>CN and then was indeed isolated *via* semi preparative HPLC and was eluted after 23 minutes at a flow rate of 3.5mL/min using 50% MeCN/ 50% H<sub>2</sub>O as the mobile phase. The HPLC solvent was removed from the mixture under a stream of nitrogen. The radioactive product was taken up in saline and subsequently flushed through a sterility filter to obtain a sterile and clean aqueous solution of [<sup>18</sup>F]FIAUProTide (**2.2**). Radiochemical reactions were carried out using starting activities between 4-15 GBq, leading to RCY of 1-5% (n=7, decay-corrected from end of bombardment (EoB)), with high radiochemical purities (98%) and specific activities of 1800 mCi/μmol. The total synthesis time was 240 min after the end of bombardment (EoB). (Analytical HPLC: (0') 95%H<sub>2</sub>O/5%ACN - (5') 50% H<sub>2</sub>O/50%CH<sub>3</sub>CN- (15') 50% H<sub>2</sub>O/50%CH<sub>3</sub>CN- (20') 95%H<sub>2</sub>O/5%CH<sub>3</sub>CN); Rt: 12.3 min.

## 8. Experimental



### 8.3.3 Experimental section from chapter 5

#### 2'-deoxy- 2'α-fluoro-5-iodouridine

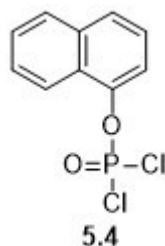


**MW:** 372.1

**MF:** C<sub>9</sub>H<sub>10</sub> FIN<sub>2</sub>O<sub>4</sub>

To a solution of 2'-α-fluoro-2'-deoxyuridine (2eq; 2g; 8.12mmol) in anhydrous acetonitrile (50 ml), iodine (1.2eq; 1.24g; 4.87mmol) and ceric ammonium nitrate (CAN) (1eq; 2.23g; 4.062mmol) were added. The reaction mixture was stirred at 75°C for 1h and it was then quenched with a saturated solution of Na<sub>2</sub>S<sub>2</sub>O<sub>3</sub> and then concentrated. The residue was re-dissolved in ethyl acetate and washed twice with brine. The organic layer was dried under MgSO<sub>4</sub>, filtered and concentrated *in vacuo* to give a pale yellow solid. Yield: 60%.

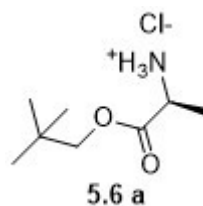
**<sup>1</sup>H NMR** (500 MHz, DMSO-*d*<sub>6</sub>): δppm 11.69 (*s*, 1H, NH), 8.53 (*s*, 1H, 6-CH), 5.86 (*d*, *J*=15.8 Hz, 1H, 1'-CH), 5.60 (*d*, *J*=6.4Hz, 1H, 3'-OH), 5.39 (*t*, *J*=4.5Hz, 1H, 3'-CH), 5.04 (*dd*, *J*=53.2, 4.1Hz, 1H, 2'-CH), 4.18 (*ddd*, *J*=23.4, 11.4, 7.2 Hz, 1H, 4'-CH), 3.90 (*d*, *J*=8.2Hz, 1H, 5'-OH), 3.85–3.79 (*m*, 1H, 5'-CH), 3.63–3.58 (*m*, 1H, 5'-CH). **<sup>13</sup>C NMR** (125 MHz, DMSO-*d*<sub>6</sub>): δ 167.88 (C=O), 165.01 (C=O), 145.02 (C-6), 125.19 (C-2'), 121.26 (C-1'), 115.81 (C-4'), 61.11 (C-5), 57.30 (C-3'), 45.87 (C-5'). **<sup>19</sup>F NMR** (470 MHz, DMSO-*d*<sub>6</sub>): δppm -202.09. **HPLC:** Rt: 2.0 min (97%). 98%H<sub>2</sub>O/2%CH<sub>3</sub>CN.

**Naphthalen-1-yl phosphorodichloridate(5.4)****MF:** C<sub>10</sub>H<sub>7</sub>Cl<sub>2</sub>O<sub>2</sub>P**MW:** 261.03

Phosphorus oxychloride (1eq; 0.912mL; 1.5g; 9.78mmol) and 1-naphtol (1eq; 1.41g; 9.78mmole) were stirred in anhydrous Et<sub>2</sub>O under nitrogen atmosphere. Anhydrous TEA (1eq; 1.36 ml; 0.990 g; 9.78mmoles) was added dropwise at -78°C. The reaction mixture was then allowed to stir for 1h and then to slowly warm to rt and stirred for other 3h. The reaction was monitored by <sup>31</sup>P NMR. The crude mixture was then filtered under nitrogen atmosphere and reduced under pressure to furnish a yellowish oil which wasn't further purified. Yield: 98%.

<sup>1</sup>H NMR (CDCl<sub>3</sub>, 500MHz): δppm 8.01-8.00 (*m*, 1H, H-8), 7.81-7.79 (*m*, 1H, H-5), 7.70-7.68 (*m*, 1H, H-4), 7.63-7.52 (*m*, 4H, H-2, H-3, H-6, H-7). <sup>31</sup>P NMR (CDCl<sub>3</sub>, 202 MHz): δppm 3.88.

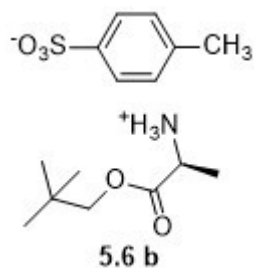
Note: Data agrees with previously published papers.<sup>85,103,156</sup>

**(S)-1-(neopentyloxy)-1-oxopropan-2-aminium – chloride. (5.6a)****MF:** C<sub>8</sub>H<sub>18</sub> Cl NO<sub>2</sub>**MW:** 195.6

Compound **5.6a** was prepared according to standard procedure A1. Thionyl chloride (2eq; 1.63mL, 2.66g, 22.44mmol), neopentyl alcohol (15eq; 12.88mL; 10.11g; 0.168mol), L-alanine (1eq; 1g; 0.0112mol) were reacted to give the product **5.6a** a yellowish oil which wasn't further purified. Yield: 57%.

**<sup>1</sup>H NMR** (500 MHz, CDCl<sub>3</sub>): δppm 8.56 (*s*, 3H, NH<sub>3</sub><sup>+</sup>), 4.92 (*s*, 2H, CH<sub>2</sub>-neopentyl), 3.92 (*m*, 1H, CH-ala), 1.39 (*d*, *J*=7.5 Hz, 3H, CH<sub>3</sub>-ala), 1.21 (*d*, *J*=6.0Hz, 9H, 3xCH<sub>3</sub>-neopentyl).

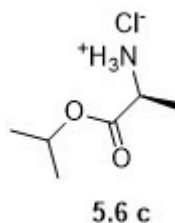
Note: Data agrees with previously published papers. <sup>85,103,156</sup>

**(S)-1-(neopentyloxy)-1-oxopropan-2-aminium - 4-methylbenzenesulfonate. (5.6b)****MF:** C<sub>15</sub>H<sub>25</sub>NO<sub>5</sub>S**MW:** 331.4

Compound **5.6b** was prepared according to standard procedure A2. L-alanine (1eq; 0.500g; 5.61mol), 2,2-dimethyl-1-propanol (15eq; 9.07mL; 7.41g; 0.084mol) and p-toluenesulfonic acid (1.1eq; 1.17g; 6.17mmol) were reacted to give as a product a white solid (**5.6b**) which wasn't further purified. Yield: 83%.

**<sup>1</sup>H NMR** (500 MHz, CDCl<sub>3</sub>): δppm 8.29 (*s*, 3H, NH<sub>3</sub><sup>+</sup>), 7.49 (*d*, J=7.9Hz, 2H, CH-tosylate), 7.13 (*d*, J=7.7Hz, 2H, CH-tosylate), 3.89 (*m*, 1H, CH-ala), 3.06 (*s*, 2H, CH<sub>2</sub>-ester), 2.30 (*s*, 3H, CH<sub>3</sub>-tosylate), 0.94 (*s*, 3H, CH<sub>3</sub>-ala), 0.86–0.79 (*m*, 9H, 3xCH<sub>3</sub>-ester).

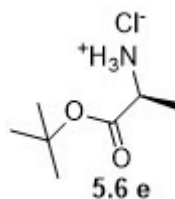
Note: Data agrees with previously published papers.<sup>85,103,156</sup>

**(S)-1-isopropoxy-1-oxopropan-2-aminium chloride. (5.6c)****MF:** C<sub>6</sub>H<sub>14</sub>ClNO<sub>2</sub>**MW:** 167.6

Compound **5.6c** was prepared according to standard procedure A1. Thionyl chloride (2eq; 1.63mL, 2.66g, 22.44mmol), 2-propanol (isopropanol) (15eq; 12.88mL; 10.11g; 0.168mol) were reacted to give **5.6c** as a white solid. Yield: 89%.

**<sup>1</sup>H NMR** (500 MHz, CDCl<sub>3</sub>): δppm 8.66 (*s*, 3H, NH<sub>3</sub><sup>+</sup>), 4.98 (*dt*, *J*=12.5, 6.2Hz, 1H, CH-ester), 3.96 (*m*, 1H, CH-ala), 1.41 (*d*, *J*=7.2Hz, 3H, CH<sub>3</sub>-ala), 1.24 (*d*, *J* = 6 Hz, 6H, 2xCH<sub>3</sub>, *i*-propyl).

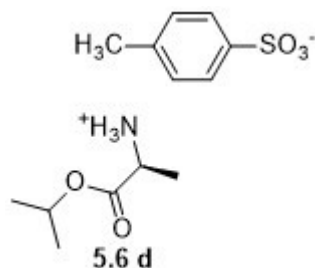
Note: Data agrees with previously published papers.<sup>85,103,156</sup>

**S)-1-(tert-butoxy)-1-oxopropan-2-aminium chloride. (5.6e)****MF:** C<sub>7</sub>H<sub>16</sub>ClNO<sub>2</sub>**MW:** 146.21

Compound **5.6e** was prepared according to standard procedure A1. Thionyl chloride (2eq; 1.63mL, 2.66g, 22.44mmol), tert-butanol (15eq; 12.88mL; 10.11g; 0.168mol) and L-alanine (1eq; 1g; 0.0112mol) were reacted to furnish compound **5.6e** as yellowish solid. Yield: 84%.

**<sup>1</sup>H NMR** (500 MHz, CDCl<sub>3</sub>): δ 8.56 (*s*, 3H, NH<sub>3</sub><sup>+</sup>), 3.99 (*m*, 1H, CH-ala), 1.36 (*d*, *J*=7.1Hz, 3H, CH<sub>3</sub>-ala), 1.19 (*s*, 9H, 3xCH<sub>3</sub>, tert-butyl).

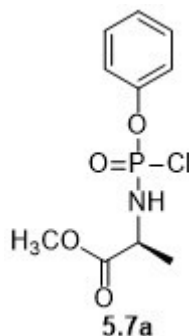
Note: Data agrees with previously published papers. <sup>85,103,156</sup>

**(S)-1-isopropoxy-1-oxopropan-2-aminium 4-methylbenzenesulfonate. (5.6d)****MF:** C<sub>13</sub>H<sub>24</sub>O<sub>5</sub>S**MW:** 171.19

Compound **5.6d** was prepared according to standard procedure A2. L-alanine (1eq; 0.500g; 5.61mol), isopropanol (15eq; 9.01mL; 7.39g; 0.081mol) and p-toluenesulfonic acid (1.1eq; 1.17g; 6.17mmol) were used as reagents to give **5.6d** as a white solid which wasn't further purified. Yield: 78%.

**<sup>1</sup>H NMR** (500 MHz, CDCl<sub>3</sub>): δppm 8.34 (*s*, 3H, NH<sub>3</sub><sup>+</sup>), 7.51 (*d*, J=7.8Hz, 2H, CH-tosylate), 7.09 (*d*, J=7.5Hz, 2H, CH-tosylate), 3.90 (*m*, 1H, CH-ala), 3.06 (*m*, 1H, CH-ester), 2.11 (*s*, 3H, CH<sub>3</sub>-tosylate), 1.11 (*s*, 3H, CH<sub>3</sub>-ala), 0.86–0.79 (*d*, J=7.2 Hz 2xCH<sub>3</sub>-ester).

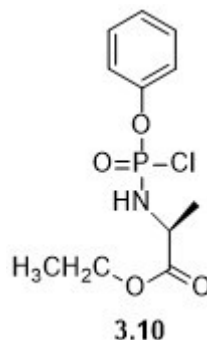
Note: Data agrees with previously published papers.<sup>85,103,156</sup>

**(2S)-methyl 2-((chloro(phenyl)phosphoryl)amino)propanoate. (5.7a)****MF:** C<sub>10</sub>H<sub>13</sub>ClNO<sub>4</sub>P**MW:** 277.6

Compound **5.7a** was prepared according to standard procedure B. Phenyl dichlorophosphate (**3.9**) (1eq; 0.250g; 1.18mmol), L-alanine methyl ester hydrochloride salt (1eq; 0.165g; 1.18mmol), triethylamine (2eq; 0.239g; 0.329mL; 2.36mmol) were used as reagents to furnish **5.7a** as a yellowish oil. Yield: 80%.

**<sup>1</sup>H NMR** (500 MHz, CDCl<sub>3</sub>): δppm 7.25-7.39 (*m*, 2H, Ar-H), 7.21-7.37 (*m*, 3H, Ar-H), 4.30 (*m*, 1H, NH), 4.19 (*m*, 1H, CH-ala), 3.50 (*s*, 3H, CH<sub>3</sub>-ester), 1.21 (*m*, 3H, CH<sub>3</sub>-ala). **<sup>31</sup>P NMR**: (202 MHz, CDCl<sub>3</sub>): δppm 7.96, 7.64.

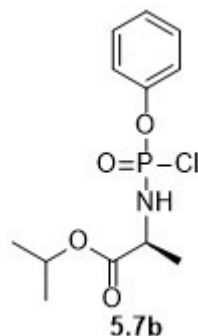
Note: Data agrees with previously published papers.<sup>85,103,156</sup>

**Ethyl (chloro(phenoxy)phosphoryl)-L-alaninate. (3.10)****MF:** C<sub>11</sub>H<sub>15</sub>ClNO<sub>4</sub>P**MW:** 291.6

Compound **3.10** was synthesised according to standard procedure B. Anhydrous triethylamine (2eq; 0.662mL; 0.480g; 4.74mmol), phenyl dichlorophosphate (**3.9**) (1 eq; 0.354mL; 0.500g; 2.37mmol) and L-alanine ethyl ester hydrochloride salt (1eq; 0.364g; 2.37mmol) were reacted to afford the product **3.10** as a yellowish oil. Yield: 95%.

**<sup>1</sup>H NMR** (500MHz, CDCl<sub>3</sub>): δppm 7.35-7.41 (*m*, 2H, Ar-H), 7.21-7.30 (*m*, 3H, Ar-H), 4.53 (*m*, 1H, NH), 4.21 (*m*, 1H,CH), 3.95 (*m*, 2H, CH<sub>2</sub>), 1.51 (*m*, 3H, CH<sub>3</sub>-ala), 1.23 (*m*, 3H, CH<sub>3</sub>-ester). **<sup>31</sup>P NMR** (202 MHz, CDCl<sub>3</sub>): δppm 8.05, 7.71.

Note: Data agrees with previously published papers.<sup>85,103,156</sup>

Isopropyl(chloro(phenoxy)phosphoryl)-L-alaninate (**5.7b**)

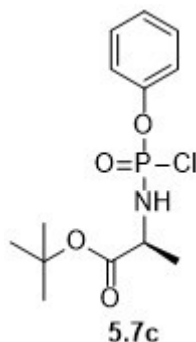
**MF:** C<sub>12</sub>H<sub>17</sub>ClNO<sub>4</sub>P

**MW:** 305.69

Compound **5.7b** was synthesised according to standard procedure B. Anhydrous triethylamine (2eq; 1.08mL; 0.78g; 7.74mmol), phenyl dichlorophosphate (**3.9**) (1eq; 0.579 ml; 0.818 g; 3.87mmol) and L-alanine isopropyl ester hydrochloride salt (1eq; 0.650g; 3.87mmol) were reacted to afford **5.7b** as a yellowish oil which wasn't further purified. Yield: 83%.

**<sup>1</sup>H NMR** (500 MHz, CDCl<sub>3</sub>): δppm 7.28 (*m*, 2H, CH-phenyl), 7.23 (*m*, 2H, CH-phenyl), 7.08 (*m*, 1H, CH-phenyl), 4.98 (*m*, 1H, CH-*i*-propyl), 4.37 (*s*, 1H, NH), 4.04 (*m*, 1H, CH-ala), 1.30 (*d*, *J*=7.5, 3H, CH<sub>3</sub>- ala), 1.16 (*dd*, *J*=9.7, 3.5Hz, 6H, 2xCH<sub>3</sub>-ester). **<sup>31</sup>P NMR** (202MHz, CDCl<sub>3</sub>): δppm 8.18, 7.84.

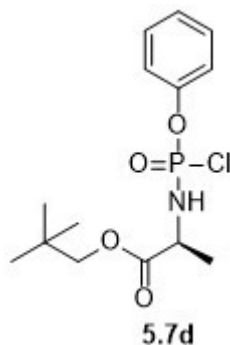
Note: Data agrees with previously published papers.<sup>85,103,156</sup>

**Tert-butyl(chloro(phenoxy)phosphoryl)-L-alaninate. (5.7c)****MW:** 319.72**MF:** C<sub>13</sub>H<sub>19</sub>ClNO<sub>4</sub>P

Compound **5.7c** was prepared according to the standard procedure B. Anhydrous triethylamine (2eq; 0.661ml; 0.48g; 4.74mmol), phenyl dichlorophosphate (**3.9**) (1eq; 0.354mL; 0.500g; 2.37mmol) and L-alanine tert-butyl ester hydrochloride salt (**5.6e**) (1eq; 0.430g; 2.37mmol) were reacted to afford **5.7c** as a yellowish oil which wasn't further purified. Yield: 91%.

**<sup>1</sup>H NMR** (500 MHz, CDCl<sub>3</sub>): δppm 7.28 (*ddd*, *J*=14.7, 9.4, 4.0Hz, 2H, CH-phenyl), 7.10–7.00 (*m*, 3H, CH-phenyl), 4.31 (*m*, 1H, NH), 3.98 (*m*, 1H, CH-ala), 1.60 (*d*, *J*=7.1Hz, CH<sub>3</sub>-ala), 1.53 (*s*, 9H, 3xCH<sub>3</sub>). **<sup>31</sup>P NMR** (202 MHz, CDCl<sub>3</sub>): δppm 8.24, 7.82.

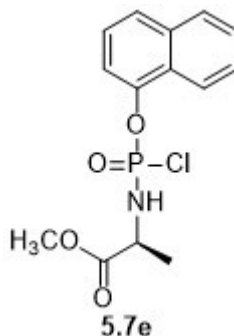
Note: Data agrees with previously published papers.<sup>85,103,156</sup>

**Neopentyl(chloro(phenoxy)phosphoryl)-L-alaninate. (5.7d)****MW:** 333.74**MF:** C<sub>14</sub>H<sub>21</sub>ClNO<sub>4</sub>P

Compound **5.7d** was synthesised according to the standard procedure B. Anhydrous triethylamine (2eq; 1.26mL; 0.918g; 9.08mmol), phenyl dichlorophosphate (**3.9**) (1eq; 0.678mL; 0.958g; 4.54 mmol) and L-alanine neopentyl ester sulfonate salt (**5.6b**) (1eq; 1.50g; 4.54mmol) were reacted to afford compound **5.7d** as a yellowish oil which wasn't further purified. Yield: 82%.

<sup>1</sup>H NMR (500MHz, CDCl<sub>3</sub>): δppm 7.33–7.21 (*m*, 2H, H-Ar), 7.11 (*m*, 3H, H-Ar), 3.97–3.83 (*m*, 1H, NH), 3.82–3.70 (*m*, 2H, CH<sub>2</sub>-ester), 3.68 (*m*, 1H, CH-ala), 0.90–0.84 (*s*, 9H, 3x CH<sub>3</sub>-ester), 0.82 (*d*, J=3.5Hz, 3H, CH<sub>3</sub>-ala). <sup>31</sup>P NMR (202 MHz, CDCl<sub>3</sub>): δppm 8.12, 7.80.

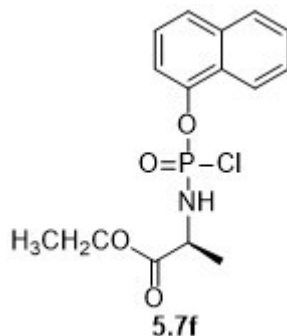
Note: Data agrees with previously published papers.<sup>85,103,156</sup>

**Methyl(chloro(naphthalen-1-yloxy)phosphoryl)-L-alaninate (5.7e)****MW:** 327.70**MF:** C<sub>14</sub>H<sub>15</sub>ClNO<sub>4</sub>P

Compound **5.7e** was prepared according to standard procedure B. Anhydrous triethylamine (2eq; 1.61mL; 1.17g; 11.54mmol), naphthyl dichlorophosphate (**5.4**) (1eq; 1.50g; 5.77mmol) and L- alanine methyl ester hydrochloride salt (1eq; 0.805g; 5.77mmol) were used as reagents to afford the compound **5.7e** as a yellowish oil which wasn't further purified. Yield: 85%.

**<sup>1</sup>H NMR** (CDCl<sub>3</sub>, 500 MHz): δppm 7.89-7.15 (*m*, 7H, Naph), 4.29-4.25 (*m*, 1H, NH), 4.31-4.20 (*m*, 1H, CH- ala), 3.81-3.64 (*s*, 3H, CH<sub>3</sub>-ester), 1.34 (*d*, J=3.5Hz, 3H, CH<sub>3</sub>-ala). **<sup>31</sup>P NMR** (CDCl<sub>3</sub>, 202 MHz): δppm 7.99, 7.87.

Note: Data agrees with previously published papers.<sup>85,103,156</sup>

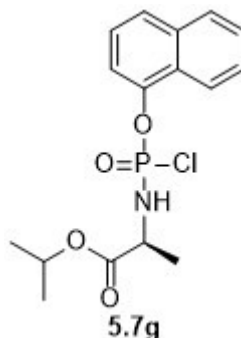
**Ethyl(chloro(naphthalen-1-yloxy)phosphoryl)-L-alaninate. (5.7f)****MF:** C<sub>15</sub>H<sub>17</sub>ClNO<sub>4</sub>P**MW:** 341.72

Compound **5.7f** was prepared according to standard procedure B. Anhydrous triethylamine (2eq; 1.61mL; 1.17g; 11.54mmol), naphthyl dichlorophosphate (**5.3**) (1eq; 1.50g; 5.77mmol) and L-alanine ethyl ester hydrochloride salt (1eq; 0.886g; 5.77mmol) were reacted to afford the product **5.7f** as a yellowish oil which wasn't further purified. Yield: 94%.

<sup>1</sup>H NMR (CDCl<sub>3</sub>, 500 MHz): δppm 8.31-8.26 (*m*, 1H, H-8, naph), 7.63-7.51 (*m*, 1H, H-6, naph), 7.74-7.71 (*m*, 1H, H-2, naph), 7.52-7.43 (*m*, 4H, naph), 4.39 (*m*, 1H, CH-ala), 4.21 (*q*, 2H, CH<sub>2</sub>-ester), 1.58-1.54 (*m*, 3H, CH<sub>3</sub>-ala), 1.41-1.29 (*d*, J=6.3Hz 3H, CH<sub>3</sub>-ester).

<sup>31</sup>P NMR (CDCl<sub>3</sub>, 202 MHz): δ 8.13, 7.89.

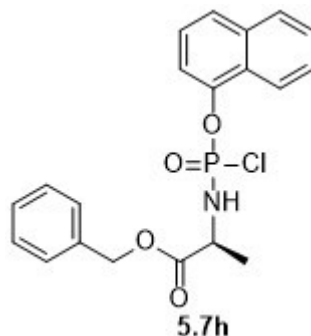
Note: Data agrees with previously published papers.<sup>85,103,156</sup>

**Isopropyl(chloro(naphthalen-1-yloxy)phosphoryl)-L-alaninate. (5.7g)****MF:** C<sub>16</sub>H<sub>19</sub>ClNO<sub>4</sub>**MW:** 355.75

Compound **5.7g** was prepared according to standard procedure B. Anhydrous triethylamine (2eq; 0.749mL; 0.54g; 5.38mmol), naphthyl dichlorophosphate (**5.4**) (1eq; 0.7g; 2.69mmol) and L-alanine isopropyl ester hydrochloride salt (**5.6c**) (1eq; 0.45g; 2.69mmol) were reacted to afford product **5.7g** as a yellowish oil which wasn't further purified. Yield: 82%.

**<sup>1</sup>H NMR** (CDCl<sub>3</sub>, 500MHz): δppm 8.09 (*m*, 1H, H-8, naph), 7.89-7.86 (*m*, 1H, H-6, naph), 7.76-7.73 (*m*, 1H, H-2, naph), 7.59-7.44 (*m*, 4H, naph), 5.12-5.05 (*m*, 1H, CH, *i*-propyl), 4.43-4.20 (*m*, 1H, CH-ala), 1.56-1.51 (*d*, J=3.1Hz, 3H, CH<sub>3</sub>-ala), 1.31-1.23 (*d*, J=4.5Hz, 6H, 2x CH<sub>3</sub>, *i*-propyl). **<sup>31</sup>P-NMR** (CDCl<sub>3</sub>, 202 MHz): δ 8.15, 7.99.

Note: Data agrees with previously published papers.<sup>85,103,156</sup>

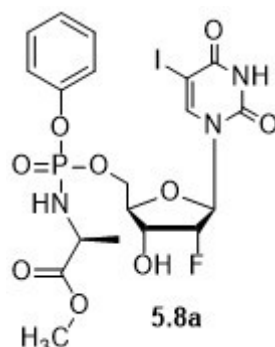
**Benzyl(chloro(naphthalen-1-yloxy)phosphoryl)-L-alaninate (5.7h)****MF:** C<sub>20</sub>H<sub>19</sub>ClNO<sub>4</sub>P**MW:** 403.79

Compound **5.7h** was prepared according to standard procedure B. Anhydrous triethylamine (2eq; 0.749mL; 0.54g; 5.38mmol), naphthyl dichlorophosphate (**5.3**) (1eq; 0.7g; 2.69mmol) and L-alanine benzyl ester hydrochloride salt (1eq; 0.45g; 2.69mmol) to furnish the product **5.7h**. Yield: 80%

<sup>1</sup>H NMR (CDCl<sub>3</sub>, 500MHz): δppm 7.83-7.35 (*m*, 12H, naph and phenyl), 5.13-5.04 (*m*, 2H, CH<sub>2</sub>Ph), 4.41-4.31 (*m*, 1H, CHCH<sub>3</sub>), 1.51-1.46 (*m*, 3H, CH<sub>3</sub>.ala). <sup>31</sup>P NMR (CDCl<sub>3</sub>, 202 MHz): δppm 8.14, 7.88.

Note: Data agrees with previously published papers.<sup>85,103,156</sup>

**Methyl((((2R,3R,4S,5R)-4-fluoro-3-hydroxy-5-(5-iodo-2,4-dioxo-3,4-dihydropyrimidin-1(2H)-yl)tetrahydrofuran-2-yl)methoxy)(phenoxy)phosphoryl)-L-alaninate. (5.8a)**



**MF:** C<sub>19</sub>H<sub>22</sub>FIN<sub>3</sub>O<sub>9</sub>P

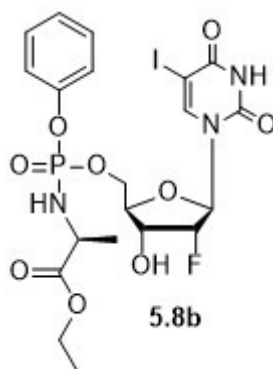
**MW:** 613.2

Compound **5.8a** was prepared according to standard procedure C. 1-(3-fluoro-4-hydroxy-5-(hydromethyl)tetrahydrofuran-2-yl)-5-iodopyrimidine-2,4(1H,3H)-dione (**2.3**) (1eq; 0.265g; 0.713mmol), NMI (5eq; 0.283mL; 0.293g; 3.567mmol) and methyl-2-(chloro(phenoxy) phosphorylamino)propanoate (**5.7a**) (3eq; 0.594g; 2.140mmol) were reacted to obtain a residue that was purified by silica gel column chromatography (CH<sub>2</sub>Cl<sub>2</sub>/CH<sub>3</sub>OH gradient from 100% CH<sub>2</sub>Cl<sub>2</sub> to 95% CH<sub>2</sub>Cl<sub>2</sub>) to obtain the product **5.8a** as a yellowish oil. Yield: 7%.

**<sup>1</sup>H NMR** (500 MHz, CDCl<sub>3</sub>): δppm 8.90 (*s*, 1H, 3-NH), 7.85 (*d*, *J* = 4.9 Hz, 1H, 6-CH), 7.26 (*td*, *J*=7.9, 2.9 Hz, 2H, CH-phenyl), 7.16 (*d*, *J*=8.6 Hz, 2H, CH-phenyl), 7.11 (*t*, *J* = 7.4 Hz, 1H, CH-phenyl), 5.78 (*ddd*, *J* = 30.9, 17.7, 1.4 Hz, 1H, 1'-CH), 4.91 (*m*, 1H, 2'-CH), 4.40 (*d*, *J* = 8.0 Hz, 2H, 5'-CH<sub>2</sub>), 4.29 (*m*, 1H, 4'-CH), 4.14 (*t*, *J* = 8.8 Hz, 1H, 3'-OH), 4.03 (*m*, 1H, 3'-CH), 3.09 (*dd*, *J* = 7.0, 4.9 Hz, 1H, CH-ala), 3.65 (*s*, 3H, CH<sub>3</sub>-ester), 1.97 (*d*, *J* = 11.9 Hz, 3H, CH<sub>3</sub>-ala). **<sup>13</sup>C NMR** (125 MHz, CDCl<sub>3</sub>): δppm 171.3 (C=O, ala) 159.70 (C=O, uridine), 158.3 (C=O, uridine), 149.46 (CH-uridine), 145.00 (C-O-Ar), 144.53 (Ar-CH), 129.88 (Ar-CH), 120.14 (Ar-CH), 93.87, 93.73 (C-3'), 92.34, 92.22 (C-1'), 90.14, 88.91 (C-4'), 81.57, 81.36 (C-5), 68.87 (C-3'), 64.71 (C-5'), 64.38 (CH<sub>3</sub>-ester), 58.49 (CH-ala), 20.94, 20.88 (CH<sub>3</sub>-ala). **<sup>19</sup>F NMR** (470 MHz, CDCl<sub>3</sub>): δppm -201.16, -202.58. **<sup>31</sup>P NMR** (202 MHz,

CDCl<sub>3</sub>): δppm 3.76, 3.30. **MS (ESI)<sup>+</sup>**: 636.0 [M+Na<sup>+</sup>]. **HPLC**: Rt: 10.1 min (97%).  
[Gradient: (0') 95%H<sub>2</sub>O/5%CH<sub>3</sub>CN - (5') 50% H<sub>2</sub>O/50%CH<sub>3</sub>CN- (15') 50% H<sub>2</sub>O/50%  
CH<sub>3</sub>CN- (20') 95% H<sub>2</sub>O/5% CH<sub>3</sub>CN].

**Ethyl-2-(((4-fluoro-3-hydroxy-5-(5-iodo-2,4-dioxo-3,4-dihydropyrimidin-1(2H)-yl)tetrahydrofuran-2-yl)methoxy)(phenoxy)phosphoryl)-L-alaninate (5.8b)**



**MF:** C<sub>20</sub>H<sub>24</sub>FIN<sub>3</sub>O<sub>9</sub>P

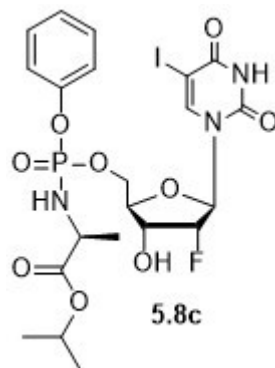
**MW:** 627.3

Compound **5.8b** was prepared according to standard procedure C. 1-(3-fluoro-4hydroxy-5-(hydromethyl)tetrahydrofuran-2-yl)-5-iodopyrimidine-2,4(1H,3H)-dione (**2.3**) (1eq; 0.159g; 0.427mmol), NMI (5eq; 0.169mL; 0.175g; 2.138mmol) and ethyl-2-(chloro(phenoxy) phosphorylamino)propanoate (**3.10**) (4.2eq; 0.524g; 1.79mmol) were reacted to obtain a residue that was purified by silica gel column chromatography (CH<sub>2</sub>Cl<sub>2</sub>/CH<sub>3</sub>OH gradient from 100% CH<sub>2</sub>Cl<sub>2</sub> to 95% CH<sub>2</sub>Cl<sub>2</sub>) to obtain the product **5.8b** as a yellowish oil. Yield: 12%.

**<sup>1</sup>H-NMR** (500 MHz, CDCl<sub>3</sub>): δppm 9.82 (s, 1H, 3-NH), 7.85 (*d*, *J*=5.1 Hz, 1H, 6-CH), 7.26 – 7.21 (*m*, 2H, CH-phenyl), 7.16 (*t*, *J*=8.0 Hz, 2H, CH-phenyl), 7.07 (*td*, *J*=7.1, 3.3 Hz, 1H, CH-phenyl), 5.78 (*ddd*, *J*=28.1, 17.8, 1.5 Hz, 1H, 1'-CH), 4.92 (*ddd*, *J* = 56.6, 52.5, 3.4 Hz, 1H, 2'-CH), 4.39 (*d*, 2H, 5'-CH<sub>2</sub>), 4.33 (*m*, 1H, 4'-CH), 4.25 (*dd*, *J*=11.7, 9.5 Hz, 1H, 3'-CH), 4.16 (*t*, *J*=6.7 Hz, 1H, 3'-OH), 4.05 (*t*, *J*=7.8 Hz, 2H, CH<sub>2</sub>-ester), 3.97 (*m*, 1H, NH-ala), 3.03 (*dd*, *J*=7.2, 4.6 Hz, 1H, CH-ala), 1.31 (*m*, 3H, CH<sub>3</sub>-ala), 1.15 (*t*, *J*=6.9 Hz, 3H, CH<sub>3</sub>-ester). **<sup>13</sup>C-NMR** (125 MHz, CDCl<sub>3</sub>): δppm 173.62 (C=O, ala), 160.29, 160.25 (C-4), 150.36 (C-2), 149.90, 149.88 (C-phenyl), 145.07, 144.63 (C-6), 129.83 - 120.25 (Ar-C), 93.87, 93.76 (C-5), 92.37, 92.25 (C-4'), 89.88, 89.05 (C-2'), 81.54, 81.35 (C-1'), 68.23 (C-

3'), 65.08, 65.04 (C-5'), 61.85, 61.83 (CH<sub>2</sub>-ester), 53.46 (CH-ala), 20.90 (CH<sub>3</sub>-ala), 14.11 (CH<sub>3</sub>-ester). **<sup>19</sup>F NMR** (470 MHz, CDCl<sub>3</sub>): δppm -201.12, -202.39. **<sup>31</sup>P-NMR** (202 MHz, CDCl<sub>3</sub>): δ 3.20, 3.48. **MS(ESI)<sup>+</sup>**: 628.03 [M+H<sup>+</sup>]. **HPLC**: Rt: 10.5 min (95%). [Gradient: (0') 95% H<sub>2</sub>O/5% CH<sub>3</sub>CN - (5') 50% H<sub>2</sub>O/50% CH<sub>3</sub>CN- (15') 50% H<sub>2</sub>O/50% CH<sub>3</sub>CN- (20') 95% H<sub>2</sub>O/5% CH<sub>3</sub>CN.

**Isopropyl((((2R,3R,4S,5R)-4-fluoro-3-hydroxy-5-(5-iodo-2,4-dioxo-3,4-dihydropyrimidin-1(2H)-yl)tetrahydrofuran-2-yl)methoxy)(phenoxy)phosphoryl)-L-alaninate. (5.8c)**



**MF:** C<sub>21</sub>H<sub>26</sub>FIN<sub>3</sub>O<sub>9</sub>P

**MW:** 641.3

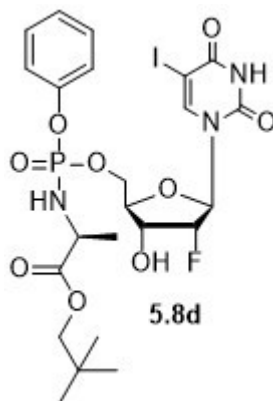
Compound **5.8c** was prepared according to standard procedure C. 1-(3-fluoro-4-hydroxy-5-(hydromethyl)tetrahydrofuran-2-yl)-5-iodopyrimidine-2,4(1H,3H)-dione (**2.3**) (1eq; 0.250g; 0.672mmol), NMI (5eq; 0.266mL; 0.275g; 3.359mmol) and isopropyl-2-(chloro(phenoxy) phosphorylamino)propanoate (**5.7b**) (3eq; 0.611g; 2.016mmol) were reacted to obtain a residue that was purified by silica gel column chromatography (CH<sub>2</sub>Cl<sub>2</sub>/CH<sub>3</sub>OH gradient from 100% CH<sub>2</sub>Cl<sub>2</sub> to 95% CH<sub>2</sub>Cl<sub>2</sub>) to obtain the product **5.8c** as a yellowish oil. Yield: 3%.

**<sup>1</sup>H NMR** (500 MHz, CDCl<sub>3</sub>): δppm 11.82 (*s*, 1H, 3-NH), 8.31 (*d*, *J*=4.9 Hz, 1H, 6-CH), 7.43–7.21 (*m*, 2H, CH-phenyl), 7.18 (*t*, *J*=9.1 Hz, 2H, CH-phenyl), 7.07 (*td*, *J*=7.1, 3.9 Hz, 1H, CH-phenyl), 6.07 (*ddd*, *J*=25.3, 15.3, 1.5 Hz, 1H, 1'-CH), 5.43 (*ddd*, *J*=54.3, 53.5, 4.4 Hz, 1H, 2'-CH), 4.98 (*d*, 2H, 5'-CH<sub>2</sub>), 4.71 (*m*, 1H, 4'-CH), 4.54 (*dd*, *J*=15.3, 9.4 Hz, 1H, 3'-CH), 4.12 (*t*, *J*=5.7 Hz, 1H, 3'-OH), 4.11 (*m*, 1H, CH-ester), 3.94 (*m*, 1H, NH-ala), 3.39 (*d*, *J*=4.7Hz, 6H, 2x CH<sub>3</sub>-ester), 3.23 (*dd*, *J*=7.2, 4.6 Hz, 1H, CH-ala), 1.41 (*m*, 3H, CH<sub>3</sub>-ala).

**<sup>13</sup>C NMR** (125 MHz, CDCl<sub>3</sub>): δppm 171.61 (C=O, ala), 161.31 (C-4), 159.26 (C-2), 153.90, 152.18 (C-phenyl), 149.7, 148.69 (C-6), 131.23 -129.24 (Ar-C), 92.7(C-5), 92.14, 92.09 (C-4'), 90.03 (C-2'), 89.53, 87.41 (C-1'), 72.51 (C-3'), 71.03 (C-5'), 55.83 (CH-ester), 52.31

(CH-ala), 21.23 (CH<sub>3</sub>-ala), 20.91 (CH<sub>3</sub>-ester). **<sup>19</sup>F NMR** (470 MHz, CDCl<sub>3</sub>): δppm -207.09, -205.19. **<sup>31</sup>P NMR** (202 MHz, CDCl<sub>3</sub>): δppm 3.42, 3.29. **MS (ESI)<sup>+</sup>** : 664.3 [M + Na<sup>+</sup>]. **HPLC**: Rt: 10.6 min (96%). [Gradient: (0') 95%H<sub>2</sub>O/5%CH<sub>3</sub>CN - (5') 50% H<sub>2</sub>O/50%CH<sub>3</sub>CN- (15') 50% H<sub>2</sub>O/50% CH<sub>3</sub>CN- (20') 95% H<sub>2</sub>O/5% CH<sub>3</sub>CN].

**Neopentyl (((2R,3R,4R,5R)-4-fluoro-3-hydroxy-5-(5-iodo-2,4-dioxo-3,4-dihydropyrimidin-1(2H)-yl)tetrahydrofuran-2-yl)methoxy)(phenoxy)phosphoryl)-L-alaninate. (5.8d)**



**MF:** C<sub>23</sub>H<sub>30</sub>FIN<sub>3</sub>O<sub>9</sub>P

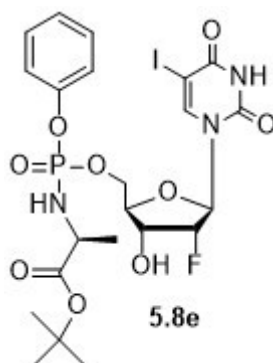
**MW:** 669.38

Compound **5.8d** was obtained according to standard procedure C. 1-(3-fluoro-4-hydroxy-5-(hydromethyl)tetrahydrofuran-2-yl)-5-iodopyrimidine-2,4(1H,3H)-dione (**2.3**) (1eq; 0.293g; 0.79mmol), NMI (5eq; 0.309mL; 0.320g; 3.98mmol) and neopentyl-2-(chloro(phenoxy) phosphorylamino)propanoate (**5.7c**) (3eq; 0.800g; 2.39mmol) were used as reagents to obtain a crude that was purified by silica gel column chromatography (CH<sub>2</sub>Cl<sub>2</sub>/CH<sub>3</sub>OH gradient from 100% CH<sub>2</sub>Cl<sub>2</sub> to 95% CH<sub>2</sub>Cl<sub>2</sub>) to obtain the product **5.8d** as a yellowish oil. Yield: 3%.

<sup>1</sup>H NMR (500 MHz, CDCl<sub>3</sub>): δppm 9.76 (s, 1H, 3-NH), 7.70 (s, 1H, 6-CH), 7.27–7.22 (m, 2H, CH-phenyl), 7.14 (t, J=7.4 Hz, 2H, CH-phenyl), 7.07 (t, J=7.4 Hz, 1H, CH-phenyl), 5.87 (m, 1H, 1'-CH), 5.04 (dd, J=52.6, 4.6 Hz, 1H, 2'-CH), 4.40 (m, 2H, 5'-CH<sub>2</sub>), 4.35 (m, 1H, 4'-CH), 4.29 (m, 1H, 3'-CH), 4.18 (m, 1H, 3'-OH), 3.81 (m, 1H, NH-ala), 3.95 (s, CH<sub>2</sub>-ester) 3.39 (m, 1H, CH-ala), 1.38 (s, 9H, 3x CH<sub>3</sub>-ester), 1.27 (d, J=7.0 Hz, 3H, CH<sub>3</sub>-ala). <sup>13</sup>C NMR (125 MHz, CDCl<sub>3</sub>): δppm 172.73 (C=O, ala), 160.13, 160.08 (C-4), 150.80 (C-2), 149.68 (C-phenyl), 145.35, 145.31 (C-6), 129.77 - 120.11 (Ar-C), 92.03, 91.83 (C-5), 91.51, 91.22 (C-4'), 89.25, 88.98 (C-2'), 82.36, 82.27 (C-1'), 82.02, 81.99 (CH<sub>2</sub>-ester), 69.65, 69.53 (C-3'), 68.97, 68.84 (C-5'), 53.64, 53.58 (CH-ala), 27.92 (CH<sub>3</sub>-neopentyl), 21.10, 21.02 (CH<sub>3</sub>-ala). <sup>19</sup>F NMR (470 MHz, CDCl<sub>3</sub>): δppm -199.18, -203.16. <sup>31</sup>P NMR (202 MHz, CDCl<sub>3</sub>):

$\delta$ ppm 3.81, 3.74. **MS (ESI)<sup>+</sup>**: 692.5 [M + Na<sup>+</sup>]. **HPLC**: Rt: 11.1 min (95%). [Gradient: (0') 95% H<sub>2</sub>O/5% CH<sub>3</sub>CN - (5') 50% H<sub>2</sub>O/50% CH<sub>3</sub>CN- (15') 50% H<sub>2</sub>O/50% CH<sub>3</sub>CN- (20') 95% H<sub>2</sub>O/5% CH<sub>3</sub>CN].

**Tert-butyl-2-(((4-fluoro-3-hydroxy-5-(5-iodo-2,4-dioxo-3,4-dihydropyrimidin-1(2H)-yl)tetrahydrofuran-2-yl)methoxy)(phenoxy)phosphoryl)-L-alaninate. (5.8e)**



**MF:** C<sub>22</sub>H<sub>28</sub>FIN<sub>3</sub>O<sub>9</sub>P

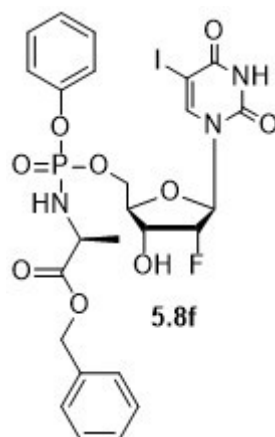
**MW:** 655.4

Compound **5.8e** was prepared according to standard procedure C. 1-(3-fluoro-4-hydroxy-5-(hydromethyl)tetrahydrofuran-2-yl)-5-iodopyrimidine-2,4(1H,3H)-dione (**2.3**) (1eq; 0.271g; 0.729mmol), NMI (5eq; 0.289mL; 0.299g; 3.649mmol) and tertbutyl-2- (chloro(phenoxy) phosphorylamino)propanoate (**5.7d**)(3eq; 0.700g; 2.189mmol) were used to obtain a crude that was purified by silica gel column chromatography (CH<sub>2</sub>Cl<sub>2</sub>/CH<sub>3</sub>OH gradient from 100% CH<sub>2</sub>Cl<sub>2</sub> to 95% CH<sub>2</sub>Cl<sub>2</sub>) to obtain the product **5.8e** as a yellowish oil. Yield: 6%.

**<sup>1</sup>H NMR** (500 MHz, CDCl<sub>3</sub>): δppm 10.31 (s, 1H, 3-NH), 8.59 (s, 1H, 6-CH), 7.51-8.43 (m, 2H, CH-phenyl), 7.29 (t, *J*=7.1 Hz, 2H, CH-phenyl), 7.13 (t, *J*=7.1 Hz, 1H, CH-phenyl), 6.01 (m, 1H, 1'-CH), 5.04 (dd, *J* = 49.3, 3.9 Hz, 1H, 2'-CH), 4.40 (m, 2H, 5'-CH<sub>2</sub>), 4.29 (m, 1H, 4'-CH), 4.23 (m, 1H, 3'-CH), 4.07 (m, 1H, 3'-OH), 3.96 (m, 1H, NH-ala), 3.27 (m, 1H, CH-ala), 1.36 (s, 9H, 3x CH<sub>3</sub>-ester), 1.21 (d, *J*=7.0 Hz, 3H, CH<sub>3</sub>-ala). **<sup>13</sup>C NMR** (125 MHz, CDCl<sub>3</sub>): δppm 179.7 (C=O, ala), 159.13,159.0 (C-4), 156.2 (C-2), 148.21 (C-phenyl), 147.91, 147.43 (C-6), 125.21-124.92 (Ar-C), 98.32, 97.89 (C-5), 94.21, 93.97 (C-4'), 92.21, 92.19 (C-2'), 85.71, 84.35 (C-1'), 82.34, 81.76 (C-ester), 69.21, 68.72 (C-3'), 68.23, 68.19 (C-5'), 54.49, 53.48 (CH-ala), 25.09 (CH<sub>3</sub>-tert butyl), 23.65, 23.63 (CH<sub>3</sub>-ala). **<sup>19</sup>F NMR** (470 MHz, CDCl<sub>3</sub>): δppm -204.3, -203.91. **<sup>31</sup>P NMR** (202 MHz, CDCl<sub>3</sub>): δppm 3.91, 3.79. **MS (ESI)<sup>+</sup>**: 678.4 [M + Na<sup>+</sup>]. **HPLC**: Rt: 11.9 min (99%). [Gradient: (0')

95% $\text{H}_2\text{O}$ /5% $\text{CH}_3\text{CN}$  - (5') 50%  $\text{H}_2\text{O}$ /50% $\text{CH}_3\text{CN}$ - (15') 50%  $\text{H}_2\text{O}$ /50%  $\text{CH}_3\text{CN}$ - (20') 95%  $\text{H}_2\text{O}$ /5%  $\text{CH}_3\text{CN}$ ].

**Benzyl((((2R,3R,4S,5R)-4-fluoro-3-hydroxy-5-(5-iodo-2,4-dioxo-3,4-dihydropyrimidin-1(2H)-yl)tetrahydrofuran-2-yl)methoxy)(phenoxy)phosphoryl)-L-alaninate. (5.8f)**



**MF:** C<sub>25</sub>H<sub>26</sub>FIN<sub>3</sub>O<sub>9</sub>P

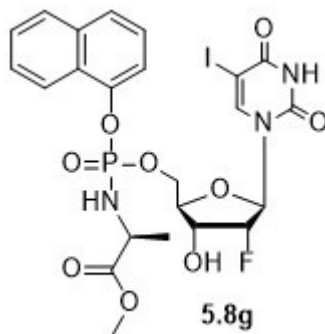
**MW:** 689.3

Compound **5.8f** was prepared according to standard procedure C. 1-(3-fluoro-4-hydroxy-5-(hydromethyl)tetrahydrofuran-2-yl)-5-iodopyrimidine-2,4(1H,3H)-dione (**2.3**) (1eq; 0.200g; 0.537mmol), NMI (5eq; 0.212mL; 0.220g; 2.68mmol) and benzyl (chloro(phenoxy)phosphoryl)-L-alaninate (**4.5**) (3eq; 0.570g; 1.61mmol) were reacted to obtain a product that was purified by silica gel column chromatography chromatography (CH<sub>2</sub>Cl<sub>2</sub>/CH<sub>3</sub>OH gradient from 100% CH<sub>2</sub>Cl<sub>2</sub> to 95% CH<sub>2</sub>Cl<sub>2</sub>) to afford the compound **5.8f** as a yellowish oil. Yield: 11%.

**<sup>1</sup>H NMR** (500 MHz, CDCl<sub>3</sub>): δ 10.59 (s, 1H, 3-NH), 7.91 (s, 1H, 6-CH), 7.41–7.38 (m, 2H, CH-phenyl), 7.32 (t, *J*=7.9 Hz, 2H, CH-phenyl), 7.37-7.35 (m, 2H, CH-benz), 7.25-7.23 (m, 2H, CH-benz) 7.22 (t, 7.9 Hz, 1H, CH-benzyl), 7.13 (t, *J*=7.2 Hz, 1H, CH-phenyl), 5.99 (m, 1H, 1'-CH), 5.42 (dd, *J*=49.6, 4.6 Hz, 1H, 2'-CH), 5.31 (m, 2H, CH<sub>2</sub>-benz), 4.68 (m, 2H, 5'-CH<sub>2</sub>), 4.52 (m, 1H, 4'-CH), 4.27 (m, 1H, 3'-CH), 4.11 (m, 1H, 3'-OH), 3.89 (m, 1H, NH-ala), 3.71 (m, 1H, CH-ala), 1.26 (d, *J*=7.0 Hz, 3H, CH<sub>3</sub>-ala). **<sup>13</sup>C NMR** (125 MHz, CDCl<sub>3</sub>): δppm 171.7 (C=O, ala), 167.31 (C-4), 158.13 (C-phenyl), 155.43 (C-benzyl), 149.09, 149.92 (C-6), 145.65 (C-2), 129.98-120.32 (Ar-C), 92.61, 92.54 (C-5), 90.54, 90.21 (C-4'), 87.76, 86.99 (C-2'), 85.13, 83.51 (C-1'), 80.07, 80.03 (C-ester), 69.21, 68.52 (C-3'), 67.54

(C-5'), 54.31 (CH-ala), 27.25 (CH<sub>3</sub>-ala). **<sup>19</sup>F NMR** (470 MHz, CDCl<sub>3</sub>): δppm -200.79, -200.12. **<sup>31</sup>P NMR** (202 MHz, CDCl<sub>3</sub>): δppm 3.90, 3.87. **MS (ESI)<sup>+</sup>**: 690.3 [M + H<sup>+</sup>]. **HPLC**: Rt: 13.2 min (98%). [Gradient: (0') 95%H<sub>2</sub>O/5%CH<sub>3</sub>CN - (5') 50% H<sub>2</sub>O/50%CH<sub>3</sub>CN- (15') 50% H<sub>2</sub>O/50% CH<sub>3</sub>CN- (20') 95% H<sub>2</sub>O/5% CH<sub>3</sub>CN].

**Methyl((((2R,3R,4S,5R)-4-fluoro-3-hydroxy-5-(5-iodo-2,4-dioxo-3,4-dihydropyrimidin-1(2H)-yl)tetrahydrofuran-2-yl)methoxy)(naphthalen-1-yloxy)phosphoryl)-L-alaninate.**  
**(5.8g)**



**MF:** C<sub>23</sub>H<sub>24</sub>FIN<sub>3</sub>O<sub>9</sub>P

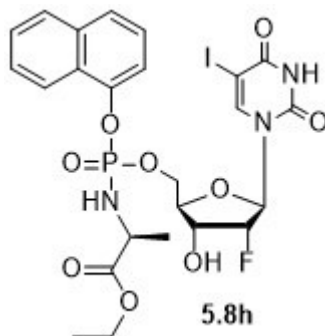
**MW:** 663.3

Compound **5.8g** was synthesised according to standard procedure C. 1-(3-fluoro-4-hydroxy-5-(hydromethyl)tetrahydrofuran-2-yl)-5-iodopyrimidine-2,4(1H,3H)-dione (**2.3**) (1eq; 0.400g; 1.07mmol), NMI (5eq; 0.424mL; 0.439g; 5.35mmol) and methyl-2-(chloro(naphthoxy) phosphorylamino)propanoate (**5.7e**) (3eq; 1.05g; 3.22mmol) were reacted to obtain a product that was purified by silica gel column chromatography (CH<sub>2</sub>Cl<sub>2</sub>/CH<sub>3</sub>OH gradient from 100% CH<sub>2</sub>Cl<sub>2</sub> to 95% CH<sub>2</sub>Cl<sub>2</sub>) to afford the compound **5.8g** as a yellowish solid. Yield: 4%.

**<sup>1</sup>H NMR** (500 MHz, CDCl<sub>3</sub>): δppm 10.91 (*d*, *J*=41.4 Hz, 1H, 3-NH), 8.23 (*d*, *J*=4.9 Hz, 1H, 6-CH), 7.91 (*m*, 2H, CH, naph), 7.86-7.4 (*m*, 5H, CH-naph), 5.54 (*ddd*, *J*=34.9, 17.6, 1.3 Hz, 1H, 1'-CH), 4.90 (*m*, 1H, 2'-CH), 4.60 (*d*, *J*=7.0 Hz, 2H, 5'-CH<sub>2</sub>), 4.31 (*m*, 1H, 4'-CH), 4.12 (*t*, *J*=8 Hz, 1H, 3'-OH), 4.13 (*m*, 1H, 3'-CH), 3.98 (*s*, 3H, CH<sub>3</sub>-ester) 3.87 (*d*, *J*=11.7 Hz, 1H, NH-ala), 3.11 (*dd*, *J*=8.0, 4.9 Hz, 1H, CH-ala), 1.28 (*dd*, *J*=10.1, 6.7 Hz, 3H, CH<sub>3</sub>-ala). **<sup>13</sup>C NMR** (125 MHz, CDCl<sub>3</sub>): δ 163.10 (C=O, ala), 151.03 (C-naph), 145.13 (C-4), 145.01 (C-2), 144.19 (C-6), 128.13-119.91 (Ar-C), 91.73 (C-5), 92.91, 92.52 (C-4'), 91.19, 89.1 (C-2'), 81.12, 81.09 (C-1'), 65.37 (C-5'), 64.9, 64.31 (CH<sub>3</sub>-ester), 56.48 (CH-ala), 51.75 (C-3'), 39.11 (C-2'), 21.93, 20.99 (CH<sub>3</sub>-ala). **<sup>19</sup>F NMR** (470 MHz, CDCl<sub>3</sub>): δppm -201.10, -201.01. **<sup>31</sup>P NMR** (202 MHz, CDCl<sub>3</sub>): δppm 3.75, 3.42. **MS (ESI)<sup>+</sup>** : 664.3 [M +

H<sup>+</sup>]. **HPLC:** Rt: 15.1 min (95%). [Gradient: (0') 95% $\text{H}_2\text{O}$ /5% $\text{CH}_3\text{CN}$  - (5') 50%  $\text{H}_2\text{O}$ /50% $\text{CH}_3\text{CN}$ - (15') 50%  $\text{H}_2\text{O}$ /50% $\text{CH}_3\text{CN}$ - (20') 95%  $\text{H}_2\text{O}$ /5% $\text{CH}_3\text{CN}$ ].

**Ethyl (((((2R,3R,4S,5R)-4-fluoro-3-hydroxy-5-(5-iodo-2,4-dioxo-3,4-dihydropyrimidin-1(2H)-yl)tetrahydrofuran-2-yl)methoxy)(naphthalen-1-yloxy)phosphoryl)-L-alaninate. (5.8h)**



**MF:** C<sub>24</sub>H<sub>26</sub>FIN<sub>3</sub>O<sub>9</sub>P

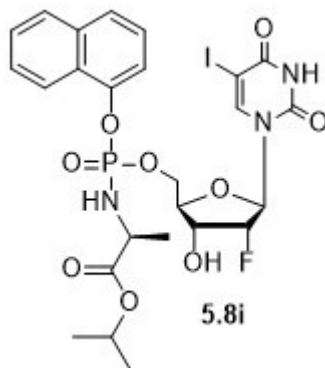
**MW:** 677.3

Compound **5.8h** was obtained according to standard procedure C. 1-(3-fluoro-4-hydroxy-5-(hydromethyl)tetrahydrofuran-2-yl)-5-iodopyrimidine-2,4(1H,3H)-dione (**2.3**) (1eq, 0.400g, 1.07mmol), NMI (5 eq; 0.424mL; 0.439g; 5.35mmol) and ethyl-2-(chloro(naphthoxy)phosphorylamino)propanoate (3eq; 1.098g; 3.22mmol) were used as reagents to obtain a crude that was purified by silica gel column chromatography (CH<sub>2</sub>Cl<sub>2</sub>/CH<sub>3</sub>OH gradient from 100% CH<sub>2</sub>Cl<sub>2</sub> to 95% CH<sub>2</sub>Cl<sub>2</sub>) to afford the compound **5.8h** as a yellowish oil. Yield: 5%.

**<sup>1</sup>H NMR** (500 MHz, CDCl<sub>3</sub>): δppm 11.9 (*d*, *J*=40.3 Hz, 1H, 3-NH), 8.19 (*d*, *J*=4.7 Hz, 1H, 6-CH), 7.83 (*m*, 2H, CH, naph), 7.81-7.2 (*m* 5H, CH-naph), 5.5 (*ddd*, *J*=32.7, 12.3, 1.4 Hz, 1H, 1'-CH), 4.73 (*m*, 1H, 2'-CH), 4.56 (*d*, *J* = 7.0 Hz, 2H, 5'-CH<sub>2</sub>), 4.21 (*m*, 1H, 4'-CH), 4.26 (*m*, 3'-OH), 4.14 (*m*, 2H, CH<sub>2</sub>-ester), 4.11 (*m*, 1H, 3'-CH), 3.89 (*d*, *J* = 10.7 Hz, 1H, NH-ala), 3.21 (*dd*, *J* = 7.0, 4.9 Hz, 1H, CH-ala), 1.27 (*d*, *J* = 6.7 Hz, 3H, CH<sub>3</sub>-ala), 1.18 (*t*, *J* = 7.9 Hz, 3H, CH<sub>3</sub>-ester). **<sup>13</sup>C NMR** (125 MHz, CDCl<sub>3</sub>): δppm 167.92 (C=O, ala), 159.03 (C-naph), 144.3 (C-4), 143.9 (C-2), 144.19 (C-6), 123.03 - 121.02 (Ar-C), 90.74 (C-5), 92.49 (C-4'), 91.21, 90.1 (C-2'), 83.1 (C-1'), 67.46 (C-5'), 62.9, 61.3 (CH<sub>3</sub>-ester), 61.9 (CH<sub>2</sub>-ester), 54.93 (CH-ala), 50.31 (C-3'), 50.10 (C-2'), 22.15, 21.79 (CH<sub>3</sub>-ala). **<sup>19</sup>F NMR** (470 MHz, CDCl<sub>3</sub>): δppm -201.39, -201.31. **<sup>31</sup>P NMR** (202 MHz, CDCl<sub>3</sub>): δppm 3.74, 3.59. **MS**

**(ESI)<sup>+</sup>**: 700.3 [M + Na<sup>+</sup>]. **HPLC**: Rt: 16.4 min (96%). [Gradient: (0') 95% H<sub>2</sub>O/5% CH<sub>3</sub>CN - (5') 50% H<sub>2</sub>O/50% CH<sub>3</sub>CN- (15') 50% H<sub>2</sub>O/50% CH<sub>3</sub>CN- (20') 95% H<sub>2</sub>O/5% CH<sub>3</sub>CN].

**Tertbutyl((((2R,3R,4R,5R)-4-fluoro-3-hydroxy-5-(5-iodo-2,4-dioxo-3,4-dihydropyrimidin-1(2H)-yl)tetrahydrofuran-2-yl)methoxy)(naphthalen-1-yloxy)phosphoryl)-L-alaninate**



**MF:** C<sub>26</sub>H<sub>30</sub>FIN<sub>3</sub>O<sub>9</sub>P

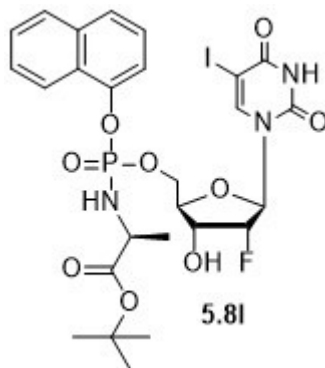
**MW:** 705.4

Compound **5.8i** was synthesised according to standard procedure C. 1-(3-fluoro-4-hydroxy-5-(hydromethyl)tetrahydrofuran-2-yl)-5-iodopyrimidine-2,4(1H,3H)-dione (**2.3**) (1 eq; 0.158g; 0.426mmol) and NMI (5eq; 0.168mL; 0.175g; 0.213mmol) and isopropyl-2-(chloro(naphoxy)phosphorylamino)propanoate (**5.7g**) (3eq; 1.05g; 3.22mmol) were reacted to obtain a crude that was purified by silica gel column chromatography (CH<sub>2</sub>Cl<sub>2</sub>/CH<sub>3</sub>OH gradient from 100% CH<sub>2</sub>Cl<sub>2</sub> to 95% CH<sub>2</sub>Cl<sub>2</sub>) to afford the compound **5.8i** as a yellowish oil. Yield: 5%.

**<sup>1</sup>H NMR** (500 MHz, CDCl<sub>3</sub>): δppm 11.89 (*d*, *J* = 42.3 Hz, 1H, 3-NH), 8.21 (*d*, *J* = 5.1 Hz, 1H, 6-CH), 7.93 (*m*, 2H, CH, naph), 7.21-7.20 (*m*, 5H, CH-naph), 5.43 (*ddd*, *J* = 34.5, 19.1, 1.9 Hz, 1H, 1'-CH), 4.89 (*m*, 1H, 2'-CH), 4.45 (*d*, *J* = 7.3 Hz, 2H, 5'-CH<sub>2</sub>), 4.19 (*m*, 1H, 4'-CH), 4.09 (*t*, *J* = 7 Hz, 1H, 3'-OH), 4.10 (*m*, 1H, 3'-CH), 3.91 (*d*, *J* = 10.9 Hz, 1H, NH-ala), 3.87 (*m*, 1H, CH-*i*-propyl), 3.09 (*dd*, *J* = 7.0, 4.7 Hz, 1H, CH-ala), 1.33 (*dd*, *J* = 10.4, 4.1 Hz, 3H, CH<sub>3</sub>-ala), 1.19 (*d*, *J* = 7.9 Hz, 6H, 2x CH<sub>3</sub>-*i*-propyl). **<sup>13</sup>C NMR**(125 MHz, CDCl<sub>3</sub>): δppm 167.12 (C=O, ala), 161.02 (C-naph), 154.11 (C-4), 149.81 (C-2), 147.23 (C-6), 129.21 - 120.97 (Ar-C), 95.23 (C-5), 92.65, 92.34 (C-4'), 91.15, 88.76 (C-2'), 81.97, 81.54 (C-1'), 71.35 (C-5'), 68.9, 68.29 (CH-*i*-propyl), 55.38 (CH-ala), 50.29 (C-3'), 41.11 (C-2'), 27.88, 27.65 (CH<sub>3</sub>-ala), 21.32-21.29 (CH<sub>3</sub>-*i*-propyl). **<sup>19</sup>F NMR** (470 MHz, CDCl<sub>3</sub>): δppm -

200.32, -200.11. **<sup>31</sup>P NMR** (202 MHz, CDCl<sub>3</sub>): δppm 3.56, 3.12. **MS (ESI)<sup>+</sup>**: 728.5 [M + Na<sup>+</sup>]. **HPLC**: Rt: 16.6 min (97%). [Gradient: (0') 95%H<sub>2</sub>O/5%CH<sub>3</sub>CN - (5') 50% H<sub>2</sub>O/50%CH<sub>3</sub>CN- (15') 50% H<sub>2</sub>O/50% CH<sub>3</sub>CN- (20') 95% H<sub>2</sub>O/5% CH<sub>3</sub>CN].

**Benzyl (((((2R,3R,4R,5R)-4-fluoro-3-hydroxy-5-(5-iodo-2,4-dioxo-3,4-dihydropyrimidin-1(2H)-yl)tetrahydrofuran-2-yl)methoxy)(naphthalen-1-yloxy)phosphoryl)-L-alaninate. (5.8I)**



**MF:** C<sub>26</sub>H<sub>30</sub>FIN<sub>3</sub>O<sub>9</sub>P

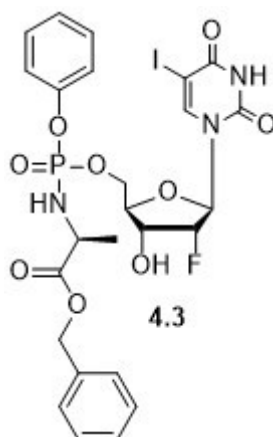
**MW:** 705.9

Compound **5.8I** was prepared according to standard procedure C. 1-(3-fluoro-4-hydroxy-5-(hydromethyl)tetrahydrofuran-2-yl)-5-iodopyrimidine-2,4(1H,3H)-dione (**2.3**) (1eq; 0.427g; 1.14mmol), NMI (5eq; 0.454mL; 0.468g; 5.7mmol) and isopropyl-2-(chloro(naphoxy) phosphorylamino)propanoate (**5.7g**) (3eq; 1.05g; 3.22mmol) were used to obtain a crude that was purified by silica gel column chromatography (CH<sub>2</sub>Cl<sub>2</sub>/CH<sub>3</sub>OH gradient from 100% CH<sub>2</sub>Cl<sub>2</sub> to 95% CH<sub>2</sub>Cl<sub>2</sub>) to afford the compound **5.8I** as a yellowish oil. Yield: 3%.

**<sup>1</sup>H NMR** (500 MHz, CDCl<sub>3</sub>): δppm 11.73 (*d*, *J* = 40.4 Hz, 1H, 3-NH), 8.64 (*d*, *J* = 4.7 Hz, 1H, 6-CH), 8.01 (*m*, 2H, CH, naph), 7.92-7.86 (*m*, 5H, CH-naph), 6.12 (*ddd*, *J* = 39.1, 14.3, 1.9 Hz, 1H, 1'-CH), 4.95 (*m*, 1H, 2'-CH), 4.65 (*d*, *J* = 7.5 Hz, 2H, 5'-CH<sub>2</sub>), 4.22 (*m*, 1H, 4'-CH), 4.17 (*t*, *J* = 7.8 Hz, 1H, 3'-OH), 4.13 (*m*, 1H, 3'-CH), 3.92 (*m*, CH-*i*-propyl), 3.87 (*d*, *J* = 9.6 Hz, 1H, NH-ala), 3.64 (*dd*, *J* = 7.9, 4.7 Hz, 1H, CH-ala), 1.29 (*dd*, *J* = 10.5, 6.3 Hz, 3H, CH<sub>3</sub>-ala), 1.21 (*d*, *J* = 7.9 Hz, 9H, 3x CH<sub>3</sub>-ester). **<sup>13</sup>C NMR**(125 MHz, CDCl<sub>3</sub>): δppm 171.08 (C=O, ala), 169.55 (C-naph), 155.17 (C-4), 153.00 (C-2), 149.23 (C-6), 131.82-129.27 (Ar-C), 99.07 (C-5), 95.76, 95.03 (C-4'), 91.09, 89.77 (C-2'), 86.54, 87.09 (C-1'), 67.02 (C-5'), 64.1, 64.01 (CH-ester), 59.76 (CH-ala), 57.32 (C-3'), 39.87 (C-2'), 22.00, 20.15 (CH<sub>3</sub>-ala), 19.78, 19.54 (CH<sub>3</sub>-ester). **<sup>19</sup>F NMR** (470 MHz, CDCl<sub>3</sub>): δppm -203.15, -202.65. **<sup>31</sup>P NMR** (202 MHz, CDCl<sub>3</sub>): δ 3.91, 3.76. **MS (ESI)<sup>+</sup>** : 706.6 [M + H<sup>+</sup>]. **HPLC**: Rt: 16.9 min (97%).

[Gradient: (0') 95% $\text{H}_2\text{O}$ /5% $\text{CH}_3\text{CN}$  - (5') 50%  $\text{H}_2\text{O}$ /50% $\text{CH}_3\text{CN}$ - (15') 50%  $\text{H}_2\text{O}$ /50%  $\text{CH}_3\text{CN}$ - (20') 95%  $\text{H}_2\text{O}$ /5%  $\text{CH}_3\text{CN}$ ].

**Benzyl (((((2R,3R,4S,5R)-4-fluoro-3-hydroxy-5-(5-iodo-2,4-dioxo-3,4-dihydropyrimidin-1(2H)-yl)tetrahydrofuran-2-yl)methoxy)(phenoxy)phosphoryl)-L-alaninate. (4.3)**



**MF:** C<sub>25</sub>H<sub>26</sub>FIN<sub>3</sub>O<sub>9</sub>P

**MW:** 689.3

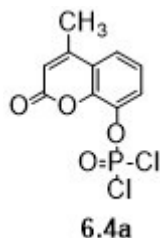
Compound **4.3** was prepared according to the standard procedure C. 1-(3-fluoro-4-hydroxy-5-(hydromethyl)tetrahydrofuran-2-yl)-5-iodopyrimidine-2,4(1H,3H)-dione (**1.66**) (1eq; 0.400g; 1.07mmol), NMI (5eq; 0.424mL; 0.439g; 5.35mmol), benzyl-2-(chloro(naphoxy)phosphorylamino)propanoate (**4.5**) (3eq; 1.05g; 3.22mmol) were reacted to obtain a residue that was purified by silica gel column chromatography (CH<sub>2</sub>Cl<sub>2</sub>/CH<sub>3</sub>OH from 100% CH<sub>2</sub>Cl<sub>2</sub> to 95% CH<sub>2</sub>Cl<sub>2</sub>) to obtain the product **4.3** as a yellowish oil. Yield: 10%.

**<sup>1</sup>H NMR** (500 MHz, CDCl<sub>3</sub>): δppm 10.59 (s, 1H, 3-NH), 7.89 (s, 1H, 6-CH), 7.53–7.48 (m, 2H, CH-phenyl), 7.45 (t, *J*=8Hz, 2H, CH-phenyl), 7.41-7.38 (m, 2H, CH-benz), 7.17-7.15 (m, 2H, CH-benz), 7.13 (t, 8Hz, 1H, CH-benzyl), 7.12 (t, *J*=7.4 Hz, 1H, CH-phenyl), 5.99 (m, 1H, 1'-CH), 5.79 (dd, *J*=47.6, 4.6 Hz, 1H, 2'-CH), 5.14 (m, 2H, CH<sub>2</sub>-benz), 4.90 (m, 2H, 5'-CH<sub>2</sub>), 4.39 (m, 1H, 4'-CH), 4.27 (m, 1H, 3'-CH), 4.19 (m, 1H, 3'-OH), 4.02 (m, 1H, NH-ala), 3.99 (m, 1H, CH-ala), 1.29 (d, *J*=7.0Hz, 3H, CH<sub>3</sub>-ala). **<sup>13</sup>C NMR** (125 MHz, CDCl<sub>3</sub>): δppm 171.9 (C=O, ala), 168.12 (C-4), 144.18 (C-2), 149.0 (C-phenyl), 147.91 (C-benzyl), 145.5, 145.1 (C-6), 128.31-121.48 (Ar-C), 94.3 (C-5), 92.10 (C-4'), 89.13 (C-2'), 83.6, 82.97 (C-1'), 81.08, 80.97 (C-ester), 69.61, 68.14 (C-3'), 67.23 (C-5'), 52.8 (CH-ala), 21.98 (CH<sub>3</sub>-ala). **<sup>19</sup>F NMR** (470 MHz, CDCl<sub>3</sub>): δppm -200.91, -201.15. **<sup>31</sup>P NMR** (202 MHz,

$\text{CDCl}_3$ ):  $\delta$ ppm 3.90, 3.86. **MS (ESI)<sup>+</sup>**: 690.3 [M + H<sup>+</sup>]. **HPLC**: Rt: 13.4 min (98%). [Gradient: (0') 95% $\text{H}_2\text{O}$ /5% $\text{CH}_3\text{CN}$  - (5') 50%  $\text{H}_2\text{O}$ /50% $\text{CH}_3\text{CN}$ - (15') 50%  $\text{H}_2\text{O}$ /50%  $\text{CH}_3\text{CN}$ - (20') 95%  $\text{H}_2\text{O}$ /5%  $\text{CH}_3\text{CN}$ ].

### 8.3.4 Experimental section from Chapter 6

#### 4-Methyl-2-oxo-2H-chromen-8-yl phosphorodichloridate

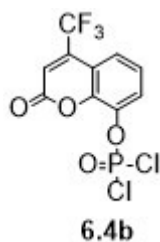


**MF:** C<sub>10</sub>H<sub>7</sub>Cl<sub>2</sub>O<sub>4</sub>P

**MW:** 293.04

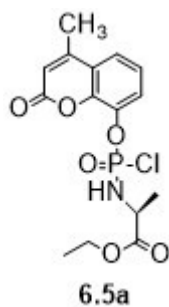
Phosphorus oxychloride (1eq, 0.434g, 0.264 mL, 2.83mmol) and 4-methylumbelliferone **6.3a** (1eq, 0.5g, 2.83mmol), were stirred in anhydrous Et<sub>2</sub>O under nitrogen atmosphere. Anhydrous TEA (2eq, 0.574g, 0.791mL, 5.676mmol) was added dropwise at -78°C. The reaction mixture was then allowed to stir for 30min and then to slowly warm to rt and stirred for 1h. The reaction was monitored by <sup>31</sup>P NMR. The crude mixture was then filtered under nitrogen atmosphere and reduced under pressure to furnish **6.4a** as a yellowish oil which wasn't further purified. Yield: 86%.

<sup>31</sup>P NMR (CDCl<sub>3</sub>, 202 MHz): δppm 4.02.

**2-Oxo-4-(trifluoromethyl)-2H-chromen-8-yl phosphorodichloridate****MF:** C<sub>10</sub>H<sub>4</sub>Cl<sub>2</sub>F<sub>3</sub>O<sub>4</sub>P**MW:** 347.01

Phosphorus oxychloride (1eq, 0.330g, 0.202mL, 2.17mmol) and 7-hydroxy-4-(trifluoromethyl)coumarin **6.3b** (1eq, 0.5g, 2.17mmol), were stirred in anhydrous Et<sub>2</sub>O under nitrogen atmosphere. Anhydrous TEA was added dropwise at -78°C. The reaction mixture was then allowed to stir for 30min and then to slowly warm to rt and stirred for 1h. The reaction was monitored by <sup>31</sup>P NMR. The crude mixture was then filtered under nitrogen atmosphere and reduced under pressure to furnish **6.4b** as a yellowish oil which wasn't further purified. Yield: 88%.

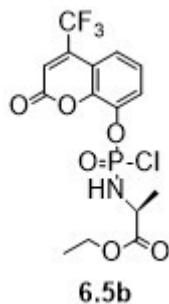
<sup>31</sup>P NMR (CDCl<sub>3</sub>, 202 MHz): δppm 4.57.

**Ethyl (chloro((4-methyl-2-oxo-2H-chromen-8-yl)oxy)phosphoryl)-L-alaninate****MF:** C<sub>15</sub>H<sub>17</sub>ClNO<sub>6</sub>P**MW:** 373.73

Compound **6.5a** was synthesised according to standard procedure B. **6.4a** phosphorodichloridate (0.650 g, 2.21 mmol), L-alanine ethyl ester (0.339g, 2.21mmol) and TEA (0.447g, 0.616ml, 4.42mmol) were used to produce **6.5a** which was used for next reaction without further purification. Yield: 71%.

<sup>31</sup>P NMR (CDCl<sub>3</sub>, 202 MHz): δppm 8.32, 7.79.

**Ethyl (chloro((2-oxo-4-(trifluoromethyl)-2H-chromen-8-yl)oxy)phosphoryl)-L-alaninate**



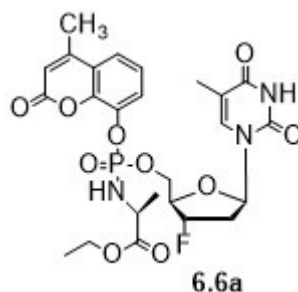
**MF:** C<sub>15</sub>H<sub>14</sub>ClF<sub>3</sub>NO<sub>6</sub>P

**MW:** 427.70

Compound **6.5b** was synthesised according to standard procedure B. **6.4b** (0.6g, 1.73mmol), L-alanine ethyl ester (0.265g, 1.73mmol) and TEA (0.351g, 0.483mL, 3.46mmol) were used to produce **6.5b** which was used for next reaction without further purification. Yield: 81%.

<sup>31</sup>P NMR (CDCl<sub>3</sub>, 202 MHz): δppm 9.51, 7.88.

**Ethyl (((((2R,3S,5R)-3-fluoro-5-(5-methyl-2,4-dioxo-3,4-dihydropyrimidin-1(2H)-yl)tetrahydrofuran-2-yl)methoxy)((4-methyl-2-oxo-2H-chromen-8-yl)oxy)phosphoryl)-L-alaninate. (6.6a)**



**MF:** C<sub>25</sub>H<sub>29</sub>FN<sub>3</sub>O<sub>10</sub>P

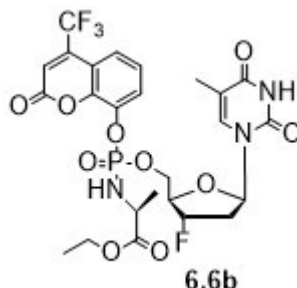
**MW:** 581.49

Compound **6.6a** was synthesised according to standard procedure D. FLT (**1.29**) (1eq, 0.146 g, 0.6 mmol), tBuMgCl (0.117 ml, 0.9 mmol) and **6.5a** phosphorochloridate (2eq, 0.450 g, 1.2 mmol) were used to produce **6.6a**. It was purified by silica gel column chromatography (CH<sub>2</sub>Cl<sub>2</sub>/CH<sub>3</sub>OH from 100% CH<sub>2</sub>Cl<sub>2</sub> to 95% CH<sub>2</sub>Cl<sub>2</sub>) to obtain a pale white solid. Yield: 5 %.

**<sup>1</sup>H-NMR** (CDCl<sub>3</sub>, 500MHz): δppm 8.59, 8.53 (*s*, 1H, NH), 7.95-7.93 (*m*, 1H, ArH), 7.51, 7.49 (*q*, *J* = 1.83 Hz; *J* = 1.6 Hz, 1H, ArH), 7.37-7.34 (*m*, 2H, ArH), 7.28-7.23 (*m*, 1H, H-1'), 6.97, 6.91, (*t*, *J* = 2, 8, 5 Hz, 1H, H-3'), 6.11-6.07 (*m*, 1H, ArH), 5.43, 5.36 (*d*, *J* = 1.8Hz, 2H, H-2'), 5.08-5.01 (*m*, 1H, H-4'), 4.99-4.88 (*m*, 2H, H-5'), 4.67-4.56 (*m*, 2H, CH<sub>2</sub> ester), 4.06-3.89 (*m*, 2H, NH, CH-ala), 2.39 (*d*, *J* = 1.6 Hz, 3H, CH<sub>3</sub>-coum), 1.91, 1.85 (*t*, *J* = 1.6 Hz, 3H, CH<sub>3</sub> thym), 1.41, 1.39 (*d*, *J* = 6.5 Hz, 3H, CH<sub>3</sub> ala), 1.12, 1.11 (*t*, *J* = 7 Hz, 3H, CH<sub>3</sub> ester). **<sup>13</sup>C NMR** (CDCl<sub>3</sub>, 125MHz): δppm 175.83 (C=O-ala), 169.98, 167.43 (C=O-thym), 157.65, 157.10 (C=O- coum), 153.78, 153.75 (ArC), 152.52, 152.43, 151.98, 151.76 (Ar-C), 151.05 (C=O-thym), 139.18, 138.79 (ArCH), 135.64, 134.34 (C-3'), 131.21, 130.11 (C-2'), 129.15, 127.54 (Ar-CH), 115.77 (Ar-C), 115.14, 114.61, 113.88, 113.43 (ArCH), 109.45, 109.21 (ArC), 107.11, 107.05, 89.43, 89.14 (C-1'), 83.21, 83.11 (C-4'), (71.88, 69.76, C-5'), 69.22, 69.10 (CH<sub>2</sub> ester), 49.88, 49.73 (CH- ala), 29.31-29.25 (CH<sub>3</sub>-coum), 20.16 (CH<sub>3</sub> ala), 19.43 (CH<sub>3</sub>-ester), 15.84, 14.34 (CH<sub>3</sub>-thym). **<sup>31</sup>P NMR** (CDCl<sub>3</sub>, 202 MHz):

$\delta$ ppm 3.01, 2.73.  $^{19}\text{F}$  NMR (470 MHz,  $\text{CDCl}_3$ ):  $\delta$ ppm-175.2, -174.8. MS (ESI) $^+$ : 582.5 [M+H $^+$ ].

**Ethyl (((((2R,3S,5R)-3-fluoro-5-(5-methyl-2,4-dioxo-3,4-dihydropyrimidin-1(2H)-yl)tetrahydrofuran-2-yl)methoxy)((2-oxo-4-(trifluoromethyl)-2H-chromen-8-yl)oxy)phosphoryl)-L-alaninate. (6.6b)**



**MF:** C<sub>25</sub>H<sub>26</sub>F<sub>4</sub>N<sub>3</sub>O<sub>10</sub>P

**MW:** 635.46

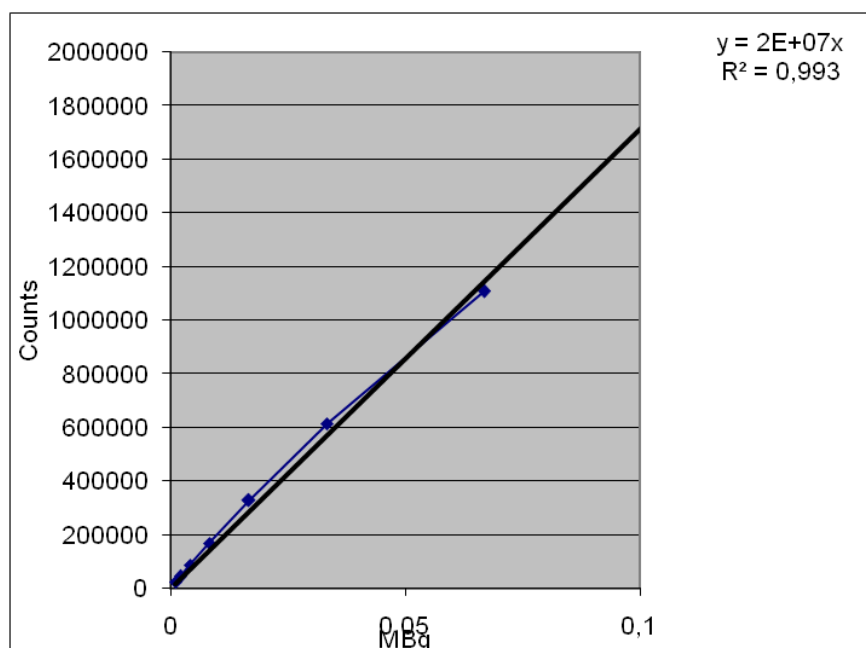
Compound **6.6b** was prepared according to standard procedure D. FLT (**1.29**) (1eq, 0.100g, 0.41mmol), tBuMgCl (0.08mL) and phosphorochloridate (0.349g, 0.82 mmol) were used to produce Protide **6.6b** that was purified by silica gel column chromatography (CH<sub>2</sub>Cl<sub>2</sub>/CH<sub>3</sub>OH from 100% CH<sub>2</sub>Cl<sub>2</sub> to 95% CH<sub>2</sub>Cl<sub>2</sub>) to obtain a pale white solid. Yield: 11%.

**<sup>1</sup>H-NMR** (CDCl<sub>3</sub>, 500MHz): δppm 8.63, 8.61 (s, 1H, NH), 7.84-7.81 (m, 1H, ArH), 7.43, 7.41 (m, 1H, ArH), 7.25-7.19 (m, 2H, ArH), 7.19-7.18 (m, 1H, H-1'), 6.76, 6.75 (t, J = 1.6, 7, 4.3 Hz, 1H, H-3'), 6.03-6.00 (m, 1H, ArH), 5.64, 5.39 (d, J = 1.7 Hz, 2H, H-2'), 4.99-4.97 (m, 1H, H-4'), 4.49-4.43 (m, 2H, H-5'), 4.25-4.21 (m, 2H, CH<sub>2</sub>- ester), 4.11 (m, 1H, NH), 4.02 (m, 1H, CH-ala), 1.95, 1.89 (t, J = 1.5 Hz, 3H, CH<sub>3</sub> thym), 1.54, 1.51 (d, J = 5 Hz, 3H, CH<sub>3</sub> ala), 1.21, 1.19 (t, J = 7 Hz, 3H, CH<sub>3</sub> ester). **<sup>13</sup>C NMR** (CDCl<sub>3</sub>, 125MHz): δppm 181.21 (C=O-ala), 165.98, 164.12 (C=O-thym), 159.65, 158.10 (C=O- coum), 153.12, 153.01 (ArC), 152.76, 152.73, 151.86, 151.54 (Ar-C), 150.3 (C-CF<sub>3</sub>), 150.11 (C=O-thym), 141.18, 140.9 (ArCH), 139.64, 139.99 (C-3'), 137.11, 137.02 (C-2'), 131.53, 131.32 (Ar-CH), 121.99 (CF<sub>3</sub>), 118.23, 117.21, 117.10, 116.98 (ArCH), 110.32, 109.87 (ArC), 108.09, 108.04, 89.43, 89.23 (C-1'), 85.76, 85.11 (C-4'), 75.99, 68.71, (C-5'), 68.19, 67.99 (CH<sub>2</sub> ester), 53.88, 53.53 (CH-ala), 20.99 (CH<sub>3</sub>-ala), 19.13 (CH<sub>3</sub>-ester), 15.99, 15.29 (CH<sub>3</sub>-

thym). **<sup>31</sup>P NMR** (CDCl<sub>3</sub>, 202 MHz): δppm: δ 3.12, 2.91. **<sup>19</sup>F NMR** (CDCl<sub>3</sub>, 470MHz):  
δppm - 64.78,-64.12,-174.3, -174.1. **MS (ESI<sup>+</sup>)**: 658.2 [M+Na<sup>+</sup>].

## 9. Appendix

1.  $^{18}\text{F}$  counts against MBq standard curve. The activity of  $[^{18}\text{F}]\text{FIAU}$  dissolved in PBS was measured and used to make serial dilutions. The range of concentrations was then measured using an automatic gamma counter.



### 2. Raw data for standard curve

Sample	Counts/min		Mean	MBq	KBq
	A	B			
HEK 1	38029	33879	35954	0.001798	1.7977
HEK 2	33052	32571	32811.5	0.001641	1.640575
HEK 3	61659	52007	56833	0.002842	2.84165
TK-HEK1	133924	124467	129195.5	0.00646	6.459775
TK-HEK2	139935	139430	139682.5	0.006984	6.984125
TK-HEK3	145572	117115	131343.5	0.006567	6.567175

**3. Radioactivity measurements from cell washes. KBq of radioactivity from the samples were generated using the standard curve in Figure 4.15**

Sample	Counts		KBq		Total	
	Supernatan	Supernatan	Supernatan	Supernatan	Count	KBq
	t 1	t 2	t 1	t 2		
					251384	125.692
TK- HEK1	2321157	192690	116.0579	9.6345	7	4
					252308	126.154
TK-HEK2	2317760	205327	115.888	10.26635	7	4
					248966	124.483
TK-HEK3	2315578	174083	115.7789	8.70415	1	1
					239915	119.957
HEK1	2269951	129205	113.4976	6.46025	6	8
					243348	121.674
HEK2	2271855	161629	113.5928	8.08145	4	2
					239571	
HEK3	2251568	144151	112.5784	7.20755	9	119.786

## 4. T-test to compare group means with the assumption of equal variances

	HEK	TK-HEK
Mean	0.1164	1.3396
St-Dev	0.0103	0.0859

Hypothesis:

$$H_0 : \mu_{TK} \leq \mu_{HeK}$$

$$H_1 : \mu_{TK} > \mu_{HeK}$$

Significance Level

$$\alpha = 0.05$$

Pooled variance:

$$S_p^2 = \frac{(3-1)0.0103^2 + (3-1)0.0859^2}{(3+3-2)} = 0.0037425$$

$$S_p = \sqrt{0.0037425} = 0.0612$$

Test Statistic:

$$t = \frac{1.3396 - 0.1164}{0.0612 \sqrt{\frac{1}{3} + \frac{1}{3}}} = 24.48$$

Degrees of Freedom:

$$df = 3 + 3 - 2 = 4$$

Critical value:

$$t_c = 2.132$$

Compare and decide:

$$t = 24.48 > t_c = 2.132 \quad \therefore \text{Reject } H_0$$

## 10. Bibliography

- (1) Cole, E. L.; Stewart, M. N.; Littich, R.; Hoareau, R.; Scott, P. J. H. Radiosyntheses Using Fluorine-18: The Art and Science of Late Stage Fluorination. *Curr. Top. Med. Chem.* **2014**, *14* (7), 875–900.
- (2) Matthews, P. M.; Rabiner, E. A.; Passchier, J.; Gunn, R. N. Positron Emission Tomography Molecular Imaging for Drug Development. *Br. J. Clin. Pharmacol.* **2012**, *73* (2), 175–186.
- (3) Rudin, M.; Weissleder, R. Molecular Imaging in Drug Discovery and Development. *Nat. Rev. Drug Discov.* **2003**, *2* (2), 123–131.
- (4) Miller, P. W.; Long, N. J.; Vilar, R.; Gee, A. D. Synthesis of  $^{11}\text{C}$ ,  $^{18}\text{F}$ ,  $^{15}\text{O}$ , and  $^{13}\text{N}$  Radiolabels for Positron Emission Tomography. *Angew. Chemie - Int. Ed.* **2008**, *47* (47), 8998–9033.
- (5) Schlyer, D. J. PET Tracers and Radiochemistry. *Ann. Acad. Med. Singapore* **2004**, *33* (2), 146–154.
- (6) Jacobson, O.; Kiesewetter, D. O.; Chen, X. Fluorine-18 Radiochemistry, Labeling Strategies and Synthetic Routes. *Bioconjug. Chem.* **2015**, *26* (1), 1–18.
- (7) Preshlock, S.; Tredwell, M.; Gouverneur, V.  $^{18}\text{F}$ -Labeling of Arenes and Heteroarenes for Applications in Positron Emission Tomography. *Chem. Rev.* **2016**, *116* (2), 719–766.
- (8) van der Veldt, A. A. M.; Smit, E. F.; Lammertsma, A. A. Positron Emission Tomography as a Method for Measuring Drug Delivery to Tumors in Vivo: The Example of [ $^{11}\text{C}$ ]docetaxel. *Front. Oncol.* **2013**, *3*, 1–7.
- (9) Daniels, S.; Tohid, S. F. M.; Velanguparackel, W.; Westwell, A. D. The Role and Future Potential of Fluorinated Biomarkers in Positron Emission Tomography. *Expert Opin. Drug Discov.* **2010**, *5* (3), 291–304.
- (10) Alauddin, M. M. Positron Emission Tomography (PET) Imaging with ( $^{18}\text{F}$ )-Based

- Radiotracers. *Am. J. Nucl. Med. Mol. Imaging* **2012**, 2 (1), 55–76.
- (11) Turkheimer, F. E.; Veronese, M.; Dunn, J. *Experimental Design and Practical Data Analysis in Positron Emission Tomography*; London, 2014.
- (12) Circular orbits | a2-level-level-revision, physics, fields-0, circular-orbits | Revision World <https://revisionworld.com/a2-level-level-revision/physics/fields-0/circular-orbits> (accessed Jan 1, 2018).
- (13) Gómez-Vallejo, V.; Gaja, V.; Gona, K. B.; Llop, J. Nitrogen-13: Historical Review and Future Perspectives. *J. Labelled Comp. Radiopharm.* **2014**, 57 (4), 244–254.
- (14) Bishop, A.; Satyamurthy, N.; Bida, G.; Hendry, G.; Phelps, M.; Barrio, J. R. Proton Irradiation of [18O]O<sub>2</sub>: Production of [18F]F<sub>2</sub> and [18F]F<sub>2</sub> + [18F] OF<sub>2</sub>. *Nucl. Med. Biol.* **1996**, 23 (3), 189–199.
- (15) Långström, B.; Antoni, G.; Gullberg, P.; Halldin, C.; Malmberg, P.; Någren, K.; Rimland, A.; Svärd, H. Synthesis of L- and D-[Methyl-11C]methionine. *J. Nucl. Med.* **1987**, 28 (6), 1037–1040.
- (16) Larsen, P.; Ulin, J.; Dahlstrøm, K.; Jensen, M. Synthesis of [11C]iodomethane by Iodination of [11C]methane. *Appl. Radiat. Isot.* **1997**, 48 (2), 153–157.
- (17) Cai, L.; Lu, S.; Pike, V. W. Chemistry with [18F]Fluoride Ion. *European J. Org. Chem.* **2008**, 2008 (17), 2853–2873.
- (18) Preshlock, S.; Tredwell, M.; Gouverneur, V. 18F-Labeling of Arenes and Heteroarenes for Applications in Positron Emission Tomography. *Chem. Rev.* **2016**, 116 (2), 719–766.
- (19) Jacobson, O.; Kiesewetter, D. O.; Chen, X. Fluorine-18 Radiochemistry, Labeling Strategies and Synthetic Routes. *Bioconjug. Chem.* **2015**, 26 (1), 1–18.
- (20) Saha, G. B. *Basics of PET Imaging : Physics, Chemistry, and Regulations*; Springer, 2010.
- (21) Berridge, M. S.; Apana, S. M.; Hersh, J. M. Teflon Radiolysis as the Major Source of Carrier in Fluorine-18. *J. Label. Compd. Radiopharm.* **2009**, 52 (13), 543–548.
- (22) Vallabhajosula, S. *Molecular Imaging : Radiopharmaceuticals for PET and SPECT*;

Springer-Verlag, 2009.

- (23) FASTlab Multi-Tracer Platform - TRACERcenter Equipment - PET Radiopharmacy - CATEGORIES [http://www3.gehealthcare.com.sg/en-gb/products/categories/pet-radiopharmacy/tracer\\_center\\_equipment/fastlab](http://www3.gehealthcare.com.sg/en-gb/products/categories/pet-radiopharmacy/tracer_center_equipment/fastlab) (accessed Jan 1, 2018).
- (24) L'Annunziata, M. F. Radiopharma instruments | Trasis <http://www.trasis.com/> (accessed Jan 1, 2018).
- (25) Scott, P. J. H.; Hockley, B. G. *Radiochemical Synthesis. Volume I, Radiopharmaceuticals for Positron Emission Tomography*; Wiley, 2012.
- (26) L'Annunziata, M. F. *Handbook of Radioactivity Analysis*; 2012.
- (27) Lindegren, S.; Jensenb, H.; Jacobsson, L. A Radio-High-Performance Liquid Chromatography Dual-Flow Cell Gamma-Detection System for on-Line Radiochemical Purity and Labeling Efficiency Determination. *J. Chromatogr. A* **2014**, *1337*, 128–132.
- (28) *The Ionising Radiations Regulations 1999*; Queen's Printer of Acts of Parliament, 1999.
- (29) Bixler, A.; Springer, G.; Lovas, R. Practical Aspects of Radiation Safety for Using Fluorine-18. *J. Nucl. Med. Technol.* **1999**, *27* (1), 14-6-9.
- (30) He, Q.; Alfeazi, I.; Sadeghi, S. No-Carrier-Added Electrochemical Nucleophilic Radiofluorination of Aromatics. *J. Radioanal. Nucl. Chem.* **2015**, *303* (1), 1037–1040.
- (31) Jacobson, O.; Chen, X. PET Designated Fluoride-18 Production and Chemistry. *Curr. Top. Med. Chem.* **2010**, *10* (11), 1048–1059.
- (32) Kim, D. W.; Ahn, D. S.; Oh, Y. H.; Lee, S.; Kil, H. S.; Oh, S. J.; Lee, S. J.; Kim, J. S.; Ryu, J. S.; Moon, D. H.; Chi, D. Y. A New Class of SN2 Reactions Catalyzed by Protic Solvents: Facile Fluorination for Isotopic Labeling of Diagnostic Molecules. *J. Am. Chem. Soc.* **2006**, *128* (50), 16394–16397.
- (33) Ganghua, T.; Xiaolan, T.; Fuhua, W.; Mingfang, W.; Baoyuan, L. A Facile and

- Rapid Automated Synthesis of 3'-Deoxy-3'-[18F]fluorothymidine. *Appl. Radiat. Isot.* **2010**, *68* (9), 1734–1739.
- (34) Cavaliere, A.; Probst, K. C.; Westwell, A. D.; Slusarczyk, M. Fluorinated Nucleosides as an Important Class of Anticancer and Antiviral Agents. *Future Med. Chem.* **2017**, *9* (15), 1809–1833.
- (35) Hollingworth, C.; Gouverneur, V. Transition Metal Catalysis and Nucleophilic Fluorination. *Chem. Commun.* **2012**, *48* (24), 2929.
- (36) Kepe, V.; Moghbel, M. C.; Långström, B.; Zaidi, H.; Vinters, H. V; Huang, S.-C.; Satyamurthy, N.; Doudet, D.; Mishani, E.; Cohen, R. M.; Høilund-Carlsen, P. F.; Alavi, A.; Barrio, J. R. Amyloid- $\beta$  Positron Emission Tomography Imaging Probes: A Critical Review. *J. Alzheimers. Dis.* **2013**, *36* (4), 613–631.
- (37) Swallow, S. Fluorine in Medicinal Chemistry. *Prog. Med. Chem.* **2015**, *54* (2), 65–133.
- (38) Buckingham, F.; Gouverneur, V. Asymmetric 18 F-Fluorination for Applications in Positron Emission Tomography. *Chem. Sci.* **2016**, *7* (3), 1645–1652.
- (39) Hoover, A. J.; Lazari, M.; Ren, H.; Narayanam, M. K.; Murphy, J. M.; Van Dam, R. M.; Hooker, J. M.; Ritter, T. A Transmetalation Reaction Enables the Synthesis of [18F]5-Fluorouracil from [18F]Fluoride for Human PET Imaging. *Organometallics* **2016**, *35* (7), 1008–1014.
- (40) Purrington, S. T.; Kagen, B. S.; Patrick, T. B. Application of Elemental Fluorine in Organic Synthesis. *Chem. Rev.* **1986**, *86* (6), 997–1018.
- (41) Casella, V.; Ido, T.; Wolf, A. P.; Fowler, J. S.; MacGregor, R. R.; Ruth, T. J. Anhydrous F-18 Labeled Elemental Fluorine for Radiopharmaceutical Preparation. *J. Nucl. Med.* **1980**, *21* (8), 750–757.
- (42) Teare, H.; Robins, E. G.; Kirjavainen, A.; Forsback, S.; Sandford, G.; Solin, O.; Luthra, S. K.; Gouverneur, V. Radiosynthesis and Evaluation of [18F]Selectfluor Bis(triflate). *Angew. Chemie Int. Ed.* **2010**, *49* (38), 6821–6824.
- (43) Bauta, W.; Schulmeier, B. E.; Burke, B.; Puente, J. F.; Cantrell, W. R.; Lovett, D.; Goebel, J.; Anderson, B.; Ionescu, D.; Ruichao, G. A New Process for

- Antineoplastic Agent Clofarabine. *Org. Proc. Res. Dev* **2004**, *8* (6), 889–896.
- (44) Anderson, H.; Pillarsetty, N.; Cantorias, M.; Lewis, J. S. Improved Synthesis of 2'-deoxy-2'-[18F]-Fluoro-1-Beta-D-Arabinofuranosyl-5-Iodouracil ([18F]-FIAU). *Nucl. Med. Biol.* **2010**, *37* (4), 439–442.
- (45) Zhang, H.; Cantorias, M. V; Pillarsetty, N.; Burnazi, E. M.; Cai, S.; Lewis, J. S. An Improved Strategy for the Synthesis of [<sup>18</sup>F]-Labeled Arabinofuranosyl Nucleosides. *Nucl. Med. Biol.* **2012**, *39* (8), 1182–1188.
- (46) Shelton, J.; Lu, X.; Hollenbaugh, J. A.; Cho, J. H.; Amblard, F.; Schinazi, R. F. Metabolism, Biochemical Actions, and Chemical Synthesis of Anticancer Nucleosides, Nucleotides, and Base Analogs. *Chem. Rev.* **2016**, *116* (23), 14379–14455.
- (47) Gallagher, B. M.; Fowler, J. S.; Gutterson, N. I.; MacGregor, R. R.; Wan, C. N.; Wolf, A. P. Metabolic Trapping as a Principle of Oradiopharmaceutical Design: Some Factors Responsible for the Biodistribution of [18F] 2-Deoxy-2-Fluoro-D-Glucose. *J. Nucl. Med.* **1978**, *19* (10), 1154–1161.
- (48) Gambhir, S. S.; Czernin, J.; Schwimmer, J.; Silverman, D. H.; Coleman, R. E.; Phelps, M. E. A Tabulated Summary of the FDG PET Literature. *J. Nucl. Med.* **2001**, *42* (5 Suppl), 1S–93S.
- (49) Adam, M. J. A Rapid, Stereoselective, High Yielding Synthesis of 2-Deoxy-2-Fluoro-D-Hexopyranoses: Reaction of Glycals with Acetyl Hypofluorite. *J. Chem. Soc. Chem. Commun.* **1982**, *0* (13), 730.
- (50) Shiue, C.-Y.; K.-C., A. P.; Wolf, A. P. A Rapid Synthesis of 2-Deoxy-2-Fluoro-D-Glucose from Xenon Difluoride Suitable for Labelling with 18F. *J. Label. Compd. Radiopharm.* **1983**, *20* (2), 157–162.
- (51) Hamacher, K.; Coenen, H. H.; Stocklin, G. Synthesis D-Glucose Using Aminopolyether Supported Nucleophilic Substitution. *J. Nucl. Med.* **1986**, *27* (February), 235–239.
- (52) Yu, S. Review of F-FDG Synthesis and Quality Control. *Biomed. Imaging Interv. J.* **2006**, *2* (4), e57.

- (53) Pankiewicz, K. W. Fluorinated Nucleosides. *Carbohydr. Res.* **2000**, 327 (1–2), 87–105.
- (54) Mangner, T. J.; Klecker, R. W.; Anderson, L.; Shields, A. F. Synthesis of 2'-Deoxy-2'-[18F]fluoro- $\beta$ -D-Arabinofuranosyl Nucleosides, [18F]FAU, [18F]FMAU, [18F]FBAU and [18F]FIAU, as Potential PET Agents for Imaging Cellular Proliferation. *Nucl. Med. Biol.* **2003**, 30 (3), 215–224.
- (55) Soloviev, D.; Lewis, D.; Honess, D.; Aboagye, E. [18F]FLT: An Imaging Biomarker of Tumour Proliferation for Assessment of Tumour Response to Treatment. *Eur. J. Cancer* **2012**, 48 (4), 416–424.
- (56) McKinley, E. T.; Ayers, G. D.; Smith, R. A.; Saleh, S. A.; Zhao, P.; Washington, M. K.; Coffey, R. J.; Manning, H. C. Limits of [18F]-FLT PET as a Biomarker of Proliferation in Oncology. *PLoS One* **2013**, 8 (3), e58938.
- (57) Tjuvajev, J. G.; Doubrovin, M.; Akhurst, T.; Cai, S.; Balatoni, J.; Alauddin, M. M.; Finn, R.; Bornmann, W.; Thaler, H.; Conti, P. S.; Blasberg, R. G. Comparison of Radiolabeled Nucleoside Probes (FIAU, FHBG, and FHPG) for PET Imaging of HSV1-Tk Gene Expression. *J. Nucl. Med.* **2002**, 43 (8), 1072–1083.
- (58) Alauddin, M. M.; Shahinian, A.; Park, R.; Tohme, M.; Fissekis, J. D.; Conti, P. S. Biodistribution and PET Imaging of [(18)F]-Fluoroadenosine Derivatives. *Nucl. Med. Biol.* **2007**, 34 (3), 267–272.
- (59) Marik, J.; Ogasawara, A.; Martin-McNulty, B.; Ross, J.; Flores, J. E.; Gill, H. S.; Tinianow, J. N.; Vanderbilt, A. N.; Nishimura, M.; Peale, F.; Pastuskovas, C.; Greve, J. M.; van Bruggen, N.; Williams, S. P. PET of Glial Metabolism Using 2-18F-Fluoroacetate. *J. Nucl. Med.* **2009**, 50 (6), 982–990.
- (60) Vingerhoets, F. J.; Schulzer, M.; Ruth, T. J.; Holden, J. E.; Snow, B. J. Reproducibility and Discriminating Ability of Fluorine-18-6-Fluoro-L-Dopa PET in Parkinson's Disease. *J. Nucl. Med.* **1996**, 37 (3), 421–426.
- (61) Miller, P. W.; Long, N. J.; Vilar, R.; Gee, A. D. Synthesis of 11C, 18F, 15O, and 13N Radiolabels for Positron Emission Tomography. *Angew. Chem. Int. Ed. Engl.* **2008**, 47 (47), 8998–9033.

- (62) Link, J. M.; Krohn, K. A.; Clark, J. C. Production of [11C]CH<sub>3</sub>I by Single Pass Reaction of [11C]CH<sub>4</sub> with I<sub>2</sub>. *Nucl. Med. Biol.* **1997**, *24* (1), 93–97.
- (63) Ametamey, S. M.; Honer, M.; Schubiger, P. A. Molecular Imaging with PET. *Chem. Rev.* **2008**, *108* (5), 1501–1516.
- (64) da Silva, E. S.; Gómez-Vallejo, V.; Llop, J.; López-Gallego, F. Efficient Nitrogen-13 Radiochemistry Catalyzed by a Highly Stable Immobilized Biocatalyst. *Catal. Sci. Technol.* **2015**, *5* (5), 2705–2713.
- (65) Tominaga, T.; Inoue, O.; Suzuki, K.; Yamasaki, T.; Hirobe, M. Synthesis of <sup>13</sup>N-Labelled Amines by Reduction of <sup>13</sup>N-Labelled Amides. *Int. J. Radiat. Appl. Instrumentation. Part A. Appl. Radiat. Isot.* **1986**, *37* (12), 1209–1212.
- (66) Martín, A.; SAN Sebastián, E.; Gómez-Vallejo, V.; Llop, J. Positron Emission Tomography with [<sup>13</sup>N]ammonia Evidences Long-Term Cerebral Hyperperfusion after 2h-Transient Focal Ischemia. *Neuroscience* **2012**, *213*, 47–53.
- (67) Hoop, B.; Smith, T. W.; Burnham, C. A.; Correll, J. E.; Brownell, G. L.; Sanders, C. A. Myocardial Imaging with <sup>13</sup>NH<sub>4</sub><sup>+</sup> and a Multicrystal Positron Camera. *J. Nucl. Med.* **1973**, *14* (3), 181–183.
- (68) Beaney, R.; Jones, T.; Lammertsma, A.; Mckenzie, C.; Halnan, K. Positron Emission Tomography for in-Vivo Measurement of Regional Blood Flow, Oxygen Utilisation, and Blood Volume in Patients with Breast Carcinoma. *Lancet* **1984**, *323* (8369), 131–134.
- (69) Al-Nahhas, A.; Win, Z.; Szyszko, T.; Singh, A.; Nanni, C.; Fanti, S.; Rubello, D. Gallium-68 PET: A New Frontier in Receptor Cancer Imaging. *Anticancer Res.* *27* (6B), 4087–4094.
- (70) Deri, M. A.; Zeglis, B. M.; Francesconi, L. C.; Lewis, J. S. PET Imaging with <sup>89</sup>Zr: From Radiochemistry to the Clinic. *Nucl. Med. Biol.* **2013**, *40* (1), 3–14.
- (71) Anderson, C. J.; Ferdani, R. Copper-64 Radiopharmaceuticals for PET Imaging of Cancer: Advances in Preclinical and Clinical Research. *Cancer Biother. Radiopharm.* **2009**, *24* (4), 379–393.
- (72) Kolb, H. C.; Finn, M. G.; Sharpless, K. B. Click Chemistry: Diverse Chemical

- Function from a Few Good Reactions. *Angew. Chem. Int. Ed. Engl.* **2001**, *40* (11), 2004–2021.
- (73) Jones, T.; Rabiner, E. A.; PET Research Advisory Company. The Development, Past Achievements, and Future Directions of Brain PET. *J. Cereb. Blood Flow Metab.* **2012**, *32* (7), 1426–1454.
- (74) Matthews, P. M.; Rabiner, E. A.; Passchier, J.; Gunn, R. N. Positron Emission Tomography Molecular Imaging for Drug Development. *Br. J. Clin. Pharmacol.* **2012**, *73* (2), 175–186.
- (75) Bergström, M.; Hargreaves, R. J.; Burns, H. D.; Goldberg, M. R.; Sciberras, D.; Reines, S. A.; Petty, K. J.; Ögren, M.; Antoni, G.; Långström, B.; Eskola, O.; Scheinin, M.; Solin, O.; Majumdar, A. K.; Constanzer, M. L.; Battisti, W. P.; Bradstreet, T. E.; Gargano, C.; Hietala, J. Human Positron Emission Tomography Studies of Brain Neurokinin 1 Receptor Occupancy by Aprepitant. *Biol. Psychiatry* **2004**, *55* (10), 1007–1012.
- (76) Van Rompay, A. R.; Johansson, M.; Karlsson, A. Substrate Specificity and Phosphorylation of Antiviral and Anticancer Nucleoside Analogues by Human Deoxyribonucleoside Kinases and Ribonucleoside Kinases. *Pharmacol. Ther.* **2003**, *100* (2), 119–139.
- (77) Chu, C. K.; Baker, D. C.; Symposium on Nucleosides as Antitumor and Antiviral Agents (1992 : San Francisco, C. . *Nucleosides and Nucleotides as Antitumor and Antiviral Agents*.
- (78) Van Rompay, A. R.; Johansson, M.; Karlsson, A.; Berg, J. M. (Jeremy M.; Tymoczko, J. L.; Stryer, L.; Stryer, L. *Biochemistry, 5th Edition*; W.H. Freeman, 2002; Vol. 100.
- (79) Balzarini, J.; Egberink, H.; Hartmann, K.; Cahard, D.; Vahlenkamp, T.; Thormar, H.; De Clercq, E.; McGuigan, C. Antiretrovirus Specificity and Intracellular Metabolism of 2',3' -Didehydro-2',3'-dideoxythymidine (Stavudine) and Its 5'-monophosphate Triester Prodrug So324. *Mol. Pharmacol.* **1996**, *50* (5), 1207–1213.

- (80) Al-Madhoun, A. S.; Tjarks, W.; Eriksson, S. The Role of Thymidine Kinases in the Activation of Pyrimidine Nucleoside Analogues. *Mini Rev. Med. Chem.* **2004**, *4* (4), 341–350.
- (81) Pradere, U.; Garnier-Amblard, E. C.; Coats, S. J.; Amblard, F.; Schinazi, R. F. Synthesis of Nucleoside Phosphate and Phosphonate Prodrugs. *Chem. Rev.* **2014**, *114* (18), 9154–9218.
- (82) Mehellou, Y. The ProTides Boom. *ChemMedChem* **2016**, *11* (11), 1–4.
- (83) Mehellou, Y.; Rattan, H. S.; Balzarini, J. The ProTide Prodrug Technology: From the Concept to the Clinic. *J. Med. Chem.* **2017**, acs.jmedchem.7b00734.
- (84) Serpi, M.; Madela, K.; Pertusati, F.; Slusarczyk, M. Synthesis of Phosphoramidate Prodrugs: ProTide Approach. *Curr. Protoc. Nucleic Acid Chem.* **2013**, Chapter 15.
- (85) McGuigan, C.; Murziani, P.; Slusarczyk, M.; Gonczy, B.; Vande Voorde, J.; Liekens, S.; Balzarini, J. Phosphoramidate ProTides of the Anticancer Agent FUDR Successfully Deliver the Preformed Bioactive Monophosphate in Cells and Confer Advantage over the Parent Nucleoside. *J. Med. Chem.* **2011**, *54* (20), 7247–7258.
- (86) Westwell, A. D. *Fluorinated Pharmaceuticals: Advances in Medicinal Chemistry*; Future Science Ltd: London, UK, 2015.
- (87) Isanbor, C.; O'Hagan, D. Fluorine in Medicinal Chemistry: A Review of Anti-Cancer Agents. *J. Fluor. Chem.* **2006**, *127* (3), 303–319.
- (88) Ismail, F. M. D. Important Fluorinated Drugs in Experimental and Clinical Use. *J. Fluor.* **2002**, *118*, 27–33.
- (89) Park, B. K.; Kitteringham, N. R.; O'Neill, P. M. Metabolism of Fluorine-Containing Drugs. *Annu. Rev. Pharmacol. Toxicol.* **2001**, *41* (1), 443–470.
- (90) Meier, C.; Knispel, T.; Marquez, V. E.; Siddiqui, M. A.; De Clercq, E.; Balzarini, J. cycloSal-Pronucleotides of 2'-Fluoro-Ara- and 2'-Fluoro-Ribo-2',3'-Dideoxyadenosine as a Strategy to Bypass a Metabolic Blockade. *J. Med. Chem.* **1999**, *42* (9), 1615–1624.

- (91) Carreras, C. W.; Santi, D. V. The Catalytic Mechanism and Structure of Thymidylate Synthase. *Annu. Rev. Biochem.* **1995**, *64* (1), 721–762.
- (92) Kaiyawet, N.; Rungrotmongkol, T.; Hannongbua, S. Effect of Halogen Substitutions on dUMP to Stability of Thymidylate Synthase/dUMP/mTHF Ternary Complex Using Molecular Dynamics Simulation. *J. Chem. Inf. Model.* **2013**, *53* (6), 1315–1323.
- (93) Malet-Martino, M.; Jolimaitre, P.; Martino, R. The Prodrugs of 5-Fluorouracil. *Curr. Med. Chem. Anticancer. Agents* **2002**, *2* (2), 267–310.
- (94) Vande Voorde, J.; Liekens, S.; McGuigan, C.; Murziani, P. G. S.; Slusarczyk, M.; Balzarini, J. The Cytostatic Activity of NUC-3073, a Phosphoramidate Prodrug of 5-Fluoro-2'-Deoxyuridine, Is Independent of Activation by Thymidine Kinase and Insensitive to Degradation by Phosphorolytic Enzymes. *Biochem. Pharmacol.* **2011**, *82* (5), 441–452.
- (95) Ghazaly, E. A.; Slusarczyk, M.; McGuigan, C.; Harrison, D.; Blagden, S. P. Abstract B46: NUC-3373: A Novel Pyrimidine Nucleotide Analogue That Overcomes Key Cancer Drug Resistance Limiting Patient Survival. *Mol. Cancer Ther.* **2015**, *14* (12 Supplement 2), B46–B46.
- (96) Blagden, S. P.; Slusarczyk, M.; Serpi, M.; McGuigan, C.; Ghazaly, E. A. Abstract CT028: First-in-Human Phase I Study of the Nucleotide Analogue NUC-3373 Designed to Overcome Fluoropyrimidine Drug Resistance Mechanisms. *Cancer Res.* **2016**, *76* (14 Supplement), CT028-CT028.
- (97) Toschi, L.; Finocchiaro, G.; Bartolini, S.; Gioia, V.; Cappuzzo, F. Role of Gemcitabine in Cancer Therapy. *Futur. Oncol.* **2005**, *1* (1), 7–17.
- (98) Eckel, F.; Schneider, G.; Schmid, R. M. Pancreatic Cancer: A Review of Recent Advances. *Expert Opin. Investig. Drugs* **2006**, *15* (11), 1395–1410.
- (99) Kroep, J. R.; Loves, W. J. P.; van der Wilt, C. L.; Alvarez, E.; Talianidis, I.; Boven, E.; Braakhuis, B. J. M.; van Groeningen, C. J.; Pinedo, H. M.; Peters, G. J. Pretreatment Deoxycytidine Kinase Levels Predict in Vivo Gemcitabine Sensitivity. *Mol. Cancer Ther.* **2002**, *1* (6), 371–376.

- (100) Heinemann, V.; Hertel, L. W.; Grindey, G. B.; Plunkett, W. Comparison of the Cellular Pharmacokinetics and Toxicity of 2',2'-difluorodeoxycytidine and 1-Beta-D-Arabinofuranosylcytosine. *Cancer Res.* **1988**, *48* (14), 4024–4031.
- (101) Beumer, J. H.; Eiseman, J. L.; Parise, R. A.; Joseph, E.; Covey, J. M.; Egorin, M. J. Modulation of Gemcitabine (2',2'-Difluoro-2'-Deoxycytidine) Pharmacokinetics, Metabolism, and Bioavailability in Mice by 3,4,5,6-Tetrahydrouridine. *Clin. Cancer Res.* **2008**, *14* (11), 3529–3535.
- (102) Bender, D. M.; Bao, J.; Dantzig, A. H.; Diseroad, W. D.; Law, K. L.; Magnus, N. A.; Peterson, J. A.; Perkins, E. J.; Pu, Y. J.; Reutzel-Edens, S. M.; Remick, D. M.; Starling, J. J.; Stephenson, G. A.; Vaid, R. K.; Zhang, D.; McCarthy, J. R. Synthesis, Crystallization, and Biological Evaluation of an Orally Active Prodrug of Gemcitabine. *J. Med. Chem.* **2009**, *52* (22), 6958–6961.
- (103) Slusarczyk, M.; Lopez, M. H.; Balzarini, J.; Mason, M.; Jiang, W. G.; Blagden, S.; Thompson, E.; Ghazaly, E.; McGuigan, C. Application of ProTide Technology to Gemcitabine: A Successful Approach to Overcome the Key Cancer Resistance Mechanisms Leads to a New Agent (NUC-1031) in Clinical Development. *J. Med. Chem.* **2014**, *57* (4), 1531–1542.
- (104) Blagden, S. P. et al. Final Results of ProGem1, the First in-Human Phase I/II Study of NUC-1031 in Patients with Solid Malignancies. | 2015 ASCO Annual Meeting | Virtual Meeting | Meeting Library. *J Clin Oncol.* 2015, p suppl; abstr 2514.
- (105) Ricci, F.; Tedeschi, A.; Morra, E.; Montillo, M. Fludarabine in the Treatment of Chronic Lymphocytic Leukemia: A Review. *Ther. Clin. Risk Manag.* **2009**, *5* (1), 187–207.
- (106) Parker, W. B.; Cheng, Y. C. Inhibition of DNA Primase by Nucleoside Triphosphates and Their Arabinofuranosyl Analogs. *Mol. Pharmacol.* **1987**, *31* (2), 146–151.
- (107) Huang, P.; Plunkett, W. Phosphorolytic Cleavage of 2-Fluoroadenine from 9-Beta-D-Arabinofuranosyl-2-Fluoroadenine by Escherichia Coli. A Pathway for 2-Fluoro-ATP Production. *Biochem. Pharmacol.* **1987**, *36* (18), 2945–2950.

- (108) Hallek, M.; Fischer, K.; Fingerle-Rowson, G.; Fink, A.; Busch, R.; Mayer, J.; Hensel, M.; Hopfinger, G.; Hess, G.; von Grünhagen, U.; Bergmann, M.; Catalano, J.; Zinzani, P.; Caligaris-Cappio, F.; Seymour, J.; Berrebi, A.; Jäger, U.; Cazin, B.; Trnecny, M.; Westermann, A.; Wendtner, C.; Eichhorst, B.; Staib, P.; Bühler, A.; Winkler, D.; Zenz, T.; Böttcher, S.; Ritgen, M.; Mendila, M.; Kneba, M.; Döhner, H.; Stilgenbauer, S.; International Group of Investigators; German Chronic Lymphocytic Leukaemia Study Group. Addition of Rituximab to Fludarabine and Cyclophosphamide in Patients with Chronic Lymphocytic Leukaemia: A Randomised, Open-Label, Phase 3 Trial. *Lancet* **2010**, *376* (9747), 1164–1174.
- (109) Von Hoff, D. D. Phase I Clinical Trials with Fludarabine Phosphate. *Semin. Oncol.* **1990**, *17* (5 Suppl 8), 33–38.
- (110) Jordheim, L. P.; Durantel, D.; Zoulim, F.; Dumontet, C. Advances in the Development of Nucleoside and Nucleotide Analogues for Cancer and Viral Diseases. *Nat. Rev. Drug Discov.* **2013**, *12* (6), 447–464.
- (111) Daly, M. B.; Roth, M. E.; Bonnac, L.; Maldonado, J. O.; Xie, J.; Clouser, C. L.; Patterson, S. E.; Kim, B.; Mansky, L. M. Dual Anti-HIV Mechanism of Clofarabine. *Retrovirology* **2016**, *13* (1), 20.
- (112) Cleij, M. C.; Steel, C. J.; Brady, F. 3'-DEOXY-3'-[\*P]FLUOROTHYnIDINE. **2001**, *1* (1 ml), 871–873.
- (113) Ghosn, J.; Quinson, A.-M.; Sabo, N.; Cotte, L.; Piketty, C.; Dorléacq, N.; Bravo, M.-L.; Mayers, D.; Harmenberg, J.; Mårdh, G.; Valdez, H.; Katlama, C. Antiviral Activity of Low-Dose Alovudine in Antiretroviral-Experienced Patients: Results from a 4-Week Randomized, Double-Blind, Placebo-Controlled Dose-Ranging Trial. *HIV Med.* **2007**, *8* (3), 142–147.
- (114) Velanguparackel, W.; Hamon, N.; Balzarini, J.; McGuigan, C.; Westwell, A. D. Synthesis, Anti-HIV and Cytostatic Evaluation of 3'-Deoxy-3'- Fluorothymidine (FLT) pro-Nucleotides. *Bioorganic Med. Chem. Lett.* **2014**, *24* (10), 2240–2243.
- (115) Klecker, R. W.; Katki, A. G.; Collins, J. M. Toxicity, Metabolism, DNA Incorporation with Lack of Repair, and Lactate Production for 1-(2'-fluoro-2'-deoxy-Beta-D-Arabinofuranosyl)-5-Iodouracil in U-937 and MOLT-4 Cells. *Mol.*

*Pharmacol.* **1994**, *46* (6), 1204–1209.

- (116) Cai, H.; Li, Z.; Conti, P. S. The Improved Syntheses of 5-Substituted 2'-[<sup>18</sup>F]fluoro-2'-deoxy-Arabinofuranosyluracil Derivatives ([<sup>18</sup>F]FAU, [<sup>18</sup>F]FEAU, [<sup>18</sup>F]FFAU, [<sup>18</sup>F]FCAU, [<sup>18</sup>F]FBAU and [<sup>18</sup>F]FIAU) Using a Multistep One-Pot Strategy. *Nucl. Med. Biol.* **2011**, *38* (5), 659–666.
- (117) Ghosh, R. K.; Ghosh, S. M.; Chawla, S. Recent Advances in Antiretroviral Drugs. *Expert Opin. Pharmacother.* **2011**, *12* (1), 31–46.
- (118) Frampton, J. E.; Perry, C. M. Emtricitabine: A Review of Its Use in the Management of HIV Infection. *Drugs* **2005**, *65* (10), 1427–1448.
- (119) By, S.; Kates, D. E. Application for Inclusion of Emtricitabine On WHO Model List of Essential Medicines. **2006**.
- (120) Pawlotsky, J. M.; Najera, I.; Jacobson, I. Resistance to Mericitabine, a Nucleoside Analogue Inhibitor of HCV RNA-Dependent RNA Polymerase. *Antiviral Therapy*. 2012, pp 411–423.
- (121) Summers, B. B.; Beavers, J. W. F.; Klibanov, O. M. Sofosbuvir, a Novel Nucleotide Analogue Inhibitor Used for the Treatment of Hepatitis C Virus. *J. Pharm. Pharmacol.* **2014**, *66*, 1653–1666.
- (122) Cha, A.; Budovich, A. Sofosbuvir: A New Oral Once-Daily Agent for the Treatment of Hepatitis C Virus Infection. *P T* **2014**, *39* (5), 345–352.
- (123) Bhatia, H. K.; Singh, H.; Grewal, N.; Natt, N. K. Sofosbuvir: A Novel Treatment Option for Chronic Hepatitis C Infection. *J. Pharmacol. Pharmacother.* **2014**, *5* (4), 278–284.
- (124) Bullard-Feibelman, K. M.; Govero, J.; Zhu, Z.; Salazar, V.; Veselinovic, M.; Diamond, M. S.; Geiss, B. J. The FDA-Approved Drug Sofosbuvir Inhibits Zika Virus Infection. *Antiviral Res.* **2017**, *137*, 134–140.
- (125) Lam, A. M.; Espiritu, C.; Bansal, S.; Micolochick Steuer, H. M.; Zennou, V.; Otto, M. J.; Furman, P. A. Hepatitis C Virus Nucleotide Inhibitors PSI-352938 and PSI-353661 Exhibit a Novel Mechanism of Resistance Requiring Multiple Mutations within Replicon RNA. *J. Virol.* **2011**, *85* (23), 12334–12342.

- (126) Wang, C.; Song, Z.; Yu, H.; Liu, K.; Ma, X. Adenine: An Important Drug Scaffold for the Design of Antiviral Agents. *Acta Pharm. Sin. B* **2015**, *5* (5), 431–441.
- (127) Couturier, O.; Luxen, A.; Chatal, J.-F.; Vuillez, J.-P.; Rigo, P.; Hustinx, R. Fluorinated Tracers for Imaging Cancer with Positron Emission Tomography. *Eur. J. Nucl. Med. Mol. Imaging* **2004**, *31* (8), 1182–1206.
- (128) Serpi, M.; Madela, K.; Pertusati, F.; Slusarczyk, M.; Serpi, M.; Madela, K.; Pertusati, F.; Slusarczyk, M. Synthesis of Phosphoramidate Prodrugs: ProTide Approach. In *Current protocols in nucleic acid chemistry / edited by Serge L. Beaucage ... [et al.]*; John Wiley & Sons, Inc.: Hoboken, NJ, USA, 2013; Vol. Chapter 15, p 15.5.1-15.5.15.
- (129) Hassan, M. Z.; Osman, H.; Ali, M. A.; Ahsan, M. J. Therapeutic Potential of Coumarins as Antiviral Agents. *Eur. J. Med. Chem.* **2016**, *123*, 236–255.
- (130) Peck, M.; Pollack, H. A.; Friesen, A.; Muzi, M.; Shoner, S. C.; Shankland, E. G.; Fink, J. R.; Armstrong, J. O.; Link, J. M.; Krohn, K. A. Applications of PET Imaging with the Proliferation Marker [<sup>18</sup>F]-FLT. *Q. J. Nucl. Med. Mol. Imaging* **2015**, *59* (1).
- (131) Fletcher, S. The Mitsunobu Reaction in the 21<sup>st</sup> Century. *Org. Chem. Front.* **2015**, *2* (6), 739–752.
- (132) Meyer, J. P.; Probst, K. C.; Trist, I. M. L.; Mcguigan, C.; Westwell, A. D. Radiochemical Synthesis of 2'-[<sup>18</sup>F]-Labelled and 3'-[<sup>18</sup>F]-Labelled Nucleosides for Positron Emission Tomography Imaging. *J. Labelled Comp. Radiopharm.* **2014**, *57* (5), 333–337.
- (133) Mitsunobu Reaction <http://www.organic-chemistry.org/namedreactions/mitsunobu-reaction.shtml> (accessed Jan 2, 2018).
- (134) Balagopala, M. I.; Ollapally, A. P.; Lee, H. J. An Improved Synthesis of Azidothymidine. *Nucleosides, Nucleotides and Nucleic Acids* **1996**, *15* (4), 899–906.
- (135) Miah, A.; Reese, C. B.; Song, Q.; Sturdy, Z.; Neidle, S.; Simpson, I. J.; Read, M.;

- Rayner, E. 2',3'-Anhydrouridine. A Useful Synthetic Intermediate. *J. Chem. Soc. Perkin Trans. 1* **1998**, 0 (19), 3277–3284.
- (136) Turkman, N.; Gelovani, J. G.; Alauddin, M. M. A Novel Method for Stereospecific Fluorination at the 2'-Arabino-Position of Pyrimidine Nucleoside: Synthesis of [18F]-FMAU. *J. Label. Compd. Radiopharm.* **2010**, 53 (13), 782–786.
- (137) Yun, M.; Oh, S. J.; Ha, H.-J.; Ryu, J. S.; Moon, D. H. High Radiochemical Yield Synthesis of 3'-deoxy-3'-[18F]fluorothymidine Using (5'-O-Dimethoxytrityl-2'-deoxy-3'-O-Nosyl-Beta-D-Threo Pentofuranosyl)thymine and Its 3-N-BOC-Protected Analogue as a Labeling Precursor. *Nucl. Med. Biol.* **2003**, 30 (2), 151–157.
- (138) Alauddin, M. M. Nucleoside-Based Probes for Imaging Tumor Proliferation Using Positron Emission Tomography. *J. Label. Compd. Radiopharm.* **2013**, 56 (3–4), 237–243.
- (139) Meyer, J.-P.; Probst, K. C.; Trist, I. M. L.; McGuigan, C.; Westwell, A. D. A Novel Radiochemical Approach to 1-(2'-deoxy-2'-[18F]fluoro-β-D-Arabinofuranosyl)cytosine (18F-FAC). *J. Label. Compd. Radiopharm.* **2014**, 57 (11), 637–644.
- (140) Wieland, D. M.; Tobes, M. C.; Manger, T. J. *Analytical and Chromatographic Techniques in Radiopharmaceutical Chemistry*; Springer New York, 1986.
- (141) Bhasin, S. K.; Gupta, R. *Pharmaceutical Organic Chemistry*; Elsevier Health Sciences APAC, 2012.
- (142) PET Tracerlab FX/FX2  
[http://www3.gehealthcare.com/en/technical/molecular\\_imaging\\_-\\_radiopharmaceutical/pet\\_tracerlab\\_fx](http://www3.gehealthcare.com/en/technical/molecular_imaging_-_radiopharmaceutical/pet_tracerlab_fx) (accessed Jan 2, 2018).
- (143) Lao, Y.; Yang, C.; Zou, W.; Gan, M.; Chen, P.; Su, W. Quantification of Kryptofix 2.2.2 in [18F]fluorine-Labelled Radiopharmaceuticals by Rapid-Resolution Liquid Chromatography. *Nucl. Med. Commun.* **2012**, 33 (5), 498–502.
- (144) Brichard, L.; Aigbirhio, F. I. An Efficient Method for Enhancing the Reactivity and Flexibility of [ F ] Fluoride Towards Nucleophilic Substitution Using

- Tetraethylammonium. *European J. Org. Chem.* **2014**, 6145–6149.
- (145) Qiu, X.-L.; Xu, X.-H.; Qing, F.-L. Recent Advances in the Synthesis of Fluorinated Nucleosides. *Tetrahedron* **2010**, *66* (4), 789–843.
- (146) Alauddin, M. M. Nucleoside-Based Probes for Imaging Tumor Proliferation Using Positron Emission Tomography. *J. Labelled Comp. Radiopharm.* *56* (3–4), 237–243.
- (147) Youn, H.; Chung, J.-K. Reporter Gene Imaging. *Am. J. Roentgenol.* **2013**, *201* (2), W206–W214.
- (148) Strimbu, K.; Tavel, J. A. What Are Biomarkers? *Curr. Opin. HIV AIDS* **2010**, *5* (6), 463–466.
- (149) Neves, A. A.; Brindle, K. M. Assessing Responses to Cancer Therapy Using Molecular Imaging. *Biochim. Biophys. Acta* **2006**, *1766* (2), 242–261.
- (150) Ponomarev, V. Nuclear Imaging of Cancer Cell Therapies. *J. Nucl. Med.* **2009**, *50* (7), 1013–1016.
- (151) Koehne, G.; Doubrovin, M.; Doubrovina, E.; Zanzonico, P.; Gallardo, H. F.; Ivanova, A.; Balatoni, J.; Teruya-Feldstein, J.; Heller, G.; May, C.; Ponomarev, V.; Ruan, S.; Finn, R.; Blasberg, R. G.; Bornmann, W.; Riviere, I.; Sadelain, M.; O'Reilly, R. J.; Larson, S. M.; Gelovani Tjuvajev, J. G. Serial in Vivo Imaging of the Targeted Migration of Human HSV-TK-Transduced Antigen-Specific Lymphocytes. *Nat. Biotechnol.* **2003**, *21* (4), 405–413.
- (152) Ruggiero, A.; Thorek, D. L. J.; Guenoun, J.; Krestin, G. P.; Bernsen, M. R. Cell Tracking in Cardiac Repair: What to Image and How to Image. *Eur. Radiol.* **2012**, *22* (1), 189–204.
- (153) Weir, J. P. Regulation of Herpes Simplex Virus Gene Expression. *Gene* **2001**, *271* (2), 117–130.
- (154) Miyagawa, T.; Gogiberidze, G.; Serganova, I.; Cai, S.; Balatoni, J. A.; Thaler, H. T.; Ageyeva, L.; Pillarsetty, N.; Finn, R. D.; Blasberg, R. G. Imaging of HSV-Tk Reporter Gene Expression: Comparison between [18F]FEAU, [18F]FFEAU, and Other Imaging Probes. *J. Nucl. Med.* **2008**, *49* (4), 637–648.

- (155) Anderson, H.; Pillarsetty, N.; Cantorias, M.; Lewis, J. S. Improved Synthesis of 2'-deoxy-2'-[18F]-Fluoro-1-Beta-D-Arabinofuranosyl-5-Iodouracil ([18F]-FIAU). *Nucl. Med. Biol.* **2010**, *37* (4), 439–442.
- (156) Derudas, M.; Quintiliani, M.; Brancale, A.; Graciela, A.; Snoeck, R.; Balzarini, J.; McGuigan, C. Evaluation of Novel Phosphoramidate ProTides of the 2'-Fluoro Derivatives of a Potent Anti-Varicella Zoster Virus Bicyclic Nucleoside Analogue. *Antivir. Chem. Chemother.* **2010**, *21*, 15–31.
- (157) Sridharan, V.; Menéndez, J. C. Cerium(IV) Ammonium Nitrate as a Catalyst in Organic Synthesis. *Chem. Rev.* **2010**, *110* (6), 3805–3849.
- (158) Lepore, S. D.; Mondal, D. Recent Advances in Heterolytic Nucleofugal Leaving Groups. *Tetrahedron* **2007**, *63*, 5103–5122.
- (159) Douglas, P. K. Catalytic Stereoselective Glycosylation Process for Preparing 2'-deoxy-2',2'-difluoronucleosides and 2'-deoxy-2'-fluoronucleosides, 1993.
- (160) Jimenez, J. C.; Tyson, D. R.; Dhar, S.; Nguyen, T.; Hamai, Y.; Bradshaw, R. A.; Evans, G. R. D. Human Embryonic Kidney Cells (HEK-293 Cells): Characterization and Dose-Response Relationship for Modulated Release of Nerve Growth Factor for Nerve Regeneration. *Plast. Reconstr. Surg.* **2004**, *113* (2), 605–610.
- (161) Morin, K. W.; Duan, W.; Xu, L.; Zhou, A.; Moharram, S.; Knaus, E. E.; McEwan, A. J. .; Wiebe, L. I. Cytotoxicity and Cellular Uptake of Pyrimidine Nucleosides for Imaging Herpes Simplex Type-1 Thymidine Kinase (HSV-1 TK) Expression in Mammalian Cells. *Nucl. Med. Biol.* **2004**, *31* (5), 623–630.
- (162) Gelderblom, H. R. *Structure and Classification of Viruses*; University of Texas Medical Branch at Galveston, 1996.
- (163) Murphy, F. A.; Nathanson, N. The Emergence of New Virus Diseases: An Overview. *Semin. Virol.* **1994**, *5* (2), 87–102.
- (164) Wiwanitkit, V. Emerging Zika Virus Infection: What Should We Know? *Asian Pac. J. Trop. Biomed.* **2016**, *6* (7), 551–553.
- (165) Bäck, A. T.; Lundkvist, A. Dengue Viruses - an Overview. *Infect. Ecol. Epidemiol.* **2013**, *3*.

- (166) Gollnest, T.; de Oliveira, T. D.; Schols, D.; Balzarini, J.; Meier, C. Lipophilic Prodrugs of Nucleoside Triphosphates as Biochemical Probes and Potential Antivirals. *Nat. Commun.* **2015**, *6*, 8716.
- (167) Stuyver, L. J.; Lostia, S.; Adams, M.; Judy, S.; Pai, B. S.; Grier, J.; Phillip, M.; Choi, Y.; Chong, Y.; Choo, H.; Chu, C. K.; Otto, M. J.; Schinazi, R. F.; Analogues, J.; Mathew, J. S.; Tharnish, P. M. Antiviral Activities and Cellular Toxicities of - Didehydrocytidine Analogues Antiviral Activities and Cellular Toxicities of Modified. **2002**, *46* (12), 3854–3860.
- (168) Petter Jordheim, L.; Durantel, D.; Zoulim, F.; Dumontet, C. Advances in the Development of Nucleoside and Nucleotide Analogues for Cancer and Viral Diseases. *Nat. Publ. Gr.* **2013**, *12*.
- (169) McGuigan, C.; Bourdin, C.; Derudas, M.; Hamon, N.; Hinsinger, K.; Kandil, S.; Madela, K.; Meneghesso, S.; Pertusati, F.; Serpi, M.; Slusarczyk, M.; Chamberlain, S.; Kolykhalov, A.; Vernachio, J.; Vanpouille, C.; Introini, A.; Margolis, L.; Balzarini, J. Design, Synthesis and Biological Evaluation of Phosphorodiamidate Prodrugs of Antiviral and Anticancer Nucleosides. *Eur. J. Med. Chem.* **2013**, *70*, 326–340.
- (170) Griengl, H.; Wanek, E.; Schwarz, W.; Streicher, W.; Rosenwirth, B.; De Clercq, E. 2'-Fluorinated Arabinonucleosides of 5-(2-Haloalkyl)uracil: Synthesis and Antiviral Activity. *J Med Chem* **1987**, *30* (7), 1199–1204.
- (171) Gentile, I.; Borgia, F.; Buonomo, A. R.; Castaldo, G.; Borgia, G. A Novel Promising Therapeutic Option against Hepatitis C Virus: An Oral Nucleotide NS5B Polymerase Inhibitor Sofosbuvir. *Curr. Med. Chem.* **2013**, *20* (30), 3733–3742.
- (172) Trials, C.; Manning, F. J.; Swartz, M.; Trials, C.; Isbn, M.; Pdf, T.; Press, N. A.; Press, N. A.; Academy, N.; Academy, N.; Press, N. A. *Review of the Fialuridine (FIAU) Clinical Trials*; 1995.
- (173) McKenzie, R.; Fried, M. W.; Sallie, R.; Conjeevaram, H.; Di Bisceglie, A. M.; Park, Y.; Savarese, B.; Kleiner, D.; Tsokos, M.; Luciano, C.; Pruett, T.; Stotka, J. L.; Straus, S. E.; Hoofnagle, J. H. Hepatic Failure and Lactic Acidosis Due to Fialuridine (FIAU), an Investigational Nucleoside Analogue for Chronic Hepatitis

- B. *N. Engl. J. Med.* **1995**, 333 (17), 1099–1105.
- (174) McKenzie, R.; Fried, M. W.; Sallie, R.; Conjeevaram, H.; Di Bisceglie, A. M.; Park, Y.; Savarese, B.; Kleiner, D.; Tsokos, M.; Luciano, C.; Pruett, T.; Stotka, J. L.; Straus, S. E.; Hoofnagle, J. H. Hepatic Failure and Lactic Acidosis Due to Fialuridine (FIAU), an Investigational Nucleoside Analogue for Chronic Hepatitis B. *N. Engl. J. Med.* **1995**, 333 (17), 1099–1105.
- (175) Staschke, K. A.; Colacino, J. M. Priming of Duck Hepatitis B Virus Reverse Transcription in Vitro: Premature Termination of Primer DNA Induced by the 5'-triphosphate of Fialuridine. *J. Virol.* **1994**, 68 (12), 8265–8269.
- (176) Colacino, J. M.; Malcolm, S. K.; Jaskunas, S. R. Effect of Fialuridine on Replication of Mitochondrial DNA in CEM Cells and in Human Hepatoblastoma Cells in Culture. *Antimicrob. Agents Chemother.* **1994**, 38 (9), 1997–2002.
- (177) Cui, L.; Yoon, S.; Schinazi, R. F.; Sommadossi, J. P. Cellular and Molecular Events Leading to Mitochondrial Toxicity of 1-(2-Deoxy-2-Fluoro-1-Beta-D-Arabinofuranosyl)-5-Iodouracil in Human Liver Cells. *J. Clin. Invest.* **1995**, 95 (2), 555–563.
- (178) Sikka, V.; Chattu, V. K.; Popli, R. K.; Galwankar, S. C.; Kelkar, D.; Sawicki, S. G.; Stawicki, S. P.; Papadimos, T. J. The Emergence of Zika Virus as a Global Health Security Threat: A Review and a Consensus Statement of the INDUSEM Joint Working Group (JWG). *J. Glob. Infect. Dis.* **2016**, 8 (1), 3–15.
- (179) McGuigan, C.; Salgado, A.; Yarnold, C.; Harries, T. Y.; De Clercq, E.; Balzarini, J. Short Communication Novel Nucleoside Phosphoramidates as Inhibitors of HIV: Studies on the Stereochemical Requirements of the Phosphoramidate Amino Acid. *Antivir. Chem. Chemother.* **1996**, 7 (4), 184–188.
- (180) McGuigan, C.; Cahard, D.; Salgado, A.; De Clercq, E.; Balzarini, J. Phosphoramidates as Potent Prodrugs of Anti-HIV Nucleotides: Studies in the Amino Region. *Antivir. Chem. Chemother.* **1996**, 7 (1), 31–36.
- (181) McGuigan, C.; Tsang, H. W.; Cahard, D.; Turner, K.; Velazquez, S.; Salgado, A.; Bidois, L.; Naesens, L.; De Clercq, E.; Balzarini, J. Phosphoramidate Derivatives of

- d4T as Inhibitors of HIV: The Effect of Amino Acid Variation. *Antiviral Res.* **1997**, *35* (3), 195–204.
- (182) Knaggs, M. H.; McGuigan, C.; Harris, S. A.; Heshmati, P.; Cahard, D.; Gilbert, I. H.; Balzarini, J. A QSAR Study Investigating the Effect of L-Alanine Ester Variation on the Anti-HIV Activity of Some Phosphoramidate Derivatives of d4T. *Bioorg. Med. Chem. Lett.* **2000**, *10* (18), 2075–2078.
- (183) Elder, D. P.; Delaney, E.; Teasdale, A.; Eyley, S.; Reif, V. D.; Jacq, K.; Facchine, K. L.; Oestrich, R. S.; Sandra, P.; David, F. The Utility of Sulfonate Salts in Drug Development. *J. Pharm. Sci.* **2010**, *99* (7), 2948–2961.
- (184) WHO | Zika Virus. *WHO* **2018**.
- (185) Kruse, C. A.; Mitchell, D. H.; Kleinschmidt-DeMasters, B. K.; Franklin, W. A.; Morse, H. G.; Spector, E. B.; Lillehei, K. O. Characterization of a Continuous Human Glioma Cell Line DBTRG-05MG: Growth Kinetics, Karyotype, Receptor Expression, and Tumor Suppressor Gene Analyses. *In Vitro Cell. Dev. Biol.* *28A* (9–10), 609–614.
- (186) Vecchi, C.; Montosi, G.; Pietrangelo, A. Huh-7: A Human “hemochromatotic” Cell Line. *Hepatology* **2010**, *51* (2), 654–659.
- (187) Gosert, R.; Egger, D.; Lohmann, V.; Bartenschlager, R.; Blum, H. E.; Bienz, K.; Moradpour, D. Identification of the Hepatitis C Virus RNA Replication Complex in Huh-7 Cells Harboring Subgenomic Replicons. *J. Virol.* **2003**, *77* (9), 5487–5492.
- (188) Chan, J. F.-W.; Yip, C. C.-Y.; Tsang, J. O.-L.; Tee, K.-M.; Cai, J.-P.; Chik, K. K.-H.; Zhu, Z.; Chan, C. C.-S.; Choi, G. K.-Y.; Sridhar, S.; Zhang, A. J.; Lu, G.; Chiu, K.; Lo, A. C.-Y.; Tsao, S.-W.; Kok, K.-H.; Jin, D.-Y.; Chan, K.-H.; Yuen, K.-Y. Differential Cell Line Susceptibility to the Emerging Zika Virus: Implications for Disease Pathogenesis, Non-Vector-Borne Human Transmission and Animal Reservoirs. *Emerg. Microbes Infect.* **2016**, *5* (8), e93–e93.
- (189) Mumtaz, N.; Jimmerson, L. C.; Bushman, L. R.; Kiser, J. J.; Aron, G.; Reusken, C. B. E. M.; Koopmans, M. P. G.; van Kampen, J. J. A. Cell-Line Dependent Antiviral Activity of Sofosbuvir against Zika Virus. *Antiviral Res.* **2017**, *146*, 161–163.

- (190) Kherlopian, A. R.; Song, T.; Duan, Q.; Neimark, M. A.; Po, M. J.; Gohagan, J. K.; Laine, A. F. A Review of Imaging Techniques for Systems Biology. *BMC Syst. Biol.* **2008**, *2* (1), 74.
- (191) Puaux, A.-L.; Ong, L. C.; Jin, Y.; Teh, I.; Hong, M.; Chow, P. K. H.; Golay, X.; Abastado, J.-P. A Comparison of Imaging Techniques to Monitor Tumor Growth and Cancer Progression in Living Animals. *Int. J. Mol. Imaging* **2011**, *2011*, 321538.
- (192) Liu, S.; Conti, P. S.; Li, Z. PET/Fluorescence Imaging: An Opportunity to Integrate Diagnosis with Surgery. *Omi. J. Radiol.* **2013**, *2* (1).
- (193) Shraddha, B.; Swati, D.; Vilasrao, K. Concise Review on Fluorescence Spectroscopy – A Commonly Utilized Technique in Study of Drugs-Protein Interaction. *Int. J. pharma Sci. Res.* **2015**, *6*, 927–933.
- (194) Wysocki, L. M.; Lavis, L. D. Advances in the Chemistry of Small Molecule Fluorescent Probes. *Curr. Opin. Chem. Biol.* **2011**, *15* (6), 752–759.
- (195) Venkata Sairam, K.; Gurupadayya, B. M.; Chandan, R. S.; Nagesha, D. K.; Vishwanathan, B. A Review on Chemical Profile of Coumarins and Their Therapeutic Role in the Treatment of Cancer. *Curr. Drug Deliv.* **2016**, *13* (2), 186–201.
- (196) Das, N.; Dhanawat, M.; Dash, B.; Nagarwal, R. C.; Shrivastava, S. K. Codrug: An Efficient Approach for Drug Optimization. *Eur. J. Pharm. Sci.* **2010**, *41* (5), 571–588.
- (197) Christie, R. M.; Lui, C.-H. Studies of Fluorescent Dyes: Part 2. An Investigation of the Synthesis and Electronic Spectral Properties of Substituted 3-(2'-Benzimidazolyl)coumarins. *Dye. Pigment.* **2000**, *47* (1–2), 79–89.
- (198) Hassan, M. Z.; Osman, H.; Ali, M. A.; Ahsan, M. J. Therapeutic Potential of Coumarins as Antiviral Agents. *Eur. J. Med. Chem.* **2016**, *123*, 236–255.
- (199) Lavis, L. D.; Raines, R. T. Bright Building Blocks for Chemical Biology. *ACS Chem. Biol.* **2014**, *9* (4), 855–866.
- (200) Torres, F. C.; Brucker, N.; Andrade, S. F.; Kawano, D. F.; Garcia, S. C.; Poser, G. L.

- von; Eifler-Lima, V. L. New Insights into the Chemistry and Antioxidant Activity of Coumarins. *Curr. Top. Med. Chem.* **2014**, *14* (22), 2600–2623.
- (201) Penta, S. *Advances in Structure and Activity Relationship of Coumarin Derivatives*.
- (202) Kashman, Y.; Gustafson, K. R.; Fuller, R. W.; Cardellina, J. H.; McMahon, J. B.; Currens, M. J.; Buckheit, R. W.; Hughes, S. H.; Cragg, G. M.; Boyd, M. R. The Calanolides, a Novel HIV-Inhibitory Class of Coumarin Derivatives from the Tropical Rainforest Tree, *Calophyllum Lanigerum*. *J. Med. Chem.* **1992**, *35* (15), 2735–2743.
- (203) Xu, Z. Q.; Flavin, M. T.; Jenta, T. R. Calanolides, the Naturally Occurring Anti-HIV Agents. *Curr. Opin. Drug Discov. Devel.* **2000**, *3* (2), 155–166.
- (204) Sancho, R.; Márquez, N.; Gómez-Gonzalo, M.; Calzado, M. A.; Bettoni, G.; Coiras, M. T.; Alcamí, J.; López-Cabrera, M.; Appendino, G.; Muñoz, E. Imperatorin Inhibits HIV-1 Replication through an Sp1-Dependent Pathway. *J. Biol. Chem.* **2004**, *279* (36), 37349–37359.
- (205) Kaushik-Basu, N.; Bopda-Waffo, A.; Talele, T. T.; Basu, A.; Costa, P. R. R.; da Silva, A. J. M.; Sarafianos, S. G.; Noël, F. Identification and Characterization of Coumestans as Novel HCV NS5B Polymerase Inhibitors. *Nucleic Acids Res.* **2008**, *36* (5), 1482–1496.
- (206) Nakamura, T.; Funahashi, M.; Takagaki, K.; Munakata, H.; Tanaka, K.; Saito, Y.; Endo, M. Effect of 4-Methylumbelliferone on Cell-Free Synthesis of Hyaluronic Acid. *Biochem. Mol. Biol. Int.* **1997**, *43* (2), 263–268.
- (207) Nagy, N.; Kuipers, H. F.; Frymoyer, A. R.; Ishak, H. D.; Bollyky, J. B.; Wight, T. N.; Bollyky, P. L. 4-Methylumbelliferone Treatment and Hyaluronan Inhibition as a Therapeutic Strategy in Inflammation, Autoimmunity, and Cancer. *Front. Immunol.* **2015**, *6*, 123.
- (208) Kosaki, R.; Watanabe, K.; Yamaguchi, Y. Overproduction of Hyaluronan by Expression of the Hyaluronan Synthase Has2 Enhances Anchorage-Independent Growth and Tumorigenicity. *Cancer Res.* **1999**, *59* (5), 1141–1145.

- (209) National Institutes of Health. National Institutes of Health Consensus Development Conference Statement: Management of Hepatitis C: 2002--June 10-12, 2002. *Hepatology* **2002**, *36* (5 Suppl 1), S3-20.
- (210) Li, X.; Zeng, H.; Wang, P.; Lin, L.; Liu, L.; Zhen, P.; Fu, Y.; Lu, P.; Zhu, H. Reactivation of Latent HIV-1 in Latently Infected Cells by Coumarin Compounds: Hymecromone and Scoparone. *Curr. HIV Res.* **2016**, *14* (6), 484–490.
- (211) Harada, K.; Kubo, H.; Tomigahara, Y.; Nishioka, K.; Takahashi, J.; Momose, M.; Inoue, S.; Kojima, A. Coumarins as Novel 17 $\beta$ -Hydroxysteroid Dehydrogenase Type 3 Inhibitors for Potential Treatment of Prostate Cancer. *Bioorg. Med. Chem. Lett.* **2010**, *20* (1), 272–275.
- (212) Hakamata, W.; Tamura, S.; Hirano, T.; Nishio, T. Multicolor Imaging of Endoplasmic Reticulum-Located Esterase As a Prodrug Activation Enzyme. *ACS Med. Chem. Lett.* **2014**, *5* (4), 321–325.
- (213) Mattoo, B. N. Absorption and Fluorescence Spectra of Coumarins. *Trans. Faraday Soc.* **1956**, *52* (0), 1184.
- (214) Lau, W. M.; White, A. W.; Gallagher, S. J.; Donaldson, M.; McNaughton, G.; Heard, C. M. Scope and Limitations of the Co-Drug Approach to Topical Drug Delivery. *Curr. Pharm. Des.* **2008**, *14* (8), 794–802.
- (215) Al-Masoudi, N. A.; Al-Salihi, N. J.; Marich, Y. A.; Markus, T. Synthesis, and Fluorescence Properties of Coumarin and Benzocoumarin Derivatives Conjugated Pyrimidine Scaffolds for Biological Imaging Applications. *J. Fluoresc.* **2015**, *25* (6), 1847–1854.
- (216) Tang, G.; Tang, X.; Wen, F.; Wang, M.; Li, B. A Facile and Rapid Automated Synthesis of 3'-deoxy-3'-[(18)F]fluorothymidine. *Appl. Radiat. Isot.* **2010**, *68* (9), 1734–1739.

